THE UNIVERSITY
of EDINBURGH

Diagnostic and prognostic value of current phenotyping methods and novel molecular markers in idiopathic pulmonary fibrosis

Dr Lisa Margaret Nicol

A thesis submitted for the degree of Doctor of Medicine

The University of Edinburgh

2018

Declaration

I declare that all of the work presented in this thesis is my own, and has been composed and performed by myself. All sources of information, including contributions by colleagues, are fully acknowledged in the text.

This work has not been submitted for candidature for any other degree or personal qualification.

Lisa Margaret Nicol

Acknowledgements

First and foremost I would like to give special thanks to my primary supervisor, Dr Nik Hirani for providing excellent support and guidance throughout my research. Thanks are given to all of the staff and patients at the Edinburgh Lung Fibrosis Clinic, with a special mention to Pauline McFarlane, Dr Hirani's research nurse. I would also like to thank Alison MacKinnon, Mairi Brittan, John Marwick, Sarah Howie, Adriano Rossi, Kevin Dhaliwal, Ian Dransfield, Ross Mills and the staff in the flow laboratory, Shonna Johnston and William Ramsey for their invaluable help and guidance over the last two years. I would like to thank Alex Przybylski, Sohan Seth and Jeremy Walker for providing statistical support and guidance for the analysis of data. Lastly I would like to thank InterMune, Chief Scientist Office, Chiesi and Galecto for funding my research and providing financial support to allow me to attend and present my work at international conferences.

Abstract

Diagnostic and prognostic value of current and novel biomarkers in idiopathic pulmonary fibrosis

Background

Idiopathic pulmonary fibrosis (IPF) is a devastating form of chronic lung injury of unknown aetiology characterised by progressive lung scarring. A diagnosis of definite IPF requires High Resolution Computed Tomography (HRCT) appearances indicative of usual interstitial pneumonia (UIP), or in patients with 'possible UIP' CT appearances, histological confirmation of UIP. However the proportion of such patients that undergo SLB varies, perhaps due to a perception of risk of biopsy and additive diagnostic value of biopsy in individual patients. We hypothesised that an underlying UIP pathological pattern may result in increased risk of death and aimed to explore this by comparing the risk of SLB in suspected idiopathic interstitial pneumonia, stratified according to HRCT appearance. Additionally we sought to determine the positive-predictive value of biopsy to diagnose IPF in patients with 'possible UIP HRCT' in our population. In patients with possible UIP who are not biopsied, the clinical value of bronchoalveolar lavage (BAL) is uncertain. We aimed to prospectively study the diagnostic and prognostic value of BAL differential cell count (DCC) in suspected IPF and determine the feasibility of repeat BAL and the relationship between DCC and disease progression in two successive BALs. We hypothesised that BAL DCC between definite and possible IPF was different and that baseline DCC and change in BAL DCC predicted disease progression. Alveolar macrophages (AMs) are an integral part of the lung's reparative mechanism following injury, however in IPF they contribute to pathogenesis by releasing pro-fibrotic mediators promoting fibroblast proliferation and collagen deposition. Expansion of novel subpopulations of pulmonary monocyte-like cells (PMLCs) has been reported in inflammatory lung disease. We hypothesised that a distinct AM polarisation phenotype would be associated with disease progression. We aimed to perform detailed phenotyping of AM and PMLCs in BAL in IPF patients. Several prognostic scoring systems and biomarkers have been described to predict

disease progression in IPF but most were derived from clinical trial patients or tertiary referral centres and none have been validated in separate cohorts. We aimed to identify a predictive tool for disease progression utilising physiological, HRCT and serum biomarkers in a unique population of incident treatment naïve IPF patients.

Methods

Between 01/01/07 and 31/12/13, 611 consecutive incident patients with suspected idiopathic interstitial pneumonia (IIP) presented to the Edinburgh lung fibrosis clinic. Of these patients 222 underwent video-assisted thoracoscopic lung biopsy and histological pattern was determined according to ATS/ERS criteria. Post-operative mortality and complication rates were examined. Fewer than 2% received IPF-directed therapy and less than 1% of the cohort were lost to follow-up. Disease progression was defined as death or ≥10% decline in VC within 12 months of BAL. Cells were obtained by BAL and a panel of monoclonal antibodies; CD14, CD16, CD206, CD71, CD163, CD3, CD4, CD8 and HLA-DR were used to quantify and selectively characterise AMs, resident PMLCs, inducible PMLCs, neutrophils and CD4+/CD8+ T-cells using flow cytometry. Classical, intermediate and non-classical monocyte subsets were also quantified in peripheral blood. Potential biomarkers (n=16) were pre-selected from either previously published studies of IPF biomarkers or our hypothesis-driven profiling. Linear logistic regression was used on each predictor separately to assess its importance in terms of p-value of the associated weight, and the top two variables were used to learn a decision tree.

Results

Based on the 2011 ATS/ERS criteria, 87 patients were categorised as ‘definite UIP’, of whom 3 underwent SLB for clinical indications. IPF was confirmed in all 3 patients based on 2013 ATS/ERS/JRS/ALAT diagnostic criteria. 222 patients were diagnosed with ‘possible UIP’; 55 underwent SLB, IPF was subsequently diagnosed in 37 patients, 4 were diagnosed with ‘probable IPF’ and 14 were considered ‘not IPF’. In this group, 30 patients were aged 65 years or over and 25/30 (83%) had UIP on biopsy. 306 patients had HRCTs deemed ‘inconsistent with UIP’, SLB was performed in 168 patients. Post-

operative 30-day mortality was 2.2% overall, and 7.3% in the 'possible UIP' HRCT group. Patients with 'definite IPF' based on HRCT and SLB appearances had significantly better outcomes than patients with 'definite UIP' on HRCT alone (P=0.008, HR 0.44 (95% CI 0.240 to 0.812)).

BAL DCC was not different between definite and possible UIP groups, but there were significant differences with the inconsistent with UIP group. In the 12 months following BAL, 33.3% (n=7/21) of patients in the definite UIP group and 29.5% (n=18/61) in the possible UIP group had progressed. There were no significant differences in BAL DCC between progressor and non-progressor groups. Mortality in patients with suspected IPF and a BAL DCC consistent with IPF was no different to those with a DCC inconsistent with IPF (P=0.425, HR 1.590 (95% CI 0.502 to 4.967)). There was no difference in disease progression in either group (P=0.885, HR 1.081 (95% CI 0.376 to 3.106)). There was no statistically significant difference in BAL DCC at 0 and 12 months in either group. There was no significant change in DCC between 0 and 12 month BALs between progressors and non-progressors. Repeat BAL was well tolerated in almost all patients. There was 1 death within 1 month of a first BAL and 1 death within 1 month of a second BAL; both were considered 'probably procedure-related'.

AM CD163 and CD71 (transferrin receptor) expression were significantly different between groups (P<0.0001), with significant increases in the IPF group vs non fibrotic ILD (P<0.0001) and controls (P<0.0001 and P<0.001 respectively). CD71 expression was also significantly increased in the IPF progressor vs non-progressor group (P<0.0001) and patients with high CD71 expression had significantly poorer survival than the $CD71^{low}$ group (P=0.040, median survival 40.5 and 75.6 months respectively). CD206 (mannose receptor) expression was also significantly higher in the IPF progressor vs non-progressor group (P=0.034). There were no differences in baseline BAL neutrophil, eosinophil or lymphocyte percentages between IPF progressor or non-progressor groups. The percentage of rPMLCs was significantly increased in BAL fluid cells of IPF patients compared to those with non-fibrotic ILD (P<0.0001) and healthy controls (P<0.05). Baseline rPMLC percentage was significantly higher in IPF

progressors vs IPF non-progressors (P=0.011). Baseline BAL iPMLC:rPMLC ratio was also significantly different between IPF progressor and non-progressor groups (P=0.011). Disease progression was confidently predicted by a combination of clinical and serological variables. In our cohort we identified a predictive tool based on two key parameters, one a measure of lung function and one a single serum biomarker. Both parameters were entered into a decision tree, and when applied to our cohort yielded a sensitivity of 86.4%, specificity of 92.3%, positive predictive value of 90.5% and negative predictive value of 88.9%. We also applied previously reported predictive tools such as the GAP Index, du Bois score and CPI Index to the Edinburgh IPF cohort.

Conclusions

SLB can be of value in the diagnosis of ILD, however perhaps due to the perceived risks associated with the procedure, only a small percentage of patients undergo SLB despite recommendations that patients have histological confirmation of the diagnosis. Advanced age is a strong predictor for IPF, and in our cohort 83% of patients aged over 65 years with 'possible UIP' HRCT appearances, had UIP on biopsy. BAL and repeat BAL in IPF is feasible and safe (<1.5% mortality). Of those that underwent repeat BAL, disease progression was not associated with a change in DCC. However, 22% of lavaged patients died or were deemed too frail to undergo a second procedure at 12 months. These data emphasise the importance of BAL in identifying a novel human AM polarisation phenotype in IPF. Our data suggests there is a distinct relationship between AM subtypes, cell-surface expression markers, PMLC subpopulations and disease progression in IPF. This may be utilised to investigate new targets for future therapeutic strategies. Disease progression in IPF can be predicted by a combination of clinical variables and serum biomarker profiling. We have identified a unique prediction model, when applied to our locally referred, incident, treatment naïve cohort can confidently predict disease progression in IPF. IPF is a heterogeneous disease and there is a definite clinical need to identify 'personalised' prognostic biomarkers which may in turn lead to novel targets and the advent of personalised medicines.

Lay Summary

Idiopathic pulmonary fibrosis (IPF) is a devastating form of lung scarring with no known cause, and an average survival time worse than many cancers at 3-5 years. There are around 5000 new patients diagnosed each year in the UK, with Scotland harbouring the highest incidence. IPF can often be diagnosed by CT scanning, however HRCT appearances are not definitive in around 50% of patients. It is recommended that these patients go on to have a biopsy of their lung to try and prove the diagnosis, however surgical lung biopsy can be a risky procedure in this group of patients, many of whom are elderly, frail and have many other health problems. We found that surgical lung biopsy can be of value in the diagnosis of IPF, however patients with 'possible IPF' have an increased risk of death following the procedure, and the majority of patients over the age of 65 years had IPF on biopsy anyway, therefore we suggest careful consideration must be given prior to subjecting these patients to a potentially dangerous and unnecessary procedure. Two drugs, pirfenidone and nintedanib, have been approved for treatment of IPF in recent years, however these drugs do not provide a cure, have many intolerable side-effects, and have strict criteria for use. Their recommendation is based on the results of clinical trials, of which eligibility criteria would have excluded a large proportion of patients we see with IPF in real-life clinical practice. Another problem faced by doctors and patients alike is that IPF can have a highly variable clinical course and it is very difficult to predict which patients will deteriorate rapidly when patients first develop symptoms. We aimed to identify patients at risk of rapid progression by using a number of different clinical variables, but also looking at the characteristics of the cells themselves. Cells were obtained from patient blood by taking a blood sample, and from the airways by inserting a camera into patients' lungs via the nose, and performing a lavage (lung wash). We found that the cells from patients with IPF and rapid progression had different surface expression markers than those of patients who did not progress. We also identified a protein that could be detected in a blood sample, that when combined with lung function data at the onset of symptoms, was highly predictive of disease progression in IPF.

Table of contents

Table of Figures

Table of Tables

List of Abbreviations

6MWD….	6 Minute Walk Distance	DLCO…..	Diffusing Capacity of the Lungs for Carbon Monoxide
ACE…….	Angiotensin-Converting Enzyme	DM/PM….	Dermatomyositis / Polymyositis
ACM……	Alveolar-Capillary Membrane	DNA….....	Deoxyribonucleic Acid
AEC….....	Alveolar Epithelial Cell	EAA.....	Extrinsic Allergic Alveolitis
AIP.....	Acute Interstitial Pneumonia	ECG….....	Electrocardiograph
ALAT…..	Latin American Thoracic Society	ECM…….	Extracellular Matrix
AM……..	Alveolar Macrophage	ELISA…..	Enzyme-Linked Immunosorbent Assay
ANOVA..	Analysis of Variance	ERS….....	European Thoracic Society
ATS…….	American Thoracic Society	FACs.....	Fluorescence Activated Cell Sorting
BAL…….	Bronchoalveolar Lavage	FDA……..	US Food and Drink Administration
BALF…..	Bronchoalveolar Lavage Fluid	FEV_1….....	Forced Expiratory Volume in 1 Second
BCA…….	Bicinchoninic Acid	FGF……..	Fibroblast Growth Factor
BMI…….	Body Mass Index	FMO.....	Fluorescence Minus One
CCL…….	CC-Chemokine	FVC……..	Forced Vital Capacity
CD……...	Cluster of Differentiation	GAP……..	Gender Age Physiology
cDNA…..	Complementary Deoxyribonucleic Acid	GRADE.....	Grades of Recommendation, Assessment, Development and Evalution
CHI3-L1..	Chitinase-3-Like Protein 1	GRO-alpha……..	Growth-Regulated Oncogene alpha
CI…….	Confidence Interval	GSH……..	Glutathine
COP.....	Cryptogenic Organising Pneumonia	HGF……..	Hepatocyte Growth Factor
COPD…..	Chronic Obstructive Pulmonary Disease	HLA……..	Human Leukocyte Antigen
CPI……...	Composite Physiologic Index	HP…….....	Hypersensitivity Pneumonitis
CRP……..	Clinical-Radiological-Physiological	HR…….....	Hazard Ratio
CTD-ILD.	Connective Tissue Disease-Associated Interstital Lung Disease	HRCT……	High Resolution Computed Tomography
CXCL…..	C-X-C Motif Chemokine	HSP….....	Heat Shock Protein
DCC…….	Differntial Cell Count	ICU.....	Intensive Care Unit
DIP.....	Desquamative Interstitial Pneumonia	IFN……	Interferon

IGF.....	Insulin-Like Growth Factor
IgG……..	Immunoglobulin G
IIP……	Idiopathic Interstitial Pneumonia
IL……	Interleukin
ILD……..	Interstitial Lung Disease
IM……....	Interstitial Macrophage
IMDM.....	Iscove's Modified Dulbecco's Medium
iNOS….....	Inducible Nitric Oxide Synthase
IPF……	Idiopathic Pulmonary Fibrosis
iPMLC…..	Inducible Pulmonary Monocyte-Like Cells
IQR.....	Interquartile Range
IRF……..	Interferon Regulatory Factor
JRS……..	Japanese Respiratory Society
KL……	Krebs Von Den Lungen
KM.....	Kaplan Meier
LED……..	Light-Emitting Diode
LPS……....	Lipopolysaccharide
M-CSF…..	Macrophage Colony-Stimulating Factor
MCP…….	Monocyte Chemoattractant Protein
MCTD.....	Mixed Connective Disease
MDC……	Macrophage-Derived Chemokine
MDT…….	Multidisciplinary Team
MIF……..	Macrophage Migration Inhibitory Factor
MMP……	Matrix Metalloproteinase
MPO….....	Myeloperoxidase
MRCD…..	Medical Research Council Dyspnoea Score
MRP……..	Multidrug Resistance Protein
MUC5B….	Mucin 5B
NAC……..	N-acetylcysteine
NE…….	Neutrophil Elastase
NET….....	Neutrophil Extracellular Trap
NICE……..	National Institute for Health and Care Excellence
NO…….	Nitric Oxide
NSIP……..	Non-Specific Interstitial Pneumonia
PACS…….	Picture Archiving and Communication System
PAI….....	Plasminogen Activator
PARC……	p53-Associated Parkin-Like Cytoplasmic Protein
PBS.....	Phosphate-Buffered Saline
PD……..	Pharmacodynamics
PDGF.....	Platelet-Derived Growth Factor
PFT……	Pulmonary Function Test
PK……..	Pharmacokinetics
PMLC….....	Pulmonary Monocyte-Like Cells
qPCR.....	Quantitative Polymerase Chain Reaction
RA.....	Rheumatoid Arthritis
RAGE….....	Receptor for Advanced Glycation Endproducts
RB-ILD….	Respiratory Bronchiolitis Associated-Interstitial Lung Disease
RML.....	Right Middle Lobe
RNA……..	Ribonucleic Acid
ROC……..	Receiver Operating Characteristic
ROSE….....	Risk Stratification Score

rPMLC.....	Resident Pulmonary Monocyte-Like Cells
SD…….....	Standard Deviation
SLB……..	Surgical Lung Biopsy
SLE.....	Systemic Lupus Erythematosus
SP…….	Surfactant Protein
SsC.....	Systemic Sclerosis
TCO……..	Lung Transfer Factor
TGF……..	Transforming Growth Factor
Th2……...	T helper type 2 Cell
TIMPs.....	Tissue Inhibitors of Matrix Metalloproteinases
TLC……..	Total Lung Capacity
TNF……..	Tumour Necrosis Factor
TOLLIP…	Toll-Interacting Protein
Tregs….....	Regulatory T-cells
TSLP….....	Thymic Stromal Lymphopoietin
UIP……...	Usual Interstitial Pneumonia
uPA.....	Urokinase-Like Plasminogen Activator
VATS…..	Video-Assisted Thorocoscopic Surgery
VEGF…..	Vascular Endothelial Growth Factor

Chapter 1

General Introduction

1.1 Introduction

The interstitial lung diseases (ILDs) are a heterogeneous group of lung disorders characterised by varying degrees of parenchymal inflammation and fibrosis. The last decade has seen marked changes in the field of ILD with an increasing incidence and a more complex, continually expanding disease classification. In their most severe forms, these diseases lead to progressive loss of lung function, respiratory failure and death. Despite significant advances, progress has been limited by a poor understanding of the pathological mechanisms of disease, and also significant patient heterogeneity, including great variability in disease progression. Distinguishing the various forms of pulmonary fibrosis is paramount in determining correct management and for predicting prognosis. The current international consensus statement recommends that around two thirds of idiopathic pulmonary fibrosis (IPF) cases can be diagnosed on the basis of typical clinical and radiological findings of usual interstitial pneumonia (UIP), however it is advocated that the remainder of patients should undergo surgical lung biopsy (SLB) to obtain a confident diagnosis[1]. In the UK, only 7.5–12% of suspected IPF patients undergo surgical lung biopsy [2], a reflection perhaps of clinicians' reluctance to refer patients for a procedure associated with significant morbidity and mortality. When we consider the multi-faceted nature of obtaining a diagnosis in ILD, it is clear that no single diagnostic test can provide a confident answer. The gold standard is that a diagnosis must be reached by a multidisciplinary team (MDT) with expertise in ILD, and must consider all clinical, radiological and histological parameters. IPF has the poorest prognosis of all of the ILDs, and with the recent addition of two newly approved drugs, pirfenidone and nintedanib, a timely and accurate definitive diagnosis is fundamental in facilitating early treatment, but also considering the longer term management for example early referral for lung transplantation, or palliative care involvement as appropriate.

This introduction begins with an overview of the background of IPF and a description of the pulmonary structure and function, including a brief summary of the pulmonary biology of the lung's response to infection and injury. This is followed by an overview of the pathogenesis, diagnosis and management of IPF, and a report of existing methods used to predict disease progression including current and novel biomarkers, concluding with a discussion of the hypothesis and aims of this thesis.

1.2 Background of Idiopathic Pulmonary Fibrosis

Idiopathic pulmonary fibrosis (IPF) is the commonest ILD and is a chronic and progressive form of lung scarring with a median survival time of 3-5 years and no curative therapy. IPF occurs worldwide however Scotland harbours the highest incidence in the UK[3]. There are approximately 5000 new cases per year in the UK, with a disease prevalence of 5-15 cases per 100,000 population[4]. The disease is becoming more common with a recently reported increase in the annual incidence of 11% between 1991 and 2003, a rise that is only partly explained by an ageing population[5]. The median age at presentation is 70 years and IPF is more prevalent in males and in smokers[4]. Patients typically present with progressive dyspnoea and a dry cough. Clinical examination findings include bibasal inspiratory "velcro-type" crackles and finger clubbing, which occurs in 25-50%[6]. It is well recognised that symptoms often precede diagnosis by a period of 1-2 years[7]. Pulmonary function tests (PFTs) may be normal at presentation, however typically show a restrictive pattern with a reduced forced vital capacity (FVC) and an impaired gas exchange indicated by a reduced diffusion lung capacity for carbon monoxide (TLco). IPF is a highly heterogeneous disease and so the natural history and clinical course in each individual patient is difficult to predict[6]. Many patients have a slow and steady deterioration over a period of years, whereas 10-15% of patients progress rapidly, often leading to death from respiratory failure in a few months. Some patients experience periods of relative stability interspersed with episodes of acute deterioration[4]. Most patients with IPF die from progression of lung fibrosis causing respiratory failure and death. However there are a number of notable comorbidities that attribute significant mortality in IPF; ischaemic heart disease, heart failure, bronchogenic carcinoma, infection and pulmonary embolism[7]. There are now two drugs, pirfenidone and nintedanib, approved by the National Institute for Health

and Care Excellence (NICE) for IPF; however at an annual cost of around £26,000 per patient and the potential for severe side-effects, accurate disease identification is essential[2].

1.3 Pulmonary structure and function

1.3.1 The upper respiratory tract

The upper respiratory tract contains the nose, nostrils, nasal cavity, mouth, pharynx and the portion of the larynx above the vocal cords. The upper airway is a collapsible, compliant tube and can withstand the suction pressures produced by the rhythmic contraction of the diaphragm that draws air into the lungs during respiration. Nasal hairs line the opening of the nostrils to catch large particles of dust, thus preventing them from being inhaled. The upper airways are lined with a mucous secreting mucous membrane which traps smaller particles like pollen and smoke. This membrane is lined with small, hair-like structures called cilia, which move the particles trapped in the mucous out of the nose. After air is sucked into the upper respiratory tract, it is moistened, warmed and cleansed by the nasal epithelium covering the turbinate bones in the nasal cavity. The pharynx is a muscular structure that contains the tonsils and adenoids, which are lymphatic tissues that fight infection by releasing T and B lymphocyte cells. The larynx forms the entrance to the lower respiratory tract and contains the epiglottis, a leaf-shaped flap that folds backwards on swallowing, therefore preventing food or fluid from entering the lower airways[8].

1.3.2 The lower respiratory tract

The major structures of the lower respiratory tract are the portion of the larynx below the vocal cords, the trachea, and within the lungs, the bronchi, bronchioles, and alveoli. The trachea is a rigid tube, held open by C-shaped hyaline cartilage rings embedded in the walls. The trachea is approximately 4.5 inches long, and then divides into the right and left main bronchi. These bronchi also contain cartilage rings, and on travelling down deeper into the lungs, branch into secondary and tertiary bronchi, which then continue to divide into the bronchioles. Bronchioles do not contain any cartilage and so

may undergo constriction and obstruction during different disease states. From the bronchi, the dividing tubes become progressively narrower with an estimated 20 to 23 divisions before ending at an alveolus. Alveoli are air sacs located at the end of the bronchioles, and cluster together to form alveolar sacs. The surface of each alveolus contains a network of capillaries and it is here that gaseous exchange occurs. Oxygen is transported from the lungs to the heart, where it is pumped out into all of the body's tissues, and carbon dioxide is transported from the blood to the lungs, where it is expelled from the body during expiration[8].

The lungs are suspended in the pleural cavity of the thorax, and are covered by two thin membranes; the visceral pleura, the inner lining covering the surface of the lung, and the parietal pleura, the outer layer covering the inner surface of the chest wall. This membrane secretes pleural fluid which lubricates the two surfaces preventing friction and allowing the lung to move freely during respiration. In addition, a negative pressure is created between the two layers, allowing the two surfaces to stick together tightly.

The lung consists of epithelial cells which form the lining of the trachea and bronchi, and mesenchymal cells which line the lungs themselves. Most of the respiratory tract is covered in ciliated pseudostratified columnar epithelium. The cilia beat in one direction, moving mucous towards the pharynx where it is swallowed. Cells of the bronchioles are more cuboidal, however are still ciliated. The walls of the bronchioles are composed of helical bands of smooth muscle cells and contain no cartilage. Glands and mucous producing goblet cells are abundant in the upper airways, but become sparser on moving down the lower respiratory tract at the level of the bronchioles. The epithelium is cuboidal between the alveoli in the earlier branches of respiratory bronchioles, but becomes progressively flatter until it is entirely squamous alveolar epithelium within the alveolar ducts. There are around 300 million alveoli in the human lung providing a huge surface area (approximately $70m^2$) for gas exchange. There are three main cell types found in the alveoli. Type I alveolar cells, or squamous pulmonary epithelial cells, form the continuous lining of the alveolus and are the cells across which gases diffuse between the lungs and the blood. Type II alveolar cells are found scattered amongst the others, and secrete pulmonary surfactant, a phospholipid, which keeps the alveolar cells moist and lowers the surface tension of the air-surface interface, helping to prevent alveolar collapse. The third major cell type is the alveolar macrophage (AM), which lie

on top of the alveolar lining provided by type I cells. AMs move freely over the surface of the alveoli and phagocytose any material that enters the alveoli. AMs are cleared via the airways and lymphatics. The layer separating blood and air is the alveolocapillary barrier, across which gases diffuse during the gas exchange process. The membrane consists of three layers, alveolar epithelial cells, capillary endothelial cells and fused basement membranes of alveolar epithelial cells and capillary endothelial cells in most areas, however in a few areas the basement membranes are separated and the interstitium containing fibroblasts, collagen and elastic fibres can be seen. The membrane is very thin at around 0.5 microns in thickness, which allows rapid diffusion of respiratory gases[8,9].

1.4 Lung responses to infection and injury and the pathogenesis of fibrosis

Tissue repair and regeneration are critical biological processes that are fundamental to survival[10]. Due to its position within the body at the interface between the host and environment, the lung is not only involved in gas exchange, but has a pivotal role in mediating host defence[11]. This border consists not only of the airway's mucociliary clearance, but also of the extensive alveolar-capillary membrane (ACM) which is composed of both immune and non-immune cells. This barrier is continuously exposed to a number of both inhaled and haematogenous stimuli, and when lung tissues are injured during infection or after toxic or mechanical injury, a complex inflammatory response is triggered by the resultant cell death or invading organism. The inflammatory response consists of recruitment, proliferation and activation of a number of haematopoietic and non-haematopoietic cells including neutrophils, macrophages, lymphoid cells, natural killer cells, B cells, T cells, fibroblasts, epithelial cells, endothelial cells and stem cells, which in normal tissue repair, results in rapid restoration of normal lung structure and function[10].

The early phases of wound healing after injury to the ACM consist of increased vascular permeability with extravasation of plasma and clotting factors into lung tissues which leads to activation of the intrinsic and extrinsic coagulation pathways. This results in

the development of a provisional wound matrix consisting of fibrin, fibronectin and platelets[12]. Platelet activation and degranulation cause an influx of a number of lipid mediators and cytokines into the matrix[11]. Following stimulation by these growth factors or chemotaxins, leukocyte, endothelial cell, fibroblast/myofibroblast, and epithelial cell activation occur[11].

Leukocyte recruitment occurs following endothelial cell activation, leukocyte activation, expression of adhesion molecules, leukocyte-endothelial cell adhesion and leukocyte extravasation via chemotactic gradients. Neutrophils are typically the first leukocyte to arrive at the site of tissue injury, however are often considered short-lived mediators of acute inflammation[13]. Their primary function is to phagocytose debris and microorganisms, however they are also capable of releasing a number of lipid and protein mediators, including neutrophil elastase (NE), which may contribute to the fibrotic process. Neutrophil elastase promotes fibroblast proliferation and myofibroblast differentiation[13]. Neutrophils are also able to release neutrophil extracellular traps (NETs) which consist of chromatin and granular proteins. Release of NETs in the lung promotes lung fibroblast proliferation and differentiation, extracellular matrix (ECM) generation and release of the pro-fibrotic cytokine IL-17, all of which may contribute to local tissue damage and inflammation[13].

After lung injury large numbers of inflammatory monocytes are recruited from the bone marrow via chemokine gradients and cell adhesion, these recruited cells often exceed the population of lung resident macrophages[10]. Macrophages are present in almost all tissues of the body and are fundamental for maintenance of homeostasis. Pulmonary macrophages are integral to the lung's host defence, and may be resident, residing in the lung tissue itself, or recruited from circulating monocytes in the blood. The distinction between resident and recruited macrophage populations may be important in the development of fibrosis as the cytokine profiles and functions can vary significantly[14]. There are two types of pulmonary macrophage in humans; alveolar macrophages (AM), which sit in the airway space, and interstitial macrophages (IM), which are located in lung parenchymal tissue. AMs express high levels of the integrin CD11c and low levels of CD11b, and are interposed between the pulmonary mucosa and the external environment. They have key roles in maintaining immune tolerance and recycling surfactant molecules produced by airway epithelial cells. AMs are long-

lived and repopulate by in situ proliferation rather than by replenishment from bone marrow[14]. IMs are derived from blood monocytes and express high levels of CD11b and have low surface expression of CD11c. They also contribute to homeostasis and secrete high levels of the anti-inflammatory cytokine IL-10[14].

As described, the innate immune system is pivotal in the initiation and termination of the inflammatory response following exposure to endogenous and exogenous stimuli[15]. Alveolar macrophages play a crucial role in the wound healing response and are a source of many key growth factors and chemokines[15].

In addition to the IM/AM macrophage subtypes, macrophage populations have also been classified according to their polarisation and activation phenotype. M1, or classically activated macrophages mature under the influence of transcription factor interferon regulatory factor (IRF)-5 and are induced by Type 1 helper T-cells or Type 1 cytokines (for example interferon γ), fungal cell wall components, degraded matrix (such as hyaluronic acid), LPS and TNFα[11]. It is well documented that M1 macrophages contribute to host defence against intracellular pathogens by producing reactive nitric oxide (NO) via inducible nitric oxide synthase (iNOS) and through the release of proinflammatory cytokines such as IL-1β, IL-12β, IL-23, TNFα and CXCL-10[14]. The large amounts of NO produced contribute to the killing of intracellular pathogens. M1 macrophages express low levels of the haemoglobin scavenger receptor CD163 and have key roles in the processes of phagocytosis, antigen presentation and T-cell activation. They are also involved in matrix degradation by direct production of matrix metalloproteinases MMP9, MMP2, MMP12 and MMP7, and indirect production of MMP13 and MMP3 by inducing myofibroblasts. MMPs are essential in remodelling extracellular matrix and promoting the resolution of fibrosis[11].

M2 macrophages are typically termed alternatively activated AMs and contribute to aberrant wound healing in the fibrotic process by producing profibrotic cytokines and growth factors such as TGFβ, PDGF, FGF 2, insulin-like growth factor-binding protein 5, CCL18 and galectin-3, and by recruiting fibrocytes (M2a). Regulatory macrophages (M2c) can promote resolution of fibrosis through a number of mechanisms including the production of suppressive cytokines such as IL10. M2 macrophages are induced by Type 2 helper T-cells and a number of Type 2 cytokines and mediators including IL-4,

IL-13, IL-10 and TGFβ, as well as apoptotic cells and corticosteroids[11]. M2 macrophages secrete the regulatory cytokines PDGF, IL-10 and TGFβ, the soluble IL-1 receptor antagonist, and increased levels of CCL18 and CCL22[15]. M2 AMs express anti-inflammatory cytokines and tissue inhibitors of MMPs (TIMPs) that impair remodelling of ECM. M2 AMs express the mannose receptor CD206, type 1 scavenger receptor, and CD163. They inhibit the M1-driven inflammatory process by expression of high levels of arginase-1, which competes with iNOS for L-arginine. Arginase-1 metabolism of L-arginine can lead to the formation of L-proline, which in turn can be used by myofibroblasts to produce collagen[11]. In addition, arginase produced by these cells promotes the production of hydroxyproline, enabling fibroblasts to increase collagen synthesis.

Numerous studies have reported that macrophage activation is dynamic and that they have the ability to adapt to the local environment and are capable of switching from one functional phenotype to another[14]. It has also been reported that pulmonary macrophages may co-express markers of M1/M2 activation, which together suggest AMs are highly pliable and that activation states may represent a transient spectrum rather than terminally differentiated polarisation subtypes, and it may be related to specific stimuli or disease microenvironment. The plasticity of these M1/M2 phenotypes may explain some of the biological heterogeneity seen in ILD[13].

AMs also produce soluble mediators that stimulate local and recruited tissue fibroblasts to differentiate into myofibroblasts that facilitate wound contraction and closure, as well as the synthesis of ECM components[10]. In normal wound healing, the accumulation and activation of fibroblasts transforms cellular granulation tissue into a more permanent scar tissue that is composed of collagen. Fibroblasts quickly move into the provisional matrix and are crucial to fibrogenesis. They proliferate rapidly in response to injury and are a principle source of ECM proteins including collagens and fibronectin. A number of proangiogenic growth factors including TGFβ1, FGF2, angiopoietin, PDGF and VEGF are also released at the site of injury as providing an adequate blood supply to the newly formed granulation tissue is an important part of wound healing. These factors contribute to revascularisation by promoting the formation of new capillaries and stimulating proliferation of endothelial cells. Fibroblasts typically differentiate into myofibroblasts during both normal wound healing and pathological fibrosis in response

to a number of mediators released following epithelial injury, activation of coagulation proteases and innate immune system activation[12]. Myofibroblasts are the main ECM-producing cells in the body and are identified by their acquisition of contractile features of smooth muscle cells, such as the expression of α-smooth muscle actin[12]. In addition to the production of the ECM, myofibroblasts are also able to remodel the ECM by secreting MMPS and TIMPs. In normal physiological conditions, myofibroblasts are then lost via apoptosis when lung tissue structure and function have been restored.

At this point in the pathway, macrophages and monocytes display a mostly anti-inflammatory phenotype. These macrophages respond to IL-10 and other inhibitory mediators, secrete a variety of anti-inflammatory mediators (such as IL-10 and TGFβ1) and express cell-surface receptors (such as programmed cell death ligands 1 and 2) that play important roles in dampening down the immune system and reducing inflammation. Disturbances at any stage of this process can lead to aberrant repair, by either uncontrolled release of inflammatory mediators and growth factors, or inadequate production of inhibitory macrophages, both contributing to the development of chronic wounds and failure of apoptosis, which then leads to pathological fibrosis[10].

1.5 Diagnosing IPF

In 2011, the American Thoracic Society (ATS), European Respiratory Society (ERS), Japanese Respiratory Society (JRS) and the Latin-American Thoracic Society (ALAT) published an international evidence-based guideline on the diagnosis and management of IPF. This guideline was revised in 2013. The consensus statement recommended that for a diagnosis of IPF, known causes of ILD such as domestic or occupational environmental exposures, connective tissue disease and drug toxicity must first be excluded. IPF could be diagnosed definitively in patients with an Usual Interstitial Pneumonia (UIP) pattern on high resolution CT scanning (HRCT), comprising reticular abnormalities, subpleural and basal disease predominance, honeycombing with or without traction bronchiectasis and an absence of features listed as 'inconsistent with UIP' pattern. In patients without honeycombing, a diagnosis of 'possible IPF' is made. The guideline is clear that if honeycombing is absent on HRCT then the diagnosis is regarded as 'possible IPF' and further investigation by means of surgical lung biopsy

(SLB) is required[16]. The histopathologic criteria for IPF are also described as UIP pattern, and include temporally heterogeneous areas of fibrosis and subepithelial fibroblastic foci. The diagnosis of IPF requires an integrated multidisciplinary approach involving ILD specialist respiratory physicians, radiologists and pathologists. The HRCT and histological features of a UIP pattern are presented in Tables 1 and 2. Recommendations for a diagnosis of IPF based on HRCT and SLB findings are described in Table 3.

Table 1. HRCT criteria for UIP Pattern.

UIP Pattern (All four features)
• Subpleural, basal predominance
• Reticular abnormality
• Honeycombing with or without traction bronchiectasis
• Absence of features listed as inconsistent with UIP
Possible UIP Pattern (All three features)
• Subpleural, basal predominance
• Reticular abnormality
• Absence of features listed as inconsistent with UIP
Inconsistent with UIP Pattern (Any of the seven features)
• Upper or mid-lung predominance
• Peribronchovascular predominance
• Extensive ground glass abnormality (greater than reticular abnormality)
• Profuse micronodules (bilateral, predominantly upper lobes)
• Discrete cysts (multiple, bilateral, away from areas of honeycombing)
• Diffuse mosaic attenuation/air-trapping (bilateral in three or more lobes)
• Consolidation in bronchopulmonary segment(s)/ lobe(s)

Adapted from reference 1

Table 2. Histopathological criteria for UIP Pattern.

UIP Pattern (All four features)
• Marked fibrosis/ architectural distortion, with or without honeycombing in a predominantly subleural/ paraseptal distribution
• Patchy involvement of lung
• Fibroblastic foci
• Absence of features against a diagnosis of UIP suggesting an alternative diagnosis
Probable UIP Pattern
• Marked fibrosis/ architectural distortion, with or without honeycombing
• Absence of either patchy involvement or fibroblastic foci, but not both
• Absence of features against a diagnosis of UIP suggesting an alternative diagnosis OR honeycomb changes only

Possible UIP Pattern (All three criteria)
• Patchy or diffuse involvement of lung parenchyma by fibrosis, with or without interstitial inflammation
• Absence of other criteria for UIP
• Absence of features against a diagnosis of UIP suggesting an alternative diagnosis
Not UIP Pattern (Any of the six)
• Hyaline membranes
• Organising pneumonia
• Granulomas
• Marked interstitial inflammatory cell infiltrate away from honeycombing
• Predominant airway- centred changes
• Other features suggestive of an alternative diagnosis

Adapted from reference 1

Table 3. Diagnostic recommendations for diagnosing IPF.

HRCT Pattern	**Surgical Lung biopsy Pattern**	**Diagnosis**
UIP	UIP or probable UIP or possible UIP or non-classifiable fibrosis	IPF
	Not UIP	Not IPF
Possible UIP	UIP or probable UIP	IPF
	Possible UIP or non-classifiable fibrosis	Probable IPF
	Not UIP	Not IPF
Inconsistent with UIP	UIP	Possible IPF
	Probable UIP or possible UIP or non-classifiable fibrosis or not UIP	Not IPF

Adapted from reference 1

The diagnostic algorithm does not allow for circumstances in which surgical lung biopsy is not performed. In our practice at the Edinburgh Lung Fibrosis Clinic, we categorise non-biopsied patients in whom clinical and HRCT appearances are 'consistent with UIP' as having a 'working diagnosis IPF'. These patients make up around 50% of our IPF population, but their natural history is not defined, their treatment options are not specifically addressed in any guideline and they are mostly ineligible for large clinical trials which usually require a diagnosis of 'definite IPF'. In the UK, SLB rates have been low, a reflection perhaps of the perceived risks of the procedure. Across all of the ILDs the 30-day mortality and morbidity is 2-4% and 10-18% respectively[3]. However the actual risk in the suspected IPF cohort, who are mostly aged over 65 years is not known. A recent single-centre retrospective study by Fell et

al showed that in biopsied patients aged over 70 years with 'fibrotic' appearances on HRCT, 95% had UIP confirmed at biopsy, implying that advanced age is a strong predictor for IPF[17]. This important observation, if replicated in an independent cohort, would impact on international guidelines. It is currently unclear whether these patients with 'possible IPF' should be treated with approved IPF therapies.

1.6 The management of IPF and recent clinical trials

Over the last ten years, there have been significant advances in our understanding of the pathogenesis of IPF. The most recent clinical trials have moved away from investigating anti-inflammatory compounds and focused more on targets involved in the wound healing cascade and fibrogenesis[18]. Despite this, results from trials have been largely disappointing, perhaps due to the large numbers of mediators, growth factors and signalling pathways involved in the pathogenesis of IPF[19].

The current ATS/ERS/JRS/ALAT guideline on the management of IPF does not recommend any treatments as a "strong yes", however a small number received a "conditional recommendation for use" and several "strong recommendation against use". This guideline is evidence-based and utilises the GRADE (Grades of Recommendations, Assessment, Development, and Evaluation) methodology to assess the quality of data[20].

N-acetylcysteine

N-acetylcysteine (NAC) is a precursor of the endogenous antioxidant glutathione (GSH) and has been investigated for use in IPF based on the assumption that an oxidant-antioxidant imbalance plays a role in the pathogenesis[19,20]. The IPFnet-sponsored PANTHER (Prednisolone, Azathioprine, and N-acetylcysteine: A Study That Evaluates Response in IPF) trial was a multicentre, randomised, double-blind, placebo-controlled trial designed to compare three therapeutic interventions. Patient eligibility criteria included; aged 35 to 85 years, FVC ≥ 50% of predicted, DLCO ≥ 30% of predicted, ability to understand and provide informed consent, diagnosis of IPF according to a

modified version of the ATS/ERS/JRS/ALAT criteria ≤ 48 months from enrollment. Patients were assigned in a 1:1:1 ratio to triple therapy, NAC (600mg three times daily), prednisolone (0.5mg/kg tapered to 0.15mg/kg over 25 weeks) and azathioprine (1-2mg/kg daily), NAC monotherapy (600mg three times daily) or placebo. A total of 77 patients were enrolled in the triple-therapy arm, 81 in the NAC monotherapy arm and 78 patients in the placebo arm. The primary outcome was the change in FVC over a 60-week period, with secondary outcomes including mortality, frequency of acute exacerbations, time to disease progression, and measures of clinical and physiological parameters[21]. A preplanned interim analysis at approximately 50% of data collection revealed that the triple therapy group, as compared with placebo, had a significantly increased number of deaths (8% vs 1%, P=0.01), hospitalisations (30% vs 9%, P<0.001) and serious adverse events (31% vs 10%, P=0.001). Consequently, the three-drug regimen arm was terminated and PANTHER was continued as a double-blind, two-group study (NAC monotherapy vs placebo)[21].

As a result of the increased risk of death and hospitalisation observed in the group of IPF patients in the combination triple therapy arm, the PANTHER trials concluded that there was compelling evidence against the use of prednisolone, azathioprine and NAC in triple combination therapy for patients with mild to moderate IPF. Following the remainder of the trial as a double blind, two group study (NAC versus placebo), it was concluded that NAC offered no significant benefit in the preservation of FVC in patients with IPF and mild to moderate lung function impairment.

Pirfenidone

Pirfenidone is an orally administered agent thought to exert anti-fibrotic, anti-inflammatory and antioxidant properties through downregulation or profibrotic growth factors, although its mechanism of action is not fully understood[19]. The CAPACITY (Clinical Studies Assessing Pirfenidone in Idiopathic Pulmonary Fibrosis: Research of Efficacy and Safety Outcomes) programme consisted of two multinational, randomised, double-blind, placebo-controlled trials (004 and 006). Eligible patients were aged 40–80 years with a diagnosis of IPF in the previous 48 months, predicted FVC was ≥50%, predicted carbon monoxide diffusing capacity (DLco) was ≥35%, either predicted FVC or predicted DLco of 90% or less, and 6-min walk test (6MWT) distance of ≥150 m. Patients younger than 50 years and those not meeting HRCT criteria for definite IPF

were required to have a lung biopsy sample showing usual interstitial pneumonia[22]. In study 004, 435 patients were assigned in a 2:1:2 dosing ratio to pirfenidone 2403mg daily, pirfenidone 1197mg daily, or placebo, study 006 enrolled 344 patients to a 1:1 ratio of pirfenidone 2403mg daily or placebo. The primary endpoint of both trials was change in percentage predicted FVC from baseline to week 72. Secondary endpoints included progression-free survival, worsening idiopathic pulmonary fibrosis, dyspnoea, 6MWT distance, percentage predicted DLco, and fibrosis on HRCT (study 006 only). The primary endpoint of change in percentage predicted FVC was met in study 004 (mean FVC change at week 72 was -8.0% in the pirfenidone 2403mg daily group and -12.4% in the placebo group, P=0.001), however this result was not replicated in study 006. Despite the differing results between the two trials, pooled analysis for pirfenidone 2403mg daily compared with placebo favoured pirfenidone (-8.5% vs 11.0%, P=0.005)[22,23].

The ASCEND (Assessment of Pirfenidone to Confirm Efficacy and Safety in Idiopathic Pulmonary Fibrosis) trial was conducted after the US Food and Drug Administration (FDA) denied approval and requested an additional phase 3, randomised, double-blind, placebo-controlled study to provide supportive evidence of efficacy of pirfenidone[19]. Eligibility criteria included patient aged between 40 and 80 years, a centrally confirmed diagnosis of idiopathic pulmonary fibrosis based on ATS/ERS/JRS/ALAT criteria, FVC between 50-90% of predicted, DLCO between 30-90% of predicted, a ratio of the forced expiratory volume in 1 second (FEV_1) to the FVC of ≥ 0.80, and a 6-minute walk distance of $\geq$150 m. Patients were randomised to either pirfenidone 801mg three times per day (n=278) or placebo (n=277). The primary end point was the change from baseline to week 52 in the percentage predicted FVC. The two key secondary endpoints were the change from baseline to week 52 in the 6-minute walk distance and progression-free survival. The study met its primary outcome of change in percentage predicted FVC from baseline to week 52 (-164ml in the pirfenidone group vs -280ml in the placebo group; absolute difference 116ml, relative difference 41.5%; P<0.0001)[19,24]. In addition, the proportion of patients with an absolute decline in percentage predicted FVC of >10% or death was significantly reduced in the pirfenidone group (16.5% vs 31.8%, P<0.001) and the proportion of patients with no decline was increased (22.7% vs 9.7%, P<0.001)[23,24]. Pirfenidone was approved by the European Medicines Agency for treatment of IPF in 2011, and by the US FDA in

October 2014[19]. The current ATS/ERS/JRS/ALAT clinical practice guideline for treatment of IPF advises a conditional recommendation for the use of Pirfenidone in patients with IPF.

Nintedanib

Nintedanib is a potent inhibitor of several tyrosine kinases including vascular endothelial growth factor (VEGF), platelet-derived growth factor (PDGF) and fibroblast growth factor (FGF), which are all thought to mediate a number of processes in the pathogenesis of IPF. The INPULSIS 1 and INPULSIS 2 trials were two identical, multinational, randomised, double blind, placebo-controlled trials to investigate the efficacy of nintedanib over 52 weeks. Eligibility criteria included aged ≥40 years, a diagnosis of IPF within the previous five years, FVC >50% predicted, DLCO 30%-79% predicted and an HRCT within the previous year. Patients with 'possible UIP' HRCT appearances were included in the studies, even in the absence of a confirmatory surgical lung biopsy. Patients were randomised in a 3:2 ratio to receive either nintedanib 150mg twice daily (n=638) or placebo (n=423). The primary endpoint was the annual rate of FVC decline and secondary outcomes included time to first exacerbation, quality of life, all-cause mortality and adverse effects[23]. Both trials met their primary endpoint with the nintedanib group reporting a lower rate of FVC decline compared with placebo (-114.7ml vs -239.9 ml, P<0.001 in INPULSIS 1 and -113.6ml vs -207.3ml, P<0.001 in INPULSIS 2)[23,25]. Nintedanib has recently been approved for the treatment of IPF in both Europe and the USA and received a conditional recommendation for use in IPF in the ATS/ERS/JRS/ALAT official clinical practice guideline for the treatment of IPF.

The natural history of IPF patients is mostly depicted from patients enrolled in large, multicentre clinical trials. Typically these studies only included a highly selected group of patients, with the majority of patients excluded due to age, disease severity or comorbid conditions. Patients in trials had relatively preserved lung function with a mean FVC of 60% and an absence of comorbid conditions, which contribute to its poor prognosis, such as pulmonary hypertension and coronary artery disease[18,23]. Follow-up was also relatively short at 2 years or less[26]. With the exception of the INPULSIS trials, most studies also only included patients with IPF defined by 'definite UIP' HRCT appearances, or a 'possible UIP' HRCT and a confirmatory UIP surgical lung biopsy. In real-life clinical practice, only a minority of patients would be eligible for these trials.

We aimed to describe the natural history of patients with IPF phenotyped according to PANTHER, CAPACITY, ASCEND and INPULSIS eligibility criteria. We hypothesised that the outcome of eligible versus ineligible patients would be different. We also aimed to determine the longterm IPF outcomes in a well-categorised, all-inclusive, real-life IPF patient cohort.

1.7 Predicting disease progression in IPF

Patients with fibrotic lung disease are typically risk stratified using a combination of clinical variables including history and examination findings, pulmonary function testing, exercise capacity, radiological appearances and histological features, however these variables are poorly reflective of disease pathogenesis and are only useful when put into scoring systems for grouping patients into large cohorts and not clinical useful in estimating individual patient risk. IPF is a heterogeneous disease and there is a need to identify 'personalised' prognostic biomarkers which may in turn lead to novel targets and the advent of personalised medicines.

Older age is a clinical feature of IPF and older age has been shown bear a poorer prognosis in a number of studies[6,7]. However Nadrous et al reported younger patients with IPF (aged <50 years) had similar mortality rates and the same poor prognosis as older patients[27]. IPF is also more common in men[7]. Data describing patient sex as a prognostic factor in IPF have been variable, however most suggest that male sex holds a poorer prognosis. Female sex has been shown to confer a significant survival benefit after adjusting for age, smoking history, TLCO and maximum desaturation area[6,28]. Reports on smoking status are largely consistent with smoking shown to increase mortality in IPF patients. A small number of studies report decreased mortality in smokers, however this is thought to relate to the 'healthy smoker' theory, a subgroup that may be over-represented in an IPF population which presents in older patients[7]. Survival in IPF has been described as being significantly associated with patient Body Mass Index (BMI). Increased BMI has been found to be protective with a Hazard Ratio of 0.93 per 1-unit increase in BMI[7,29]. Baseline and change in 6 minute walk distance (6MWD) have also been reported as being predictive of mortality[6]. A baseline 6MWD of <250m and a 24-week decline of >50m are both independent predictors of mortality[4].

There are also a number of comorbidities in IPF that are reported to significantly reduce survival, these include pulmonary arterial hypertension, significant emphysema, significant coronary artery disease and bronchogenic carcinoma[7]. Studies describing the association of baseline pulmonary function tests and survival have yielded variable results. However the clinical variables that are most commonly associated with prognosis are FVC, TLC and TLCO. Change in PFT values over time has been shown to be more predictive of prognosis and have improved clinical prediction models. A significant (>10%) or marginal (>5-10%) decline in FVC over 6 or 12 months is highly predictive of mortality[6]. A reduced TLCO is also associated with a poorer prognosis. Numerous studies have concluded that changes in FVC and TLCO over 6-12 months were more predictive of prognosis over time than most baseline characteristics including histopathologic diagnosis[7,30,31]. As mentioned previously, HRCT scanning is pivotal in diagnosing IPF in most patients, and a number of studies have investigated whether HRCT appearances at baseline can accurately predict clinical outcomes. A number of parenchymal abnormalities can be assessed including extent of disease, ground glass, consolidation, reticulation, honeycombing and traction bronchiectasis. Reticulation and honeycombing are often combined to give an extent of fibrosis score. A UIP pattern on HRCT is associated with the poorest survival[7,32]. The extent of fibrosis and honeycombing on HRCT have also been shown to predict mortality and correlate with %predicted FVC and TLCO[6,33–35]. The presence of traction bronchiectasis on HRCT has also been described as an independent predictor of mortality[4,33].

Several prognostic scoring systems, based on different combinations of clinical, physiological, radiological and serological parameters, have been described to stage and predict survival in IPF[4]. However at present there is no single risk model that has been validated, widely accepted and adopted in clinical practice. King et al proposed the Clinical-Radiological-Physiological (CRP) scoring system used to predict survival in 238 patients with IPF. A number of clinical variables were included in the model; age, smoking status, finger clubbing, degree of fibrosis and pulmonary hypertension, chest radiography, total lung capacity and partial pressure of arterial oxygen at maximal exercise[36]. The model was deemed too complicated for use in clinical practice as many of the variables were not routinely measured. Wells et al described the Composite Physiologic Index (CPI). They reported that a combination of FVC, FEV_1 and TLCO values correlated with the extent of fibrosis on HRCT[37]. Ley and colleagues proposed

the GAP Index as a prognostic staging system in IPF developed using data from three large distinct patient cohorts (N=558). Four baseline clinical variables (gender, age, FVC and TLCO) are included in the model. Patients are given a GAP Index score and categorised into three severity groups with 1-year mortality risks of 6%, 16% and 39% respectively. The same group also reported a longitudinal GAP model that included the relative change in %predicted FVC over a 24 week period, and the number of respiratory hospitalisations. This improved the risk stratification significantly[38,39]. Du Bois et al devised a scoring system capable of independently predicting mortality using data from two clinical trials (N=1099). Age, respiratory hospitalisations, %predicted FVC and change in %predicted FVC over a 24 week period well all incorporated into the model. The 1-year mortality predicted by the model was consistent with the observed data. The same group then added 6MWD and 24 week change in 6MWD which improved the ability of the model to predict 1-year survival[40,41]. Mura and colleagues described a risk model predicting survival and disease progression in a prospective cohort of 70 IPF patients. The Risk Stratification Score (ROSE) comprised a number of clinical variables including a Medical Research Council dyspnoea score (MRCDs) of >3, a 6MWD of <72% predicted and a Composite Physiologic Index (CPI) of >41 at diagnosis, and significantly predicted 3-year mortality with 100% specificity. The results of this study were also confirmed in an independent retrospective cohort of 68 patients[42]. Kinder et al added serum levels of SP-A and SP-D to clinical variables and improved their prediction model of 1-year mortality in IPF[43]. Song et al reported a predictive model of survival in IPF combining clinical and serological variables. They included serum MMP7, SP-A and KL-6 levels, %predicted FVC and TLCO, age and change in FVC at 6 months in the model and found that adding biomarker data improved predictive accuracy compared to clinical variables alone[44]. Finally, Richards and colleagues described a model using physiological and biomarker variables to predict survival in 140 IPF patients. They analysed serum concentrations of 95 cytokines, chemokines, matrix metalloproteinases (MMPs) and markers of apoptosis and epithelial injury and added this to clinical variables including gender, %predicted FVC and %predicted TLCO. They identified five markers (MMP7, intracellular adhesion molecule 1, IL8, vascular cell adhesion molecule 1 and S100A12) that were predictive of patient outcome regardless of age, sex and baseline PFTs. This was then validated in a second cohort of 101 patients[45]. As previously described, several prognostic scoring

systems, based on clinical, physiological, radiological and serological parameters, have been reported to predict survival in IPF[2]. These studies are summarised in Table 4.

Table 4. Proposed predictive scoring systems in IPF.

Scoring system	Patients	Variables	Outcome	Reference
Clinical-Radiological-Physiological (CRP) scoring system	238 IPF	Age, smoking status, finger clubbing, profusion of fibrosis and pulmonary hypertension, chest radiography, total lung capacity, partial pressure of arterial oxygen at maximal exercise	Model deemed too complicated for use in clinical practice as many of the variables were not routinely measured	King et al[6,36]
Composite Physiologic Index	212 IPF	FVC, FEV1, TLCO	A combination of FVC, FEV_1 and TLCO values correlated with the extent of fibrosis on HRCT	Wells et al[6,37]
GAP Index	558 IPF	Gender, age, FVC, TLCO	GAP Index score used to categorise patients into three severity groups with 1-year mortality risks of 6%, 16% and 39% respectively	Ley et al[6,38,39]
Du Bois score	1099 IPF from 2 clinical trials	Age, respiratory hospitalisations, %predicted FVC, change in %predicted FVC over a 24 week period	The 1-year mortality predicted by the model was consistent with the observed trial data	Du Bois et al[6,40,41]
The Risk Stratification Score (ROSE)	70 IPF	Medical Research Council dyspnoea score (MRCDs) of >3, a 6MWD of <72% predicted,a Composite	Significantly predicted 3-year mortality with 100% specificity	Mura et al[42]

		Physiologic Index (CPI) of >41 at diagnosis		
Prediction model of survival in IPF	82 IPF	Age, smoking status, FVC, TLCO, alveolar-arterial oxygen gradient, BAL fluid neutrophil%, serum SP-A, serum SP-D	Adding serum SP-A and SP-D levels improved prediction model of 1-year mortality	Kinder et al[43,46]
Prediction model of survival in IPF	118 IPF	Serum MMP7, SP-A and KL-6 levels, %predicted FVC and TLCO, age and change in FVC at 6 months	Adding biomarker data improved predictive accuracy compared to clinical variables alone	Song et al[44,46]
Prediction model of survival in IPF	140 IPF	Serum concentrations of 95 cytokines, chemokines, matrix metalloproteinases (MMPs) and markers of apoptosis and epithelial injury added to clinical variables including gender, %predicted FVC and %predicted TLCO	Five markers (MMP7, intracellular adhesion molecule 1, IL8, vascular cell adhesion molecule 1 and S100A12) were predictive of patient outcome regardless of age, sex and baseline PFTs	Richards et al[45]

An important caveat of all of the above scoring systems is that they were all derived from either patients recruited to clinical trials or patients referred to tertiary referral centres, which undoubtedly leads to bias. There are very few studies of large numbers of IPF patients directly referred from the community and followed longitudinally. At present there is no single risk model that has been validated, widely accepted and adopted in clinical practice.

In summary, the clinical variables available to predict the risk of mortality and disease progression in IPF are currently inadequate. Additional non-invasive and reproducible

markers are required to improve existing risk model templates. In recent years large numbers of BAL and peripheral blood proteins and cytokines have been studied as potential biomarkers of disease progression in IPF. Biomarkers may have many different applications including predisposition to disease, diagnostic, prognostic, prediction of response to treatment and acting as a surrogate endpoint in clinical trials, however their main function is to meet an unmet clinical need. Good biomarkers should have high sensitivity/specificity, be cost effective, non-invasive, easily reproducible and widely available[46].

1.8 Investigating current and novel biomarkers in IPF

In order for a molecular biomarker to seem plausible, it would ideally reflect the pathobiological mechanism driving disease progression in IPF. Our understanding of the pathogenesis of IPF is mostly extrapolated from histological appearances in subgroups of biopsied patients. It is logical to propose that macrophages play a central role in IPF. Macrophages are integral to lung tissue repair and homeostasis, however in UIP it has been proposed that the process of normal tissue homeostasis and healing is aberrant. Many contributing mechanisms have been reported including angiogenesis, coagulation, fibrogenesis, tissue repair, inflammation, epithelial damage, matrix remodelling and oxidative stress[47]. The most notable paradigm is one in which the alveolar epithelium is repeatedly injured creating localised 'wounds' over a prolonged period of time, which leads to focal epithelial hyperplasia and activation. The dysfunctional epithelial cells then activate profibrotic signalling pathways involving growth factors and chemokines such as TGF-β1[48]. This leads to the accumulation of fibroblasts in 'fibroblastic foci', areas of intense collagen generation, and differentiation of myofibroblasts, resulting in increased extracellular matrix (ECM) deposition[48].

Despite evidence that inflammation may not play a predominant role in IPF, there is evidence that markers of inflammation and immunity may provide useful information. Brittan et al reported the presence of novel subpopulations of pulmonary monocyte-like cells (PMLC) in the human lung; resident PMLC (rPMLC, HLA-DR+CD14++CD16+ cells) and inducible PMLC (iPMLC, HLA-DR+CD14++CD16- cells)[49] . Their data

showed that PMLC represented a significant proportion of cells present in BAL fluid following inhalation of lipopolysaccharide (LPS), implying PMLC may play a significant role in the inflammatory response. Resident PMLC were found to have a significantly increased expression of the mature macrophage markers CD206 (mannose receptor), CD71 (transferrin receptor) and 25 F9, and a significantly increased expression of the proliferation antigen Ki67, compared to iPMLC[50]. There is also evidence to suggest autoimmunity and abnormalities in B and T cells may play a role in the progression of IPF[46]. C-X-C motif chemokines (CXCL)-13, a chemokine involved in B-cell trafficking, has been shown to be elevated in both lung tissue and peripheral blood of IPF patients compared to healthy controls and COPD patients, and was found to be predictive of early mortality[46,51]. Gilani et al described that CD28, a marker of effector memory T cells on circulating CD4 T cells, is downregulated in IPF, furthermore this was associated with a decline in lung function and survival in a cohort of 89 IPF patients[46,52]. Heat shock protein (HSP) 70 has been shown to induce CD4 T cells from IPF patients[46]. This leads to proliferation and production of profibrotic cytokines (IL4) and anti-HSP70 antibody production, which in turn leads to monocyte activation and IL8 production[46]. In a small, single-centre study, IgG autoantibodies to HSP70 was associated with disease progression and reduced 1-year survival in IPF patients[53,54]. Regulatory T cells (Tregs) are an important component of the adaptive immune response. It has also been reported that there is a significant impairment of Treg suppressor function in IPF, which is evident in BALF and the peripheral blood. This correlates well with clinical markers of disease progression. It has been proposed that the reduced numbers and Treg dysfunction found in IPF patients may contribute to inefficient control of the pre-existing overactive Th2 response, or contribute to a Th2 skew[5,55]. Schematic representation of previously described potential biomarkers in IPF and proposed relationship to the possible pathogenesis is shown in Figure 1[48].

Figure 1. Schematic representation of previously described potential biomarkers in IPF and proposed relationship to the possible pathogenesis.

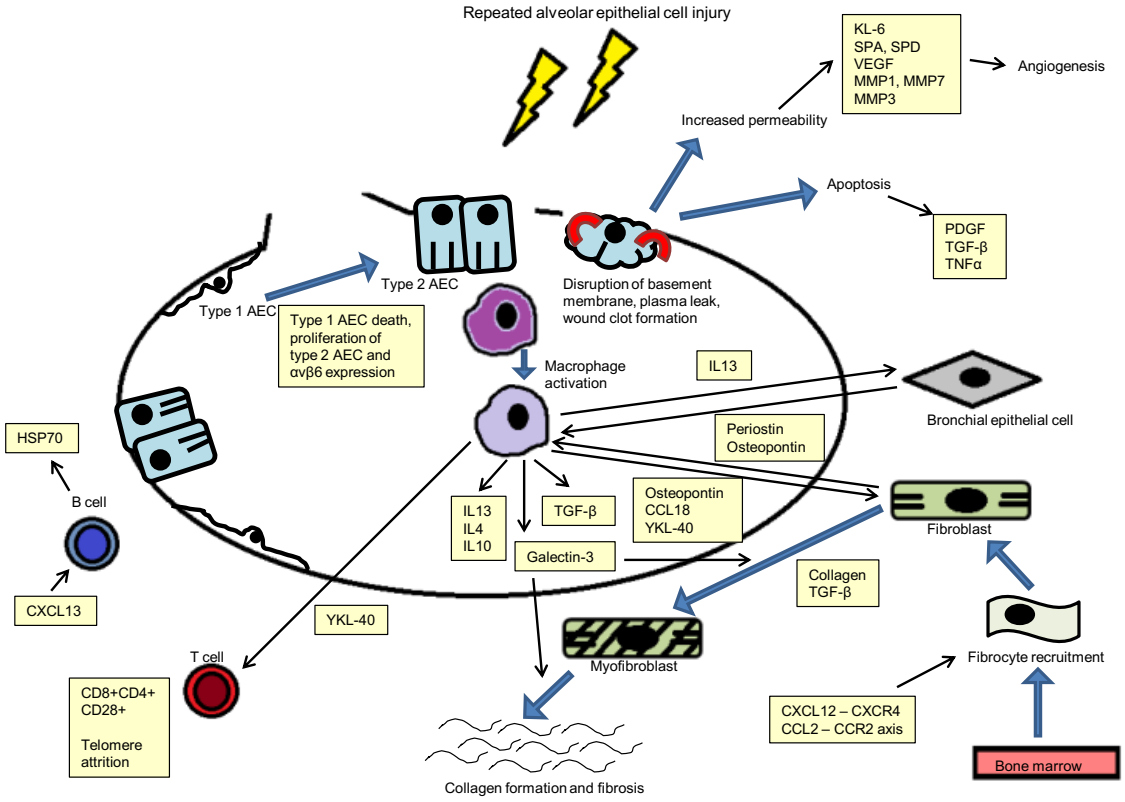

Adapted from reference 48

As mentioned, IPF has been classified as a Th2-skewed disorder, with the presence of an 'M2' polarised lung macrophage phenotype. Mediators associated with M2 macrophage polarisation are associated with disease progression and severity[56]. However, a comprehensive classification of the M2 phenotype is questionable, and there is some recognition that a distinct M2 'pro-repair' phenotype may exist and that macrophage phenotypes are dynamic and liable to change as disease evolves[57]. Perhaps one of the most promising potential biomarkers in IPF is CC-chemokine (CCL)-18, as reported by Prasse and colleagues. CCL18 is produced by alveolar macrophages and regulated by Th2 cytokines. It plays an important role in inflammatory cell migration and is involved in stimulating collagen production and the differentiation of fibroblasts. Prasse at al prospectively measured serum CCL18 levels in 72 IPF patients, and found it was a strong and independent predictor of mortality[7,58]. Serial CCL18 measurements correlated well with pulmonary function and baseline serum levels were highly

predictive of subsequent disease progression. Serum levels of >150ng/ml were independently associated with death (HR 7.98, 95%CI 2.49-25.51, P=0.005)[48,58]. Surfactant proteins (SP) A and D have also been extensively studied as potential biomarkers in IPF. SP-A and SP-D are secreted by alveolar type II pneumocytes and are present in peripheral blood following the breakdown of the epithelium. Significantly elevated serum levels of both SP-A and SP-D have been reported in IPF patients versus healthy controls, and increased serum levels in IPF have been described as being independent predictors of mortality[7,43,59]. Serum Krebs Von Den Lungen (KL-6) is a mucin-like glycoprotein expressed by alveolar type II cells and bronchiolar cells in response to epithelial damage[48]. KL-6 levels are reported to be significantly elevated in IPF and have also been linked to survival, however specificity for IPF is poor[48]. Matrix metalloproteinases (MMPs) are a family of zinc-dependant enzymes involved in the breakdown of the extracellular matrix, they share a wealth of potential pro-inflammatory and pro-fibrotic properties. Rosas et al demonstrated serum MMP1 and MMP7 levels were significantly increased in a cohort of 74 IPF patients compared to hypersensitivity pneumonitis, sarcoidosis and COPD[48,60]. MMP7 appears to be associated mechanistically with lung fibrosis as MMP7 knockout mice are relatively protected from fibrosis[61]. MMP7 expression is upregulated in BALF and lung tissue in many of the ILDs, which may hinder it's use as a diagnostic biomarker in IPF[46]. However serum MMP7 levels are strongly associated with mortality in IPF, independent of disease severity[46], and levels negatively correlate with FVC and DLCO[60]. Galectin-3 is a member of the lectin family of carbohydrate-binding proteins and it is implicated in a number of cellular processes including macrophage activation, chemoattraction, cell growth, differentiation and apoptosis. Galectin-3 binds to itself and to TGFβ receptors, forming lattices that hold the receptors at the cell surface thus altering TGFβ signal transduction. Galectin-3 inhibition has been shown to modify macrophage phenotype, inhibiting the polarisation to M2 cells and reduce tissue scarring in animal models of lung, kidney and cardiac fibrosis[62–64]. Organ fibrosis occurs due to the activation of macrophages and the recruitment and activation of myofibroblasts, galectin-3 drives both of these pathways. TGFβ has been shown to play a key role in pulmonary fibrosis by inducing EMT, ECM production and apoptosis of AECs. It has also been shown that pulmonary fibrosis can be reduced by inhibiting TGFβ activity[143]. TD139 is a specific inhibitor of the galactoside binding pocket of galectin-3. It was developed by a team of scientists from Lund University, Sweden, and

Edinburgh University, UK, and is formulated for inhalation, which enables direct targeting the fibrotic tissue in the lungs, while minimizing systemic exposure. Dr Alison MacKinnon (a senior scientist and principal investigator in my laboratory group) demonstrated previously that TD139 blocked TGF-β-induced β-catenin activation in vitro and in vivo and attenuated the late-stage progression of lung fibrosis after bleomycin. In addition, they found that patients with stable IPF had elevated levels of galectin-3 in BAL fluid and in serum when compared with patients with NSIP and controls. They also found that galectin-3 levels rose sharply during an acute exacerbation of IPF, and therefore suggested that galectin-3 may be a marker of active fibrosis in IPF[62,143]. Following on from these findings, a phase IIa, randomised, double-blind, multicenter, placebo-controlled trial was designed to assess the safety, tolerability, PK and PD characteristics of TD139 in 24 IPF patients. The study was designed and funded by Galecto. When I joined the lab group, I was recruited as a Co-Investigator on this trial. My main aim was to perform flow cytometry and Luminex Magnestic Screening Assays on BAL and plasma samples to assess whether there were any notable differences in a number of proteins of interest linked to IPF-pathogenesis, after patients were treated with an inhaled galectin-3 inhibitor for a two week period. Inhibition of galectin-3 may have the potential to reduce pulmonary fibrosis in man, and a further phase IIb study is currently in development.

There are also a number of neutrophil-related proteins described as being elevated in IPF in the literature. IL8, a member of the CXC chemokine family, and S100A12, a calcium-binding protein, are both pro-inflammatory markers involved in neutrophil recruitment and activation, with IL8 also playing a role in angiogenesis[47]. Both IL8 and S100A12 are reported as being significantly upregulated in IPF patients versus healthy controls, and also correlate negatively with FVC and TLCO values[47]. IL8 has been shown to be increased in both BALf and plasma of IPF patients and is associated with significantly worse outcomes[61]. Vascular endothelial growth factor (VEGF) is a glycoprotein expressed in AEC, it promotes vascular permeability and regulates angiogenesis[48]. BAL VEGF levels are reported as significantly reduced in IPF patients versus controls, however serum levels are significantly increased in IPF. Elevated serum VEGF levels have been described as being associated with poorer gas exchange, and for levels higher than the cohort median, shorter survival time[48]. Periostin is an extracellular matrix (ECM) protein that promotes ECM deposition, mesenchymal cell

proliferation and parenchymal fibrosis. It is secreted by bronchial cells in response to IL13. Serum periostin levels are increased in IPF and appear to correlate with disease progression[48]. Periostin may have a role in the pathological mechanism in IPF as it has been shown to be upregulated after bleomycin-induced lung injury in mice, and periostin-null mice appear protected from developing fibrosis[48]. Osteopontin is a phosphorylated glycoprotein involved in the tissue repair of many organs, it may also play a role in many TGF-β-mediated processes[53]. It induces upregulation of MMP7 in AECs and is reported to be elevated in BALf and serum of IPF patients versus controls, however it is also elevated in many of the other ILDs[48]. YKL-40 is a chitinase-like protein elevated in many inflammatory disorders, and is involved in the regulation of cell proliferation and survival. It is mediated through Th2-lymphocyte/IL13 signalling pathways, however it's role in IPF remains unclear[48]. It is thought to perhaps play a role in the release of fibrotic and inflammatory mediators from alveolar macrophages[48]. Korthagen et al predicted two distinct survival patterns in a cohort of 79 IPF patients using a serum cut off value of 79ng/ml (HR 10.9, 95%CI 1.9-63.8, $P<0.01$)[61,65]. Significantly increased levels have been reported in BALf, serum and lung tissue of IPF patients versus controls, and elevated levels appear to be associated with reduced survival[48,65]. Fibrocytes are bone marrow-derived mesenchymal cells that co-express CD34 or CD45 and extracellular matrix protein type 1 collagen. Some reports indicate they may be capable of producing ECM and differentiating into fibroblasts and myofibroblasts[53]. Elevated levels of circulating fibrocytes have been reported in IPF, and also increased further during episodes of acute exacerbation[7,66]. Levels do not appear to correlate with disease severity but do appear to be an independent predictor of early mortality, with >5% circulating fibrocytes being associated with poorer survival[7,53]. These 'known' candidate biomarkers are summarised in Tables 5 and 6. Whilst several studies have identified circulating mediators that may predict disease progression, they have not been validated in 'real-life' patient cohorts, outside of clinical trials. To date there are no proven biomarkers that predict progression or response to treatment.

Table 5. Summary of 'known' candidate biomarkers in serum.

Mediator	N=(Mean +/- SD) baseline serum concentration unless otherwise stated.	REFERENCE
CCL18	N= 72 IPF (162+/-77 ng/ml) (Range 72-400)	Prasse A et al
MMP7	N=74 IPF, 53 controls <1.99ng/ml No SD available	Rosas et al
	N=24 IPF >4.3ng/ml (survival) >4.4ng/ml (progression-free survival) No SD available	Richards et al
	N=118 IPF (13.7+/-7.6 ng/ml)	Song et al
Periostin	N=37 IPF (107.1 +/-11.9 ng/ml)	Okamoto et al
	N=54 IPF No mean value but 1 SD = 116.97ug/ml, and range is 0.14-403.43ug/ml	Naik et al
Osteopontin	N=17 IPF, 9 sarcoid, 20 controls ROC curve cut off=300-380ng/ml	Kadota J et al
KL-6	N=152 IIP, 67 collagen disease related ILD Mean in IIPs = 943Um/L(range 182-9000) Mean in CTD-ILD= 912Um/L (range 105-6770)	Satoh H et al
CXCL13	N=95 IPF, 128 COPD in plasma (94+/-8 pg/ml)	Vuga et al
SP-A	N=136 IPF (100ng/ml in Denver cohort, 70mg/ml in Iowa cohort)	Greene et al
	N= 82 IPF (106ng/ml +/1 49ng/ml) (range 27-270)	Kinder et al
	N=118 IPF (105.8+/- 72.4ng/ml)	Song et al
SP-D	N=142 (400ng/ml in Denver group and 380ng/ml in Iowa group)	Greene et al
VEGF	N=41 IPF, 43 controls Mean in IPF = 207.4pg/ml (range 10.9-589.5)	Ando et al
YKL-40	N=85 IPF, 83 controls Mean in IPF = 109.4ng/ml (IQR 76.6-237.7)	Korthagen et al

Table 6. Summary of 'known' candidate biomarkers in BAL fluid.

Protein	Number of pts	Result/significance	Reference
RAGE, SP-C, TIMP-1, fibronectin, eotaxin, IL-17A, IL-23, PARC, RANTES, TSLP, PIGF, FGFb, tissue factor	11 IPF 11 HP 10 controls	ANOVA stats not significant	Willems S et al
HGF		Increased (P=0.053)	
IL-8		Increased (P=0.018)	
IL-12p40		Decreased (P=0.072)	
MCP-1		Increased (P=0.0011)	
MDC		Increased (P=0.0044)	
MPO		Increased (P=0.015)	
MMP-8		Increased (P=0.038)	
MMP-9		Increased (P=0.010)	
Active PAI-1		Increased (P=0.0022)	
Protein C		Increased (P=0.045)	
VEGF		Decreased (P=0.0014)	
CCL18, CCL2, IL8, Calgranulin B (S100A9)		Increased	Bargagli E et al
MIF		Increased	
MRP14	54 IPF, 19 controls	Increased(P=<0.001)	Korthagen NM et al
CCL22	19 IPF, 6 controls	Increased(P=<0.001)	Yogo Y et al
CCL17		Increased(P=<0.05)	
IL-13	16 IPF, 8 controls	Increased(P=<0.05)	Park SW et al
IL-4		Increased (P=<0.05)	
M-CSF	24 IPF, 26 controls	Increased (P=0.01)	Baran CP et al
CCL 2		Increased (P=0.001)	
IGF-1	11 IPF, 6 controls	Increased (significant)	Pala L et al
IGFBP-3		Increased (significant)	

1.9 Hypothesis and aims

I hypothesise that a diagnosis of IPF and disease progression can be confidently predicted by a combination of HRCT scoring and serum/BAL biomarker profiling. In addition to an unbiased approach, I hypothesise that there is a relationship between cytokine and mediators specifically associated with alveolar macrophage polarisation and disease progression in IPF. Lastly I hypothesise that Galectin-3 inhibition in patients with IPF will modify alveolar macrophage phenotype and reduce expression of M2-associated cytokines and mediators.

Aim 1. Interrogate the Scottish Interstitial Lung Disease (ScILD) database and integrate this with the Edinburgh ILD database to determine the safety and utility of surgical lung biopsy in patients with suspected IPF.

Aim 2. Investigate the diagnostic and prognostic value of BAL differential cell count in the diagnosis of IPF.

Aim 3. Study potential prognostic biomarkers in the Edinburgh IPF cohort by first measuring a defined panel of protein biomarkers previously described in the literature as being associated with IPF disease progression in serum and BAL, then performing semi-biased and unbiased proteomic arrays to identify additional key protein candidates. I will then perform BAL proteomics on paired BAL samples performed at 0 and 12 months, a unique resource, to identify the protein signature of IPF progressors vs non-progressors.

Aim 4. Determine the relationship between alveolar macrophage subtypes (including PMLCs) and prognosis in IPF.

Aim 5. Perform detailed phenotyping of alveolar macrophages and measure BAL and serum macrophage-related proteins from patients with IPF who have received TD139 (an inhaled Galectin-3 inhibitor) or placebo as part of a Phase 2a clinical trial.

Chapter 2

Materials and Methods

2.1 Patient Selection and the Edinburgh Lung Fibrosis Clinical Database and Biobank

The Edinburgh Lung Fibrosis research database was established in 2002, and was designed to capture the natural history of ILD in patient's referred to the specialist adult ILD clinic. The dataset from 01/01/02-31/12/14 is summarised in Table 7. All subjects were fully consented and ethical approval was obtained for all protocols and procedures (LREC 06/S0703/53). Study cohorts consisted of locally referred, consecutively presenting patients with ILD presenting since 01/01/02. For all patients, diagnosis, investigation, management and follow-up was as per the Edinburgh local policy. This included a detailed clinical history, examination, autoantibody screen, HRCT and pulmonary function testing. Follow-up included 6 monthly PFTs and clinic review, with less than 1% of the study population being lost to follow-up**.** Disease progression was defined as death or ≥10% decline in FVC within 12 months of BAL. All HRCT scans were reviewed by an expert thoracic radiologist and discussed in a multidisciplinary meeting with at least two respiratory physicians with ILD subspecialty expertise. Patient HRCT scans were categorised into 'definite', 'probable' or 'inconsistent with' UIP patterns based on 2011 ATS/ERS criteria. In patients with 'probable UIP' HRCT appearances, surgical lung biopsy was performed after consideration of disease severity, comorbidities and the patient's wishes. Lung histology was reviewed in a multidisciplinary meeting by an experienced pulmonary pathologist, a member of the UK ILD pathology reference panel. In the Edinburgh cohort, 15% of all ILD patients were biopsied and in those with suspected IPF in whom the HRCT was deemed 'probable UIP', 1 in 5 patients underwent SLB. All diagnoses of definite and probable IPF were made by multidisciplinary integration of clinical, HRCT and where available histological findings, and were made based on the ATS/ERS consensus guideline.

In addition to this dataset, since 2007 a unique biobank has been collected comprising of baseline and serial samples from 575 patients including BAL from 155 patients , 47

of whom have had 'serial' lavage at 0 and 12 months, and DNA from 520 patients. Baseline BAL samples were obtained from 94 IPF patients (32 progressors, 62 non-progressors) and repeat BAL was performed at 12 months in 60 patients (16 progressors, 44 non-progressors). Baseline serum samples were obtained in 216 IPF patients (102 progressors, 114 non-progressors) and 118 patients went on to have successive serum samples 12 months later (38 progressors, 80 non-progressors). Most of the patients had matched BAL and serum samples, and less than 2% had received IPF-directed therapy. The Edinburgh Lung Fibrosis study cohort is summarised in Tables 7 and 8.

Table 7. The Edinburgh Lung Fibrosis study cohort.

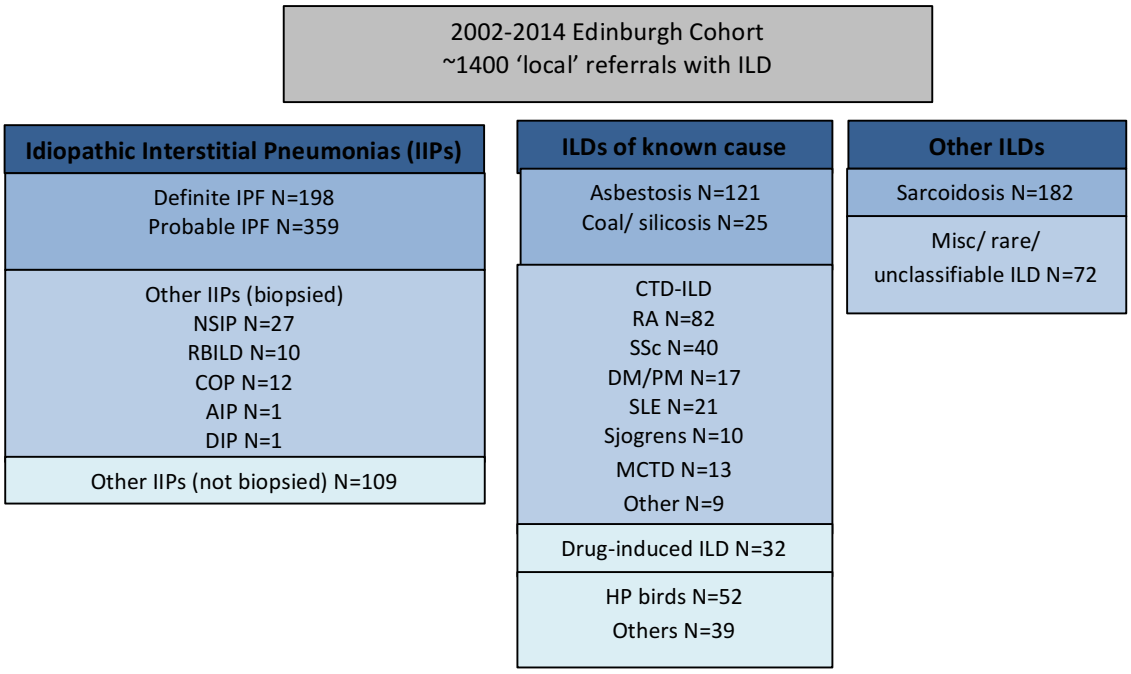

Table 8. Summary of the available samples in the Edinburgh IPF biobank according to patient phenotype.

	Progressors		**Non-Progressors**		**Controls (aged matched healthy volunteers)**
	Definite IPF Age (SD)	Probable IPF Age (SD)	Definite IPF Age (SD)	Probable IPF Age (SD)	Controls Age (SD)
Baseline serum samples	N=38 73.9 years (9.5)	N=64 74.0 years (7.8)	N=46 71.2 years (8.7)	N=68 73.6 years (8.1)	N=64 67.1 years (9.3)
0 and 12 month serum samples	N=25 73.8 years (9.1)	N=13 75.3 years (5.3)	N=33 71.0 years (8.1)	N=47 73.5 years (7.1)	0
Baseline BAL samples	N=15 66.9 years (9.0)	N=17 76.1 years (5.8)	N=27 71.3 years (6.8)	N=35 72.1 years (5.9)	N=9 62.6 years (7.8)
0 and 12 month BAL samples	N=8 69.6 years (10.3)	N=8 74.8 years (4.2)	N=20 71.3 years (7.5)	N=24 70.8 years (6.4)	0

2.2 Patient selection and study design for phase 2a clinical trial of TD139

I was Co-Investigator on a phase 2a clinical trial of TD139, an inhaled small molecule inhibitor for galectin-3. The study was designed, performed and funded by Galecto Biotech, a small company founded in 2011 in Lund, Sweden. Galectins have been shown to be involved in several pathological conditions and galectin-3 is a -galactoside binding lectin highly expressed in fibrotic lung and macrophages from IPF patients. Galectin-3 has many biological roles including cross-linking of cell surface and extracellular glycoproteins, modulating cell adhesion and signalling of cell surface receptors including TGF- and VEGF. This study was a randomised, double-blind, multicentre, placebo-controlled, phase 2a trial to assess the safety, tolerability,

pharmacokinetics (PK) and pharmacodynamics (PD) of TD139 in 24 IPF patients. Three dose cohorts of 8 subjects were recruited using a 5:3 ratio (active: placebo). Suitable patients were recruited from the Edinburgh Lung Fibrosis clinic. TD139 was inhaled using the Plastiape inhaler device at doses of 0.3mg, 3mg and 10mg once daily for 14 days. IPF patients underwent BAL prior to dosing and at 14 days. TD139 drug concentration was measured in the BAL cell pellets and plasma by laboratory staff at Simbec Research, BAL fluid samples for analysis of macrophage morphology, ex-vivo macrophage function, macrophage phenotypic and mRNA expression pattern and BAL analysis of protein biomarkers was performed by myself and Dr Alison MacKinnon, PhD. Samples from Royal Brompton Hospital, Newcastle University Hospital and Royal Devon and Exeter Hospital were also processed and analysed by myself.

Galectin-3 expression on BAL macrophages was measured by flow cytometry by myself. Real time PCR was used to assess changes in a panel of pre-selected cytokines and mediators.

Patient suitability for the trial was assessed in the 28 days prior to dosing by means of comprehensive screening which included informed consent, medical history, measurement of vital signs, physical examination, a 12-lead ECG, detailed lung function testing, urine screen and blood testing for a full blood count, kidney and liver function, and blood born virus screen. Suitable patients were then recruited into the trial and randomised to TD139 or placebo. Patients attended for BAL on day -1 and then received 14 days of treatment. Patients attended the clinical research facility on days -1, 1, 2, 3, 7, 14 and 15 for assessments including vital signs, lung function testing, 12-lead ECG, physical examination, blood testing for routine bloods and also PK/PD measurements, exhaled breath condensate for PD measurements and adverse event reporting. Patients were also reviewed at day 26 to 30 for a post-study assessment.

Trial inclusion criteria were a male or female subject of non child-bearing potential with IPF confirmed at MDT, aged between 45 and 85 years of age, FVC >45% predicted and an FEV_1/FVC ratio >0.7, TLCO >25%, oxygen saturations >90% on air, negative urinary drugs of abuse screen, negative HIV, hepatitis B and C screen, normal ECG, normal routine bloods and able to undergo BAL. Exclusion criteria included unacceptable risk for bronchoscopy, history of malignancy within 5 years, asthma,

active cigarette smoking, significant comorbidity limiting life expectancy to less than 12 months, HRCT appearances of emphysema greater than fibrosis, evidence of poorly controlled diabetes or renal, hepatic, central nervous system or metabolic dysfunction or use of systemic immunosuppressants within 30 days of dosing, and participation in a previous clinical study of an unlicensed drug within 4 months.

2.3 Protocols

2.3.1 Processing of BALF and serum

BALF was filtered through a 40µm cell strainer and total cell count obtained using an automated NucleoCounter. BALF was then centrifuged at 1200rpm for 10 mins at 4°C and the supernatant was removed and stored at -80°C. Cells were resuspended in IMDM at a concentration of 1 million cells per ml for flow cytometry. One million cells were removed for cytospin processing, briefly 10x100µl aliquots were cytocentrifued onto superfrost glass slides at 300g for 3 mins. Slides were then placed in methanol for 2 minutes and allowed to dry. One slide was then placed in DiffQuick Red for 2 minutes, then DiffQuick Blue for 90 seconds for staining.

Serum samples were centrifuged at 2500rpm for 10 minutes at 4°C and then serum was collected and stored at -80°C.

2.3.2 Flow cytometry and Fluorescence Activated cell sorting (FACS)

Whole blood (50µl) or BALF (100,000 cells) were incubated with antibodies against specific cell surface antigens (Table 9) for 30 minutes on ice. Unstained cells, single antibody stains and fluorescence minus one (FMO) controls were used. Erythrocytes were lysed by incubation at room temperature for 20 minutes in 650µl of FACSlyse. Samples were washed in 2ml PBS, centrifuged at 300g for 5 minutes and then reuspended in 450µl FACSlyse, for analysis using a LSR Fortessa cell analyser with

FACSDiva software. A SORT tube was prepared by adding 50ul PBS, 8ul CD14-AF647, 8ul CD16-PE and 8ul HLA-DR-V450. BAL fluid cells were centrifuged at 300g for 5 mins and resuspended in 800ul 1% serum and IMDM, then added to sort tube. Cells were incubated on ice for 20 mins, then 2mls sterile PBS added and centrifuged at 300g for 5 mins to wash. Cells were resuspended in 800ul 1% IMDM and taken to sorter with unstained sample. A BD FACSAriaII cell sorter was used with FACSDiva software. Cells were collected in 10% IMDM after sort, then pelleted and stored at -80°C. RNA extraction and cDNA conversion was then performed with future plans to perform qPCR on all AM, iPMLC and rPMLC pellets. FlowJo was used for data analysis. The gating strategies used to identify cell subpopulations within BAL fluid and blood are outlined in Figures 2 and 3.

Table 9. Primary antibodies used for flow cytometry and FACS.

Antibody	**Clone**	**Fluorochrome**	**Manufacturer and catalogue number**	**Laser filter**
AM, PMLC and neutrophil panel				
Anti-hCD14	HCD14	PerCP/Cy5.5	BioLegend 325622	Blue
Anti-hCD16	3G8	APC/Cy7	BioLegend 302018	Red
Anti-hHLA-DR	G46-6	V450	BD Horizon 561359	Violet
Anti-hCD206	15-2	PE	BioLegend 321106	Y/G
Anti-hCD71	CY1G4	FITC	BioLegend 334104	Blue
Anti-hCD163	GHI/61	APC	BioLegend 333610	Red
T cell panel				
Anti-hCD3	UCHT1	FITC	BioLegend 300405	Blue
Anti-hCD4	OKT4	APC/Cy7	BioLegend 317418	Red
Anti-hCD8		AF647	BioLegend	
FACS Panel				
Anti-hCD14	M5E2	AF647	BioLegend 301818	Red
Anti-hCD16	3G8	PE	BioLegend 302008	Blue
Anti-hHLA-DR	G46-6	V450	BD Horizon 561359	Violet

Figure 2. Flow cytometry gating strategies for alveolar macrophage polarisation phenotype.

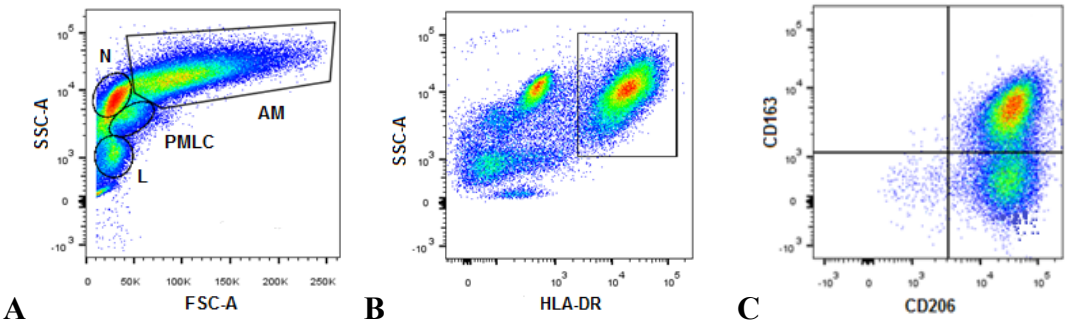

Figure 2. Flow cytometry gating strategies. Cells were identified in BAL fluid based upon their position on flow cytometry dot plots of size versus granularity (**A**). Alveolar macrophages (AM) were selected as HLA-DR+ (**B**), and were divided into $CD206^{low}CD163^{low}$, $CD206^{high}CD163^{low}$ and $CD206^{high}CD163^{high}$ subpopulations based on cell surface CD163 and CD206 expression (**C**). PMLC: Pulmonary monocyte-like cells, N: Neutrophils, L: Lymphocytes.

Figure 3. Flow cytometry gating strategies for BAL fluid cells.

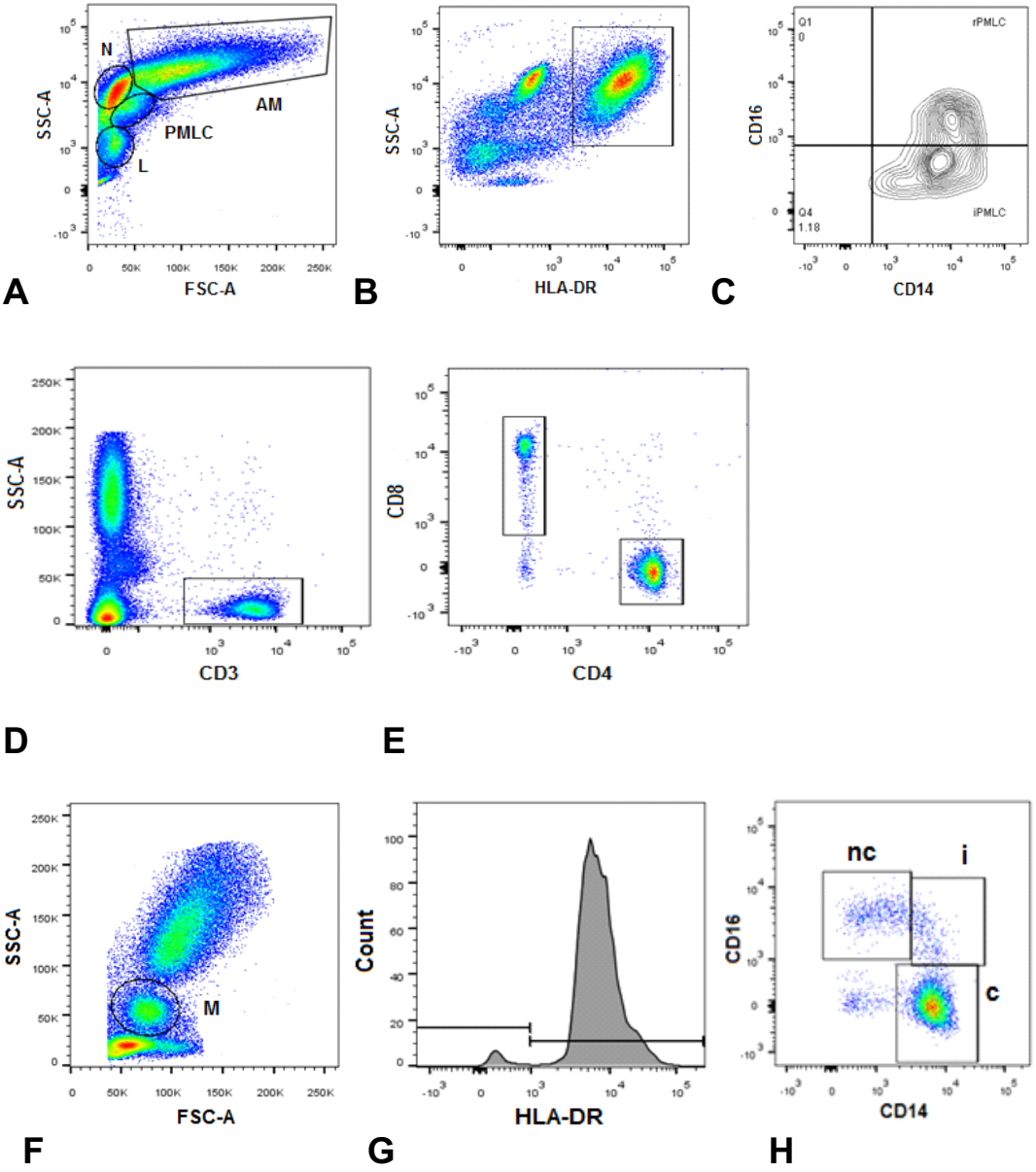

Figure 3. Flow cytometry gating strategies. Cells were identified in BAL fluid based upon their position on flow cytometry dot plots of size versus granularity (**A**). PMLCs were selected as HLA-DR+ (**B**), and were divided into rPMLC and iPMLC subpopulations based on their CD14 and CD16 expression (CD14++CD16+ and CD14++CD16- respectively) **(C**). Lymphocytes (L) were further selected for CD3 expression (**D**) and then subdivided into CD8+ and CD4+ T-cells (**E**). Cells were identified in whole blood based upon their position on flow cytometry dot plots of size versus granularity (**F**). Blood monocyte subsets (M) were identified as HLA-DR+ (**G**), and were then subdivided into classical (c), intermediate (i) and non-classical (nc) monocyte subpopulations based on their CD14 and CD16 expression (**H**). AM: Alveolar macrophages, N: Neutrophils.

2.3.3 ELISAs

Analysis of cytokines and mediators in BALF and serum were performed using DuoSet ELISA kits from R&D Systems, according to the manufacturer's instructions. All samples were ran in duplicate. Briefly, Capture Antibody was diluted to the working concentration in PBS and each well of a 96-well microplate was coated with 100L. The plate was sealed and incubated overnight at room temperature. Each well was then aspirated and washed with Wash Buffer (0.05% Tween 20 in PBS) a total of 3 times. The plates were then blocked by adding 300L of Reagent Diluent (1% BSA in PBS) and incubated at room temperature for 1 hour. The wash step was then repeated. Patient samples and standards were prepared to the working concentration in Reagent Diluent and 100L was added to each well, the plate was covered with an adhesive strip and incubated for 2 hours at room temperature. The wash step was then repeated. Detection Antibody was diluted to a working concentration in Reagent Diluent, and 100L was added to each well, the plate was covered with a new adhesive strip and incubated at room temperature for 2 hours. The wash step was repeated. One hundred microlitres of the working dilution of Streptavidin-HRP was added to each well, the plate was covered and incubated for 20 minutes at room temperature. The wash step was repeated. Substrate Solution (1:1 mixture of Colour Reagent A (H_2O_2) and Colour Reagent B (Tetramethylbenzidine)) was prepared and 100L was added to each well, then plates were incubated for 20 minutes at room temperature. Fifty microlitres of Stop Solution (2 N H_2SO_4) was added to each well, and mixed gently.

ELISA plates were analysed using a Synergy-HT microplate reader using Gen5 data analysis software. The optical density of each well was determined by setting the microplate reader to 450nm with wavelength correction set at 570nm to correct for optical imperfections in the plate.

2.3.4 Proteomic Arrays

Initially, unbiased semi-quantitative commercially bought proteomic array kits were used to detect proteins of interest in BALF (R&D, Human Angiogenesis Array cat# ARY007, Human Chemokine Array cat# ARY017, Human Protease/Protease Inhibitor

Array cat# ARY025 and Human Soluble Receptor, Non-haematopoietic Panel Array cat# ARY012). Protocols were followed as per manufacturer's instruction, however briefly capture antibodies were spotted in duplicate on nitrocellulose membranes, BAL samples were pooled, diluted and mixed with a cocktail of biotinylated detection antibodies and sample/antibody mixtures were then incubated with the array. Any analyte/detection antibody complexes present were bound by their cognate immobilised capture antibody on the membrane, Streptavidin-Horseradish Peroxidase and chemiluminescent detection reagents were then added, and a signal was produced in proportion to the amount of analyte bound. IPF Progressor and Non-Progressor groups were compared by pooling fluid containing 50µg of protein (protein determined via Pierce BCA assay, ThermoFisher cat# 23225) each from four IPF patients from each group. Pixel density was measured using ImageJ. Proteins from this array were selected on the basis of showing a 2-fold difference between IPF progressors versus IPF non-progressors AND compatibility with the Luminex Magnetic Screening Assay kits (R&D) which was subsequently used to quantify the mediators. The proteins selected for the Luminex assay are reported in Table 10.

Table 10. Analytes included in Luminex Magnetic Screening Assay.

Analyte	Analyte	Analyte	Analyte
Amphiregulin	**Chi3-L1**	**IL-10**	**Osteopontin**
CCL2/MCP-1	**CXCL1/GRO alpha**	**IL-12 p70**	**Pentraxin 3**
CCL5/RANTES	**CXCL8/IL-8**	**IL17E/IL-25**	**Periostin/OSF-2**
CCL18/PARC	**CXCL10/IP-10**	**IL-33**	**SP-D**
CCL26/Eotaxin-3	**EGF**	**MMP-1**	
VEGF	**Galectin-3**	**MIF**	

Protocols were followed as per manufacturer's instructions, however briefly analyte-specific antibodies were pre-coated onto magnetic microparticles, microparticles, standards and samples were pipetted into wells and immobilised antibodies were bound to the analyte of interest, plates were washed, then a biotinylated antibody cocktail specific to analytes of interest were added, plates were again washed, then Steptavidin-

PE was added to bind to the biotinylated antibody. Plated were again washed, then read using the Bio-Plex 200 HTF analyser (one LED identifies analyte and one determines magnitude of PE-derived signal, which is directly proportional to amount of analyte bound). Patients were categorised into Definite IPF Progressor, Probable IPF Progressor, Definite IPF Non-Progressor, Probable IPF Non-Progressor and Healthy Control groups. Luminex Magnetic Screening Assay was performed on BALF and serum, first in a Test Cohort of 4 patients per group, then in a Validation Cohort of 8 patients per IPF group and 5 controls. BALF was normalised to 10μg of protein per sample (protein determined via Pierce BCA assay, ThermoFisher cat# 23225) and serum was utilised at either 1:2 or 1:50 dilution depending on manufacturer's instruction. Definite and probable IPF groups were combined to allow an N=24 IPF progressors and N=24 IPF Non-Progressors for statistical analysis.

2.3.5 RNA extractions

RNA extraction was performed using Qiagen RNeasy Mini Kit (cat nos 74104 and 74106) and the Quick Start Protocol, according to the manufacturer's instructions. Briefly, RLT buffer mix was prepared by adding 50μl of mercaptoethanol to 5ml RLT buffer, 350μl of the mix was added to a cell pellet containing 1 million cells, and resuspended. Three hundred and fifty microlitres of 70% ethanol was added to the lysate, then 700μl of the sample was transferred to an RNeasy Mini spin column, and was centrifuged at 10,000 rpm for 1 minute. The flow-through was discarded and the column was washed by adding 700μl of RW1 buffer to the column and centrifuging for 1 minute at 10,000rpm. Flow-through was discarded and 500μl of RPE buffer (with 70% ethanol added) was added to each column and centrifuged at 10,000rpm for 1 minute. The RPE wash was repeated with a further 500μl of RPE buffer. Samples were centrifuged at 10,000rpm for another minute, flow through was discarded and the RNeasy spin column was placed in a new 2ml collection tube. Samples were then centrifuged at 10,000rpm for 2 minutes. The column was placed in a new 1.5ml tube and 30μl of RNAse-free water was pipetted onto the membrane. Samples were centrifuged for 1 minute at 10,000rpm and the column discarded. A NanoDropTM 1000 spectrophotometer (Thermo Scientific) was used to directly quantify 1μl of RNA

sample. The purity of all RNA samples were confirmed by having the optimal ratio of absorbance at 260 nm/280 nm (1.9-2.3) and 260 nm: 230 nm (>2.2).

2.3.6 Reverse transcription and quantitative PCR

Reverse transcription was performed using Qiagen QuantiTect Reverse Transcription Kit (cat nos 205310, 205311, 205313 and 205314). All protocols were followed according to manufacturer's instructions. Briefly, 12 µl of RNA (1-2µg) and 2µl of DNA wipe-out buffer were added to each PCR tube and incubated for 5 minutes at 42C. The Reverse-transcription master mix was prepared and 6 µl of the mix was added to each PCR tube (1 µl of Quantiscript Reverse Transcriptase (RT), 1 µl of RT primer mix and 4 µl of Quantiscript RT buffer), making a total volume of 20 µl per tube. Samples were incubated at 42C for 30 minutes and then 95C for 3 minutes, the latter being to inactivate the reaction.

The expression of genes of interest was quantified by qPCR using an ABI PRISM® 7000 Sequence Detection System (Applied Biosystems) and the QuantiTect SYBR Green PCR Kit (Qiagen). Complementary DNA was diluted to a 1:10 dilution by adding 180µl of RNAse-free water to each 20µl cDNA sample to make the template. Eight genes of interest were selected and primer mixes with forward and reverse primers were prepared for actin (house-keeping), galectin-3, CCL18, CD163, CD206, TGF, IL-10 and CD80. Each reaction mixture contained 5µl QuantiTect SYBR Green PCR master mix, 4µl of cDNA template and 1µl of primer to a final volume of 10µl. Each reaction was performed in duplicate in a 384-well plate (Applied Biosystems) under the following thermocycling conditions: 15 min at 95 °C for initial activation and then 40 cycles of 15 s at 94 °C, 30 s at 56 °C and 30 s at 72 °C. The controls, including no reverse transcriptase and no template control, produced no amplification.

2.4 Statistical analysis

GraphPad prism (version 6, GraphPad Software Inc., CA, USA) was used for data analysis. Normally distributed data were analysed by unpaired or paired t-test and expressed as mean (SD). Data that were not normally distributed were reported as median (interquartile range) and analysed by Mann Whitney U test or Wilcoxon signed rank test. Kruskal-Wallis test with Dunn's Multiple Comparison Test was used to calculate differences between multiple groups. Predictors of mortality and disease progression by diagnostic category were estimated using Cox models on SPSS. *P* values of <0.05 were considered significant.

Chapter 3

Clinical trial eligibility and surgical lung biopsy in the Edinburgh IPF cohort

3.1 Introduction

3.1.1 General introduction

The interstitial lung diseases are a protean group of lung disorders with substantial overlap in terms of diagnosis, prognosis and management. Idiopathic pulmonary fibrosis is the commonest fibrotic ILD and is characterised by chronic and progressive lung scarring with a median survival time of 3- 5 years and no curative therapy. In 2011, the American Thoracic Society (ATS), European Respiratory Society (ERS), Japanese Respiratory Society (JRS) and the Latin-American Thoracic Society (ALAT) published an international evidence-based guideline on the diagnosis and management of IPF. This guideline was revised in 2013. The consensus statement recommended that for a diagnosis of IPF, known causes of ILD such as domestic or occupational environmental exposures, connective tissue disease and drug toxicity must first be excluded. IPF could be diagnosed definitively in patients with an Usual Interstitial Pneumonia (UIP) pattern on HRCT scanning, comprising reticular abnormalities, subpleural and basal disease predominance, honeycombing with or without traction bronchiectasis and an absence of features listed as 'inconsistent with UIP' pattern. In patients without honeycombing, a diagnosis of 'possible IPF' is made. The guideline is clear that if honeycombing is absent on HRCT then the diagnosis is regarded as 'possible IPF' and further investigation by means of surgical lung biopsy is required[1]. The histopathologic criteria for IPF are also described as UIP pattern, and include temporally heterogeneous areas of fibrosis and subepithelial fibroblastic foci. The diagnosis of IPF requires an integrated multidisciplinary approach involving ILD specialist respiratory physicians, radiologists and pathologists. However, even with the benefits of an experienced ILD MDT and surgical lung biopsy, around 10% of ILD patients are deemed to have unclassifiable disease, with significant overlap between conditions[67]. Diagnostic

uncertainty can have major implications in terms of uncertainties in management. In recent years landmark phase 3 clinical trials in IPF have changed clinical practice. The generalisability of clinical trial data to real world patients is of importance to patients and clinicians. These well-executed studies have used similar end-points but their selection criteria have differed. These differences have arisen because in general efficacy-driven clinical trials strive to avoid heterogeneity amongst trial subjects and to enrich subjects that will meet the primary end-point, decline in FVC in the case if IPF trials.

The diagnostic criteria for IPF have been established since the ATS/ERS/JRS/ALAT consensus document of 2011[1]. However in real-world practice, diagnostic criteria used for IPF have evolved organically based on new knowledge of disease phenotype and disease progression. For example in elderly patients, clinicians increasingly make a multidisciplinary team diagnosis of IPF based on an HRCT pattern that is deemed 'possible UIP' by 2011 consensus criteria, without lung biopsy[1,16,68,69]. Diagnostic criteria for IPF in clinical trials is also evolving as exemplified by eligibility criteria for the INPULSIS trials which allowed subjects that were not biopsied but had 'possible UIP plus bronchiolar dilatation' on HRCT scanning[25,70], a pattern which was not based on the 2011 consensus document. Diagnostic classification is particularly important because the treatment of IPF is different from that of the more immunologically driven ILDs such as non-specific interstitial pneumonia (NSIP) and chronic hypersensitivity pneumonitis which may respond or even resolve with anti-inflammatory and immunosuppressive therapy[70,71]. In contrast corticosteroids and azathioprine have been shown to be harmful in IPF[21]. Furthermore the emergence of two FDA approved drug treatments for IPF make establishing a precise diagnosis increasingly relevant in everyday clinical practice.

3.1.2 Hypothesis and aims

Accurate phenotyping of patients in routine clinical practice also enhances the value of epidemiological studies. Whilst there are numerous reports of the natural history of ILDs in the literature, the vast majority have inherent bias because they are derived from specialist tertiary referral centres and are not consecutively present incident cases

or, in the case of IPF in particular, they are derived from subgroups of patients enrolled into the placebo arm of clinical trials. One way of assessing generalisability of clinical trial subjects to real-world patients is to compare the natural history of disease in patients deemed eligible or non-eligible. We aimed to describe the natural history of patients with IPF phenotyped according to PANTHER, CAPACITY, ASCEND and INPULSIS eligibility criteria. We hypothesised that survival and lung function decline would differ between eligible and non-eligible patients both within and between studies.

There is also a definite need to better define the risks and potential value of SLB in suspected IPF, and to understand the true natural history of well defined groups of ILD patients in an unbiased setting. Surgical lung biopsy enhances diagnostic certainty, however biopsy rates and thresholds in ILD vary[72], a reflection of the perceived risks of the procedure and the perceived actual diagnostic value in an individual, enhanced by the more recent observation that patients with advanced age predicts a UIP biopsy in patients[17]. Across all of the ILDs the 30-day mortality and morbidity are 2-4% and 10-18% respectively[73,74] The recent single-centre retrospective study by Fell et al showed that in biopsied patients aged over 70 years with 'fibrotic' appearances on HRCT, 95% had UIP confirmed at biopsy, implying that advanced age is a strong predictor for IPF[17]. However the positive predictive value for UIP depends on the underlying prevalence of IPF in the population and the diagnostic value and mortality of SLB specifically in 'possible UIP' based on strict ATS/ERS criteria have not been described.

We aimed to determine the mortality, complication-rate following elective SLB and the clinical utility of SLB in suspected idiopathic interstitial pneumonia, stratified according to HRCT category, in our population of consecutively presenting incident cases of ILD. We hypothesised that an underlying UIP pathological pattern may result in increased risk of death. Additionally we sought to determine the positive-predictive value of biopsy to diagnosis of IPF in patients with 'possible UIP' HRCT pattern in our population.

3.1.3 Methodology

Patient selection

The Edinburgh Lung Fibrosis research database was established in 2002, and was designed to capture the natural history of ILD patients referred to the specialist adult ILD clinic. All subjects were fully consented and ethical approval was obtained for all relevant protocols and procedures (LREC 06/S0703/53). The dataset from 01/01/02 – 31/12/13 is summarised in Figure 4. Study cohorts consisted of locally referred, consecutively presenting, incident patients with ILD presenting since 01/01/02. For all patients, diagnosis, investigation, management and follow-up was as per the Edinburgh local policy. This included a detailed clinical history, examination, autoantibody screen (PR3 and MPO ANCA, immunoglobulins IgA, IgG and IgM, aspergillus precipitans, avian precipitans, farmers lung precipitans and CTD screen including ANA, DNA, C3, C4, CCP and ENA screen (antibodies to Ro, La, Sm, RNP, Scl70, Jo1)), HRCT and pulmonary function testing. Follow-up included lung function testing at a minimum of 3 monthly and maximum of 6 monthly for at least 3 years. Disease progression was defined as death or 10% decline in VC over any 12 month period. Patients deemed to be stable at 3 years had at least 12 monthly lung function testing. Three subjects (less than 1% of the cohort) were lost to follow-up. The mean duration of follow-up was 3.4 years (range 8 days to 12.8 years). Less than 2% of the IPF cohort received IPF-directed therapy including prednisolone >30mg/day, azathioprine or N-acetylcysteine. No patients received pirfenidone or nintedanib and only one subject was recruited to a phase 3 clinical trial in the period relevant to this study. All HRCT scans were reviewed by an expert thoracic radiologist with 20 years experience and discussed in a multidisciplinary meeting with at least two respiratory physicians with ILD subspecialty expertise of at least 10 years experience. Prior to 2011, we categorised HRCT patterns as Category 1 >95% confidence of UIP, Category 2 70% confidence of UIP or Category 3 <70% confidence of UIP based on local criteria that were identical to the 2011 ATS/ERS 'definite', 'possible' and 'inconsistent with' UIP criteria except for the following[1]; 1. We defined 'basal dominance' as >50% of the ILD is below the inferior pulmonary veins. ATS/ERS/JRS/ALAT criteria has no definition of 'basal dominance'. 2. We defined 'honeycombing' if cysts are 2mm and there is at least one

site where there is a ‘stack’ of more than one row of cyts. ATS/ERS criteria do not specifically define ‘honeycombing’. 3. For HRCTs that exhibited diffuse mosaic attenuation, we categorised the scan as ‘inconsistent with UIP’ if the mosaicism was the ‘dominant’ pattern of disease. ATS/ERS/JRS/ALAT criteria defined diffuse mosaicism involving both lungs and in three or more lobes as ‘inconsistent with UIP’[1]. A retrospective analysis of 100 randomly selected HRCT scans pre- and post 2011 showed that reclassification according to Edinburgh and ATS/ERS criteria occurred in 2% of patients (data not shown). In patients with possible UIP HRCT appearances, surgical lung biopsy was performed after consideration of disease severity, comorbidities and the patient’s wishes. Lung histology was reviewed in a multidisciplinary meeting by an experienced pulmonary pathologist with 20 years lung pathology experience and a member of the UK ILD pathology reference panel. All diagnoses of definite and possible IPF were made by multidisciplinary integration of clinical, HRCT and where available histological findings, and were made based on the ATS/ERS/JRS/ALAT consensus guideline[1].

Figure 4. The Edinburgh Lung Fibrosis Research Cohort from 2002 -2013.

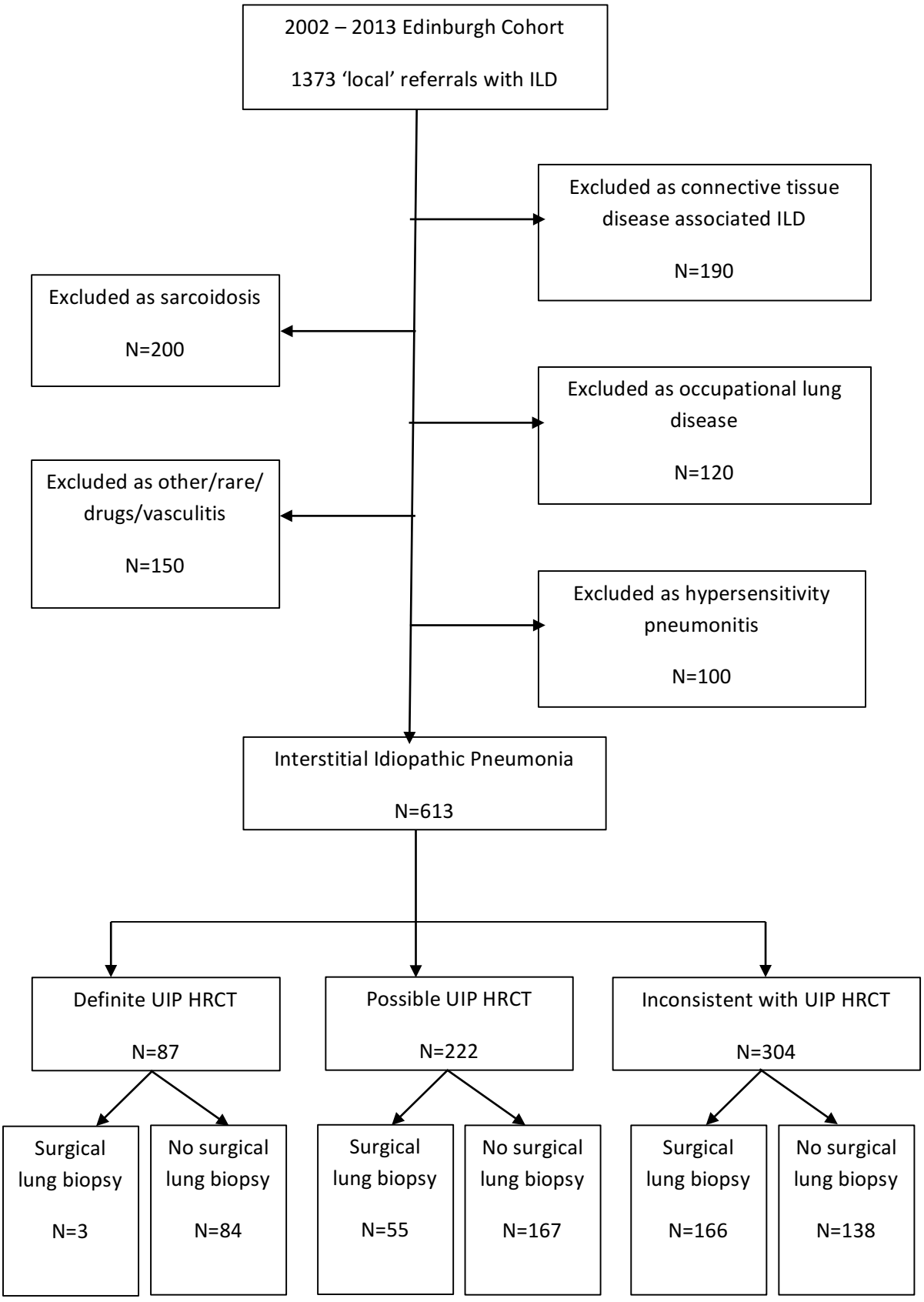

Allocation of patients according to trial eligibility criteria

Published eligibility criteria for PANTHER, CAPACITY, ASCEND and INPULSIS trials were applied to the Edinburgh cohort and patients were excluded hierarchically based on diagnostic certainty (definite vs possible IPF), then on lung function criteria and then on age criteria[21,22,24,25]. Other eligibility/ non-eligibility criteria that were defined in the protocols of these trials, such as co-morbidities, history of cancer or walking distance were not applied to our Edinburgh cohort, Figure 5.

Figure5. Clinical trials exclusion criteria applied to Edinburgh cohort.

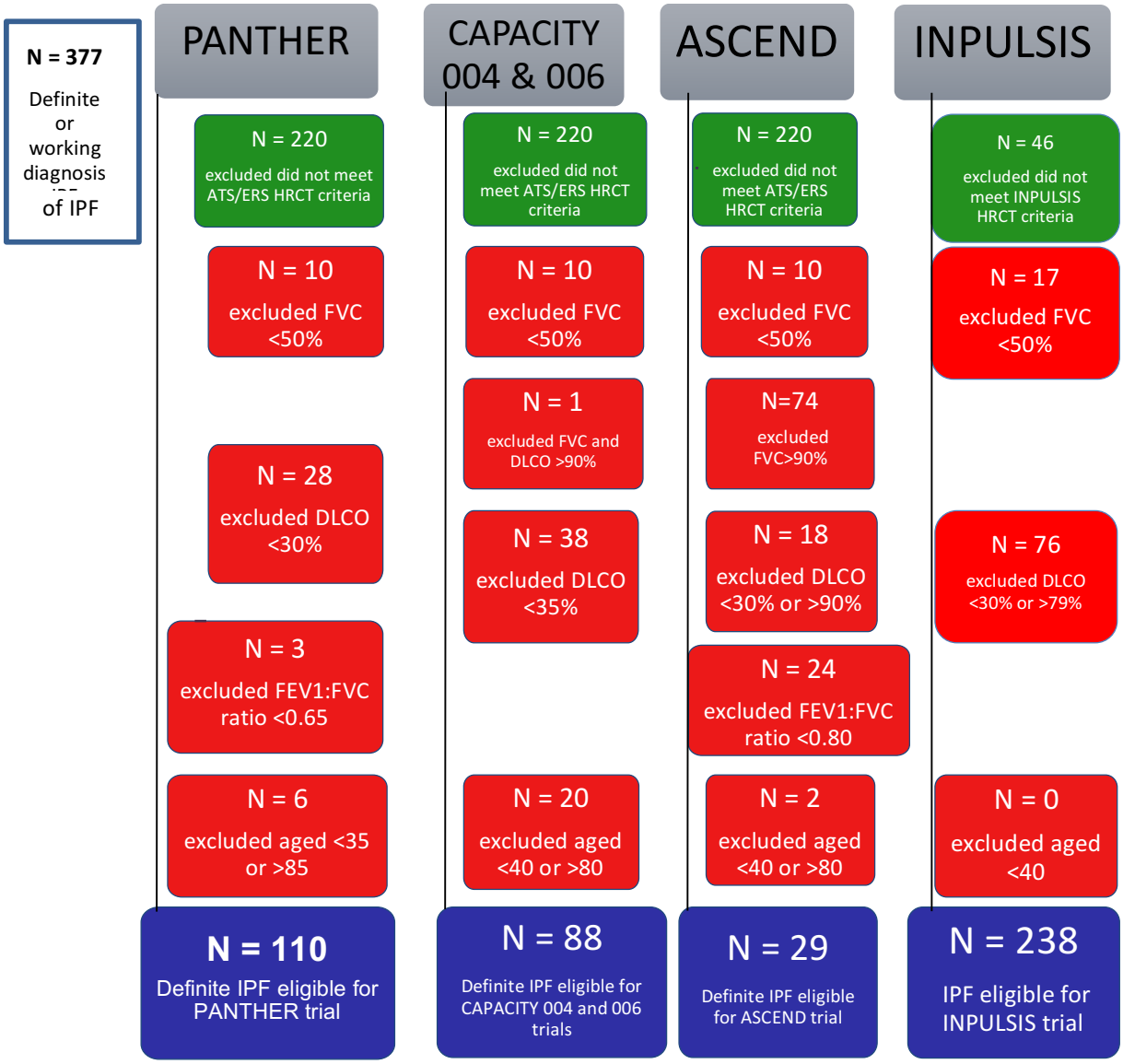

Data sources and measurement

Using a standard protocol I reviewed electronic case-notes, and HRCT images and reports on PACS to identify a) indication for biopsy (e.g. suspected ILD) and b) baseline characteristics likely predictive of final diagnosis (e.g. presence of known cause of fibrotic lung disease, lung function, and HRCT appearance categorised into 'definite UIP', 'possible UIP' and 'inconsistent with UIP' based on ATS/ERS criteria and the virtually identical Edinburgh pre-defined criteria. Cause of death and hospitalisation and rates of complication post SLB (including pain, persistent leak, pneumonia etc) were obtained from electronic case note review (including PACS). Results obtained from coding were validated by review of electronic and paper case notes. I assessed risk factors for mortality using multiple logistic regression, adjusting for age, gender, smoking status, type of operation (thoracoscopic versus open), baseline lung function (percentage of predicted FVC and TCO) and co-morbidity. Post-operative complications were assessed using the Clavien-Dingo Classification of Surgical Complications grading system, this is described in Table 11[75].

Table 11. Clavien-Dingo Classification of Surgical Complications.

Grade	Definition
Grade I	Any deviation from the normal postoperative course without the need for pharmacological treatment or surgical, endoscopic and radiological interventions.
	Allowed therapeutic regimens are: drugs as antiemetics, antipyretics, analgetics, diuretics and electrolytes and physiotherapy. This grade also includes wound infections opened at the bedside.
Grade II	Requiring pharmacological treatment with drugs other than such allowed for grade I complications. Blood transfusions and total parenteral nutrition are also included.
Grade III	Requiring surgical, endoscopic or radiological intervention
Grade IV	Life-threatening complication (including CNS complications)‡ requiring IC/ICU-management. Also including single and multi organ dysfunction
Grade V	Death of a patient

Statistical analysis

Normally distributed data were expressed as mean (standard deviation) and data that were not normally distributed were reported as median (interquartile range). Kaplan-Meier survival curves were calculated using IBM SPSS Statistics (IBM Corp. Released 2012. IBM SPSS Statistics for Windows, Version 21.0. Armonk, NY: IBM Corp), differences in survival curves were evaluated using the log-rank test. IBM SPSS Statistics (IBM Corp. Released 2012. IBM SPSS Statistics for Windows, Version 21.0. Armonk, NY: IBM Corp) was also used to perform survival curves and cox proportional hazards modelling to identify predictors of mortality and disease progression and to adjust for the following factors contributing to mortality: age, sex, smoking status, height, baseline percentage predicted FVC, baseline percentage predicted TCO, and eligibility group. The estimated trial and group-specific FVC decline rates reported are derived from an unconditional linear growth model; the estimates thus represent the average FVC decline rate for patients in each group. GraphPad prism (version 6, GraphPad Spftware Inc., CA, USA) was also used for data analysis. Normally distributed data were analysed by unpaired or paired t-test and expressed as mean (SD). Data that were not normally distributed were reported as median (interquartile range) and analysed by Mann Whitney U test or Wilcoxon signed rank test. Kruskal-Wallis test with Dunn's Multiple Comparison Test was used to calculate differences between multiple groups. *P* values of <0.05 were considered significant. Patients with missing values were excuded from statistical analysis. Missing patient data in demographics is highlighted in each table in the results section appropriately.

3.2 Results

3.2.1 The natural history of IPF in the Edinburgh IPF patient cohort

Patient data and demographics

There were 377 patients with a diagnosis of definite or probable IPF recorded on the Edinburgh Lung Fibrosis Clinical database between 01/01/02 and 31/12/14. The mean age (SD) for all IPF patients was 74.0 (8.6) years and 229 (60.7%) were male. 157 patients had definite IPF while 220 had probable IPF. Age, smoking status and baseline FEV_1 and FVC were similar for both, but those with definite IPF had lower TCO percent predicted and less emphysema at baseline than those with probable IPF. This is described in table 12 below.

Table 12. Patient demographic and baseline lung function data.

	All patients	Definite IPF	Probable IPF	P-value
N	377	157	220	
Age in years (SD)	74.0 (8.6)	73.0 (9.4)	74.0 (8.2)	0.159
Male sex (%)	229 (60.7)	95 (60.5)	125 (56.8)	0.473
Never smoked (%)	93 (24.7)	36 (22.9)	55 (25.0)	0.639
Smoked <20 pack years (%)	71 (18.8)	23 (14.6)	48 (21.8)	0.078
Smoked 20-40 pack years (%)	118 (31.3)	54 (34.4)	64 (29.1)	0.275
Smoked > 40 pack years (%)	48 (12.7)	19 (12.1)	29 (13.2)	0.753
Current Smoker (%)	47 (12.5)	25 (15.9)	22 (10.0)	0.088
Height in metres (SD)	1.66 (0.10)	1.67 (0.10)	1.65 (0.10)	0.897
FEV_1 in Litres (SD)	2.17 (0.63)	2.16 (0.65)	2.18 (0.62)	0.536
FEV_1 percent predicted (SD)	92 (21)	89 (22)	95 (20)	0.087
VC in Litres (SD)	2.73 (0.82)	2.68 (0.84)	2.77 (0.81)	0.667
VC percent predicted (SD)	90 (21)	85 (22)	94 (20)	0.075
TCO mm/min/mmHg (SD)	4.05 (1.42)	3.95 (1.29)	4.12 (1.51)	0.105
TCO percent predicted (SD)	53.0 (16.0)	50.3 (15.2)	55.3 (16.4)	0.003
Emphysema 0% (%)	188 (49.8)	113 (72)	75 (34.1)	<0.0001
Emphysema 1-5% (%)	110 (29.2)	40 (25.5)	70 (31.8)	0.185
Emphysema 5 to 19.9% (%)	53 (14)	13 (8)	40 (18)	0.006
Emphysema ≥20% (%)	26 (7)	15 (10)	11 (5)	0.062

No patients were lost to follow-up. Two hundred and twenty five patients died during follow-up and the remainder were censored at November 21st 2014. Median (inter-quartile range (IQR)) follow-up for survivors was 44 (30-61) months. Patients were followed-up for a median of 5 visits (IQR 3 to 8) over a median of 2.5 years (IQR 1 to 4). One or more visits were missed for 69 patients, the majority of whom (56) missed 3 or fewer visits.

Of the patients with HRCT appearances indicative of 'probable UIP', in whom surgical lung biopsy under the current guidelines would be advocated, 14.1% (36/255) underwent the procedure. Those who had a biopsy were on average younger (66.2 vs 75.5 years) and had higher absolute FVC and TCO values (3.28 vs 2.68 and 4.30 vs 3.38 respectively) but similar percent predicted FVC and TCO values (87.0 vs 89.1 and 48.0 vs 47.3) to patients who did not have a biopsy.

Mortality

Overall, 225 patients (59.7%) died during the follow-up period. One hundred patients (63.7%) with definite IPF and 125 patients (56.8%) with probable IPF died during follow-up (Table 13). Median survival was worse for patients with definite IPF than with probable IPF (3.4 and 4.5 years respectively, Table 13). The unadjusted hazard ratio for death for patients with definite compared to probable IPF was 1.42 (95% CI 1.08 to 1.87, P=0.013) however the association was attenuated after adjusting for gender, age, FVC, TCO and smoking status at baseline, with a hazard ratio of 0.79 (95% CI 0.59 to 1.05, P=0.106). Compared to patients with probable IPF, the difference in mortality was greater for patients with definite IPF confirmed on HRCT than on biopsy (HR 1.72; 95% CI 1.26 to 2.36, P=0.001, and HR 0.941; 95% CI 0.61 to 1.45 respectively). Mortality was also greater in patients with definite UIP on HRCT, than patients with definite IPF with a probable UIP HRCT and UIP biopsy, 3.0 years versus 5.80 years, HR 1.72 (95% CI 1.13 to 2.61). This data is shown in Figure 6 below.

Table 13. Mortality by diagnostic category and CT phenotype.

	Definite IPF	Probable IPF	P-value
N	157	220	
Deaths	100	125	0.179
Median survival in years (IQR)	3.4 (1.32, 4.25)	4.5 (1.40, 5.19)	0.013
Hazard ratio Unadjusted (95% CI)	1.42 (1.08 to 1.87)	1	0.013
Hazard ratio Adjusted (95% CI)	0.79 (0.59 to 1.05)	1	0.106

Figure 6. Mortality in definite vs probable IPF.

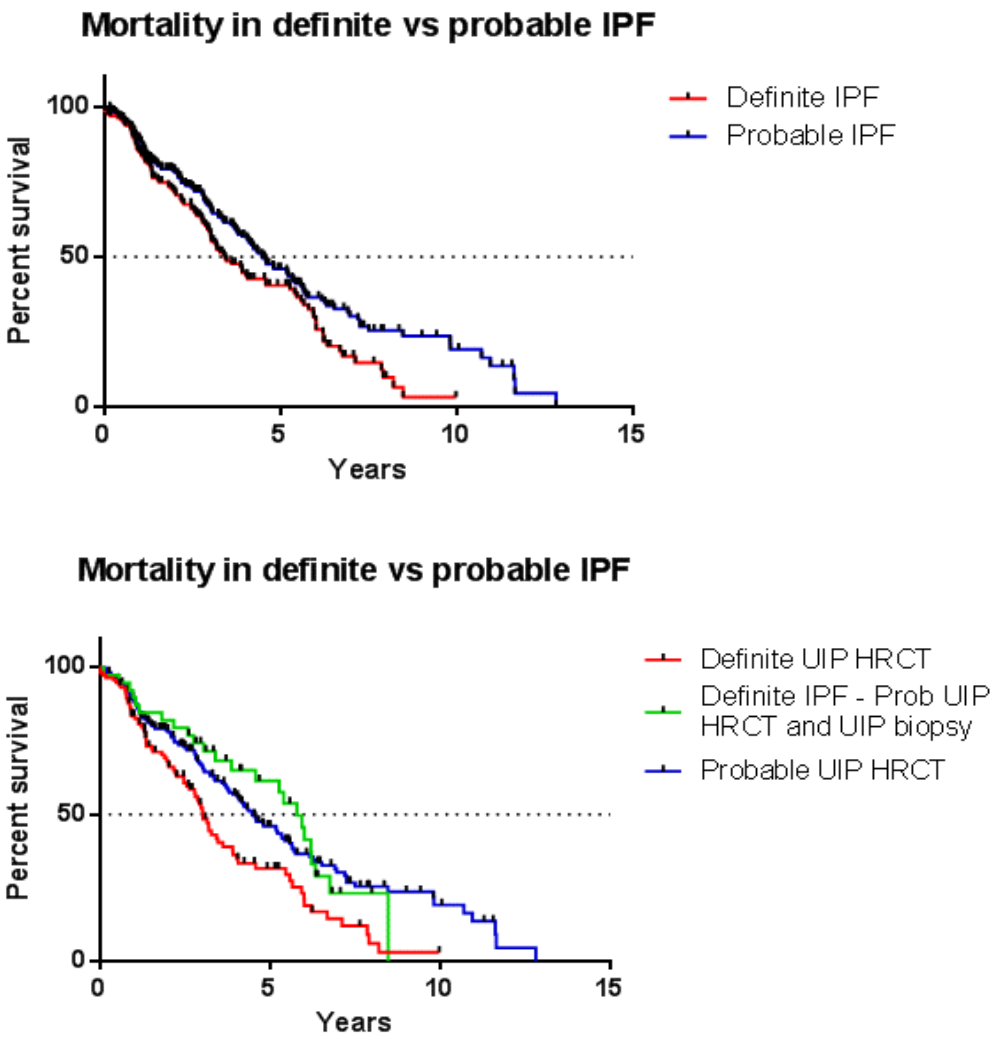

Baseline VC was the most important predictor of mortality, and very similar hazard ratios according to baseline VC were found for patients with definite IPF (HR 0.90 per 100ml; 95% CI 0.86 to 0.95, P<0·001) and probable IPF (HR 0.91 per 100ml; 95% CI 0.85 to 0.97, P= 0·004) across the follow-up period.

Decline in VC

The average overall absolute decline in VC in all IPF patients (definite and probable) was calculated using linear mixed models by Dr David McAllister, PhD, and was found to be 115 (standard deviation 109) ml/year. Patients who died during the follow-up period had a faster decline in FVC than those who did not (90 ml/year faster decline; 95% CI 50.0 to 140.0, P<0.001). Patients with definite IPF had an estimated decline in FVC of 157 ml/year and patients with probable IPF had an 85 ml/year decline (difference 71 ml/year, 95% CI 26.0 to 117.0 ml/year, P=0.001). These findings were similar after adjusting for age, sex and smoking status at baseline. Rates of FVC decline were also similar regardless of whether or not definite IPF was confirmed on biopsy (difference 73 ml/year, 95% CI 8.0 to 138.0 and difference 63 ml/year, 95% CI 9.0 to 117.0 respectively, P=0.267). Similar differences in decline in lung function were evident for VC percent predicted.

TLCO

TLCO was not obtained at baseline in 45 (11.9%) patients, because of poor test compliance or advanced disease, all of whom subsequently died. The median survival in patients with and without baseline TLCO measures was 4.58 years (IQR 1.44, 5.27) and 2.64 years (IQR 0.90, 2.85) respectively (P<0.0001). Mortality between the two groups remained significantly different when the curves were adjusted for age, sex, smoking status and baseline percentage predicted FVC (P<0.0001). When the cohort was split into definite and probable IPF groups, mortality remained significantly different in those able to perform a baseline TCO measurement compared to those who could not. In the definite IPF group, median survival was 3.91 years (IQR 1.33, 4.67) versus 2.04 years (IQR 1.06, 2.85) (P=0.034 adjusted) and in the possible IPF group,

median survival was 4.80 years (IQR 1.54, 5.48) in those with a baseline TCO value and 2.85 years (IQR 0.89, 2.84) in those who were unable to perform the test (P=0.002 adjusted). Among the 88.1% of patients in whom it was measured, lower TCO at baseline was associated with higher mortality in patients with definite IPF (HR 2.38 per mmol/min/kPa; 95%CI 1.67 to 3.33, P<0·001) and probable IPF (HR 1.61 per mmol/min/kPa; 95%CI 1.22 to 2.13, P=0·004) adjusting for age, sex and smoking status. Change in TLCO over the initial 6 months of follow-up was measured in 284 (75%) patients, among whom a 15% decline in TLCO relative to baseline was associated with increased mortality (HR 1.85; 95%CI 1.05 to 3.25, P=0·03). Decline in TCO over time was calculated by Dr David McAllister, PhD, and was found to be 0.37 mmol/min/kPa/year in the definite IPF group and 0.26 mmol/min/kPa/year on those with possible IPF (difference 0.11 mmol/min/kPa/year; 95%CI 0.02 to 0.20, P=0·01).

3.2.2 Recent clinical trial eligibility criteria applied to the Edinburgh IPF cohort

Patient data and demographics

Between 01/01/02 and 31/12/14, around 1396 locally referred, consecutive patients with suspected ILD presented to the Edinburgh Lung Fibrosis clinic. Seven hundred and twelve patients had suspected IIP, with 377 patients having a working diagnosis of IPF. Of the 712 patients, 139 underwent surgical lung biopsy to confirm the diagnosis. Of the biopsied patients, 43 were confirmed as UIP, and 96 had another IIP or unclassifiable fibrosis. Of the 450 patients that were not biopsied, 114 had ‘definite UIP’ HRCT appearances, 220 had ‘possible UIP’ HRCT appearances and 116 had HRCT appearances deemed ‘inconsistent with UIP’. Based on the ATS/ERS/JRS/ALAT IPF diagnostic criteria, 157 patients were categorised as ‘definite IPF’ and 220 patients were given a working diagnosis of IPF or ‘possible IPF’. The baseline demographics of patients included in the Edinburgh IPF study cohort are displayed in Table 14. For the survival analyses, the date of presentation was defined as the patient’s first HRCT scan confirming ILD. The census date was 21/11/14. Only

one patient underwent a lung transplant thus a time-to transplant or death analysis was not performed.

Table 14. Patient demographics of the Edinburgh IPF study cohort.

	ALL IPF **N=377**	**DEFINITE IPF** **N=157**	**WORKING DIAGNOSIS IPF** **N=220**	**P-value**
DEFINITE IPF?	30.8% met 'definite UIP' criteria on HRCT 41.6% were diagnosed with IPF based on ATS/ERS/JRS/ALAT criteria			
Surgical lung biopy (%)	43 (11.4)	43 (27.4)	0	N/A
Age (SD)	74.0 (8.6)	73.0 (9.4)	74.0 (8.2)	0.159
Male (%)	229 (60.7)	95 (60.5)	125 (56.8)	0.473
Never smoked (%)	93 (24.7)	36 (22.9)	55 (25.0)	0.639
FVC % predicted	90.5 (76.5,106.6)	89.4 (70.4,100.9)	92.3 (79.4,109.9)	0.075
TCO % predicted	50.8 (31.7,61.2)	47.7 (38.4,57.4)	51.9 (41.0,66.8)	0.003

Data presented as median (interquartile range) unless otherwise stated

Baseline and Longitudinal lung function

Clinical evaluation and baseline pulmonary function testing were performed within 3 months of presentation in most patients (305 of 377, 80.9%). Patients unable to perform baseline VC or TLCO were deemed non-eligible for recruitment, consistent with the study protocol for all 4 of these trials. Eight patients did not have any baseline spirometry; 4 were deemed too frail, 2 were unable to perform the test due to dementia, 1 patient died prior to PFT testing and 1 patient declined testing. Forty five patients did not have a TCO performed at baseline as they were too frail to perform the test. Baseline PFT data were consistent with IPF in the majority of cases. There were 254 of 369

(68.8%) patients with a normal baseline FVC (defined as >80% predicted) and 21 of 332 (5.7%) with a TCO ≥80% predicted. Only 20 out of the 369 patients (5.4%) had a normal FVC and TCO at presentation. Of the 254 patients with normal baseline FVC, follow-up at 12 months revealed 48 patients were deemed too frail to undergo further PFTS, and 45/206 (21.8%) patients had suffered an FVC decline of ≥10%, with 25/206 (12.1%) below the 80% threshold of normality. There were also 8 deaths (3.1%) in this group. There were 104/369 (28.2%) with an FVC of 50-79% of predicted at baseline. At 12 month follow-up, 25 patients were too frail for further PFTs and 19/79 (24.1%) had a ≥10% decline in FVC. There were 14 deaths (13.5%) in this group. There were 11/369 (3.0%) patients with a baseline FVC of <50% predicted. Follow-up at 12 months revealed 6 patients were too frail for further PFTs and 2/5 (40.0%) had a ≥10% decline in FVC. There were 3 (27.3%) deaths in this group.

Of the 21 patients with normal TCO at baseline, at 12 month follow-up, 2 patients were deemed too frail for further PFTs, and 9/19 (47.4%) patients had suffered a TCO decline of ≥10%, with 9/19 (47.4%) below the 80% threshold of normality. There were no deaths in this group. There were 150/332 (45.2%) patients with a baseline TCO of 50-79% of predicted and 52/102 (51.0%) had a ≥10% drop in % predicted TCO at 12 months. Thirty one patients were deemed too frail for further PFTs. There were 3 (2.0%) deaths in this group. There were 161/332 (48.5%) patients with a TCO of <50% predicted at baseline, of those, 52 were too frail to undergo repeat PFTs at 12 months and 40/109 (36.7%) had suffered a ≥10% decline in %predicted TCO. There were 12 (7.5%) deaths in this group.

The annualised VC rate of decline was also estimated for patients in ‘definite IPF eligible’, ‘definite IPF ineligible’ and ‘possible IPF non-eligible’ groups based on eligibility criteria for each of the 4 trials. This data is shown in Figure 7 below.

Figure 7. Annual rate of VC decline in Edinburgh cohort grouped by PANTHER, CAPACITY, ASCEND and INPULSIS eligibility criteria.

STUDY	Definite IPF eligible	Definite IPF ineligible	Working diagnosis IPF	P-value definite IPF eligible vs definite IPF not eligible
PANTHER	-149.1 ml/yr (95%CI -179.9, -118.3)	-158.0 ml/yr (95% CI -244.4, -71.8)	-101.6 ml/yr (95% CI -128.9, -74.3)	<0.001
CAPACITY	-161.0 ml/yr (95% CI -195.7, -126.2)	-124.4 ml/yr (95% CI -184.6, -64.2)	-101.6 ml/yr (95% CI -128.9, -74.3)	<0.001
ASCEND	-168.1 ml/yr (95% CI -239.8, -96.4)	-137.4 ml/yr (95% CI -170.2, -104.6	-101.6 ml/yr (95% CI -128.9, -74.3)	<0.001
	IPF eligible	**IPF ineligible**	**Working diagnosis IPF non-eligible**	**P-value (95% CI) definite IPF eligible vs definite IPF not eligible**
INPULSIS	-126.6 ml/yr 95% CI -151.2, -102.4)	-103.3 ml/yr (95% CI -176.6, -29.9)	-102.5 ml/yr (95% CI -135.2, -69.7)	0.006

PANTHER

When eligibility criteria for the PANTHER trial were applied to the Edinburgh IPF cohort[21], 377 IPF patients were screened and of those, 110 (29.2%) definite IPF patients would have been eligible for the trial. Two hundred and twenty patients were excluded as they did not meet HRCT and/or lung biopsy criteria, 10 patients were excluded as baseline FVC was <50% predicted, 28 were excluded as baseline TLCO was <30% predicted and 3 were excluded as baseline FEV_1:FVC ratio was <0.65. Six patients were excluded as they were aged <35 or >85 years. Demographic data for patients with

definite IPF and eligible for PANTHER, definite IPF and non-eligible for PANTHER and working diagnosis of IPF, therefore excluded from PANTHER are shown in Table 15 below.

Table 15. Edinburgh IPF cohort patient demographic data based on eligibility for PANTHER trial .

	ELIGIBLE	NON-ELIGIBLE	**Working diagnosis IPF**	**P-value eligible vs non-eligible**
Number	N=110	N=47	N=220	
AGE (years)	71 (8.8)	77 (9.8)	74 (8.0)	0.0004
FVC % pred	92·7 (21·5)	81·1 (27·1)	93·8 (23·5)	0.017
TLCO % pred	51·7 (12·1)	32·7 (16·2)	53·4 (17·2)	<0.0001

Data presented as mean (standard deviation)

There were significant differences in patient age and lung function (% predicted FVC and % predicted TLCO) between the three groups. Survival curve analysis showed there were significant differences in mortality amongst the three groups with the median survival in the 'Definite IPF Eligible' group reported as 5.41 years (IQR 1.57, 5.45), compared to 1.91 years (IQR 0.87, 2.74) in the 'Definite IPF Non-eligible' group and 4.49 years (IQR 1.40, 5.19) in the 'Working diagnosis of IPF' group (P<0.0001). The unadjusted hazard ratio for patients ineligible versus eligible for PANTHER was 4.49 (95% CI 2.59-7.80, P<0.001). Cox proportional hazards modelling revealed sex, eligibility group and baseline % predicted TCO were all significant predictors of mortality (P=0.001, P=0.037 and P<0.0001 respectively). Using cox proportional hazards modelling, the curves were adjusted for age, sex and smoking status which revealed a hazard ratio for patients with 'definite IPF' and ineligible versus 'definite IPF' and eligible of 2.62 (95% CI 1.68 – 4.09, P<0.0001). The hazard ratio for patients with 'possible IPF' and therefore ineligible, versus 'definite IPF' and eligible was 0.94 (95% CI 0.68 – 1.28, P=0.667). The curves were then adjusted for age, sex, smoking status, height, baseline %predicted FVC and %predicted TLCO, which significantly

improved the model and reported a hazard ratio for patients with 'definite IPF' ineligible versus eligible for the PANTHER trial of 1.65 (95% CI 1.04 – 2.64, P=0.035) and 'possible IPF ineligible' versus 'definite IPF eligible' of 0.95 (95%CI 0.69 – 1.31, P=0.767). The annual VC rate of decline was also estimated for each of the three groups and was reported as -149.1ml (95%CI -179.9, -118.3, P<0.001) in the 'definite IPF eligible' group, -158.0ml (95% CI -244.4, -71.8, P<0.001) in the 'definite IPF ineligible' group and -101.6ml (95% CI -128.9, -74.3, P<0.001) in the 'possible IPF non-eligible' group. Unadjusted and adjusted survival curves are shown in Figure 8 below.

Figure 8. Survival curves and hazard ratios of patients eligible and non-eligible for PANTHER trial.

(a) Unadjusted KM curve for patients ineligible versus eligible

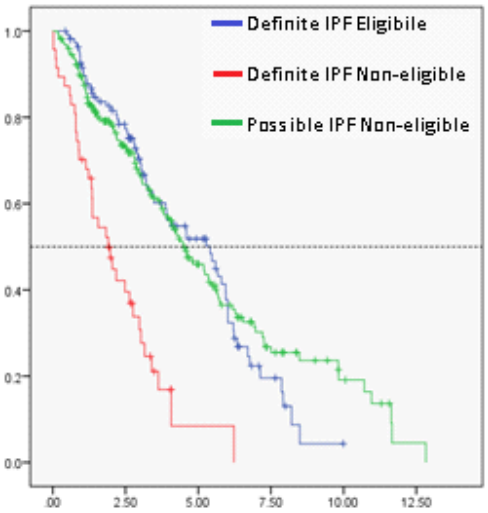

(b) Adjusted for age, sex, smoking status height, baseline %predicted FVC and %predicted TLCO

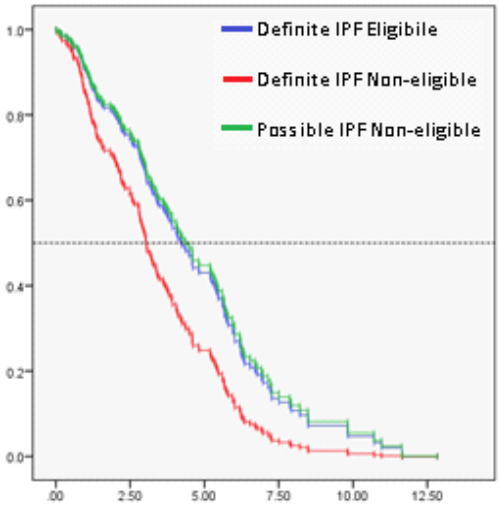

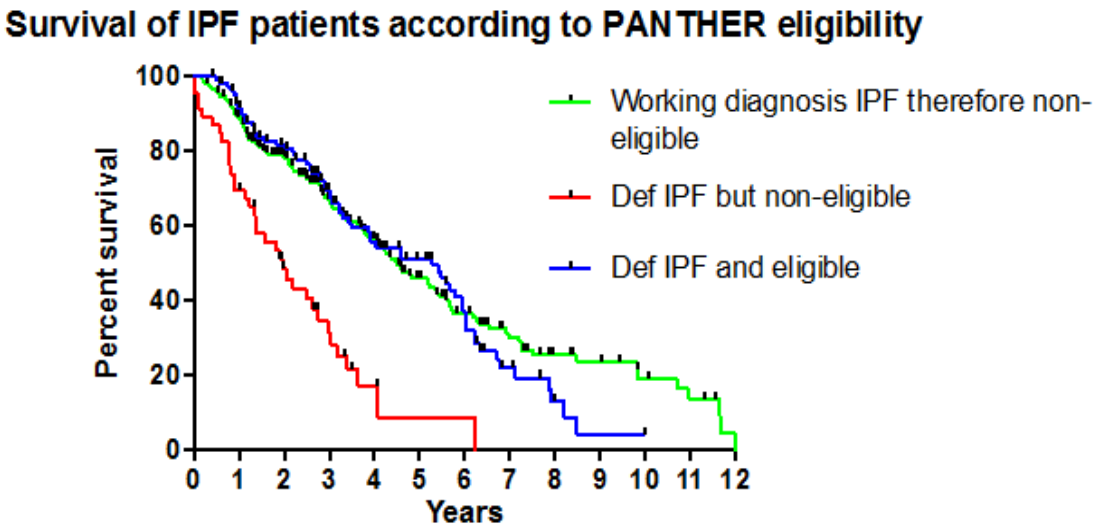

Definite IPF Non-eligible vs Definite IPF Eligible for PANTHER

Unadjusted	**HR 4.49**	**[95% CI 2.59 – 7.80]**	**P<0.0001**
Adjusted for age, sex, smoking status and eligibility group	**HR 2.62**	**[95% CI 1.68 – 4.09]**	**P<0.0001**
Adjusted for age, sex, smoking status, height, baseline %predicted FVC, %predicted TLCO and eligibility group	**HR 1.65**	**[95% CI 1.04 – 2.64]**	**P=0.035**

Possible IPF Non-eligible vs Definite IPF Eligible for PANTHER

Unadjusted	**HR 0.93**	**[95% CI 0·68 – 1·26]**	**P=0.636**
Adjusted for age, sex, smoking status and eligibility group	**HR 0.94**	**[95% CI 0.68 – 1.28]**	**P=0.677**
Adjusted for age, sex, smoking status, height, baseline %predicted FVC, %predicted TLCO and eligibility group	**HR 0.95**	**[95% CI 0.69 – 1.31]**	**P=0.767**

CAPACITY 004 and 006

When eligibility criteria for the CAPACITY trials were applied to the Edinburgh IPF cohort[22], 377 IPF patients were screened and of those, 88 (23.3%) definite IPF patients would have been eligible for this trial. Two hundred and twenty patients were excluded as they did not meet HRCT and/or lung biopsy criteria, 10 patients were excluded as baseline FVC was <50% predicted, 1 patients was excluded as baseline FVC and TLCO were >90% predicted, 38 were excluded as baseline TLCO was <35% predicted and 20 patients were excluded as they were aged <40 or >80 years. Demographic data for patients with definite IPF and eligible for CAPACITY, definite IPF and non-eligible for CAPACITY and working diagnosis of IPF, therefore excluded from CAPACITY are shown in Table 16 below.

Table 16. Edinburgh IPF cohort patient demographic data based on eligibility for CAPACITY trials.

	ELIGIBLE	NON-ELIGIBLE	**Working diagnosis IPF**	**P-value eligible vs non-eligible**
Number	N=88	N=69	N=220	
AGE	69 (7.6)	78 (9.5)	74 (8.0)	<0.0001
FVC % pred	90.9 (21.2)	87.3 (27.0)	93.8 (23.5)	0.361
TLCO % pred	54.0 (11.1)	37.6 (16.2)	53.4 (17.2)	<0.0001

Data presented as mean (standard deviation)

There were significant differences in age and % predicted TLCO between the three groups. Unadjusted survival curve analysis showed there were significant differences in mortality amongst the three groups with the median survival in the 'Definite IPF Eligible' group reported as 4.59 years (IQR 1.61, 5.60), compared to 2.76 years (IQR 1.18, 3.16) in the 'Definite IPF Non-eligible' group and 4.49 years (IQR 1.40, 5.19) in the 'Working diagnosis of IPF' group (P=0.002). The unadjusted hazard ratio for patients ineligible versus eligible for CAPACITY was 2.03 (95% CI 1.32-3.12, P=0.002). Cox proportional hazards modelling revealed sex, age, and baseline % predicted TCO were all significant predictors of mortality (P=0.002, P=0.048 and P<0.0001 respectively). Using cox proportional hazards modelling, the curves were adjusted for age, sex and smoking status which revealed a hazard ratio for patients in

the ‘definite IPF ineligible’ versus ‘definite IPF eligible’ group of 1.63 (95% CI 1.05 – 2.54, P=0.030) and ‘possible IPF ineligible’ versus ‘definite IPF eligible’ of 0.89 (95% CI 0.63 – 1.23, P=0.497). The curves were then adjusted for age, sex, smoking status, height, baseline %predicted FVC and %predicted TLCO, providing a final hazard ratio for patients in the ‘definite IPF ineligible’ versus ‘definite IPF eligible’ for CAPACITY of 0.92 (95% CI 0.58 – 1.47, P=0.730) and of 0.81 (95% CI 0.57 – 1.14, P=0.223) in the ‘possible IPF ineligible’ versus ‘definite IPF eligible’ group. The estimated annual VC rate of decline was reported as -161.0 ml (95% CI -195.7, -126.2, P<0.001) in the ‘definite IPF eligible’ group, -124.4ml (95% CI -184.6, -64.2, P<0.001) in the ‘definite IPF ineligible group, and -101.6ml (95% CI -128.9, -74.3, P<0.001) in the ‘possible IPF non-eligible’ group. Unadjusted and adjusted survival curves are shown in Figure 9 below.

Figure 9. Survival curves and hazard ratios of patients eligible and non-eligible for CAPACITY trials.

(a) Unadjusted KM curve for patients ineligible versus eligible

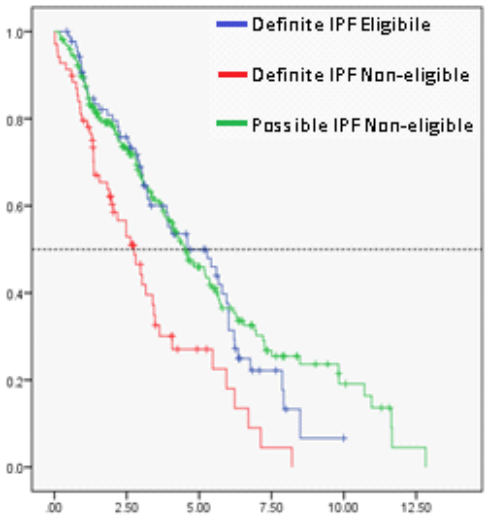

(b) Adjusted for age, sex, smoking status, height, baseline %predicted FVC and %predicted TLCO

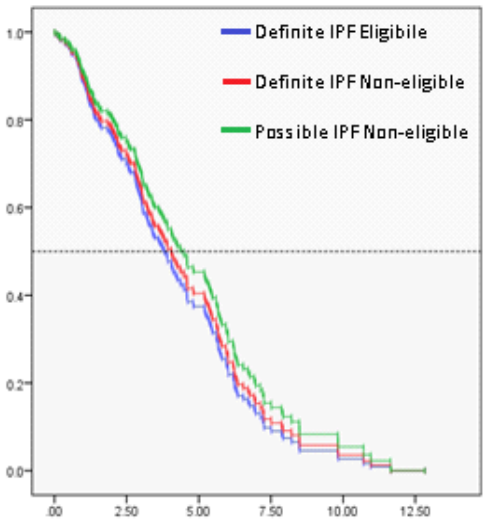

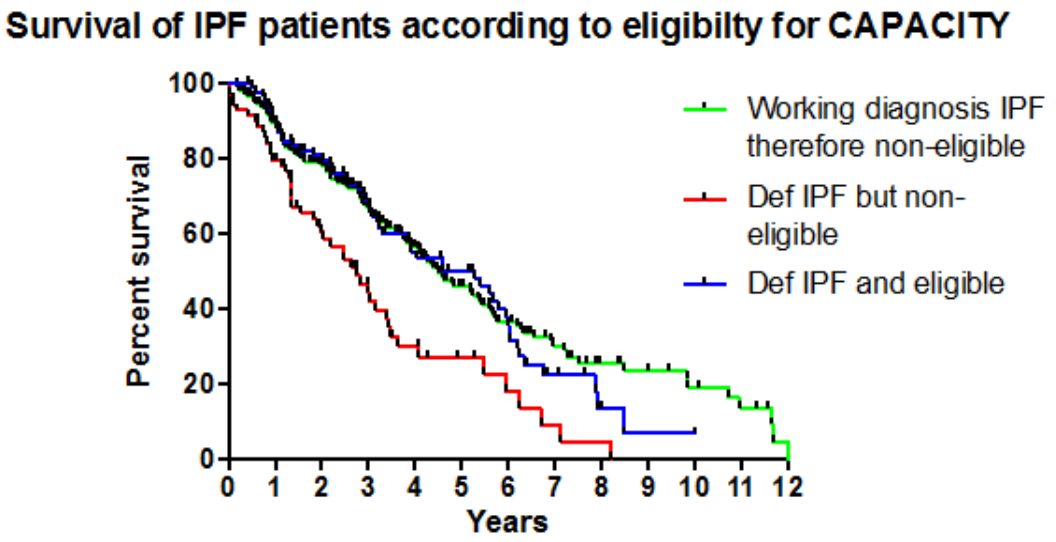

Definite IPF Non-eligible vs Definite IPF Eligible for CAPACITY 004 and 006

Unadjusted	**HR 2.03**	**[95% CI 1.32-3.12]**	**P=0.002**
Adjusted for age, sex, smoking status and eligibility group	**HR 1.63**	**[95% CI 1.05 – 2.54]**	**P=0.030**
Adjusted for age, sex, smoking status, height, baseline %predicted FVC, %predicted TLCO and eligibility group	**HR 0.82**	**[95% CI 0.51 – 1.32]**	**P=0.415**

Possible IPF Non-eligible vs Definite IPF Eligible for CAPACITY 004 and 006

Unadjusted	**HR 0.92**	**[95% CI 0.66 – 1.27]**	**P=0.593**
Adjusted for age, sex, smoking status and eligibility group	**HR 0.89**	**[95% CI 0.63 – 1.23]**	**P=0.497**
Adjusted for age, sex, smoking status, height, baseline %predicted FVC, %predicted TLCO and eligibility group	**HR 0.81**	**[95% CI 0.57 – 1.14]**	**P=0.223**

ASCEND

When eligibility criteria for the ASCEND trial were applied to the Edinburgh IPF cohort[24], 377 IPF patients were screened and of those, 29 (7.7%) definite IPF patients would have been eligible for the trial. Two hundred and twenty patients were excluded as they did not meet HRCT and/or lung biopsy criteria, 10 patients were excluded as baseline FVC was <50% predicted, 74 were excluded as FVC was >90% of predicted, 18 were excluded as TLCO was <30% or >90% predicted and 24 were excluded as their FEV_1:FVC ratio was <0.80. Two patients were excluded as they were aged <40 or >80 years old. Demographic data for patients with definite IPF and eligible for ASCEND, definite IPF and non-eligible for ASCEND and working diagnosis of IPF, therefore excluded from ASCEND are shown in Table 17 below.

Table 17. Edinburgh IPF cohort patient demographic data based on eligibility for ASCEND.

	ELIGIBLE	**NON-ELIGIBLE**	**Working diagnosis IPF**	**P-value eligible vs non-eligible**
Number	N=29	N=128	N=220	
AGE	69 (8.8)	74 (9.3)	74 (8.0)	0.011
FVC % pred	73.0 (10.0)	93.0 (24.5)	93.8 (23.5)	<0.0001
TLCO % pred	49.0 (11.7)	47.6 (16.3)	53.4 (17.2)	0.664

Data presented as mean (standard deviation)

There were significant differnces in age and % predicted FVC between the three groups. When ASCEND trial eligibility criteria were applied to the Edinburgh IPF study cohort, survival curve analysis did not demonstrate any significant differences in mortality amongst the three groups, however only 29 patients would have been eligible for by ASCEND criteria. Median survival in the 'Definite IPF Eligible' group was reported as 2.60 years (IQR 1.04, 4.04), compared to 3.63 years (IQR 1.35, 4.32) in the 'Definite IPF Non-eligible' group and 4.49 years (IQR 1.40, 5.19) in the 'Working diagnosis of IPF' group (P=0.078). The unadjusted hazard ratio for patients ineligible versus eligible for ASCEND was 0.69 (95% CI 0.38-1.13, P=0.078). Cox proportional hazards modelling revealed sex, age and baseline % predicted TCO were all significant predictors of mortality in the model (P=0.001, P=0.012 and P<0.0001 respectively).

Using cox proportional hazards modelling, the curves were adjusted for age, sex and smoking status which revealed a hazard ratio for patients in the 'definite IPF ineligible' group versus 'definite IPF eligible' of 0.61 (95% CI 0.37 – 0.99, P=0.048) and of 0.48 (95% CI 0.30 – 0.78, P=0.003) in the 'possible IPF ineligible' versus 'definite IPF eligible' group. The curves were then adjusted for age, sex, smoking status, height, baseline %predicted FVC and %predicted TLCO, revealing a final hazard ratio for patients with 'definite IPF ineligible' versus 'definite IPF eligible' for ASCEND of 0.62 (95% CI 0.37 – 1.05, P=0.074) and of 0.63 (95% CI 0.38 – 1.03, P=0.065) in the 'possible IPF ineligible' versus 'definite IPF eligible' group. The estimated annual VC rate of decline was reported as -168.1ml (95% CI -239.8, -96.4, P<0.001) in the 'definite IPF eligible' group, -137.4ml (95% CI -170.2, -104.6, P<0.001) in the 'definite IPF non-eligible' group, and -101.6 ml (95% CI -128.9, -74.3, P<0.001) in the 'possible IPF non-eligible' group. Unadjusted and adjusted survival curves are shown in Figure 10 below.

Figure 10. Survival curves and hazard ratios of patients eligible and non-eligible for ASCEND trial.

(a) Unadjusted KM curve for patients ineligible versus eligible

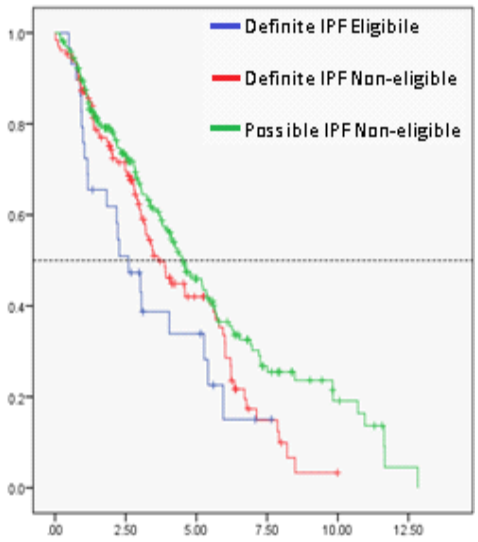

(b) Adjusted for age, sex, smoking status height, baseline %predicted FVC and %predicted TLCO

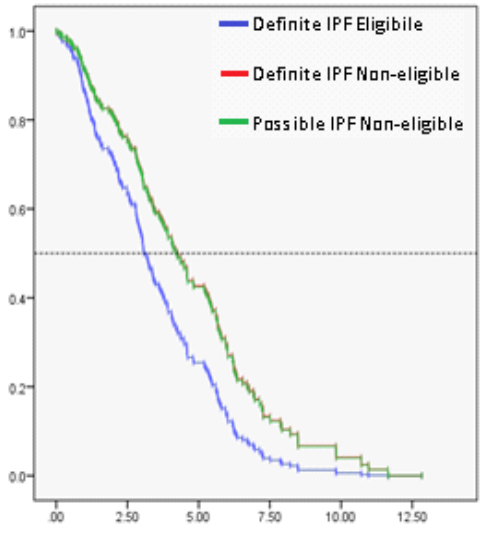

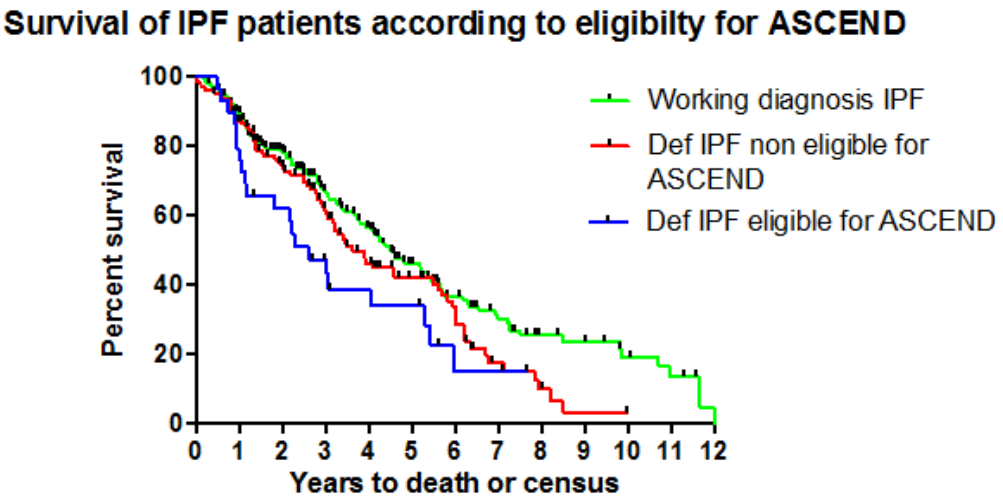

Definite IPF Non-eligible vs Definite IPF Eligible for ASCEND

Unadjusted	**HR 0.69**	**[95% CI 0.38 – 1.13]**	**P=0.078**
Adjusted for age, sex, smoking status and eligibility group	**HR 0.61**	**[95% CI 0.37 – 0.99]**	**P=0.048**
Adjusted for age, sex, smoking status, height, baseline %predicted FVC, %predicted TLCO and eligibility group	**HR 0.63**	**[95% CI 0.37 – 1.06]**	**P=0.083**

Possible IPF Non-eligible vs Definite IPF Eligible for ASCEND

Unadjusted	**HR 0.59**	**[95% CI 0.29 – 0.90]**	**P=0.022**
Adjusted for age, sex, smoking status and eligibility group	**HR 0.48**	**[95% CI 0.30 – 0.78]**	**P=0.003**
Adjusted for age, sex, smoking status, height, baseline %predicted FVC, %predicted TLCO and eligibility group	**HR 0.63**	**[95% CI 0.38 – 1.03]**	**P=0.065**

INPULSIS

Eligibility criteria for the INPULSIS trials were applied to the Edinburgh IPF cohort[25], 377 IPF patients were screened and of those, 238 (63.1%) IPF patients would have been eligible for the trial. Forty six patients were excluded as they did not meet the unique HRCT criteria for INPULSIS that required traction bronchiectasis as well as the other features of 'possible UIP' as per the ATS/ERS consensus criteria. Seventeen patients were excluded as baseline FVC was <50% predicted and 76 were excluded as baseline TLCO was <30% or >79% predicted. There were no patients under the age of 40. Demographic data for patients with IPF and eligible for INPULSIS, IPF and non-eligible for INPULSIS, and working diagnosis of IPF, therefore excluded from INPULSIS are shown in Table 18 below.

Table 18. Edinburgh IPF cohort patient demographic data based on eligibility for INPULSIS 1 and 2.

	ELIGIBLE	NON-ELIGIBLE	Working diagnosis IPF but no traction bronchiectasis	P-value eligible vs non-eligible
Number	N=238	N=93	N=46	
AGE	73 (8.8)	75 (8.9)	74 (7.2)	0.036
FVC % pred	92.8 (20.9)	85.8 (29.3)	98.9 (22.4)	0.089
TLCO % pred	51.4 (11.4)	44.9 (24.7)	57.6 (17.7)	0.087

There was a significant difference in age between the three groups, but no differences in lung function. When INPULSIS trial eligibility criteria were applied to the Edinburgh IPF study cohort, survival curve analysis revealed significant differences in mortality amongst the three groups. Median survival in the 'IPF Eligible' group was reported as 4.37 years (IQR 1.56, 5.26), compared to 2.76 years (IQR 1.26, 4.14) in the 'IPF Non-eligible' group and 5.37 years (IQR 2.76, 6.43) in the 'Working diagnosis of IPF, non-eligible' group (P=0.007). The unadjusted hazard ratio for patients ineligible versus eligible for INPULSIS was 1.29 (95% CI 1.13 – 2.05, P=0.007). This difference in eligible versus non-eligible was smaller than the equivalent comparisons for PANTHER, CAPACITY and ASCEND. Cox proportional hazards modelling revealed

sex and baseline % predicted TCO were significant predictors of mortality in the model (P=0.001 and P<0.0001 respectively). Using cox proportional hazards modelling, the curves were adjusted for age, sex and smoking status which revealed a hazard ratio for patients in the 'IPF ineligible' group versus 'IPF eligible' of 1.58 (95% CI 1.15 – 2.17, P=0.005) and of 0.78 (95% CI 0.52 – 1.17, P=0.230) in the 'working diagnosis IPF ineligible' group versus 'IPF eligible'. The curves were then adjusted for age, sex, smoking status, height, baseline %predicted FVC and %predicted TLCO, demonstrating a final hazard ratio for patients with IPF deemed ineligible versus IPF eligible for INPULSIS of 1.44 (95% CI 1.02 – 2.04, P=0.041) and patients with 'working diagnosis of IPF non-eligible' versus 'IPF eligible' of 0.86 (95% CI 0.57 – 1.31, P=0.487). The estimated annual VC rate of decline was calculated as -126.8 ml (95% CI -151.2, -102.4, P<0.001) in the 'IPF eligible' group, -103.3 ml (95% CI -176.6, -29.9, P<0.006) in the 'IPF non-eligible' group, and -102.5ml (95% CI -135.2, -69.7, P<0.001) in the 'working diagnosis IPF Non-eligible' group. Unadjusted and adjusted survival curves are shown in Figure 11 below.

Figure 11. Survival curves and hazard ratios of patients eligible and non-eligible for INPULSIS trials.

(a) Unadjusted KM curve for patients ineligible versus eligible

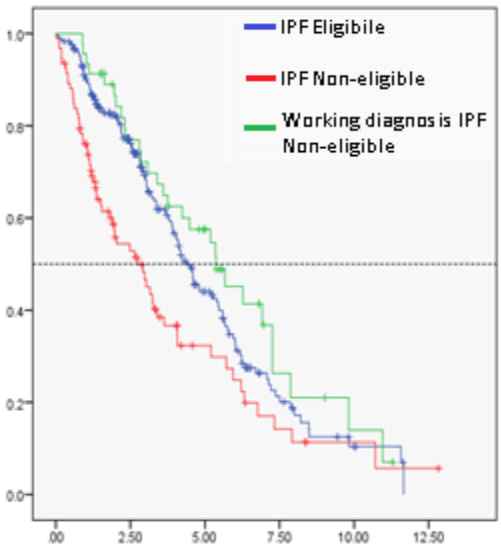

(b) Adjusted for age, sex, smoking status height, baseline %predicted FVC and %predicted TLCO

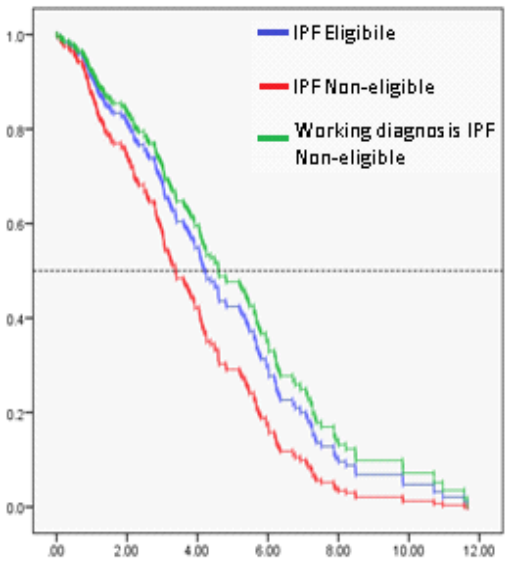

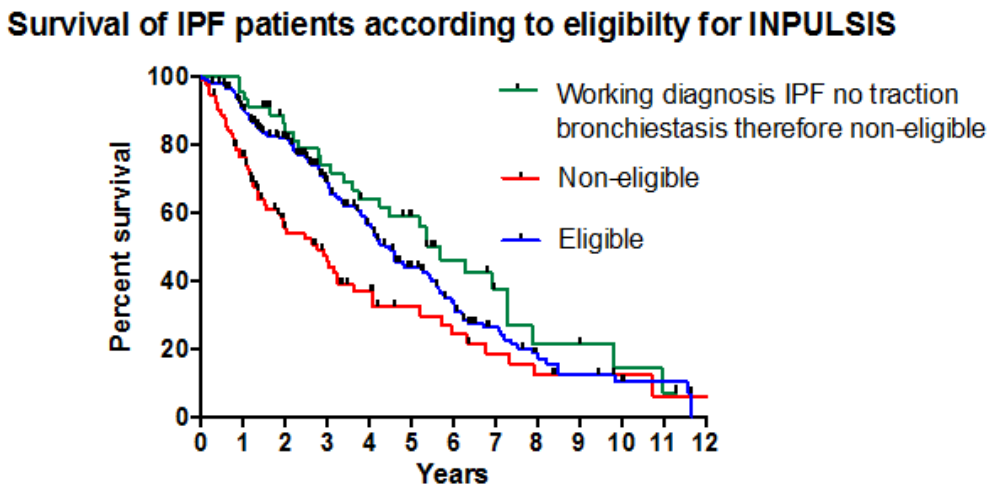

IPF Non-eligible vs IPF Eligible for INPULSIS 1 and 2

Unadjusted	**HR 1.29**	**[95% CI 1.13 – 2.05]**	**P=0.007**
Adjusted for age, sex, smoking status and eligibility group	**HR 1.58**	**[95% CI 1.15 – 2.17]**	**P=0.005**
Adjusted for age, sex, smoking status, height, baseline %predicted FVC, %predicted TLCO and eligibility group	**HR 1.47**	**[95% CI 1.04 – 2.08]**	**P=0.030**

Working diagnosis IPF Non-eligible vs IPF Eligible for INPULSIS 1 and 2

Unadjusted	**HR 0.80**	**[95% CI 0.55 – 1.17]**	**P=0.263**
Adjusted for age, sex, smoking status and eligibility group	**HR 0.78**	**[95% CI 0.52 – 1.17]**	**P=0.230**
Adjusted for age, sex, smoking status, height, baseline %predicted FVC, %predicted TLCO and eligibility group	**HR 0.86**	**[95% CI 0.57 – 1.31]**	**P=0.487**

3.2.3 Surgical lung biopsy in ILD

Between 01/01/07 and 31/12/13, 555 consecutive, locally-referred, incident patients with suspected IIP presented to the Edinburgh Lung Fibrosis clinic. Of these patients 166 underwent video-assisted thoracoscopic lung biopsy. Based on the 2011 ATS/ERS HRCT criteria, 87 patients were categorised as 'definite UIP' of whom 3 underwent SLB for clinical indications. Two hundred and nine patients were diagnosed with 'probable UIP' and 42 underwent SLB. Two hundred and fifty nine patients had HRCTs deemed 'inconsistent with UIP', SLB was performed in 121 patients. A further 60 patients were referred from outwith Lothian (tertiary referrals) with suspected IIP for SLB. Thirteen patients had 'probable UIP' appearances on HRCT and 47 patients had 'inconsistent with UIP' HRCTs. Significant differences in age, lung function and smoking status were noted between patients who underwent SLB and those who did not undergo SLB in the 'probable UIP' HRCT appearances group. Patient demographics are shown in Table 19 below.

Table 19. Patient demographics of referrals to Edinburgh Lung Fibrosis Clinic.

	Definite UIP HRCT pattern and no SLB **N=84**	Definite UIP HRCT pattern and SLB **N=3**	P-value	Probable UIP HRCT pattern and no SLB **N=167**	Probable UIP HRCT pattern and SLB **N=55**	P-value	Inconsistent with UIP HRCT pattern and no SLB **N=138**	Inconsistent with UIP HRCT pattern and SLB **N= 168**	P-value
Age in years (SD)	76.0 (+/- 8.4)	67.3 (+/- 4.62)	0.073	75.0 (+/- 7.8)	65.1 (+/-8.0)	<0.0001	68.0 (+/-12.1)	60.3 (+/-12.9)	0.032
Male (%)	58 (69.0%)	3 (100.0%)	0.268	102 (61.1%)	36 (65.5%)	0.560	71 (51.4%)	67 (39.9%)	0.045
Never smoked (%)	19 (22.6%)	1 (33.3%)	0.667	44 (26.3%)	13 (23.6%)	0.692	42 (30.4%)	68 (43.5%)*	0.019
Ex-smoker (%)	60 (71.4%)	2 (66.7%)	0.861	112 (67.1%)	29 (52.7%)	0.055	67 (48.6%)	53 (34.0%)*	0.009
Current smoker (%)	5 (6.0%)	0	0.718	11 (6.6%)	13 (23.6%)	0.0004	29 (21.0%)	35 (22.4%)*	0.768
VC in Litres (IQR)	2.70 (2.08,3.16)	3.76 (3.44,3.78)	0.040	2.66 (1.92,3.21)	2.80 (2.27,3.64)	0.0008	2.60 (2.08,3.41)	2.59 (2.10,3.50)	0.643
VC % predicted in Litres (IQR)	89.4 (72.7,100.7)	84.0 (77.0,89.0)	0.593	88.8 (76.4,104.3)	90.0 (77.0,100.0)	0.691	90.0 (75.6,103.6)	91.0 (71.0,107.0)	0.541
TLCO (mm/min/ mmHg) (IQR)	3.17 (2.24,4.34)	4.38 (4.14,5.10)	0.057	3.59 (2.90,4.57)	4.22 (3.48,5.40)	0.0002	4.32 (3.19,5.71)	4.50 (3.40,5.83)	0.325
TLCO %predicted (IQR)	43.7 (31.2,55.0)	44.0 (41.5,54.5)	0.548	50.9 (40.0,61.7)	52.0 (43.0,62.0)	0.894	58.0 (46.0,72.1)	56.0 (44.0,69.0)	0.892

*No smoking status recorded for 12 patients

Two hundred and twenty two patients in our cohort had HRCT appearances consistent with 'probable UIP'. Fifty five of those patients went on to have SLB. In this group, 30 patients were aged over 65 years, and 25/30 (83%) had UIP on biopsy. Six patients were aged over 75 years, and IPF was confirmed with a UIP biopsy in 6/6 (100%). There were no significant differences in the numbers of SLBs performed each year of the study period; there were 19 SLBs in 2007, 33 in 2008, 29 in 2009, 26 in 2010, 47 in 2011, 35 in 2012 and 37 in 2013. The full histopathology results are described in Table 20 below. In the 'probable UIP' HRCT group, the positive predictive value of a UIP biopsy in diagnosing IPF was 100% and the negative predictive value was 88%. The sensitivity and specificity of a UIP biopsy in diagnosing IPF were 95% and 100% respectively. In the patient group with HRCT appearances 'inconsistent with UIP', the positive predictive value of a UIP biopsy for an IPF diagnosis was 62% and the negative predictive value 100%, sensitivity and specificity were 100% and 95% respectively.

Table 20. SLB histopathology.

Definite UIP HRCT pattern and SLB **N=3**	**Probable UIP HRCT pattern and SLB** **N=55**	**Inconsistent with UIP HRCT pattern and SLB** **N= 168**
Definite UIP – 1***	Definite UIP – 32***	Hypersensitivity pneumonitis – 30
Possible UIP – 1***	Probable UIP – 4***	Non-classifiable fibrosis – 25
Probable UIP – 1***	Possible UIP – 2**	Fibrotic NSIP – 19
	Non-classifiable fibrosis – 3**	Definite UIP – 15*
		Sarcoidosis – 16
	Hypersensitivity pneumonitis – 5	RB-ILD – 14
		COP –11
	Fibrotic NSIP – 2	Bronchiolitis – 9
	COP – 2	Mixed cellular/ fibrotic NSIP – 6
	Cellular NSIP – 1	Langerhans histiocytosis – 5
	Sarcoidosis – 1	Wegeners granulomatosis – 5
	Bronchitis – 1	Lipoid pneumonitis – 3
	No abnormality – 1	Tuberculosis – 2
	Occupational lung disease – 1	Silicosis – 2
		Emphysema – 2
		Diffuse nodular lymphoid hyperplasia – 1
		Aspiration pneumonitis – 1
		Non-specific inflammation – 1
		CTD-ILD – 1

Key:*IPF, **Probable IPF, *Possible IPF based on ATS/ERS recommendations. **NSIP**: Non-specific interstitial pneumonia; **COP:** Cryptogenic organising pneumonia; **RB-ILD:** Respiratory bronchiolitis-associated interstitial lung disease; **CTD-ILD:** Connective tissue disease-associated interstitial lung disease.*

Post-operative mortality and morbidity

Post-operative complications were assessed using the Clavien-Dingo Classification of Surgical Complications grading system, and occurred in 39% (89/226) of procedures. In the 'definite UIP' HRCT group, 67% of patients (2/3) suffered severe complications. There were no mild-moderate postoperative complications in this group. The most common complications were persistent air-leak requiring prolonged intercostal chest drain insertion (67%) and postoperative pneumonia (33%). Sixty seven percent (2/3) of patients required admission and treatment in a critical care area in the post-operative period. The median (IQR) length of hospital stay was 9 (6-9.5) days. One patient (33%) was readmitted to hospital within one month of discharge, this was due to post-operative pneumonia and a persistent air-leak post VATS, the patient died during admission.

In the 'possible UIP' HRCT cohort, 20% (11/55 patients) suffered mild-moderate postoperative complications and 11% (6/55) suffered severe postoperative complications. In this group, the most common postoperative complications were persistent air-leak (9%), of which 40% required prolonged intercostal chest drain insertion, pneumonia (7%), and respiratory failure secondary to acute exacerbation of IPF (7%). Other complications included persistent chest pain (4%), pulmonary embolism (2%) and empyema (2%). 9% (5/55) of patients required treatment in a critical care area during admission, and 9% (5/55) were readmitted to hospital within one month, with 100% of readmissions due to a postoperative complication. The median (IQR) length of hospital stay was 3 (3-4) days. SLB was performed as an elective procedure in 98% of patients (54/55), however one patient underwent a non-elective procedure due to ongoing deterioration during admission.

In the group with HRCT appearances 'inconsistent with UIP' mild-moderate postoperative complications were observed in 36% (61/168) of patients, and severe in 5% (9/168 patients). In this cohort the most common complication was persistent air-leak (13%), of which 23% required prolonged intercostal chest drain insertion, prolonged chest pain post-procedure (11%), postoperative pneumonia (7%), wound infection (4%) and exacerbation of ILD (3%). Other complications included urinary retention (2%), lung abscess (0.6%) and small bowel ileus (0.6%). Five patients (3%) were converted to mini-thoracotomy during the procedure and this was associated with

a significantly increased complication rate. The majority of procedures were performed electively (96%), however 7/168 patients had a non-elective SLB due to deterioration as an inpatient. Five percent (9/168) of patients required critical care input and spent time in a critical care area during admission. The median (IQR) length of hospital stay was 3 (3-4) days. Eleven percent (18/168) of patients were readmitted to hospital within one month, with 100% of readmissions due to a postoperative complication.

There were 210 deaths (34.1% of the cohort) at the census date, which allowed for 12 months of follow-up following study completion. Forty six deaths (20.4%) were reported in the surgical lung biopsy cohort; 100% (3/3) in the 'definite UIP' HRCT group, 38% (21/55) in the 'probable UIP' HRCT group and 13% (22/168) in the group with HRCT appearances 'inconsistent with UIP'. The most common cause of death was idiopathic fibrosis, followed by pneumonia and lung cancer.

With regard to early deaths, in the 'definite UIP' HRCT group, in-hospital mortality was 33% (1 death), 30-day mortality was 33% (1 death) and 90-day mortality was 33% (1 death). In the 'probable UIP' HRCT cohort, in-hospital was 3% (2 deaths), 30-day mortality was 7% (4 deaths) and 90-day mortality was 7% (4 deaths). In the group with HRCT appearances 'inconsistent with UIP' in-hospital was 0.6% (1 death), 30-day mortality was 0.6% (1 death) and 90-day mortality was 1% (2 deaths). For the SLB cohort as a whole, the in-hospital mortality was 1.8% (4/226), 30-day mortality was 2.7% (6/226) and 90-day mortality was 3.5% (8/226). Postoperative complication rates and mortality data are described in Tables 21 and 22 below.

Table 21. SLB postoperative mortality and morbidity rates.

	Definite UIP HRCT pattern and no SLB **N=84**	Definite UIP HRCT pattern and SLB **N=3**	Probable UIP HRCT pattern and no SLB **N=167**	Probable UIP HRCT pattern and SLB **N=55**	Inconsistent with UIP HRCT pattern and no SLB **N=138**	Inconsistent with UIP HRCT pattern and SLB **N= 168**
Mild-moderate postoperative complication (Clavien-Dingo Grade I-II)	N/A	0	N/A	11 (20%)	N/A	61 (36%)
Severe postoperative complication (Clavien-Dingo Grade III-V)	N/A	2 (67%)	N/A	6 (11%)	N/A	9 (5%)
30-day mortality post-SLB	N/A	1 (33%)	N/A	4 (7%)	N/A	1 (0.6%)
Deceased on census date 19/12/14	49 (58%)	3 (100%)	88 (53%)	21 (38%)	27 (20%)	22 (13%)

Table 22. Cause of death of biopsy patients.

Total deaths	46 (100.0%)
Idiopathic pulmonary fibrosis	15 (32.6%)
Pneumonia	11 (23.9%)
Lung cancer	4 (8.7%)
Cancer (excluding lung cancer)	2 (4.3%)
Pulmonary embolism	2 (4.3%)
Hypersensitivity pneumonitis	2 (4.3%)
Empyema	1 (2.2%)
Chronic obstructive pulmonary disease	1 (2.2%)
Fibrotic non-specific interstitial pneumonia	1 (2.2%)
No data	7 (15.2%)

The mean survival time following SLB was 76.2 months (95% CI 71.3 – 81.1). All-cause mortality following SLB amongst the three groups was significantly different (P<0.0001). Mean survival was 21.5 months in the 'definite UIP' HRCT group (95%CI

0.0 – 58.7), 60.3 months in the 'probable UIP' HRCT group (95% CI 51.3 – 69.3) and 82.8 months (95% CI 77.8 – 87.8) in the 'inconsistent with UIP' HRCT group. Risk factors for all-cause mortality following SLB were identified as male sex (HR 2.28 (95% CI 1.04 – 4.99), P=0.039), increased comorbidity as evidenced by the Updated Charlson Index[76]. An Updated Charlson Index of ≥4 was significantly associated with increased mortality following SLB (HR 5.29, (95% CI 1.21 – 23.12), P=0.027). HRCT group was also significantly associated with mortality post-SLB (P=0.015) with patients in 'probable UIP' and 'inconsistent with UIP' HRCT groups having reduced mortality compared to those in the 'definite UIP' HRCT group (HR 0.27 (95% CI 0.06 – 1.20), P=0.085, and HR 0.12 (95% CI 0.02 – 0.58), P=0.008 respectively). Reduced baseline TCO was also an important risk factor (HR 0.02, 95% CI 0.02 – 0.22), P=0.001).

When SLB results and HRCT appearances were combined, patients were grouped into three groups; definite IPF based on an UIP HRCT alone, definite IPF based on a possible UIP HRCT combined with a UIP biopsy, and possible IPF or not IPF based on an inconsistent with UIP HRCT and a definite or probable UIP biopsy. Mortality was significantly different between the three groups with a mean survival of 40.7 months in the definite UIP HRCT group (95% CI 33.2 – 48.2), 62.1 months in the possible UIP HRCT and UIP biopsy group (95% CI 50.7 – 73.5) and 109.7 months in the possible IPF or not IPF group based on an inconsistent with UIP HRCT and a definite or probable UIP SLB (95% CI 59.6 – 159.8), P=0.014 (Figure 12).

Figure 12. Kaplan-Meier Survival Curve adjusted for age, sex, smoking status, Updated Charlson Index, HRCT group and baseline lung function.

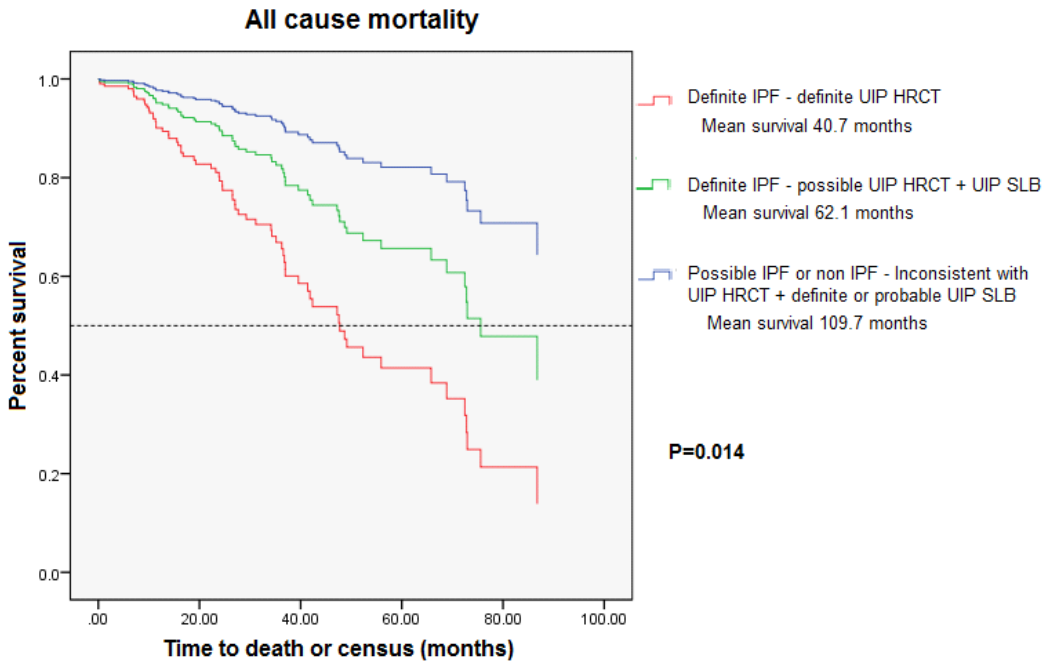

No significant risk factors for death within 30 days or 90 days of biopsy were identified, however HRCT group was a significant risk factors for death within 12 months (P=0.006). Subgroup analysis of the 'probable UIP HRCT' cohort revealed significant risk factors for death following SLB were age (HR 0.867 (95% CI 0.775 – 0.969), P=0.012) and an overall percentage of fibrosis on HRCT of >50% (HR 14.857 (95% CI 2.416 – 91.359), P=0.004). Additional important risk factors were male sex (HR 6.330 (95% CI 0.966 – 41.485), P= 0.054) and an Updated Charlson Index of ≥4 (HR 32.194, (95% CI 0.692 – 1496), P=0.076). No significant risk factors specifically for 30 day, 90 day and 1 year mortality were identified in this group.

Unadjusted mortality rates between patients with 'definite UIP' on HRCT alone, definite IPF with a 'probable UIP' HRCT and UIP biopsy, and 'probable UIP' HRCT appearances were significantly different (P=0.008, HR 0.44 (95% CI 0.240 – 0.812)). Patients with 'definite UIP' HRCT appearances had the poorest prognosis with a median survival of 35.1 months (95% CI 24.8 - 45.5), patients with 'probable UIP' HRCT appearances and who did not undergo further investigation by means of SLB

had a median survival of 51.0 months (95% CI 43.9 – 58.1). Patients with 'probable UIP' HRCT appearances, but went on to have 'definite IPF' confirmed by means of a UIP biopsy had the best prognosis, with a median survival of 72.4 months (95% CI 59.4 – 85.5). Approximately 20% of patients died within the first 12 months of diagnosis, regardless of how the diagnosis was made. When these curves were adjusted for age, sex, smoking status and baseline % predicted FVC and TLCO, there were no significant differences in survival between the three groups. Unadjusted and adjusted Kaplan-Meier survival curves for patients with suspected IPF are demonstrated in Figures 13 and 14.

Figure 13. Unadjusted Kaplan-Meier Survival Curve: Definite versus Probable UIP.

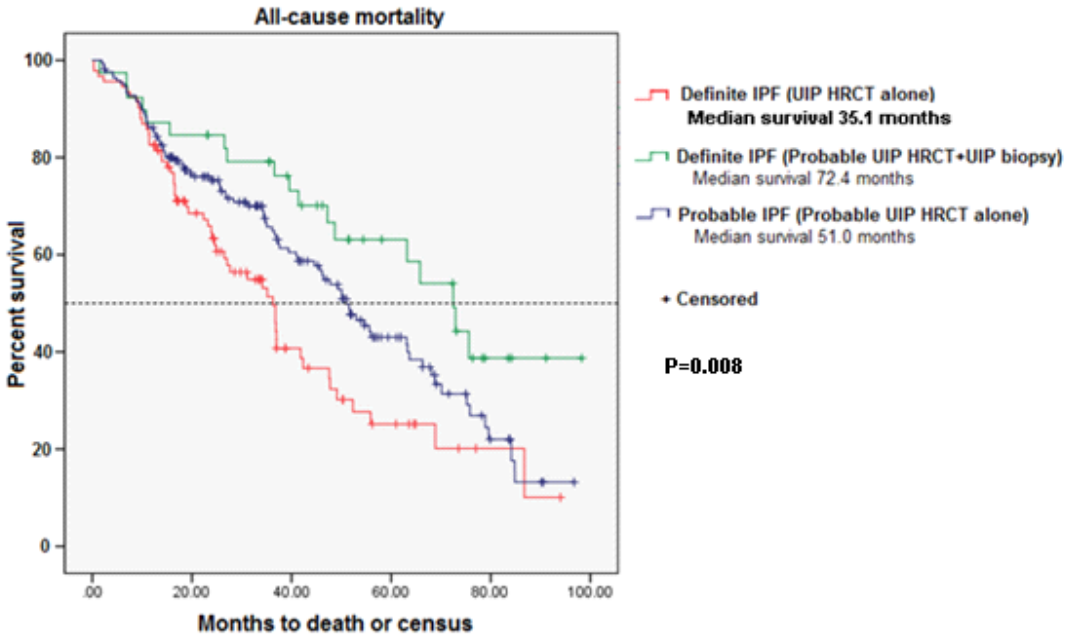

Figure 14. Kaplan-Meier Survival Curve adjusted for age, sex, smoking status and baseline lung function: Definite versus Probable UIP.

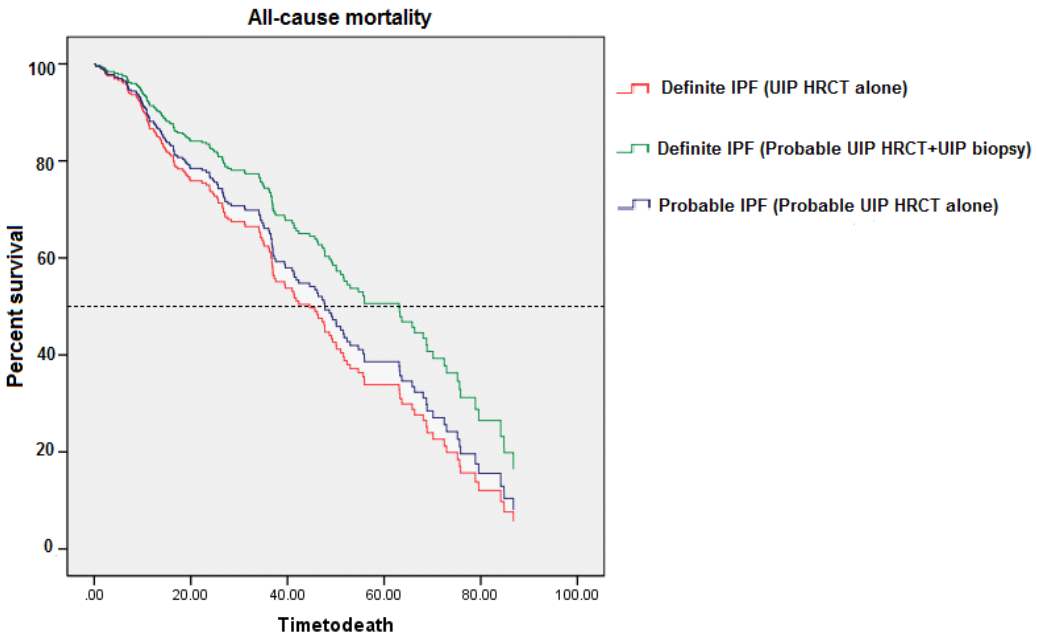

3.3 Discussion

The ILDs are a heterogeneous group of lung disorders characterised by varying degrees of parenchymal inflammation and fibrosis. Because of their heterogeneous nature, diagnostic accuracy and phenotyping are important components of both ILD and clinical practice and of epidemiological study.

We found that mortality could be predicted by serial change in VC and a related IPF Index, in patients with definite IPF and probable IPF to a similar degree. For both definite and probable IPF we found that a 5 to 10% decline in VC relative to baseline was associated with a 3-fold higher risk of mortality, similar to the hazard ratio reported by Du Bois et al[77]. In our cohort, the (relative) risk of mortality for change in VC appeared to be similar across the full spectrum of values for both definite and probable IPF, suggesting that clinicians may use change in VC as a prognostic indicator for patients with both definite and probable IPF, although a larger study would be required to validate this. For definite IPF, we found a similar median survival (3.4 years) but slightly higher one year mortality (14.6%) as previous studies, in which estimates

ranged from 2 to 4 years[32,78,79] and 2.7 to 9.0% respectively[22,80,81]. We also obtained similar estimates for decline in VC to previous groups, in which decline in VC was reported as an absolute change in FVC of 190 ml/year[80,82], an absolute change in percent predicted FVC of 3.5 to 8.0%[22,83], and change as a percentage of baseline FVC of -7.4%[84]. We found that two recently reported scoring systems for prognostication in IPF, the IPF Index and GAP Index, predicted (relative) mortality similarly in patients with definite and probable IPF. Furthermore, among patients in whom surgical lung biopsy would be advocated according to international guidelines, after adjusting for these IPF scores there was no difference in mortality among patients who did and did not have a biopsy. Consequently, patients with HRCT scans consistent with UIP have a similar prognosis according to the IPF score and GAP Index, whether or not their diagnosis was confirmed on biopsy.

The PANTHER, CAPACITY, ASCEND and INPULSIS trials have demonstrated that large randomised, placebo-controlled multicentre trials are feasible, and these studies have all changed clinical practice. Nintedanib and pirfenidone have been licensed for use and clinicians no longer use corticosteroids and azathioprine in the treatment of IPF. The nature of most interventional clinical trials dictates that the subjects are drawn from a relatively select population of patients. This is turn means that clinicians have to choose how to interpret the findings and apply them to 'real world' patients. Trials in IPF are no exception and perhaps this dilemma is exacerbated further because IPF is a heterogeneous disease that is subject to diagnostic variation despite attempts to refine the diagnosis by criteria-led consensus. The generalisabilty of IPF clinical trial data to real world patients is important to clinicians and patients. By comparing the baseline characteristics and the natural history of IPF patients who were deemed eligible or not eligible for recent landmark trials that have changed clinical practice, we found that the INPULSIS trials are more generalisable to real world IPF patients than PANTHER, CAPACITY and ASCEND. It is well recognised that very few real-life IPF patients meet inclusion criteria for clinical trials, and this was reflected in our study. In the Edinburgh IPF cohort 29.2% (110/377) patients would have been eligible for the PANTHER trial, 23.3% (88/377) eligible for CAPACITY, 7.7% (29/377) patients eligible for ASCEND and 63.1% (238/377) eligible for INPULSIS. There was a significant difference in survival between patients eligible versus non-eligible for PANTHER, CAPACITY and INPULSIS trials, with patients in the eligible group

displaying longer survival times in all three trials. Interestingly however, there was no significant difference in survival between patients categorised as 'definite IPF eligible' versus 'possible IPF non-eligible' in any of the trials, when adjusted for age, sex, smoking status, height, baseline %predicted FVC and %predicted TLCO.

There are very few observational studies detailing the natural history and characteristics of patients with IPF outside of clinical trials. The Edinburgh Lung Fibrosis cohort provided a unique opportunity because the patients were accurately phenotyped according to diagnostic criteria that were very similar or identical to ATS/ERS criteria, very few patients were lost to follow up and the majority of patients did not receive IPF-directed therapies. Most past IPF studies have recruited patients that are younger and have more preserved lung function than real world patients[80,81,85–88], and our data show the PANTHER and CAPACITY eligibility criteria promote this 'younger/milder' phenotype. Applying ASCEND eligibility criteria to our real world cohort yielded a young population with much lower VC than non-eligible patients. Only INPULSIS criteria generated eligible patients that were of a similar age and lung function as non-eligible.

Young age and preserved lung function are two of the reasons that the mortality in IPF trials has historically been low[89–91]. The 1 year mortality in the placebo arm of PANTHER study was around 2% even though subjects were rigorously ascertained to have definite IPF with almost 50% of subjects undergoing lung biopsy[21]. At the time this finding was surprising, but our data shows that applying the same lung function and age eligibility criteria as PANTHER to real world patients with definite IPF selects out a group of patients with relatively benign disease, such that 8% of eligible patients died with 12 months of presentation, but 30% of non-eligible patients died in the same period. The median survival in eligible patients was also correspondingly higher than in non-eligible patients (5·4 v 1·9 years) and there was less rapid decline in VC in the study-eligible patients.

This phenomenon of selecting out relatively benign disease was observed when we applied CAPACITY lung function and age criteria to our cohort of patients. A post-hoc analysis of subjects recruited to the CAPACITY 004 and 006 trial allowed investigators

to identify lung function characteristics that predicted faster decline in FVC and death, and these were applied to the subsequent ASCEND trial in an attempt to enrich the recruited pool of subjects with 'progressive disease'. Although the ASCEND study met its primary end-point and showed pirfenidone attenuated FVC decline over one year, the enrichment strategy was not particularly successful: the baseline characteristics of the subjects, the 1 yr mortality (5·6%) and the FVC decline were similar to the earlier CAPACITY studies[24,92]. This gives credence to subsequent pooled analyses of CAPACITY 004, 006 and ASCEND. However when applied to our real world cohort, the ASCEND eligibility criteria dramatically reduced the number of patients that would have been eligible to 8% of all IPF patients and 18% of patients with definite IPF. In stark contrast to the trial patients, almost 40% of real world eligible for ASCEND were dead by 12 months, suggesting a very different population of patients in the real world compared to ASCEND trial subjects.

The INPULSIS trial was unusual in that the investigators adopted HRCT criteria, specifically traction-bronchiectasis for defining patients with 'UIP-like' disease in the absence of lung biopsy, that were not defined or described in the consensus ATS/ERS guidelines. This immediately yielded a large number of our real-world cohort patients eligible for INPULSIS. These eligible patients had better survival than non-eligible patients with IPF, but the difference though statistically significant, was not as large as it was for PANTHER and CAPACITY. The same was true for the differences in VC decline. This suggests that INPULSIS eligible and non-eligible patients are more similar than corresponding eligible and non-eligible patients from other reported trials. Of interest, we also describe for the first time the survival and VC decline in a novel group of patients with 'possible UIP HRCT' (by ATS/ERS criteria) without traction bronchiectasis and without biopsy. Only 46 patients fulfilled these criteria, and they had a median survival of just under 6 years and an annualised rate of VC decline of 102ml/yr. There is as yet no data to show that antifibrotic drugs impact on this group of patients, but our analysis of these small numbers suggest there is disease progression and associated mortality in this group.

International consensus guidelines state that lung biopsy should be performed to distinguish IPF from other fibrotic interstitial lung diseases such as fibrotic NSIP or idiopathic HP, if patients do not meet 'definite UIP' HRCT criteria. The justification

for performing SLB is to identify patients with alternative diagnoses that may be amenable to treatment, or to provide patients and clinicians with prognostic information. However the evidence for treatment efficacy in patients with non-IPF fibrotic interstitial lung disease is very scarce, and is based on case series rather than controlled clinical trials[93,94]. Furthermore, recent data shows that using such evidence to inform treatment decisions may be harmful[21]. With regard to prognosis, our findings suggest that among patients with clinical features consistent with IPF and probable UIP on HRCT, lung biopsy appears to offer little additional prognostic information over simple clinical measures.

We report the proportion of patients with confirmed UIP on SLB, and complication rates and mortality following SLB by indication, age, sex and other baseline characteristics. Although patients undergoing SLB differ from those who do not have a biopsy, these patients are younger and more likely to have atypical findings on HRCT. Consequently, rates of alternative diagnoses are likely to overestimate the true negative predictive value of the test, which is conservative with respect to our hypothesis that SLB is of limited clinical utility in older patients with suspected IPF. Advanced age is a strong predictor for IPF, and in our cohort 83% of patients aged over 65 years and 100% of patients over 75 years with 'possible UIP' HRCT appearances had UIP on biopsy, therefore confirming the diagnosis of IPF. We suggest that advanced age and fibrotic appearances on HRCT negate the need for biopsy in this cohort. Fell et al found that in patients without honeycomb change on HRCT (ie 'probable UIP' appearances), older age and modest amounts of fibrosis were highly predictive of a diagnosis of IPF[17]. However it is important to note that the ATS/ERS consensus statement which details the IPF HRCT classification criteria was published after the Fell paper, and that the description of HRCT scans used by Fell and colleagues had a different scoring system. Our study is the only one to use the current ATS/ERS classification of 'possible' or 'probable' UIP, and therefore all patients in the 'probable UIP' category had an absence of honeycombing on HRCT.

In our cohort, a diagnosis of IPF was confirmed in 100.0% (3/3) of patients with 'definite UIP' and 67.3% (37/55) of patients with 'probable UIP' HRCT appearances following SLB. Based on histolological findings, a further 7.3% (4/55) were diagnosed with probable IPF according to ATS/ERS guidelines. Histology revealed an alternative

diagnosis in 24.1% (14/58) of patients with a 'definite' or 'probable' UIP HRCT, consequently leading to a change in management. These findings support the recommendation that SLB can be of value in the diagnosis of ILD, however it should be considered with caution in the subgroup of patients with suspected IPF, and 'probable UIP' HRCT appearances. Complications were relatively common following SLB, with 31.9% (72/226) suffering a mild-moderate complication and 7.5% (17/226) developing a serious complication in the postoperative period. Readmission rates for treatment of a postoperative complication were also reasonably high, the commonest cause of death in the postoperative period was pneumonia.

Despite international recommendations that patients have histological confirmation of the diagnosis, mortality between patients diagnosed by HRCT or by biopsy was similar, but the 30-day mortality for SLB was 7.3%. This figure was higher than typically reported in the literature, however these findings are similar to results of a large study reviewing in-hospital mortality following SLB for ILD in the USA over an 11-year study period, published recently by Hutchinson and colleagues. This study concluded that increasing age and comorbidity were the main risk factors for mortality following SLB, however male sex, open surgery and a diagnosis of suspected IPF or CTD-ILD were also associated with an increased risk[73]. With regards to our SLB cohort as a whole, in-hospital mortality was 1.8% (4/226), 30-day mortality was 2.7% (6/226) and 90-day mortality was 3.5% (8/226). These figures are slightly higher than the 30 and 90-day mortality rates following lobectomy for non-small cell lung cancer (both 2.3%), a potentially curative rather than diagnostic procedure. Risk factors for all-cause mortality following SLB were identified as increased comorbidity as evidenced by an Updated Charlson Index of ≥4, 'definite UIP' HRCT appearances and reduced baseline TCO. No significant risk factors for death within 30 or 90 days of biopsy were identified, however a 'definite UIP' HRCT scan was a significant risk factor for death within 12 months. The observation that around a fifth of patients were deceased at 12 months, regardless of how the diagnosis was made, is important. These patients are 'rapid progressors' and cannot be identified by HRCT or biopsy characteristics. There are several prognostic scoring systems based on clinical, physiological, radiological and serological parameters described in the literature to predict survival in IPF. However an important caveat of all of them is that they were all derived from either patients recruited to clinical trials or patients referred to tertiary referral centres, which undoubtedly leads

to bias. There are very few studies of large numbers of IPF patients directly referred from the community and followed longitudinally. At present there is no single risk model that has been validated, widely accepted and adopted in clinical practice.

Limitations of the study

Our study has some limitations. Whilst our cohort of IPF subjects was prospectively recruited as consecutive incident cases, the analyses were entirely retrospective. Diagnosis of IPF was made by expert consensus, but over the period of the study diagnostic criteria and level of experience was changed. We have attempted to be consistent with our diagnostic pathway, but we did not perform independent validation of diagnoses. That said, the natural history of IPF we describe is consistent with other cohorts. Another limitation is that lung biopsies were reviewed by a single pathologist, albeit one with a specialist interest in interstitial lung disease and using internationally accepted criteria for the diagnosis of UIP. Our cohort represented consecutively presenting patients referred to a respiratory clinic and not patients with acute, rapidly progressive ILD that may have presented as inpatients, and could not perform baseline lung function tests pre-treatment. Our laboratory routinely records VC rather than FVC. In patients with restrictive lung disease, it is reasonable to assume that these two measures will be similar[95]. There is no standard method to assess 'generalisabilty' of clinical trial data with real world patients. We have used one way to determine generalisabilty, that is a description of the natural history of disease in patients that would or would not be eligible for clinical trials and we are assuming that smaller differences in the natural history imply more generalisability. However there may be other methods of assessing generalisability that we have not considered. Importantly, our study is not designed to address efficacy of treatment in real-world IPF patients and should not be interpreted as such. Patients that are not eligible for a clinical trial but have the same disease entity as trial patients should respond in the same way as trial patients if the study is robust, large and well conducted, as was the case in all studies described in this paper. However with heterogeneous disease that may or may not include different disease entities, clinicians and policy makers need to decide how to extrapolate trial data to the real world.

3.4 Conclusions

Patients diagnosed with definite IPF have a slightly poorer prognosis and a faster decline in lung function than those with probable IPF, however the differences are not significant. Change in VC over the first six months from presentation predicts mortality similarly in definite and probable IPF and clinicians may use these clinical measures and a related prognostic IPF index to make prognostic statements in both groups. This may diminish the value of confirming a diagnosis of definite IPF by means of surgical lung biopsy. SLB can be of value in the diagnosis of ILD, however it should be considered with caution in the subgroup of patients with suspected IPF, and 'possible UIP' HRCT appearances. Despite international consensus guidelines that patients have histological confirmation of the diagnosis, the mortality between patients diagnosed by CT scan or by biopsy were similar, but the 30-day mortality for SLB was 7.5%. Advanced age is a strong predictor for IPF and the majority of patients in our cohort aged over 65 years with 'possible UIP' HRCT appearances had UIP on biopsy, therefore confirming the diagnosis of IPF and negating the need for biopsy in this age-group. The observation that around 20% of patients were deceased at 12 months, regardless of how the diagnosis was made, is important. These patients are 'rapid progressors' and cannot be identified by HRCT or biopsy characteristics. There is a need to identify this phenotype of rapidly progressive disease, perhaps through biomarker profiling.

My data indicates that treatment for IPF with either Pirfenidone or Nintedanib, may be beneficial in patients who are both more severe and less severe than those in randomised clinical trials, and also that the natural history of patients with 'definite IPF' and 'possible IPF' is very similar, and so such treatments could also be effective in the latter group.

It has been well documented that the mortality in IPF is high (around 20% per year), mortality in the placebo arms of the most recent clinical trials was much lower, ranging from 2.3% to 7.8%[91], suggesting the patients included in the trials are poorly reflective of a real life IPF patient population. The duration of follow-up was greater in the Edinburgh study cohort than any of the RCTs with a mean of 3.4 years (rnge 8 days to 12.8 years). Mortality was also greater in the Edinburgh IPF population than that of

which was reported in the trials (59.7% at censor date in Edinburgh cohort vs 5.8% in PANTHER, 6.2% in CAPACITY, 1.6% in ASCEND and 6.4% in INPULSIS). A higher rate of comorbidity was also documented in the Edinburgh cohort, highlighting the need for future clinical trials that include patients with common comorbidities such as diabetes, peripheral vascular disease, ischaemic heart disease, emphysema, reflux and pulmonary hypertension, as this would clearly represent a truer IPF patient population.

Patients recruited to clinical trials in IPF fall between defined age limits, present fewer comorbidities, and have well characterised disease severity. Consequently, they do not always reflect the real-life IPF patient population observed in clinical practice. The majority of our Edinburgh IPF cohort would have been excluded from recent trials and the outcome of excluded patients may be different to eligible patients. An interesting finding was that patients who did not meet ATS/ERS diagnostic criteria for 'definite IPF' and so were termed 'possible IPF' or 'Working diagnosis IPF' and deemed ineligible for clinical trials, had very similar survival curves to those in the 'definite IPF eligible' group. This may have implications on the suitability of those patients for treatment with anti-fibrotic drugs. Overall these findings may limit generalisability of clinical trials to our everyday clinical practice.

Chapter 4

A distinct alveolar macrophage polarisation phenotype and pattern of cell surface marker expression is associated with disease progression in IPF

4.1 Introduction

4.1.1 General introduction

The interstitial lung diseases (ILDs) are a heterogeneous group of lung disorders characterised by varying degrees of parenchymal inflammation and fibrosis. Idiopathic pulmonary fibrosis (IPF) is the commonest ILD and has a chronic, progressive nature. There is no proven cure and it carries the worst prognosis with a median survival of 3 years. IPF occurs worldwide however Scotland harbours the highest incidence in the UK. There are approximately 5000 new cases per year in the UK, with a disease prevalence of 5-15 cases per 100,000 population. In 2011, the American Thoracic Society (ATS), European Respiratory Society (ERS), Japanese Respiratory Society (JRS) and the Latin-American Thoracic Society (ALAT) published an international evidence-based guideline on the diagnosis and management of IPF. This guideline was revised in 2013. The consensus statement recommended that IPF could be diagnosed definitively in patients with an Usual Interstitial Pneumonia (UIP) pattern on high resolution CT scanning (HRCT), however in patients without honeycombing, a diagnosis of 'possible IPF' is made and further investigation by means of surgical lung biopsy (SLB) is required. The diagnostic algorithm does not allow for circumstances in which biopsy is not performed. Prior to the 2011 guideline, differential cell count (DCC) in bronchoalveolar lavage (BAL) was considered integral to the diagnosis of IPF, however in 2011 BAL was completely removed from the diagnostic algorithm. This shift remains controversial as BAL is a well-tolerated and safe procedure, with far fewer risks than SLB. Studies investigating the additional utility of BAL in the

diagnosis of IPF, largely conclude that BAL DCCs are of additional diagnostic benefit, even in patients with 'definite UIP' HRCT appearances. A study by Ohshimo et al demonstrated a BAL lymphocyte count of >30% was favourably discriminative for a diagnosis of IPF. In their study of 74 IPF patients, all of whom met ATS/ERS IPF criteria, 8% had a BAL lymphocyte count of >30, which changed diagnostic perception in all 6 of the 74 patients[96].

IPF is a highly heterogeneous disease and so the natural history and clinical course in each individual patient is difficult to predict. Many patients have a slow and steady deterioration over a period of years, whereas 10-15% of patients progress rapidly, often leading to death from respiratory failure in a few months. Our understanding of the pathogenesis of IPF is mostly extrapolated from histological appearances in subgroups of biopsied patients. It is thought that low-grade inflammation, oxidative cell injury and an abnormal healing process play a role in the development of usual interstitial pneumonia (UIP), the histological pattern that defines IPF. It is logical to propose that macrophages play a central role in IPF. Macrophages are integral to lung tissue repair and homeostasis, however in UIP it has been proposed that the process of normal tissue homeostasis and healing is aberrant. Many contributing mechanisms have been reported including angiogenesis, coagulation, fibrogenesis, tissue repair, inflammation, epithelial damage, matrix remodelling and oxidative stress. The most notable paradigm is one in which the alveolar epithelium is repeatedly injured creating localised 'wounds' over a prolonged period of time, which leads to focal epithelial hyperplasia and activation. The dysfunctional epithelial cells then activate profibrotic signalling pathways involving growth factors and chemokines, which lead to the accumulation of fibroblasts in 'fibroblastic foci', areas of intense collagen generation and differentiation of myofibroblasts, resulting in increased extracellular matrix (ECM) deposition.

Despite evidence that inflammation may not play a predominant role in IPF, there is evidence that markers of inflammation and immunity may provide useful information. Brittan et al reported the presence of novel subpopulations of pulmonary monocyte-like cells (PMLCs) in the human lung; resident PMLC (rPMLC, HLA-DR+CD14++CD16+ cells) and inducible PMLC (iPMLC, HLA-DR+CD14++CD16- cells). Their data showed that PMLCs represented a significant proportion of cells present in BAL following inhalation of lipopolysaccharide (LPS), implying PMLC may play a

significant role in the inflammatory response. Resident PMLC were found to have a significantly increased expression of the mature macrophage markers CD206 (mannose receptor), CD71 (transferrin receptor) and 25 F9, and a significantly increased expression of the proliferation antigen Ki67, compared to inducible PMLC[49,50].

IPF has been classified as a Th2-skewed disorder, with the presence of an 'M2' or 'alternatively activated' polarised lung macrophage phenotype. Mediators associated with M2 macrophage polarisation are associated with disease progression and severity. However, a comprehensive classification of the M2 phenotype is questionable, and there is some recognition that a distinct M2 'pro-repair' phenotype may exist and that macrophage phenotypes are dynamic and liable to change as disease evolves. This may, at least in part, explain some of the heterogeneity seen in IPF.

4.1.2 Hypothesis and aims

Reliable methods of predicting disease progression and survival are of great clinical value in IPF. We hypothesised that a distinct AM polarisation phenotype would be associated with disease progression in IPF. We aimed to quantify and perform detailed phenotyping of AMs and PMLCs in bronchoalveolar lavage (BAL) to determine the relationship between AM subtypes, PMLC populations and disease progression. We also aimed to determine the proportion of patients diagnosed with IPF on clinical and radiological grounds, in whom BAL differential count was inconsistent with IPF based on international pre-defined criteria. We aimed to explore the predictive value of BAL neutrophilia and BAL lymphocytosis on patient survival, the safety and feasibility of repeat BAL in IPF patients, and whether change in DCC between two successive BALs performed one year apart was an indicator of disease progression. We hypothesised that BAL DCC between definite and possible IPF was different and that baseline DCC predicted disease progression. Furthermore, we hypothesised that change in BAL DCC would be associated with disease progression.

4.1.3 Experimental methodology

Patient selection and the Edinburgh Lung Fibrosis Biobank

Between 01/01/2009 and 31/12/2013, 325 consecutive patients with suspected idiopathic interstitial pneumonia (IIP) presented to the Edinburgh ILD clinic. Of these 325 patients, 198 were diagnosed with definite or probable IPF based on pre-defined criteria (Figure 15). One hundred and twenty seven patients were diagnosed with another form of IIP. Of the 325 patients, 128 underwent a BAL at presentation. 197 patients did not have a BAL for the following reasons: patient not approached for consent within 3 months of presentation (n=48); consent declined by patient (n=11); patient deemed too frail or hypoxic (Sp02<92% on 2L oxygen) for BAL (n=65), BAL not indicated as clinical-radiological picture consistent with diagnosis or ILD mild (n=73). The 128 patients that did undergo BAL were grouped into 'definite IPF' (n=22), 'probable IPF' (n=62) and 'inconsistent with IPF' (n=44). Of the 84 patients with definite or probable IPF, 39 patients had a repeat BAL twelve months later. 45 patients did not have a repeat BAL for the following reasons: deceased within 12 months of first BAL (n=13), 12 months not yet elapsed from first BAL (n=10), patient declined second BAL (n=8), patient not approached for second BAL (n=8), patient deemed too frail or hypoxic for second BAL (n=6). Less than 1% of our study cohort has been lost to follow-up. All patient mortality data was collected via electronic patient records. Patient demographic data and BAL cell count data were collected via the Edinburgh ILD database. This is a unique ethically approved prospective database designed to capture the natural history of ILD (LREC 06/S0703/53). Ethical approval was obtained for all protocols and procedures. A flow diagram of patient selection is shown in Figure 16.

Figure 15. The Edinburgh Lung Fibrosis Group HRCT algorithm for IPF.

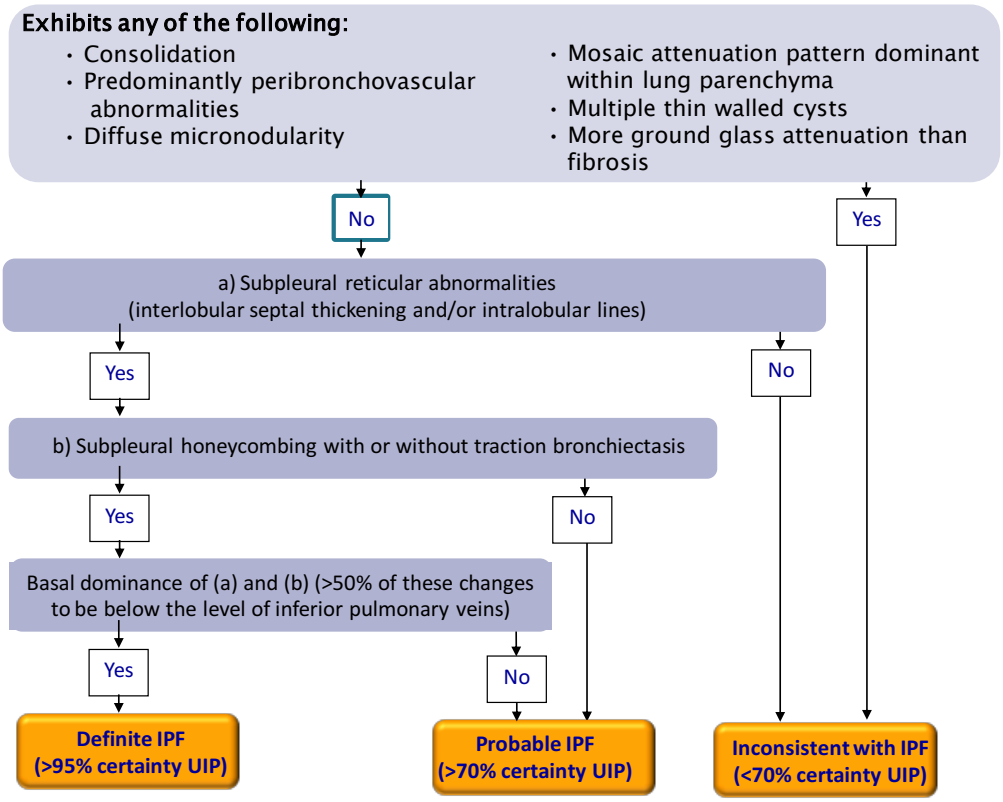

Figure 16. Flow diagram of patient selection.

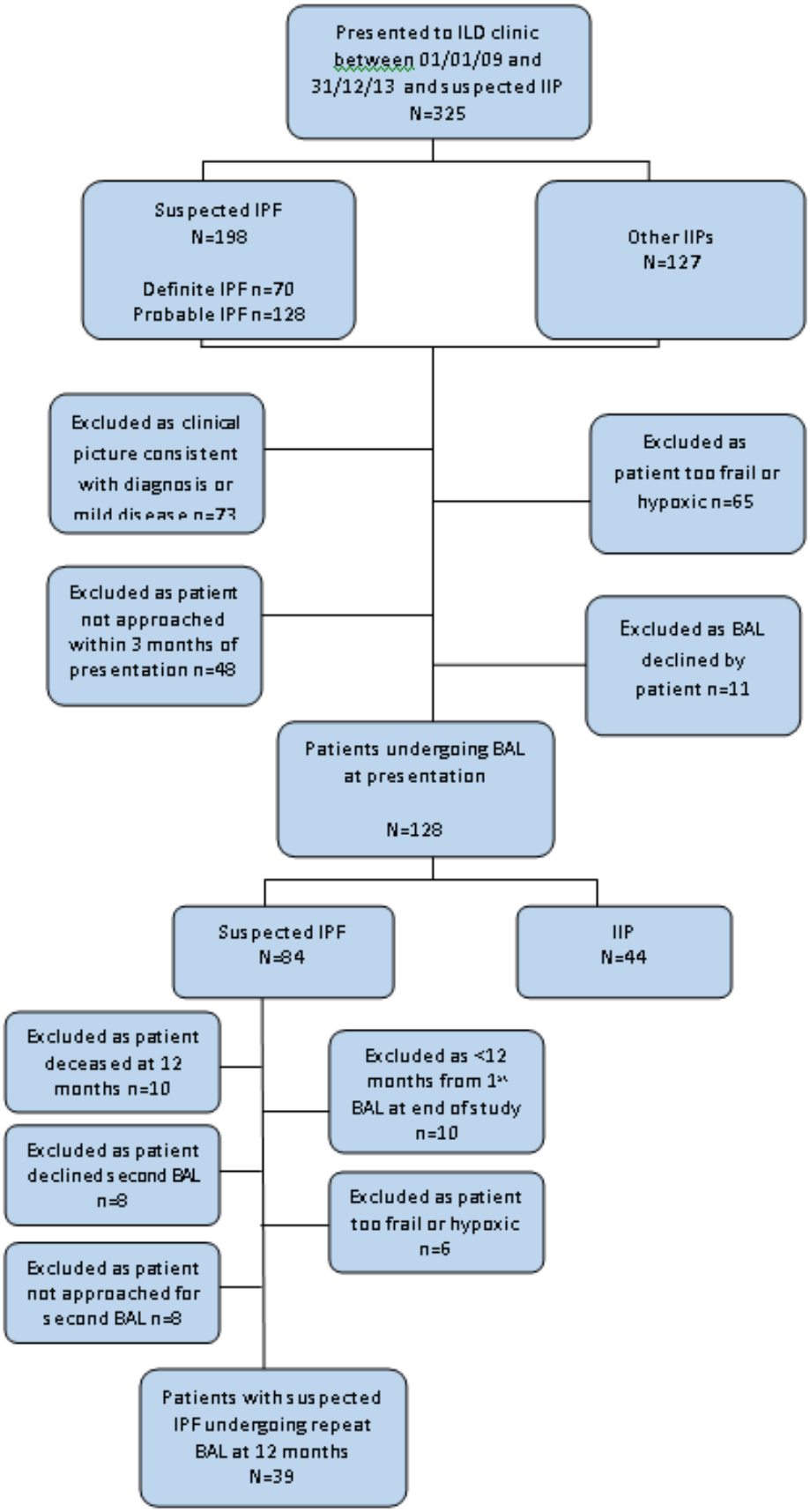

Diagnosis, investigation and management

Investigation, management and follow-up of all consecutive patients presenting at the Edinburgh Lung Fibrosis clinic was as per our local protocol. This included a detailed clinical history, physical examination, autoantibody screen (PR3 and MPO ANCA, immunoglobulins IgA, IgG and IgM, aspergillus precipitans, avian precipitans, farmers lung precipitans and CTD screen including ANA, DNA, C3, C4, CCP and ENA screen (antibodies to Ro, La, Sm, RNP, Scl70, Jo1)), HRCT and pulmonary function testing (PFTs). All HRCT scans were reviewed by a single expert thoracic radiologist (JTM) and discussed in a multidisciplinary meeting with at least two chest physicians with sub-specialty ILD expertise (NH, GAS). Surgical lung biopsies were performed as a video-assisted thoracoscopic procedure. Lung histology was reviewed in a multidisciplinary meeting by an experienced pulmonary pathologist (WAW), a member of the UK ILD pathology reference panel.

Lung Function Testing

Detailed lung function tests were performed within one month of the BAL procedure and then at 6 monthly intervals. Total lung capacity (TLC), FEV_1, FVC, lung volume-pressure relationship, and one-breath carbon monoxide diffusion capacity (TLCO) were measured. Patients were considered to have disease progression if they had a ≥10% decline in FVC or death due to a lung cause within 12 months of first BAL.

BAL

BAL was performed by standardised method according to consensus recommendations. Briefly, a flexible bronchoscope was wedged into a segmental branch of the right middle lobe (RML) and up to 240 ml of sterile saline in 40 ml aliquots instilled, with gentle aspiration after each aliquot. Patients were lightly sedated during the procedure. A total of at least 50ml of BAL fluid was retrieved per patient and this was immediately processed in the laboratory. Samples were filtered through a 40um cell strainer and then 50ul of fluid removed and counted on a cell Nucleocounter. Samples were then centrifuged at 1200rpm for 10 minutes at 4 degrees celsius and then 10 standard cytospins performed. One was stained with DiffQuick and the other 9 fixed in 90%

superdry acetone and 10% methanol mix for 10 minutes. A differential cell count was performed on fixed and stained cytopsins by an independent observer blinded to the clinical diagnosis.

Flow cytometry and Fluorescence Activated Cell Sorting (FACS)

Whole blood (50µl) or BAL fluid (100,000 cells) were incubated with antibodies against specific cell surface antigens (Table 23) for 30 minutes on ice. Unstained cells, single antibody stains and fluorescence minus one (FMO) controls were used. Erythrocytes were lysed by incubation at room temperature for 20 minutes in 650µl of FACSlyse. Samples were washed in 2ml PBS, centrifuged at 300g for 5 minutes and then resuspended in 450µl FACSlyse, for analysis using a LSR Fortessa cell analyser with FACSDiva software. A SORT tube was prepared by adding 50µl PBS, 8µl CD14-AF647, 8µl CD16-PE and 8µl HLA-DR-V450. BAL fluid cells were centrifuged at 300g for 5 minutes and resuspended in 800µl 1% serum and IMDM, then added to the sort tube. Cells were incubated on ice for 20 minutes, then 2ml sterile PBS added and centrifuged at 300g for 5 minutes to wash. Cells were resuspended in 800µl 1% serum and IMDM and taken to the sorter with an unstained sample. A BD FACSAria II cell sorter was used with FACSDiva software. Cells were collected in 10% IMDM after sorting, then pelleted and stored at -80°C. FlowJo was used for data analysis. The gating strategies used to identify cell subpopulations within BAL fluid and blood are outlined in Figures 17 and 18. Sorted AM, rPMLC and iPMLC cell pellets were the sent to Professor Mark Lindsay at the University of Bath for RNA gene sequencing.

Table 23. Primary antibodies used for flow cytometry and FACS.

Antibody	Clone	Fluorochrome	Manufacturer and catalogue number	Laser filter
AM, PMLC and neutrophil panel				
Anti-hCD14	HCD14	PerCP/Cy5.5	BioLegend 325622	Blue
Anti-hCD16	3G8	APC/Cy7	BioLegend 302018	Red
Anti-hHLA-DR	G46-6	V450	BD Horizon 561359	Violet
Anti-hCD206	15-2	PE	BioLegend 321106	Y/G
Anti-hCD71	CY1G4	FITC	BioLegend 334104	Blue
Anti-hCD163	GHI/61	APC	BioLegend 333610	Red
T cell panel				
Anti-hCD3	UCHT1	FITC	BioLegend 300405	Blue
Anti-hCD4	OKT4	APC/Cy7	BioLegend 317418	Red
Anti-hCD8		AF647	BioLegend	
FACS Panel				
Anti-hCD14	M5E2	AF647	BioLegend 301818	Red
Anti-hCD16	3G8	PE	BioLegend 302008	Blue
Anti-hHLA-DR	G46-6	V450	BD Horizon 561359	Violet

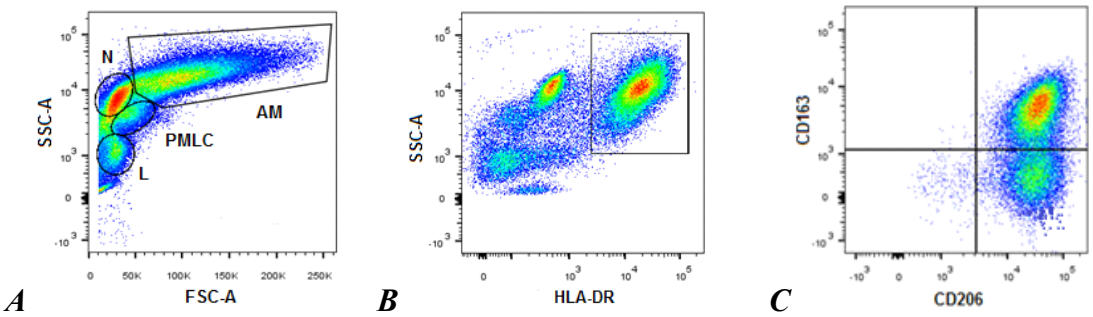

Figure 17. Flow cytometry gating strategies. Cells were identified in BAL fluid based upon their position on flow cytometry dot plots of size versus granularity (**A**). Alveolar macrophages (AM) were selected as HLA-DR+ (**B**), and were divided into $CD206^{low}CD163^{low}$, $CD206^{high}CD163^{low}$ and $CD206^{high}CD163^{high}$ subpopulations based on cell surface CD163 and CD206 expression (**C**). PMLC: Pulmonary monocyte-like cells, N: Neutrophils, L: Lymphocytes.

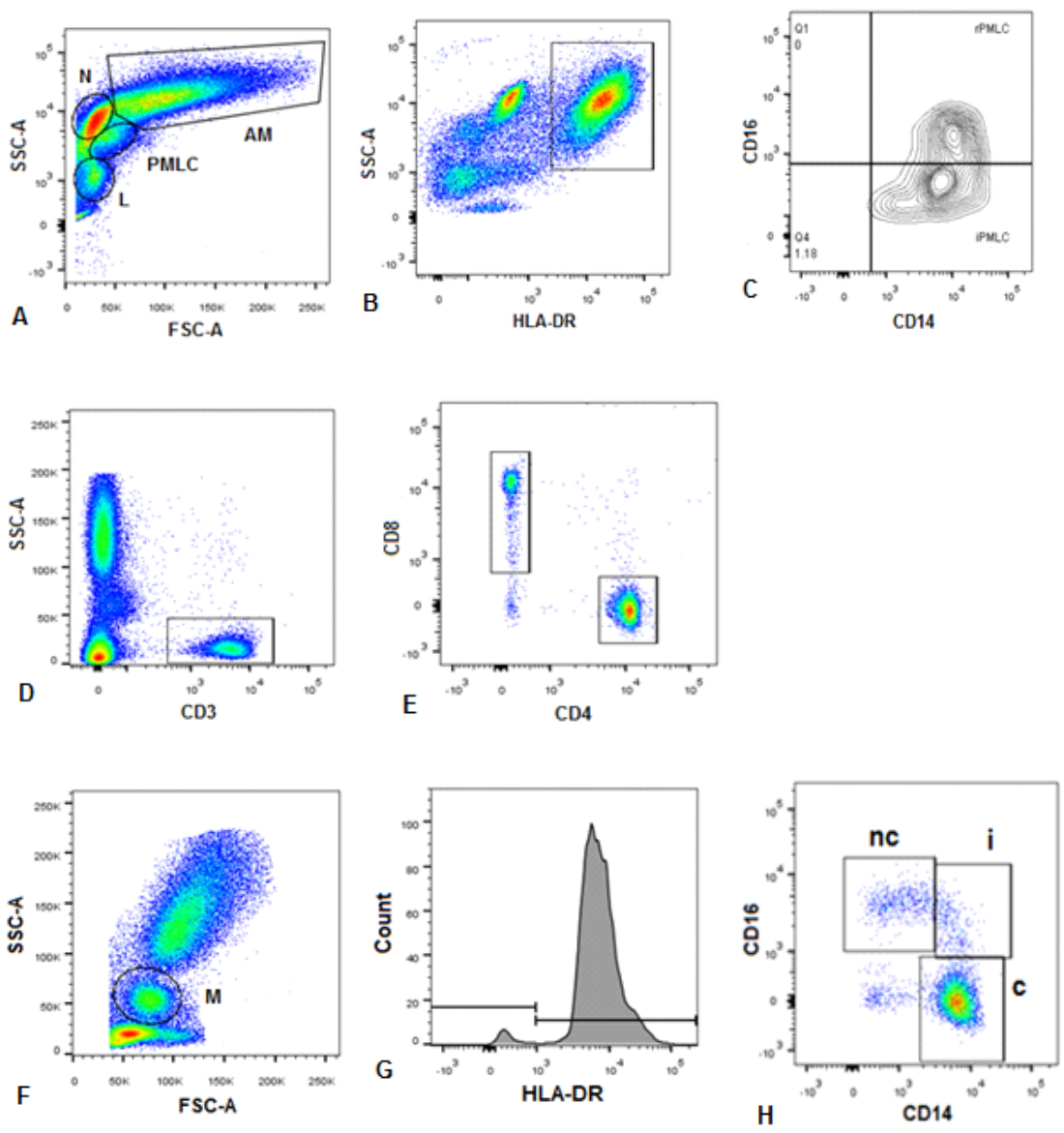

Figure 18. Flow cytometry gating strategies. Cells were identified in BAL fluid based upon their position on flow cytometry dot plots of size versus granularity (**A**). PMLCs were selected as HLA-DR+ (**B**), and were divided into rPMLC and iPMLC subpopulations based on their CD14 and CD16 expression (CD14++CD16+ and CD14++CD16- respectively) **(C**). Lymphocytes (L) were further selected for CD3 expression (**D**) and then subdivided into CD8+ and CD4+ T-cells (**E**). Cells were identified in whole blood based upon their position on flow cytometry dot plots of size versus granularity (**F**). Blood monocyte subsets (M) were identified as HLA-DR+ (**G**), and were then subdivided into classical (c), intermediate (i) and non-classical (nc) monocyte subpopulations based on their CD14 and CD16 expression (**H**). AM: Alveolar macrophages, N: Neutrophils.

Case definition

All diagnoses were made by multidisciplinary integration of clinical, HRCT and where available histological findings. Suspected idiopathic interstitial pneumonia was defined by the exclusion of known causes of fibrotic lung disease based on history and clinical assessment and HRCT appearances consistent with interstitial pneumonia. HRCT scans were classified as 'UIP pattern', 'probable UIP pattern' and 'inconsistent with UIP' by consensus on pre-specified radiographic criteria (*Figure 15*).

HRCT appearances were considered indicative of 'definite' UIP if they fulfilled all of the following criteria:
a) Subpleural reticular abnormalities consisting of interlobular septal thickening and/or intralobular lines with basal involvement
b) Basal subpleural honeycombing with or without traction bronchiectasis or bronchiolectasis
c) Ground-glass change to involve less lung volume than that affected by a and b combined
d) Basal dominance of a and b (>50% of these changes to be below level of inferior pulmonary veins)

HRCT appearances were considered indicative of 'probable UIP' if they did not fulfil all the criteria for 'definite UIP', but did fulfil all of the following:
a. Subpleural basal reticular abnormalities consisting of interlobular septal thickening and/or intralobular lines
b. Ground-glass change to involve less lung volume than that affected by 'a'.

HRCT appearances that did not fulfill all the criteria for either definite or probable UIP, or that exhibited any of the following were categorised as 'inconsistent with UIP': extensive ground glass change (more extensive than reticular abnormalities); consolidation; predominantly peribronchovascular abnormalities; diffuse micronodularity; mosaic attenuation pattern dominant within lung parenchyma; multiple thin walled cysts. These criteria are similar to the 2011 ATS/ERS criteria for 'UIP pattern' and 'possible UIP pattern'. Patients who underwent biopsy were categorised after integration of histological criteria.

Statistical analysis

GraphPad prism (version 6, GraphPad Software Inc., CA, USA) was used for data analysis. Normally distributed data were analysed by unpaired or paired t-test and expressed as mean (SD). Data that were not normally distributed were reported as median (interquartile range) and analysed by Mann Whitney U test or Wilcoxon signed rank test. Kruskal-Wallis test with Dunn's Multiple Comparison Test was used to calculate differences between multiple groups. Predictors of mortality and disease progression by diagnostic category were estimated with SPSS using Cox models. Statistical analysis of RNA gene sequencing was performed by Alex Przybylski (PhD student) and was performed using edgeR package software. *P* values of <0.05 were considered significant.

Organisation and analysis of cell differential data after initial BAL procedure

Differential cell counts from the first BAL were collated for patients with 'definite IPF', 'probable IPF' and 'inconsistent with IPF' HRCT patterns. As cell counts did not follow pattern of normal distribution, Interquartile Ranges (IQR) and median values were calculated for each cell type in each category. A one-way ANOVA test and unpaired t-test with assumptions verified were performed to compare differences in means between cell counts between groups.

Determining inconsistency in diagnosis between BAL and HRCT pattern

The differential cell counts from the first BAL procedure of patients in 'definite' and 'probable' IPF groups (n=83) were analysed. A granulocyte count of less than 3% or a lymphocyte count of greater than 20% was deemed inconsistent with a diagnosis of IPF in accordance with international guidelines.

Determining the predictive value of BAL neutrophilia on patient survival

Absolute total neutrophil count and BAL neutrophil percentage was calculated in all patients in the 'definite' and 'working diagnosis' IPF groups (n=84) from the first BAL procedure. Patients were categorised into those with a neutrophil count of $\geq$3% and

<3%. Length of time in days was calculated for each subject from the date of the first BAL procedure to 31/07/14 or date of decease. Subjects were censored if they were still alive on this date. The maximum length of time between these dates was 2002 days. Kaplan Meier Analysis was used to determine the survival patterns. Survival distributions between the two categories was analysed using the Log-rank (Mantel-Cox) test.

Determining the association between changes in BAL differential cell count from first BAL to repeat BAL at 12 months with disease progression

Lung function testing was used as an objective measure of disease progression in all patients. Disease progression was defined as a decrease in vital capacity (VC) of ≥10% in the 12 month period following BAL. Based on lung function results, patients were categorised into 'progressors' and 'non-progressors'. Patients were also considered a 'progressor' if death due to a lung cause occurred within 12 months of BAL. In order to detect any significant change in the differential cell count between successive procedures, the Wilcoxon signed rank test was performed for each cell type in both progressor and non-progressor groups.

Determining the safety of BAL

Deaths within 1 and 3 months of BAL were considered clinically important indicators for BAL safety. The number of deaths in each case was counted from the total number of patients undergoing the first BAL (n=128).

4.2 Results

4.2.1 Cellular components of bronchoalveolar lavage

Between 01/01/09 and 31/12/13, 325 consecutive incident patients with IIP presented to the Edinburgh Lung Fibrosis clinic. Based on 2011 ATS/ERS criteria, 70 were

categorised as 'definite UIP', 128 as 'probable UIP' and 127 as 'inconsistent with UIP'. Of the 325 patients, 128 underwent BAL at presentation. BAL granulocytes ≥3% and lymphocytes <20% were considered consistent with IPF. BAL DCC was consistent with IPF in 90.9% (n=20/22) of patients with 'definite IPF' and 85.5% (n=53/62) of patients with 'probable IPF'. Of the 11 patients with BAL DCC inconsistent with IPF, two underwent SLB and histology was consistent with IPF in both. There were no significant differences between gender, smoking status or surgical biopsy rates between the three groups, however patients with HRCT appearances inconsistent with UIP were significantly younger and had better lung function than those with 'definite' or 'probable' UIP HRCT appearances. Patient demographic and cellular data are presented in Tables 24 and 25 below.

Table 24. Demographic Data for Patients defined by HRCT category (n=128). Values presented as mean (+/- standard deviation).

	Definite UIP HRCT appearance *N=22*	***Probable UIP HRCT appearance*** *N=62*	***Inconsistent with UIP (other) HRCT appearance*** *N=44*	***P-value***
Age in years (SD)	71.1 (+/- 8.1)*	71.0 (+/- 7.4)$^{+}$	62.1 (+/- 9.9)*$^{+}$	<0.0001*$^{+}$
Male (%)	16 (72.7%)	44 (71.0%)	31 (70.5%)	0.880
Never smoked (%)	5 (22.7%)	17 (27.4%)	19 (43.2%)	0.105
Ex smokers (%)	13 (59.1%)	36 (58.1%)	16 (36.4%)	0.084
Current smokers (%)	4 (18.2%)	9 (14.5%)	9 (20.5%)	0.682
VC in Litres (SD)	2.79 (+/- 0.76)	2.78 (+/- 0.79)	3.18 (+/- 1.03)	0.055
VC % predicted (SD)	89.5 (+/- 28.6)	85.7 (+/- 19.8)	87.9 (+/- 20.7)	0.749
TLCO (mm/min/mmHg)(SD)	3.58 (+/- 1.1)*	4.21 (+/- 1.3)$^{+}$	5.22 (+/- 2.1)*$^{+}$	0.0002 *0.0004 $^{+}$0.005
TLCO % predicted (SD)	46.44 (+/- 13.4)*	52.8 (+/- 13.5)	59.6 (+/- 19.4)*	0.005 *0.005
Surgical lung biopsy performed (%)	3 (13.3%)	15 (24.2%)	13 (29.5%)	0.287

Table 25. Cellular data from first BAL procedure of all patients (n=128).

	Definite UIP N=22	**Probable UIP** N=62	**Inconsistent with IPF (Other)** N=44	**P-value**
Total cell count	$18.2x10^6$ ($12.5x10^6$, $31.3x10^6$)	$23.4x10^6$ ($14.6x10^6$, $34x10^6$)	$20.1x10^6$ ($10.8x10^6$, $28.5x10^6$)	0.551
% Neutrophils in BAL (IQR)	13 (5,35)*	9 (5,17)$^+$	5 (2,11)*$^+$	0.005*, 0.009$^+$
% Eosinophils in BAL (IQR)	4 (2,11)*	3 (1,5)$^+$	1 (1,3)*$^+$	0.008*, 0.016$^+$
% Lymphocytes in BAL (IQR)	3 (2,5)	2 (2,8)	5 (2,14)	0.090
% Macrophages in BAL (IQR)	71 (59,82)	79 (64,88)	84 (76,89)	0.103
Number of patients with <3% granulocytes (%)	1 (4.5%)	6 (9.8%)	8 (18.2%)	0.129
Number of patients with >20% lymphocytes (%)	1 (4.5%)	4 (6.5%)	5 (11.4%)	0.362

Data presented as median and interquartile range, *statistically significant difference between groups, $^+$statistically significant difference between groups

Comparing differential cell counts between patient cohorts

The one-way ANOVA test indicated statistically significant differences between the baseline differential cell counts of patients in the three HRCT determined categories (n=128). A statistically significant difference was noted in baseline neutrophil percentage (P=0.005) and baseline eosinophil percentage (P=0.009). Post test analysis with Dunns multiple comparison test revealed statistically significant differences in baseline neutrophil and eosinophil percentages between 'definite IPF' and 'inconsistent with IPF' groups (P=0.005 and P=0.008 respectively), and also between 'probable IPF' and 'inconsistent with IPF' groups (P=0.009 and P=0.016 respectively). No statistically significant differences were noted in baseline lymphocyte and macrophage percentages between the groups. When the same comparison was made between 'definite' and 'probable' IPF groups, there were no significant differences in any of the baseline cell percentages (Table 25). The lack of any significant difference between differential cell counts of patients in the 'definite' and 'probable' IPF categories allowed us to consider them as one group in the remaining analyses. This data is shown in Figure 19.

Figure 19. Baseline BAL DCC in 'definite', 'probable' and 'inconsistent with' UIP groups.

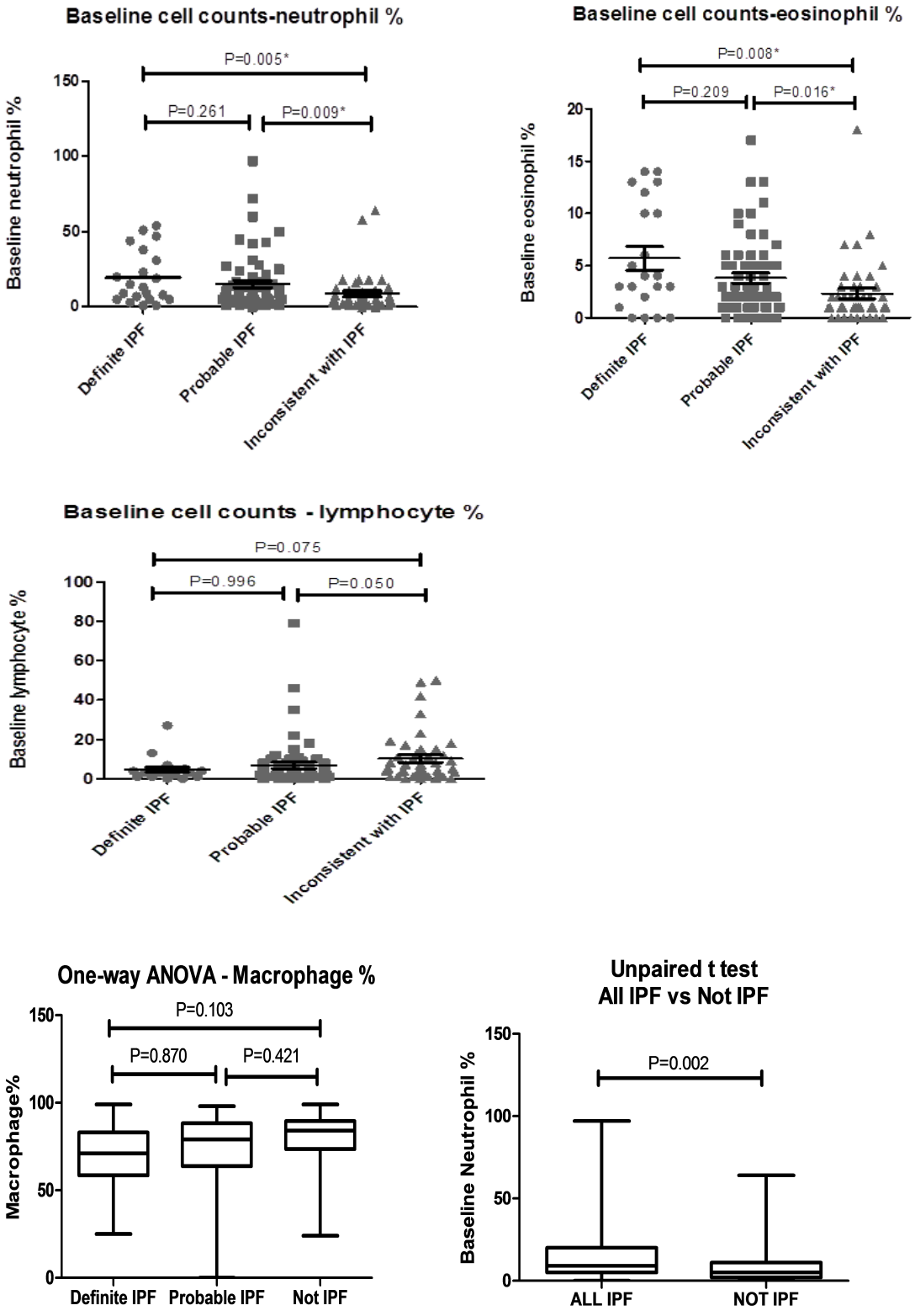

In the 12 months following BAL, 36.4% (n=8/22) of patients in the 'definite UIP' group and 30.6% (n=19/62) in the 'probable UIP' group had progressed. There were no significant differences in BAL differential cell percentage or absolute cell count in any cell type between progressor and non-progressor groups, BAL cell percentage data are demonstrated in Figure 20. Mortality in patients with suspected IPF and a BAL DCC consistent with IPF was no different to those with a DCC inconsistent with IPF (P=0.425, HR 1.590 (95% CI 0.502 to 4.967)). There was no difference in disease progression in either group (P=0.885, HR 1.081 (95% CI 0.367 to 3.106)). Kaplan-Meier curves are shown in Figure 21.

Figure 20. Baseline BAL DCC between IPF progressor and non-progressor groups.

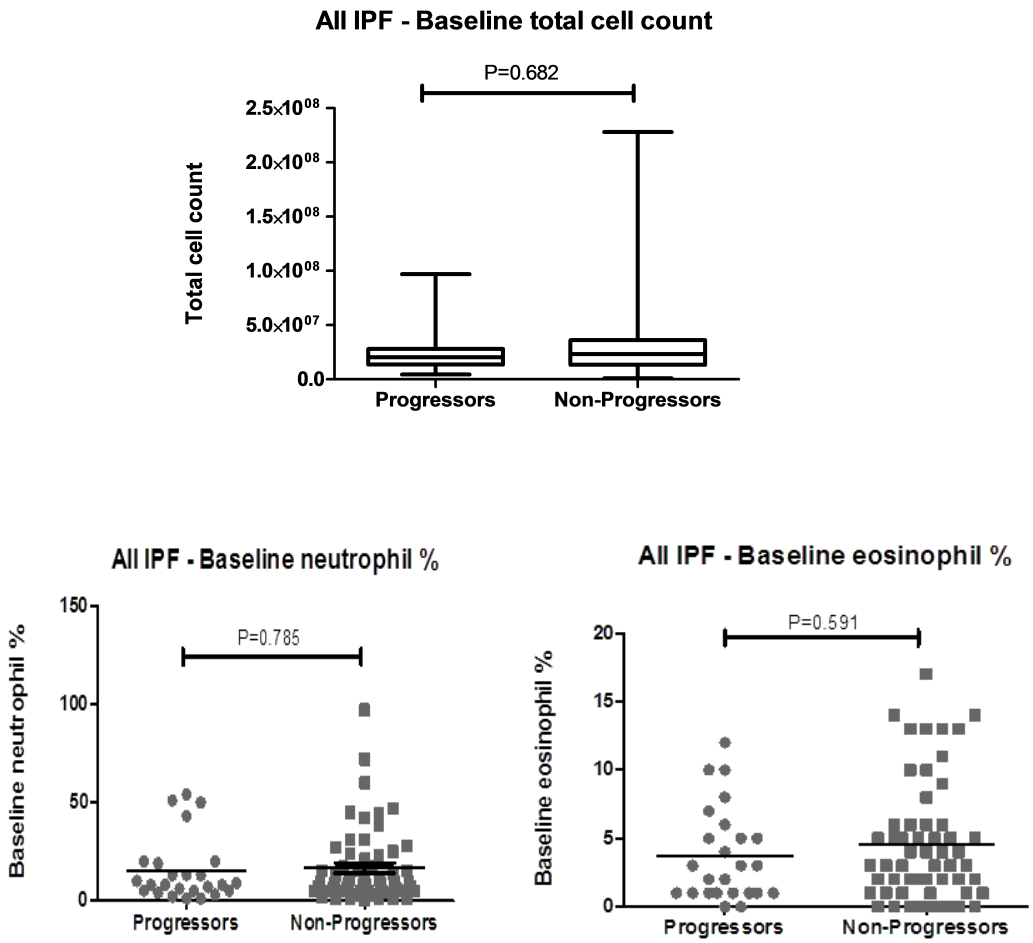

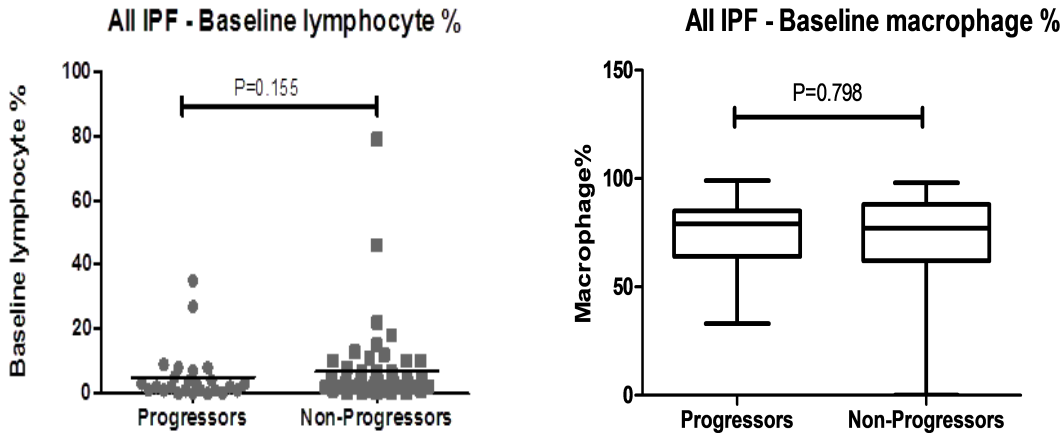

Determining Inconsistency in Diagnosis between BAL and HRCT

BAL differential cell counts were considered consistent with IPF if granulocytes were ≥3% and lymphocytes were <20%. BAL differential cell count was inconsistent with a diagnosis of IPF (granulocytes <3% or lymphocytes >20%) in 9.1% of patients in the 'definite IPF' group (n=2/22), as categorised by HRCT appearances. *Staphylococcus aureus* and *Haemophilus influenzae* were cultured from BAL fluid. Both of these patients were deemed too unfit for a second 12-month BAL, and surgical lung biopsy was not indicated. 14.5% of patients in the 'probable IPF' group had baseline differential cell counts that were inconsistent with a diagnosis of IPF (n=9/62). *Mycoplasma pneumoniae* was cultured in BAL fluid from one patient in this group. Of these 9 patients, 5 went on a repeat BAL 12 months later, and differential cell counts on repeat BAL were consistent with IPF in 4 patients. One patient had BAL differential cell count that remained inconsistent with IPF on repeat BAL. Two of the patients in this group underwent surgical lung biopsy, histology was consistent with UIP in both cases and so confirmed the diagnosis of IPF.

Determining the predictive value of baseline BAL neutrophilia and lymphocytosis on patient survival

Both 'definite IPF' and 'probable IPF' groups were combined, and a comparison of mortality and disease progression in IPF patients with both consistent (BAL

granulocytes >3% and BAL lymphocytes <20%) and inconsistent (BAL granulocytes <3% and BAL lymphocytes >20%) BAL DCCs was performed using the Log-rank (Mantel-Cox) test. There was no significant difference in survival or disease progression between the groups. Median survival was 4.5 years in the group with BAL DCC consistent with IPF, versus an undefined median survival in the group with BAL DCC inconsistent with IPF (P=0.425, HR 1.590 (95% CI 0.509 to 4.966). The median time to disease progression in the group with BAL DCC consistent with IPF was 4.9 years, versus an undefined time to progression in the group with BAL DCC inconsistent with IPF (P=0.885, HR 1.081 (95% CI 0.376 to 3.106). Figure 21.

Figure 21. Mortality and disease progression in IPF patients with consistent and inconsistent BAL DCC.

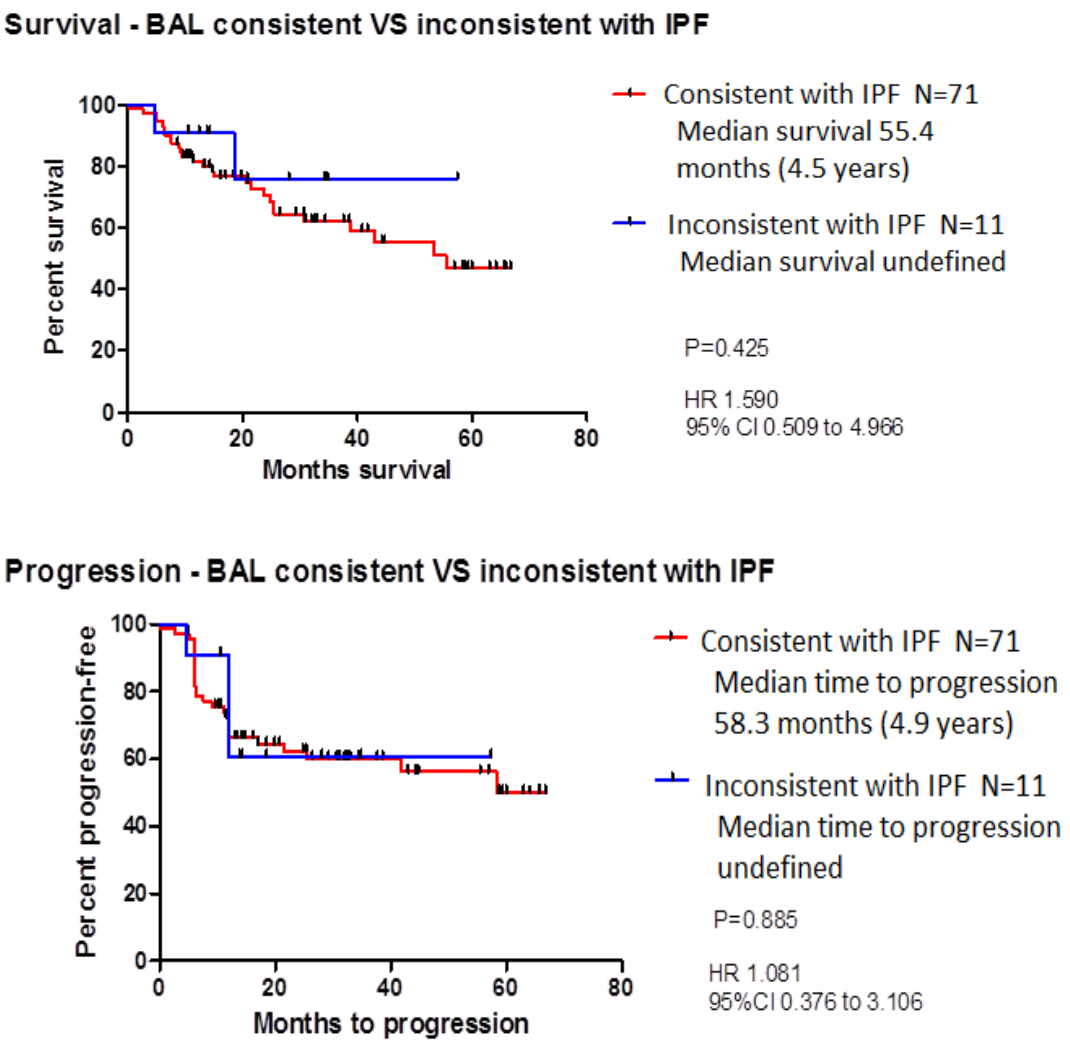

There was no significant difference in survival between patients with a baseline BAL neutrophil percentage of >3% vs <3% (median survival 52.1 vs 53.3 months respectively, P=0.400, HR 1.403 (95%CI 0.638 – 3.086)). Similarly, no difference in mortality was found between patients with a baseline BAL lymphocyte percentage of <20% vs >20% (median survival 53.3 months and undefined respectively, P=0.349, HR 1.935, (95%CI 0.580 – 4.720)). Two and five year mortality was also reviewed in IPF patients with baseline BAL neutrophils of >3% vs <3% and with baseline BAL lymphocytes of <20% and >20%, however there were no significant differences in either 2 or 5 year survival between the groups. This data is shown in Figures 22 – 27 below.

Figure 22. Kaplan Meier survival curve of patients with baseline BAL neutrophil percentage of >3% vs <3%.

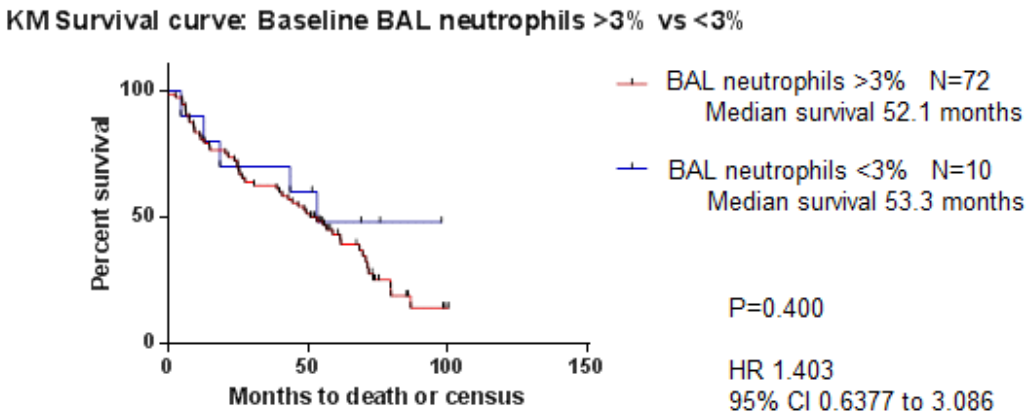

Figure 23. Kaplan Meier survival curve of patients with baseline BAL lymphocyte percentage of <20% vs >20%.

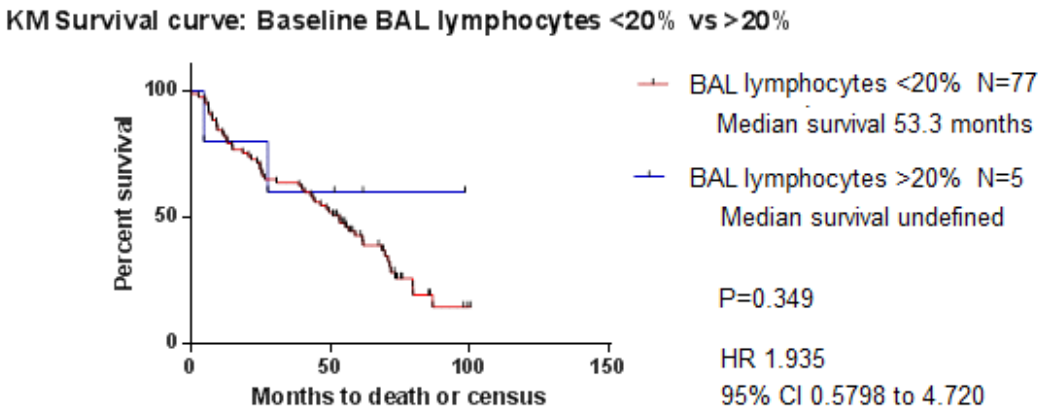

Figure 24. Kaplan Meier 2 year survival curve of patients with baseline BAL neutrophil percentage of >3% vs <3%.

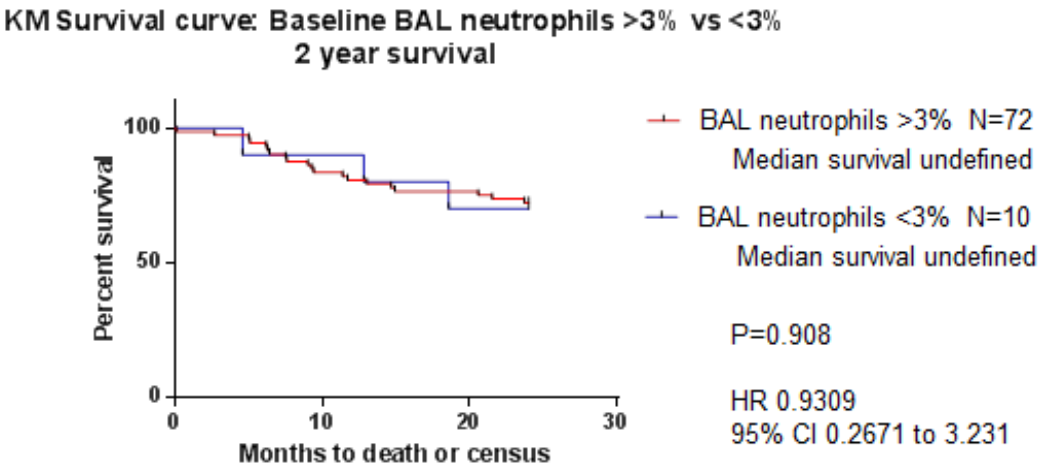

Figure 25. Kaplan Meier 5 year survival curve of patients with baseline BAL neutrophil percentage of >3% vs <3%.

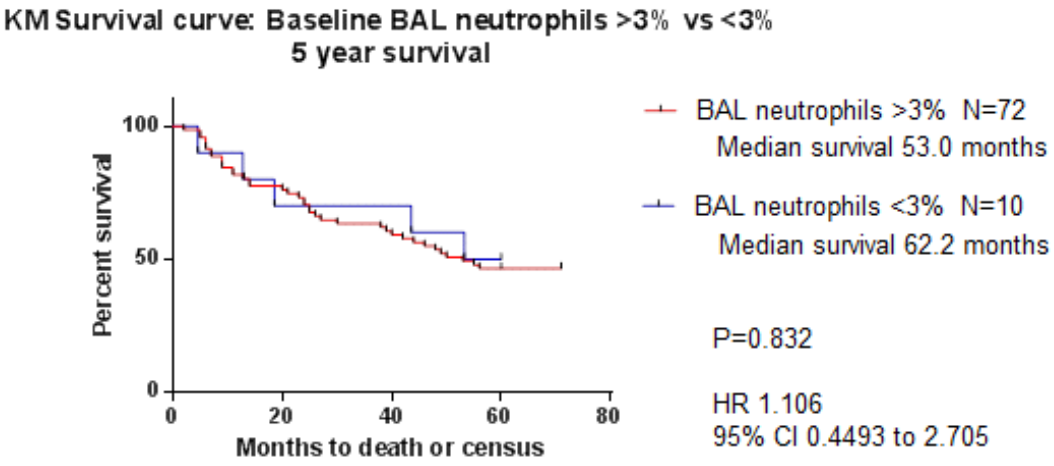

Figure 26. Kaplan Meier 2 year survival curve of patients with baseline BAL lymphocyte percentage of <20% vs >20%.

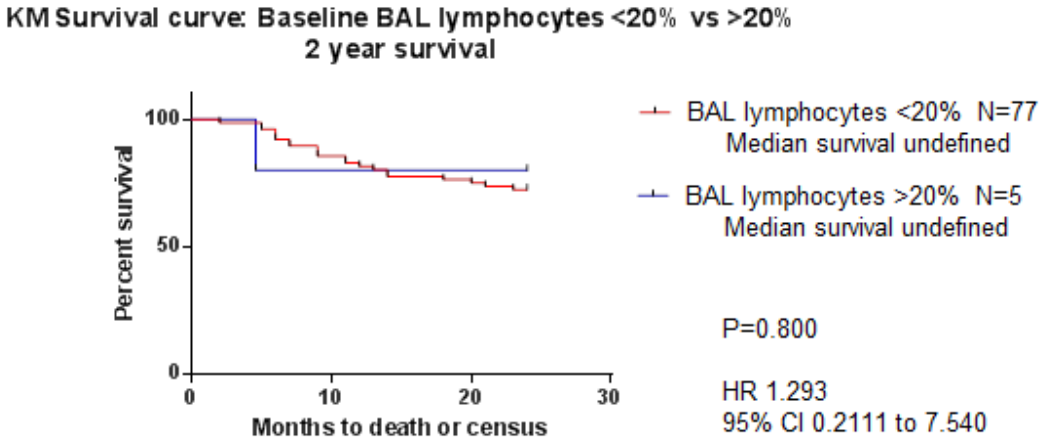

Figure 27. Kaplan Meier 5 year survival curve of patients with baseline BAL lymphocyte percentage of <20% vs >20%.

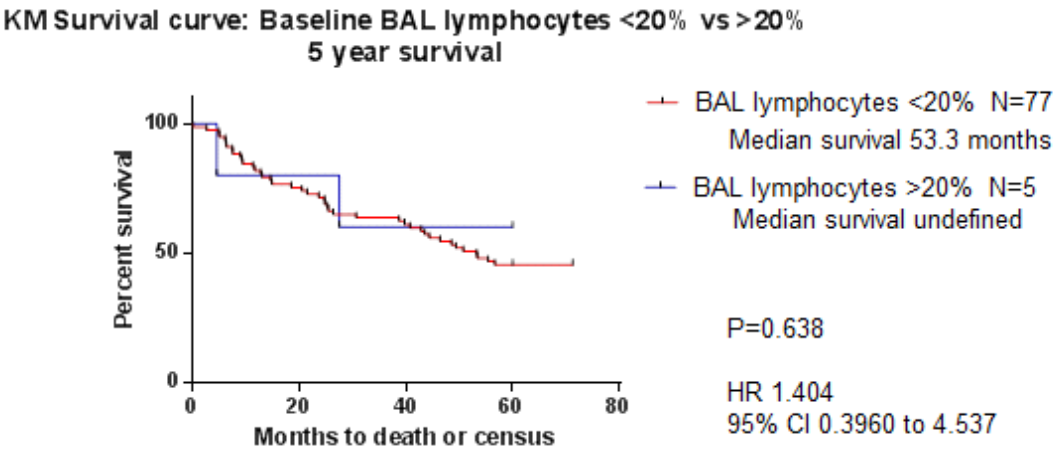

Determining the association between changes in BAL differential cell count from first BAL to repeat BAL at 12 months with disease progression

There are no studies that specifically describe the value of repeated BAL in IPF. We aimed to determine the feasibility of repeat BAL in IPF and the relationship between DCC and disease progression in two successive BALs. Of the 84 patients with 'definite' or 'probable' IPF, 39 had repeat BAL twelve months later. The reasons for patients not undergoing repeat BAL were death within 12 months of first BAL (n=13), patient not approached within 3 months of repeat BAL due date (n=12), patient declined (n=6) and

patient deemed too frail (n=5). Nine patients were awaiting repeat BAL. Patients were categorised into 'progressors' (n=8) and 'non-progressors' (n=31). Patient demographic and cellular data are shown in Tables 26 and 27. There was a significant decrease in absolute VC, percentage predicted VC, absolute TLCO and percentage predicted TLCO in the progressors between 0 and 12 month BALs. There was a significant increase in absolute VC and percentage predicted VC between BALs in the non-progressor group. There was a significant change in absolute VC, percentage predicted VC and absolute TLCO between 0 and 12 month BALs between the progressor and non-progressor groups. The Wilcoxon signed rank test was used to compare both cell percentage and absolute cell count for each of the cell types at 0 and 12 months in both progressor and non-progressor groups. There were no statistically significant differences in total cell count between 0 and 12 month BALs in either group (progressors 0 vs 12 months, P=1.000, non-progressors 0 vs 12 months, P= 0.592). There was no statistically significant difference in any of the cell types between 0 and 12 month BALs in either group (neutrophil %: progressors 0 vs 12 months, P=0.400; non-progressors 0 vs 12 months, P=0.241, lymphocyte %: progressors 0 vs 12 months, P=0.944, non-progressors 0 vs 12 months, P=0.318, eosinophil %: progressors 0 vs 12 months, P=0.374, non-progressors 0 vs 12 months, P=0.205, macrophage %: progressors 0 vs 12 months, P=0.933, non-progressors 0 vs 12 months, P=0.090). The change in the differential cell count between 0 and 12 month BALs did not appear to predict disease progression. Change in total cell count and DCC percentages between 0 and 12 month BAL is demonstrated in Figure 28.

The Mann Whitney test was used to compare the change in differential cell count for each of the four cell types measured between 0 and 12 month BALs and between progressor and non-progressor groups. There was no significant change in absolute total cell count between 0 and 12 month BALs between progressor and non-progressor groups, (P=0.682) and no significant change in absolute cell counts in each of the cell types. There was no significant difference in the change of DCC percentages between 0 and 12 month BALs between progressors and non-progressors (change in neutrophil % progressors vs non-progressors, P=1.000, change in lymphocyte % progressors vs non-progressors, P=0.794, change in eosinophil % progressors vs non-progressors, P=0.215, change in macrophage % progressors vs non-progressors, P=0.434). Change

in DCC cell percentages is shown in Figure 29. Repeat BAL was well tolerated in almost all patients.

Table 26. Patient demographic data.

	Progressors N=8 *(definite IPF n=2, possible IPF n=6)*			**Non-Progressors N=31** *(definite IPF n=9, possible IPF n=22)*			
BAL	**Baseline 0 months**	**12 months**	**Change**	**Baseline 0 months**	**12 months**	**Change**	**P-value (Change)**
VC in Litres (IQR)	3.23 (2.67,3.86)	2.85 (2.29,3.16)	-0.42 (-0.61, -0.29)	3.06 (2.54,3.32)	3.16 (2.45,3.52)	-0.02 (-0.10, 0.16)	<0.0001
	P<0.0001			P=0.015			
VC %predicted (%) (IQR)	91.5 (73.5,96.5)	79.0 (68.5,81.8)	-10.0 (-15.0, -9.0)	86.1 (81.0,101.1)	89.6 (80.0,104.2)	0 (-3.0,4.7)	<0.0001
	P<0.0001			P=0.006			
TLCO (mm/min/mm Hg)	4.65 (3.23,5.47)	3.92 (2.98,4.80)	-0.76 (-0.96, -0.25)	3.92 (3.02,5.25)	3.83 (2.89,5.09)	-0.20 (-0.56, -0.02)	0.018
	P=0.0004			P=0.138			
TLCO % predicted (%) (IQR)	54.5 (39.3,64.3)	46.0 (35.3,56.0)	-8.3 (-10.9, -2.5)	52.9 (45.0,60.0)	51.5 (40.8,58.3)	-2.1 (-7.6,0.1)	0.061
	P=0.0004			P=0.236			

Table 27. Patient cellular data.

	Progressors N=8 *(definite IPF n=2, possible IPF n=6)*			**Non-Progressors N=31** *(definite IPF n=9, possible IPF n=22)*			
BAL	**Baseline 0 months**	**12 months**	**Change**	**Baseline 0 months**	**12 months**	**Change**	**P-value**
Total cell count	$25x10^6$ ($20.5x10^6$, $34x10^6$)	$29.5x10^6$ ($19.3x10^6$, $37.3x10^6$)	*+$7x10^5$ (-$10.4x10^6$, +$17.5x10^6$)	$18x10^6$ ($9.5x10^6$, $33.2x10^6$)	$25.3x10^6$ ($13.8x10^6$, $31x10^6$)	*+$2.7x10^6$ (-$10.4x10^6$, +$10.9x10^6$)	*P=0.982
	P=0.844			P=0.813			
Neutophil % (IQR)	11 (6,21)	7 (5,20)	-4* (-15,4)	9 (5,21)	8 (4,13)	-4* (-11,4)	*P=1.000
	P=0.400			P=0.241			
Lymphocyte % (IQR)	2 (1,7)	4 (1,10)	-1* (-3,5)	4 (2,10)	4 (1,7)	-1* (-3,2)	*P=0.794
	P=0.944			P=0.318			
Eosinophil % (IQR)	1 (1,3)	3 (1,8)	1* (-1,1)	3 (1,6)	2 (1,5)	-1* (-4,2)	*P=0.215
	P=0.374			P=0.205			
Macrophage % (IQR)	79 (65,89)	74 (63,90)	1* (-8,10)	76 (62,86)	81 (68,89)	7* (-9,20)	*P=0.434
	P=0.933			P=0.090			

Figure 28. BAL DCC at 0 and 12 months in IPF progressor and non-progressor groups.

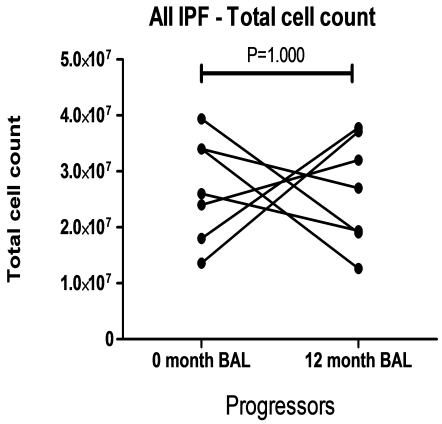

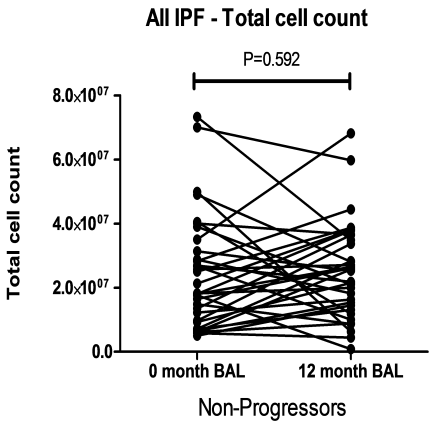

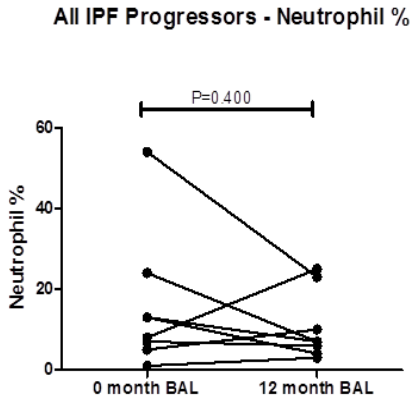

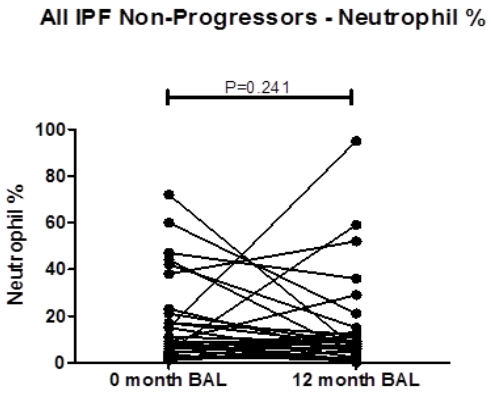

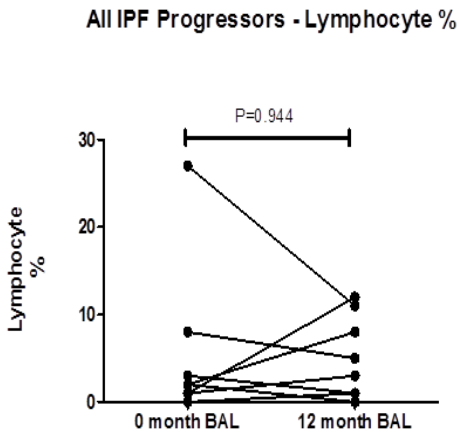

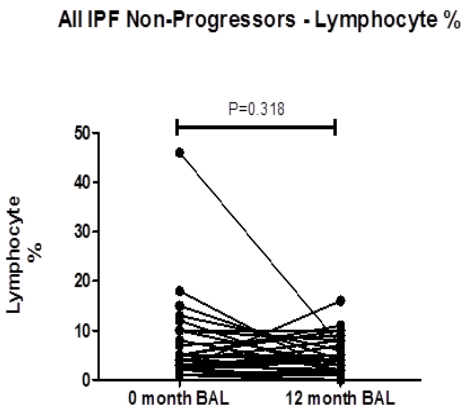

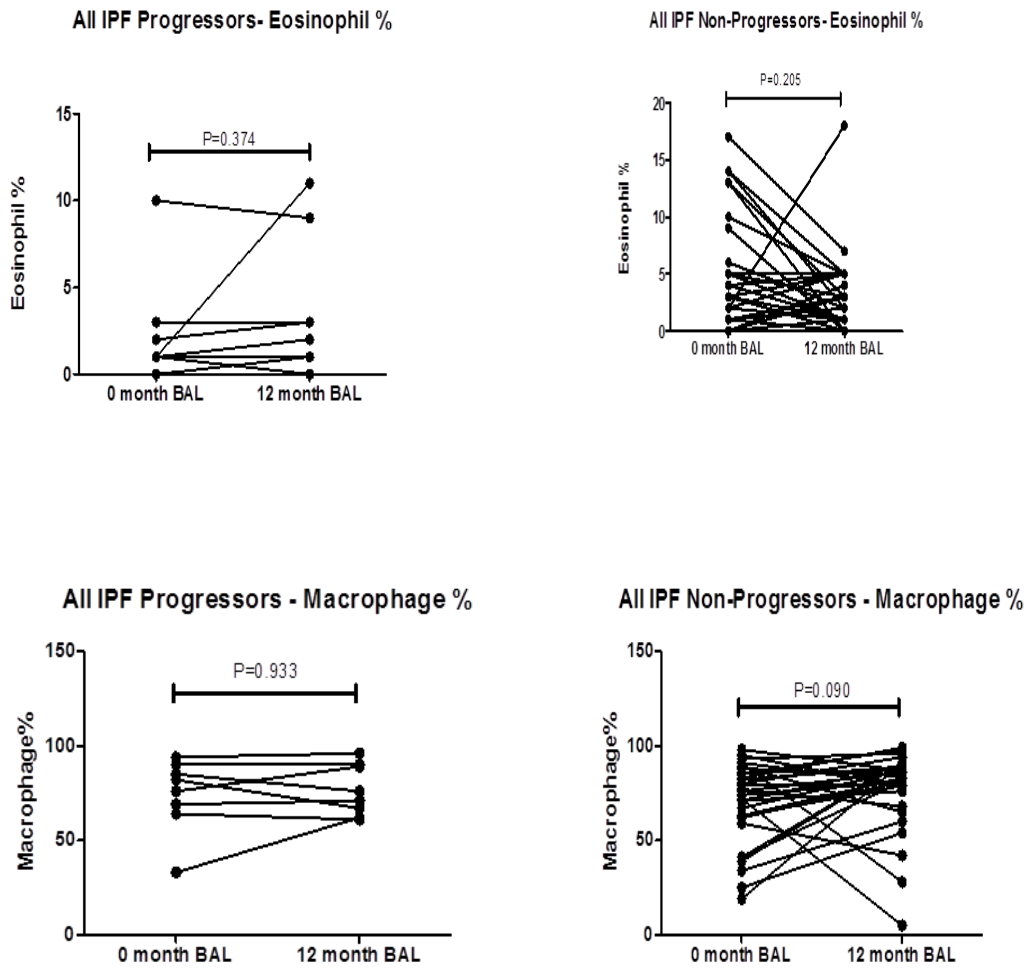

Figure 29. Change in DCC between 0 and 12 month BALs between progressors and non-progressors.

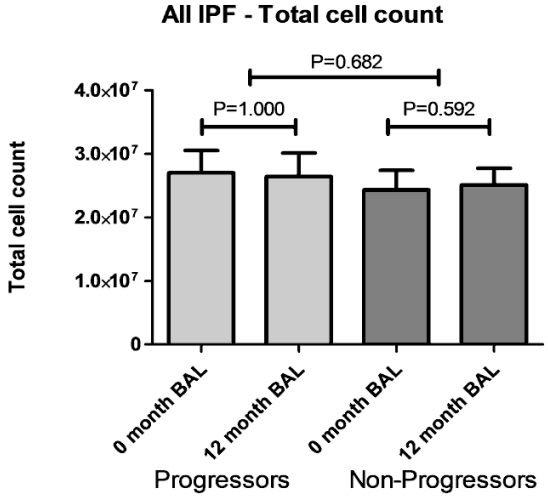

All IPF - Change in absolute total cell count from 0-12 months

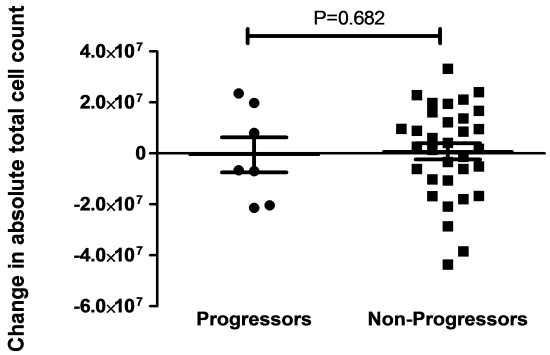

All IPF- Neutrophil %

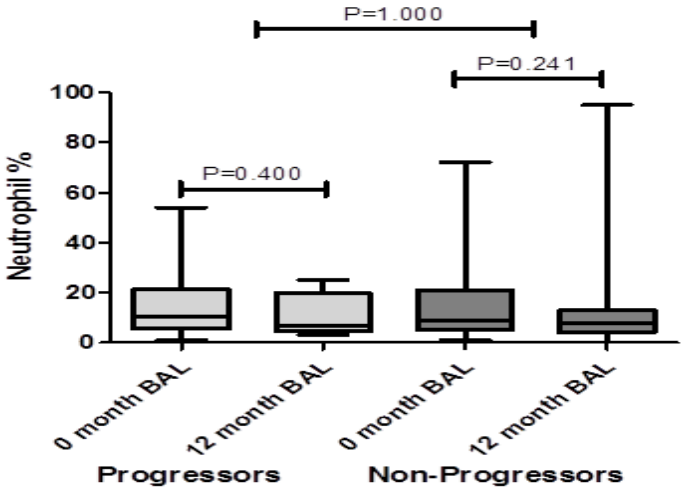

Change in neutrophil % between 0 and 12 month BALs

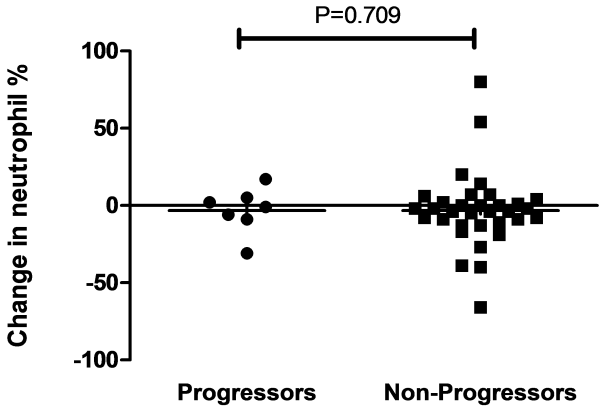

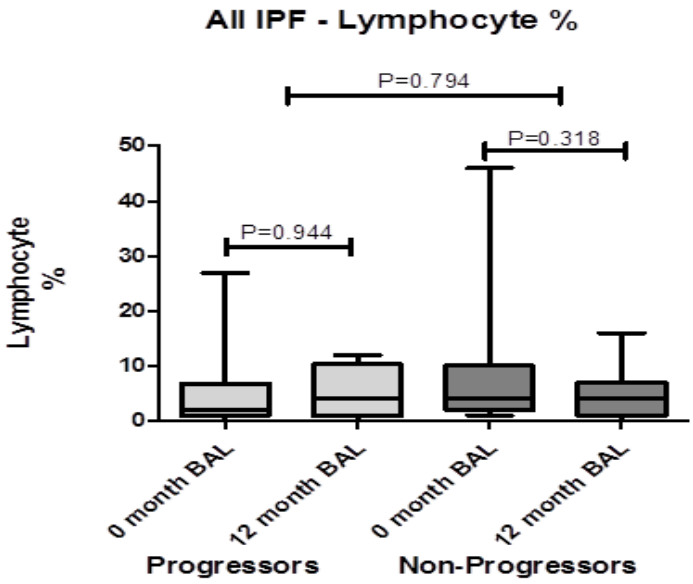

Change in lymphocyte % between 0 and 12 month BALs

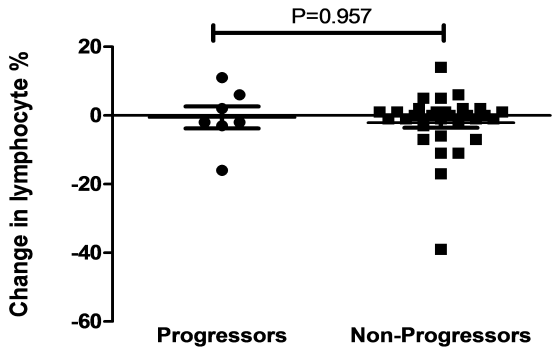

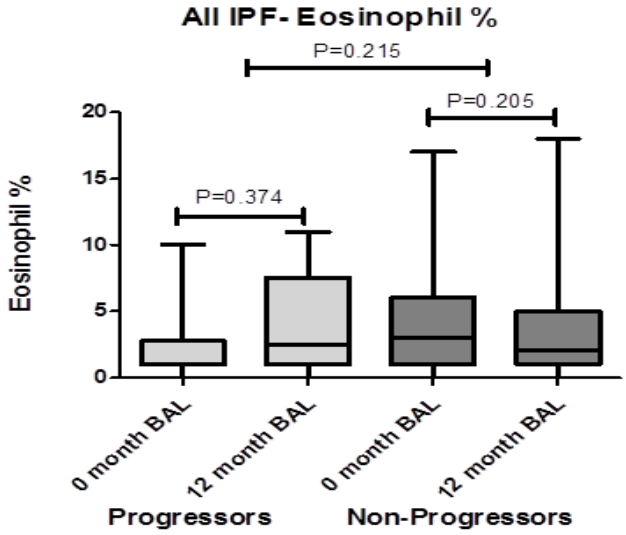

Change in eosinophil % between 0 and 12 month BALs

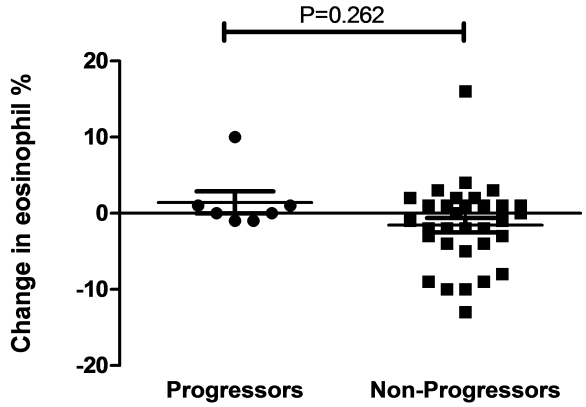

All IPF - Macrophage %

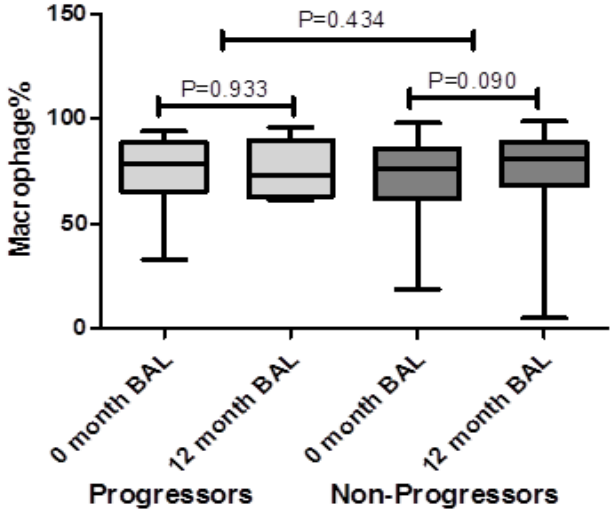

All IPF - Change in macrophage %

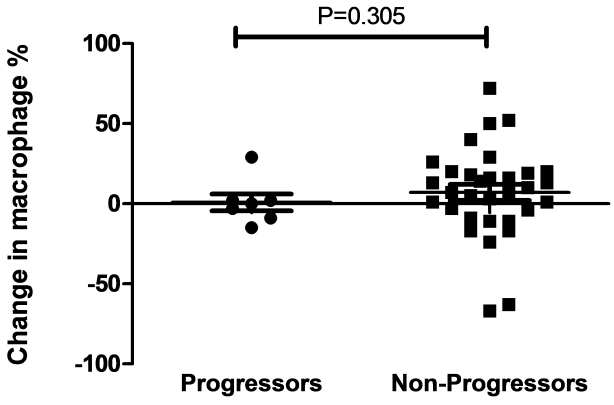

In our study, 128 patients underwent BAL at presentation; 84 patients suspected to have IPF and 44 patients unlikely to have IPF based on clinical and radiological appearances. Thirty nine patients underwent a repeat BAL procedure 12 months following initial BAL. No immediate serious complications were observed in our study and the procedure was well tolerated in most patients. There was 1 death within 1 month of a first BAL procedure, 1 death within 1 month of a second BAL procedure and 1 death within 3 months of a first BAL procedure. The first two deaths were considered to be 'probably procedure-related'. The first death occurred in 78 year old man with probable IPF three days after a first BAL procedure. The cause of death was pneumonia. The lavage fluid from the procedure was negative on culture. The second death occurred in an 80 year old man with probable IPF, 13 days following his second BAL procedure. The lavage fluid was negative on culture, however the cause of death was considered to be pulmonary oedema and fast atrial fibrillation secondary to pneumonia.

4.2.2 Alveolar macrophage phenotype in disease progression

Cells were obtained by BAL from 42 patients with IPF; 14 progressors, 28 non-progressors. A panel of monoclonal antibodies; CD14, CD16, CD206, CD71, CD163 and HLA-DR were used to quantify and selectively characterise AMs using flow cytometry. Twenty one patients underwent repeat BAL 12 months later; 5 progressors, 16 non-progressors. AMs are typically described as classical M1 ($CD206^{low}CD163^{low}$) activated AMs or alternatively activated M2a ($CD206^{high}CD163^{low}$) and M2c ($CD206^{high}CD163^{high}$) AMs. All IPF patients had significantly increased $CD206^{high}CD163^{low}$ AM polarisation versus $CD206^{high}CD163^{high}$ ($P<0.001$) and vs $CD206^{low}CD163^{low}$ ($P<0001$) at 0 month BALs. All IPF patients had significantly increased $CD206^{high}CD163^{low/high}$ AM subpopulations compared to $CD206^{low}CD163^{low}$ AM subsets at 0 and 12 month BALs ($P=0.01$ and $P<0.001$ respectively). However, there were no significant differences between progressor and non-progressor groups.

CD71 (transferrin receptor) expression was significantly increased in IPF progressors versus non-progressors at baseline BAL (P<0.0001). ROC curve analysis of baseline CD71 expression revealed a baseline CD71 expression >91.91% yielded 80% sensitivity and 92.3% specificity for IPF progression, area under curve 0.846. CD71, CD206 and CD163 expression was reported as being high or low by obtaining the mean of all values, values above the mean were termed 'high' and values below the mean were termed 'low'. KM survival curves for CD71+ high (>87.5%) vs low (≤87.5%) revealed median survivals of 40.5 months and 75.6 months respectively (P=0.015, HR 0.196 (95% CI 0.052 – 0.730)) when adjusted for sex, age, smoking status, %predicted FVC and % predicted TCO. There was also increased expression of CD206 (mannose receptor) in IPF progressors at both baseline (P=0.034) and at 12 month BAL (P=0.027) compared to the non-progressor group. CD163 expression was significantly reduced in the progressor group vs the non-progressor group at baseline BAL (P=0.019), however there was no significant difference between groups at 12 months. Graphical representation of this data is shown in Figures 30-35. Characteristic predictors of 'stable' disease at presentation were, low CD71+ (p=0.001), low CD206+ (p=0.034) and high CD163+ (p=0.019) AMs, and a higher M2 (and specifically M2a) population relative to M1 macrophages at presentation (P < 0.0001), and at 12 months, CD206 low (P=0.027) AMs. KM survival curves for $CD71^{high}CD206^{high}CD163^{low}$ vs intermediate phenotype ($CD71^{high/low}CD206^{high/low}CD163^{low/high}$) vs $CD71^{low}CD206^{low}CD163^{high}$ revealed median survivals of 23.3 months, 75.6 months and undefined survival respectively (P=0.041, HR 0.005 (95%CI 0.003-0.889)) when adjusted for sex, age, smoking status, %predicted FVC and % predicted TCO. These data are shown in Figure 36.

Figure 30. AM polarisation at 0 and 12 month BALs in IPF progressors and non-progressors.

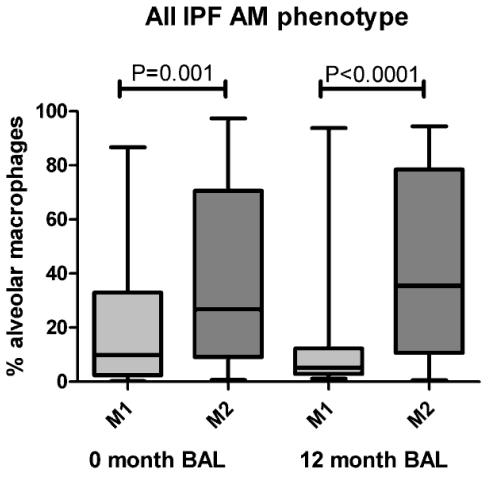

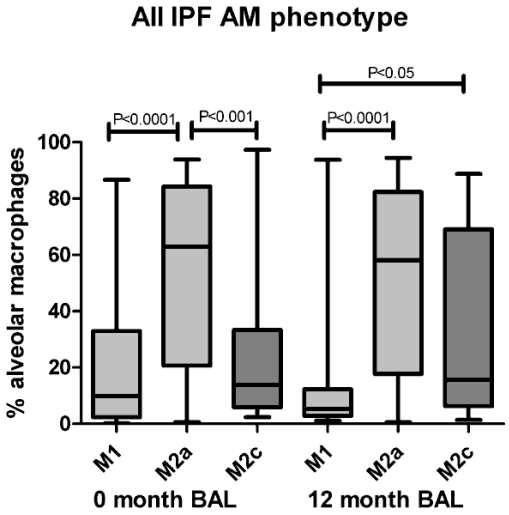

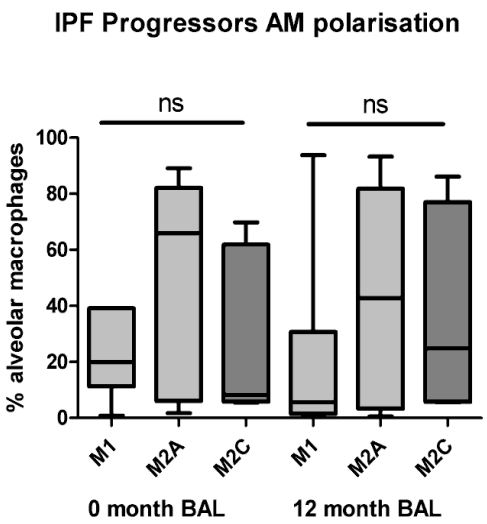

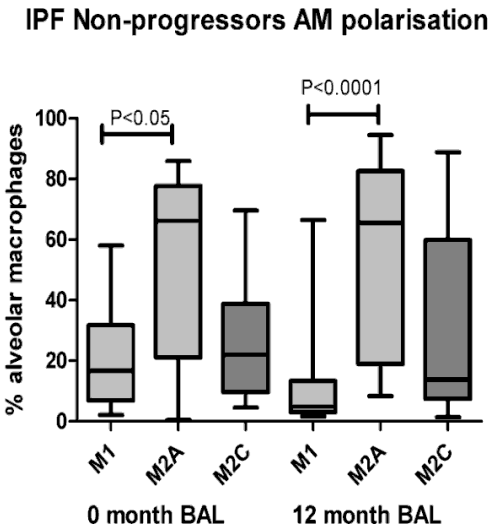

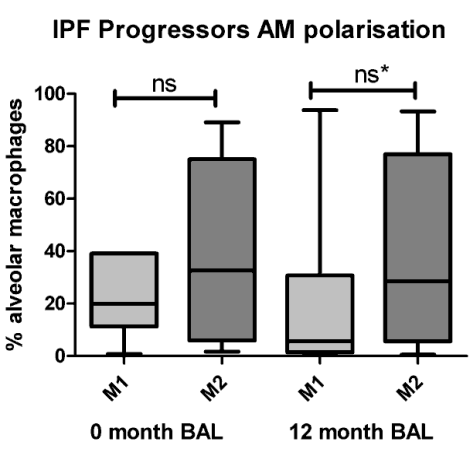

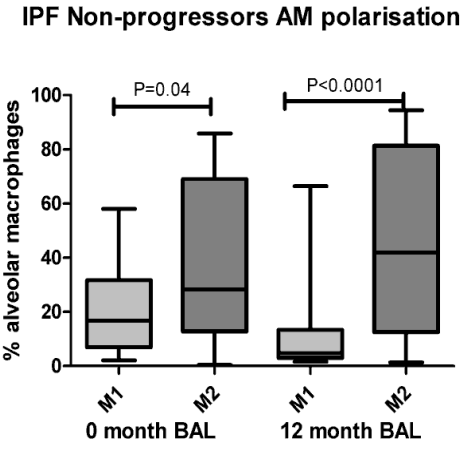

Figure 31. AM CD71 expression at 0 and 12 month BALs in IPF progressors and non-progressors.

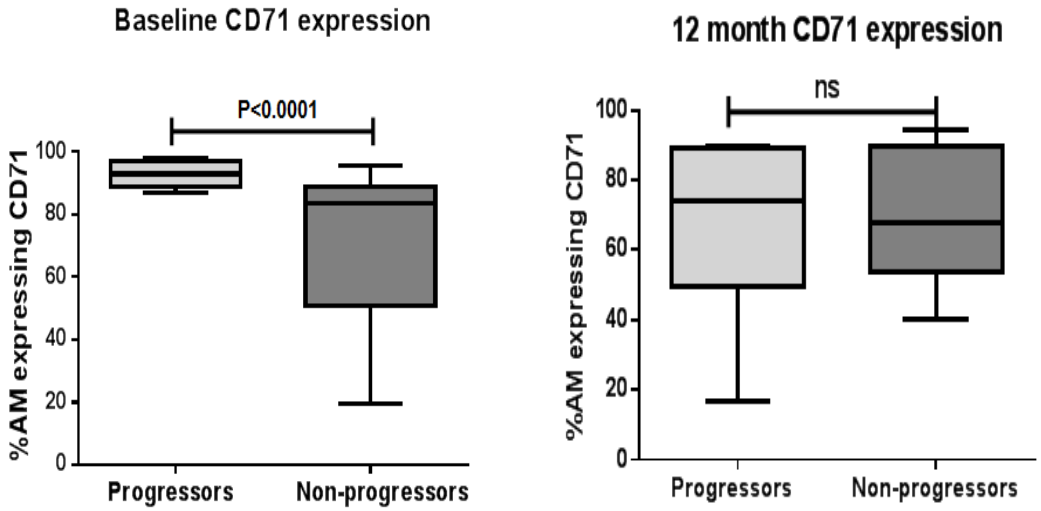

Figure 32. ROC curve of baseline %CD71+ AMs.

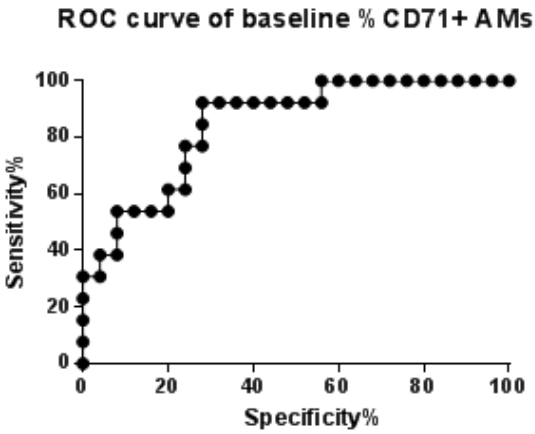

*ROC curve analysis
-Area under curve 0.846
-Baseline CD71 >91.91% yields 80% sensitivity and 92.3% specificity for IPF progression

Figure 33. KM survival curves CD71+ high vs low.

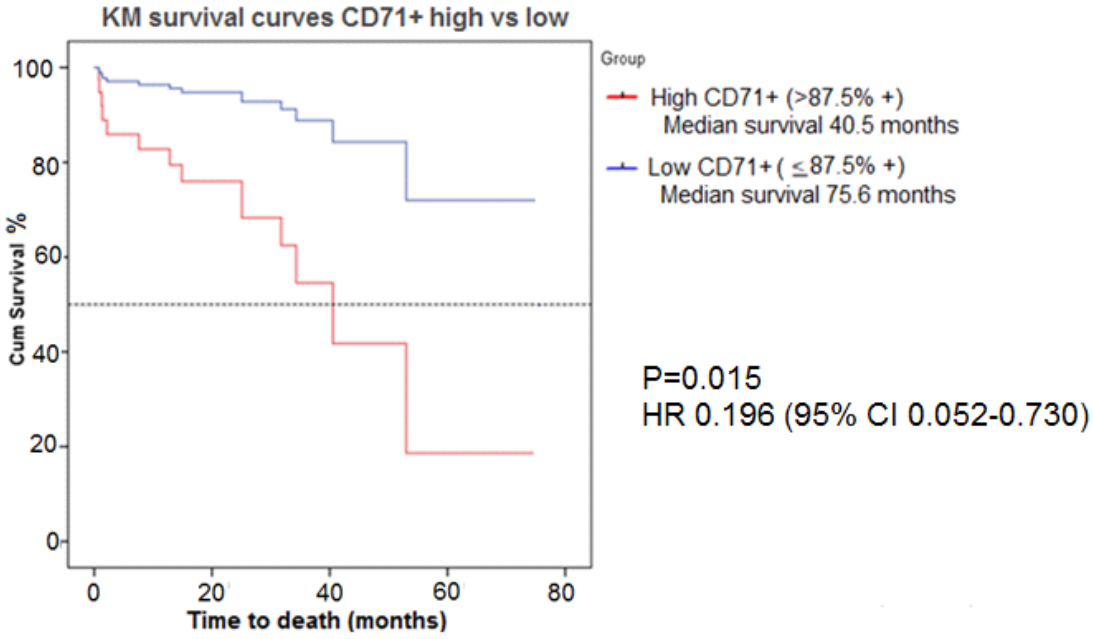

Figure 34. AM CD206 expression at 0 and 12 month BALs in IPF progressors and non-progressors.

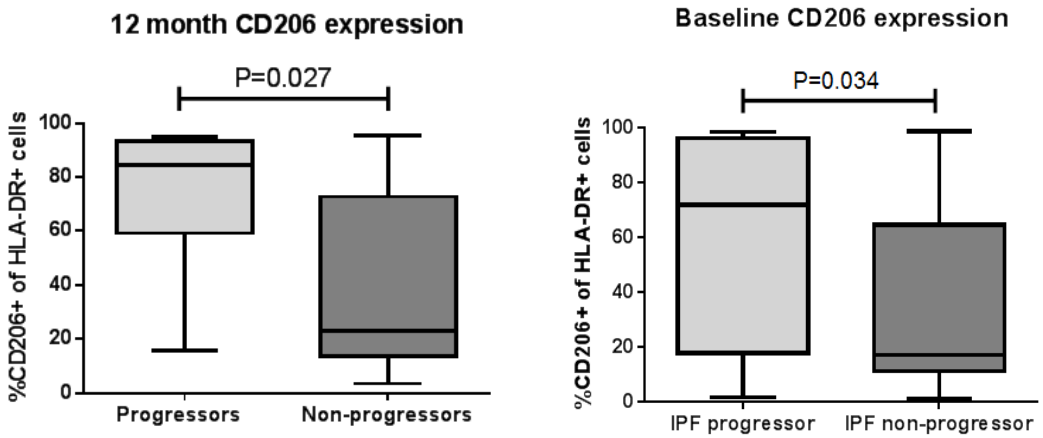

Figure 35. AM CD163 expression at 0 and 12 month BALs in IPF progressors and non-progressors.

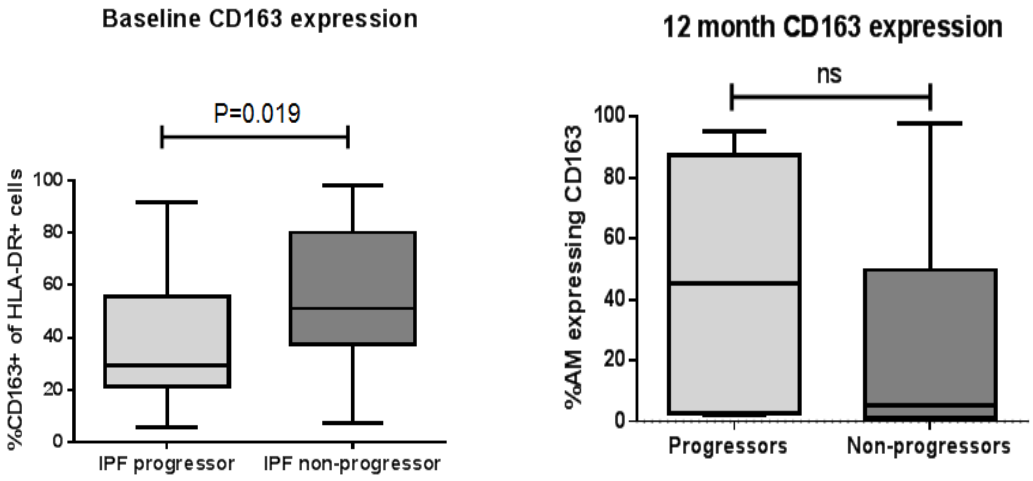

Figure 36. KM survival curve AM polarisation phenotype.

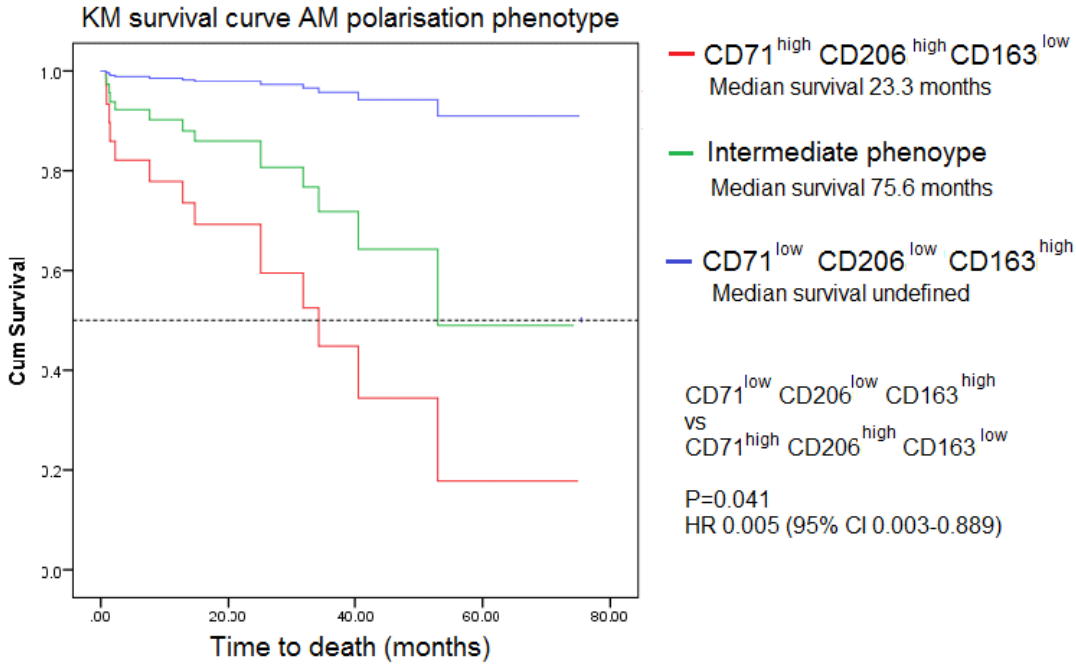

4.2.3 Pulmonary monocyte-like cells

Expansion of novel subpopulations of PMLCs, resident PMLC (rPMLC, HLA-DR+CD14++CD16+ cells) and inducible PMLC (iPMLC, HLA-DR+CD14++CD16- cells), have been reported in inflammatory lung diseases[49]. BAL fluid cells were obtained from a Test Cohort of IPF patients, 7 progressors and 19 non-progressors. BAL was performed at presentation and 12 months later. A panel of monoclonal antibodies, as described previously, were used to quantify and selectively characterise alveolar macrophages (AMs), rPMLCs and iPMLCs by cell sorting. In the Test Cohort, disease progression in IPF was associated with a significantly increased baseline BAL %rPMLC subpopulation (P=0.010) and a significantly decreased baseline BAL %iPMLC subpopulation (P=0.011). The baseline BAL iPMLC:rPMLC ratio was also significantly decreased in the IPF progressor group (P=0.01). There was a trend to suggest IPF progressors had increased %PMLC of all cells, however this did not reach significance. There were no significant changes in %rPMLC or %iPMLC between 0 and 12 month BALs in the progressor or non-progressor groups. This data is demonstrated in Figure 37.

Figure 37. %iPMLC and %rPMLC in Test Cohort by cell sorting, 0 and 12 month BALs.

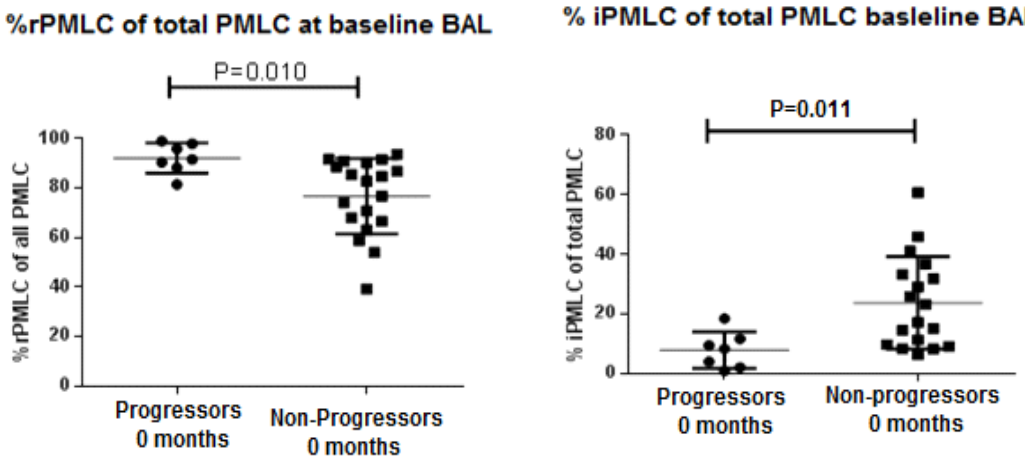

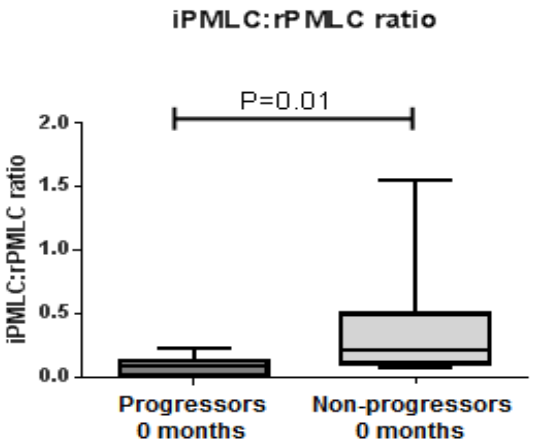

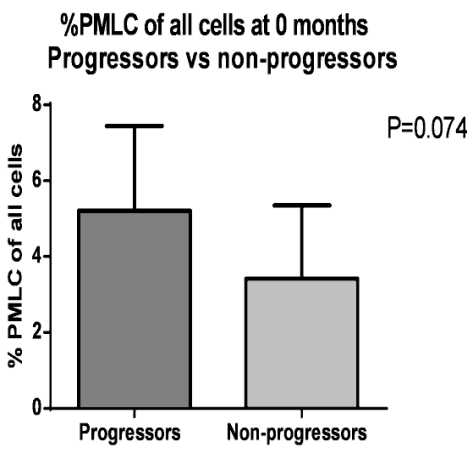

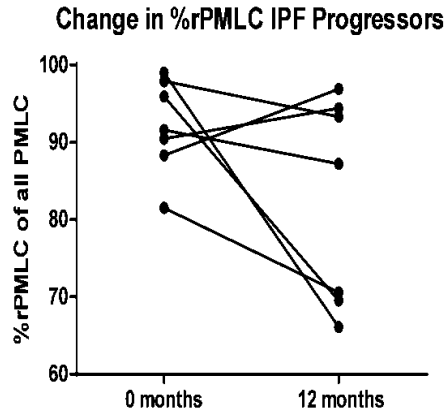

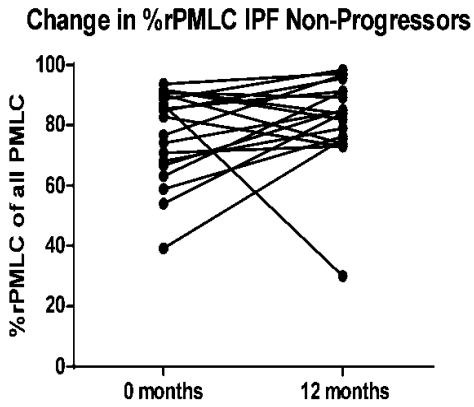

BAL fluid cells were then obtained from a Validation Cohort of ILD patients; 42 patients with IPF (14 progressors, 28 non-progressors), 30 patients with non-fibrotic ILD (18 IIP, 5 sarcoidosis, 3 CTD-ILD, 2 NSIP, 2 Bird Fancier's Lung), and 6 healthy controls. Patient demographic data are described in Table 28. Baseline lung function was significantly worse in the IPF progressors versus the IPF non-progressors, non-fibrotic ILD and healthy control groups. A panel of monoclonal antibodies; CD14, CD16, CD3, CD4, CD8 and HLA-DR were used to quantify and selectively characterise AMs, rPMLCs, iPMLCs, neutrophils and CD4/CD8+ T-cells using flow cytometry as previously described. Classical, intermediate and non-classical monocyte subsets were also quantified in peripheral blood. The percentage of rPMLCs was significantly higher in BAL fluid cells of IPF patients compared to those with non-fibrotic ILD ($P<0.0001$) and healthy controls ($P<0.05$). Baseline rPMLC percentage was significantly higher in IPF progressors compared to the IPF non-progressor group ($P=0.011$). There were no

significant differences in BAL lymphocyte populations between groups. This data is shown in Figure 38. There were no significant differences in blood classical, intermediate and non-classical monocyte population percentages in patients with IPF compared to patients with non-fibrotic ILD or healthy controls. This data is shown in Figure 39.

Table 28. Patient demographic data.

	IPF Progressor N=14	**IPF Non progressor N=28**	**Non-fibrotic ILD N=30 (18 IIP, 5 sarcoidosis, 3 CTD-ILD, 2 NSIP, 2 Bird Fancier's Lung)**	**Healthy Control N=6**	**P-value**
Age in years (SD)	70.6 (8.2)	73.5 (6.6)*$^{+}$	66.1 (9.3)*	59.8 (9.9)$^{+}$	0.0005 *0.006 $^{+}$0.002
Male (%)	13 (92.9)	18 (64.3)	20 (66.7)	2 (33.3)	
Never smoked (%)	6 (42.9)	11 (39.3)	12 (40.0)	2 (33.3)	
Ex-smoker (%)	8 (57.1)	15 (53.6)	13 (43.4)	2 (33.3)	
Current smoker (%)	0	2 (7.1)	5 (16.7)	2 (33.3)	
VC in Litres (IQR)	2.78 (2.40,3.33)	2.89 (2.35,3.42)	2.96 (2.38,3.66)	2.47 (2.37,3.48)	0.268
VC %predicted in Litres (IQR)	76.0*+^ (66.8,97.0)	95.0*° (84.3,108.8)	86.0+° (75.7,100.8)	95.0^ (87.0,101.5)	<0.0001 *°<0.0001 $^{+}$0.005 ^0.002
TLCO (mm/min/ mmHg) (IQR)	3.91* (3.06,4.79)	4.10^{+} (3.30,5.12)	4.75*$^{+}$ (3.81,6.25)	Not performed	<0.0001 *$^{+}$<0.0001
TLCO %predicted (IQR)	49.0*$^{+}$ (38.5,55.7)	55.0*^ (48.0,62.7)	60.0^{+}^ (52.0,69.8)	Not performed	<0.0001 *$^{+}$<0.0001 ^0.0002

Figure 38. BAL rPMLC, iPMLC and lymphocyte subset percentages in IPF vs non-fibrotic ILD and healthy controls.

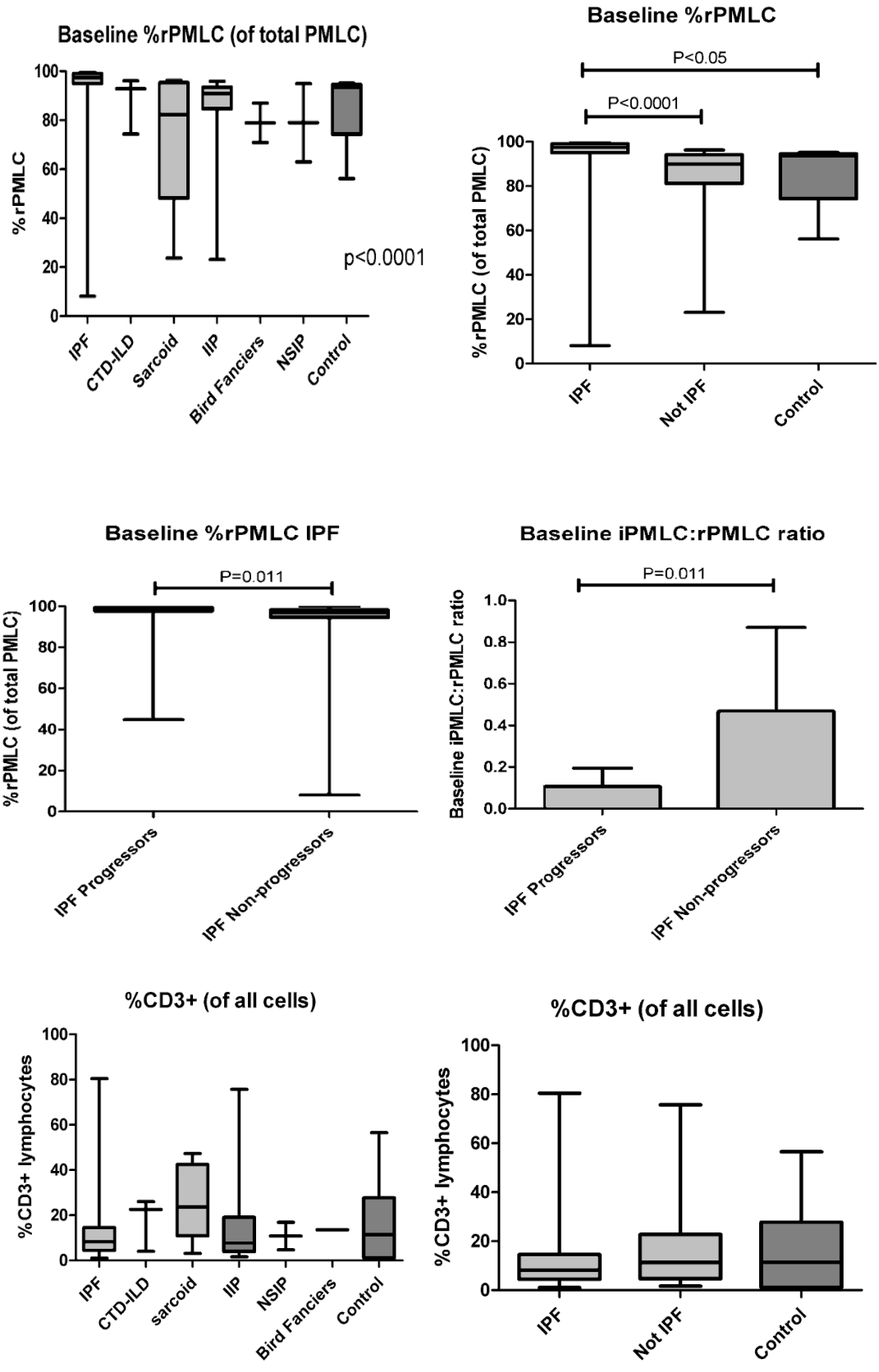

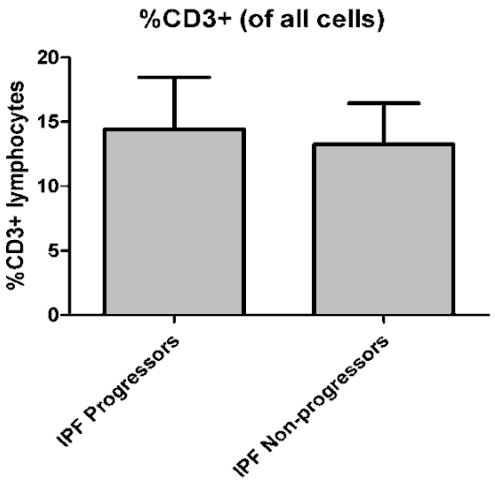
%CD3+ (of all cells)
%CD3+ lymphocytes
20
15
10
5
0
IPF Progressors
IPF Non-progressors

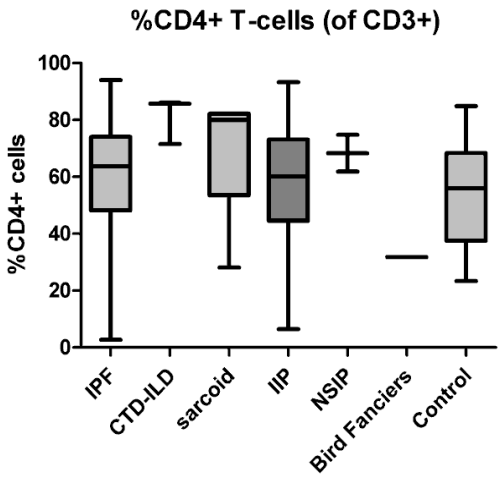
%CD4+ T-cells (of CD3+)
%CD4+ cells
100
80
60
40
20
0
IPF
CTD-ILD
sarcoid
IIP
NSIP
Bird Fanciers
Control

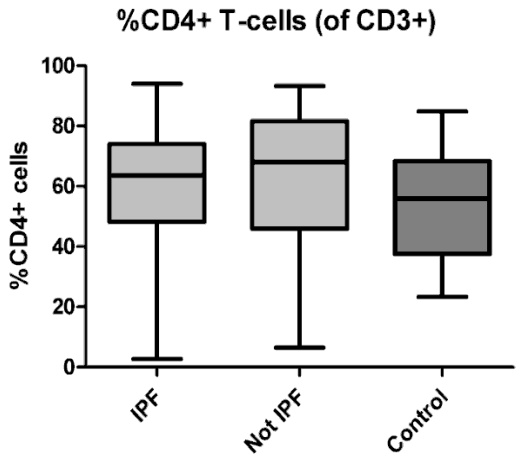
%CD4+ T-cells (of CD3+)
%CD4+ cells
100
80
60
40
20
0
IPF
Not IPF
Control

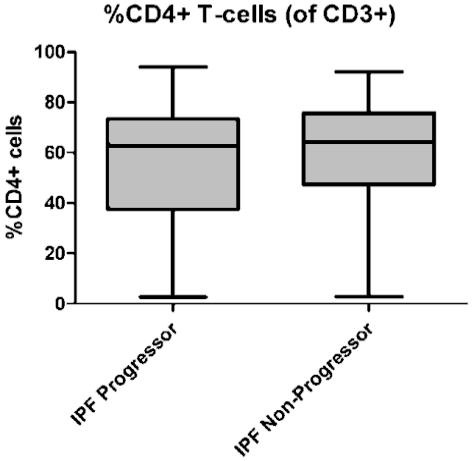
%CD4+ T-cells (of CD3+)
%CD4+ cells
100
80
60
40
20
0
IPF Progressor
IPF Non-Progressor

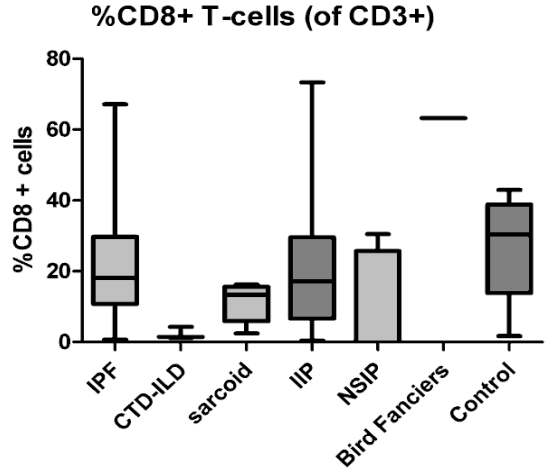
%CD8+ T-cells (of CD3+)
%CD8 + cells
80
60
40
20
0
IPF
CTD-ILD
sarcoid
IIP
NSIP
Bird Fanciers
Control

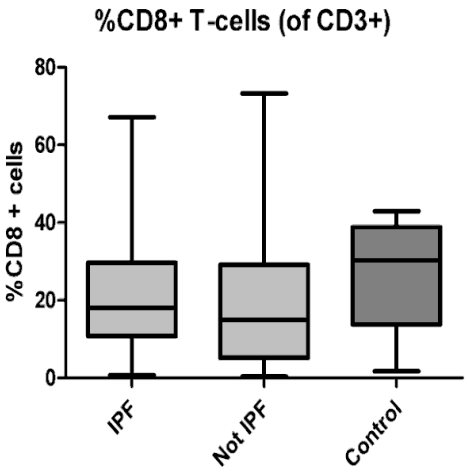
%CD8+ T-cells (of CD3+)
%CD8 + cells
80
60
40
20
0
IPF
Not IPF
Control

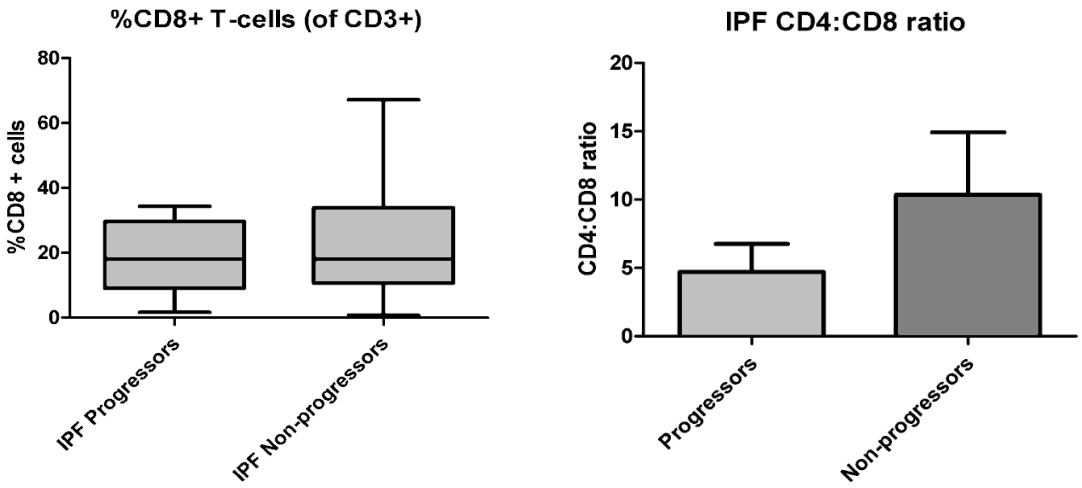

Figure 39. Whole blood classical, intermediate and non-classical monocyte population percentages in IPF vs non-fibrotic ILD and healthy control.

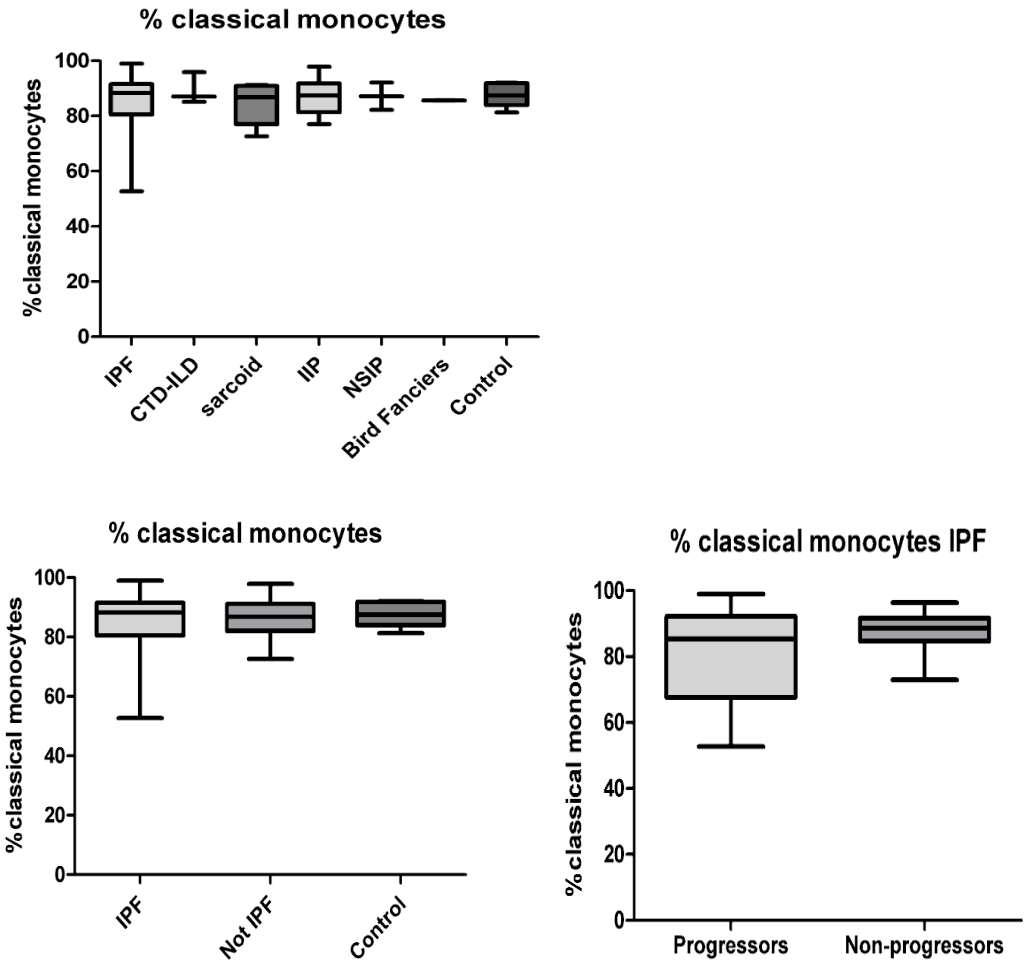

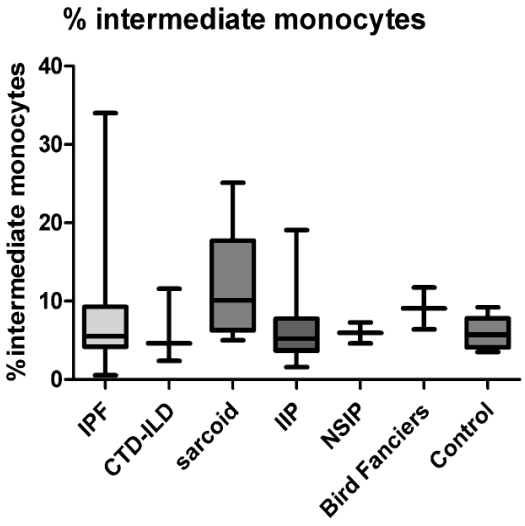
% intermediate monocytes
% intermediate monocytes
40
30
20
10
0
IPF
CTD-ILD
sarcoid
IIP
NSIP
Bird Fanciers
Control

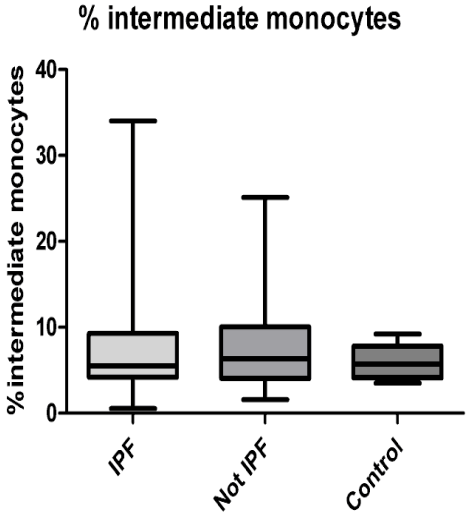
% intermediate monocytes
% intermediate monocytes
40
30
20
10
0
IPF
Not IPF
Control

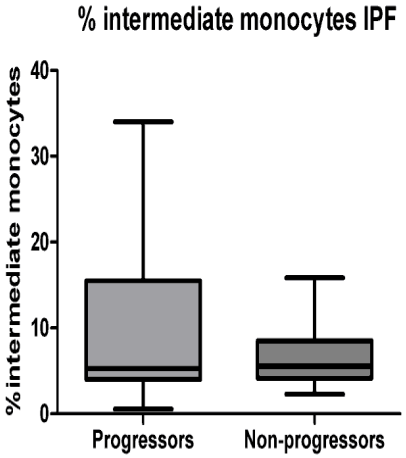
% intermediate monocytes IPF
% intermediate monocytes
40
30
20
10
0
Progressors
Non-progressors

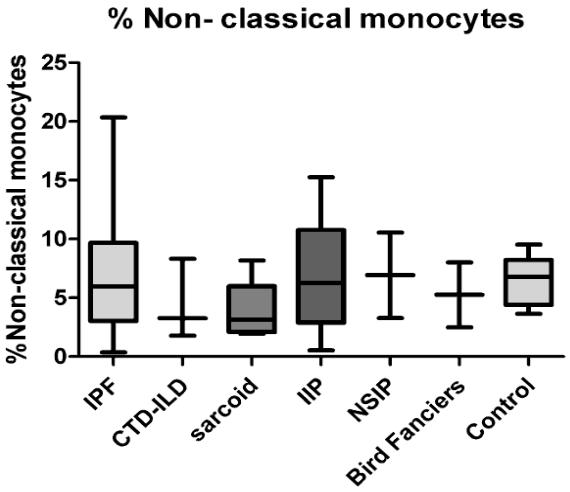
% Non- classical monocytes
% Non-classical monocytes
25
20
15
10
5
0
IPF
CTD-ILD
sarcoid
IIP
NSIP
Bird Fanciers
Control

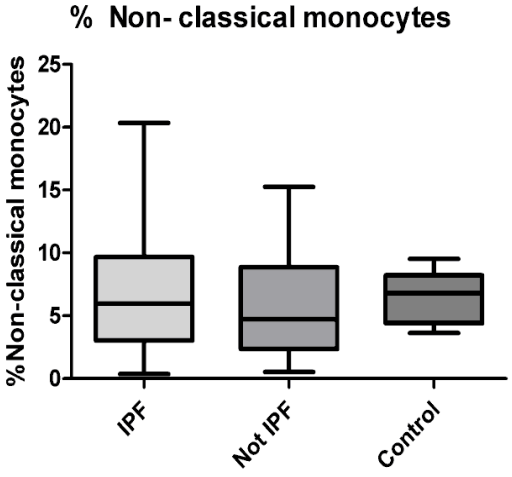
% Non- classical monocytes
% Non-classical monocytes
25
20
15
10
5
0
IPF
Not IPF
Control

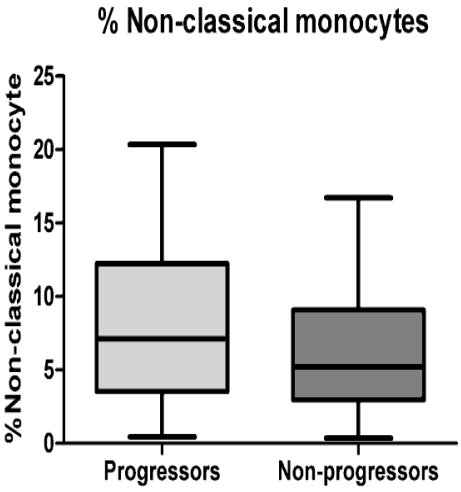
% Non-classical monocytes
% Non-classical monocyte
25
20
15
10
5
0
Progressors
Non-progressors

Real-time PCR profiling of AMs, rPMLCs and iPMLCs

After demonstrating that AMs, rPMLCs and iPMLCs are different in terms of cell size and cell surface expression markers, in order to evaluate whether these cells were different functionally, sorted AM, rPMLC and iPMLC cell pellets were sent to Professor Mark Lindsay at the University of Bath for RNA gene sequencing. Analysis of the RNA gene sequencing was performed by Alex Przybylski (PhD student) using edgeR package software. Briefly, Alex used the Human Gene Set annotation file from Ensembl to map the genes. A multidimensionality scaling plot was used to visualise the data and identify outliers. Two outliers were identified and were removed from subsequent analysis. The gene set was filtered to remove genes with 0 or near -0 counts using a Counts-Per-Million threshold. The following data is preliminary as further work is ongoing to fine-tune the analysis to ensure too many genes have not been removed, therefore losing potentially interesting results, but also to ensure too many genes have not been included, therefore increasing the likelihood of false positives and performing unnecessary comparisons. From an original set of 58,395 genes, 21,881 genes were included in the analysis. Generalised Linear Models were used to test the differences between AM, rPMLC and iPMLC groups. For each gene (21,881), Alex calculated the $\log_2$fold change (logFC) where positive values indicate upregulation of a gene in *x* versus *y*. Data showing the top twenty differentially expressed genes between AMs vs rPMLC, AMs vs iPMLC and iPMLCs vs rPMLCs is shown in Tables 29, 30 and 31 below. Heatmaps of the top twenty differentially expressed genes between AMs vs rPMLCs, AMs vs iPMLCs and iPMLCs vs rPMLCs, and histograms of the top two differentially expressed genes between each of the groups are shown in Figures 40, 41 and 42 below.

Table 29. Top twenty differentially expressed genes between AMs and rPMLCs by RNA gene sequencing.

Gene	Gene biotype	logFC	P-Value
ANGPT2	Protein coding	5.15	1.4793E-07
SPAG5	Protein coding	1.78	9.90444E-07
AC013457.1	Antisense	3.54	1.63553E-06
OPRK1	Protein coding	4.90	2.30513E-06
CENPU	Protein coding	1.56	2.80612E-06

XK	Protein coding	3.35	3.10922E-06
CDCP1	Protein coding	1.06	3.41095E-06
ESPL1	Protein coding	1.92	4.14562E-06
IER5L	Protein coding	-1.56	4.74144E-06
SNAI2	Protein coding	6.07	4.98143E-06
TBC1D4	Protein coding	1.80	6.88406E-06
OR6K3	Protein coding	4.46	7.04207E-06
HMMR	Protein coding	2.39	8.86836E-06
MYBL2	Protein coding	3.62	8.92384E-06
KIFC1	Protein coding	2.64	1.03686E-05
AXL	Protein coding	1.63	1.16976E-05
CHRM3	Protein coding	4.57	1.21527E-05
PBK	Protein coding	4.21	1.25077E-05
ASF1B	Protein coding	2.99	1.27664E-05
THBS1	Protein coding	2.12	1.41019E-05

Table 30. Top twenty differentially expressed genes between AMs and iPMLCs by RNA gene sequencing.

Gene	**Gene biotype**	**logFC**	**P-Value**
PDGFA	Protein coding	-3.18	1.303E-06
GPSM1	Protein coding	-3.10	1.737E-06
CYSLTR1	Protein coding	1.45	3.01E-06
XK	Protein coding	3.73	3.769E-06
FAM118A	Protein coding	-2.17	3.782E-06
ABCB10	Protein coding	0.98	5.201E-06
AC044849.1	Antisense	-1.96	6.056E-06
TBC1D4	Protein coding	1.98	6.089E-06
ELFN1	Protein coding	-3.18	6.171E-06
CYP4V2	Protein coding	1.55	6.566E-06
DTWD2	Protein coding	1.39	8.819E-06
ESR1	Protein coding	1.38	8.825E-06
ACKR3	Protein coding	1.86	1.069E-05
AK3	Protein coding	1.19	1.165E-05
SMIM14	Protein coding	1.06	1.249E-05
AC013457.1	Antisense	3.25	1.354E-05
PLBD1	Protein coding	1.37	1.433E-05
CDCP1	Protein coding	1.01	1.459E-05
THBS1	Protein coding	2.31	1.601E-05
HMMR	Protein coding	2.42	1.652E-05

Table 31. Top twenty differentially expressed genes between iPMLCs and rPMLCs by RNA gene sequencing.

Gene	Gene biotype	logFC	P-Value
MMP19	Protein coding	1.23	0.0002
ALDH1A2	Protein coding	1.26	0.00022
IL36RN	Protein coding	3.85	0.00043
CSPG4	Protein coding	1.05	0.00045
LINC01050	LincRNA	3.88	0.00051
IL1RN	Protein coding	1.38	0.00067
GEM	Protein coding	2.95	0.00085
PDE2A	Protein coding	1.42	0.00096
AC009951.1	TEC	0.75	0.00103
AL390719.1	Transcribed unprocessed pseudogene	2.82	0.00151
PIGV	Protein coding	-0.59	0.00155
TNFRSF18	Protein coding	2.59	0.00167
AP001330.5	LincRNA	1.93	0.00198
HRH4	Protein coding	-1.82	0.00211
CEMIP	Protein coding	2.19	0.00218
NUDT7	Protein coding	-1.48	0.00221
AC084871.1	Transcribed processed pseudogene	1.00	0.00232
ELOVL3	Protein coding	-1.56	0.00234
MAP2K6	Protein coding	-0.97	0.00234
PDCD1	Protein coding	2.95	0.00256

Figure 40. Heatmap of top 20 differentially expressed genes and histogram of top 2 differentially expressed genes between AMs and rPMLCs.

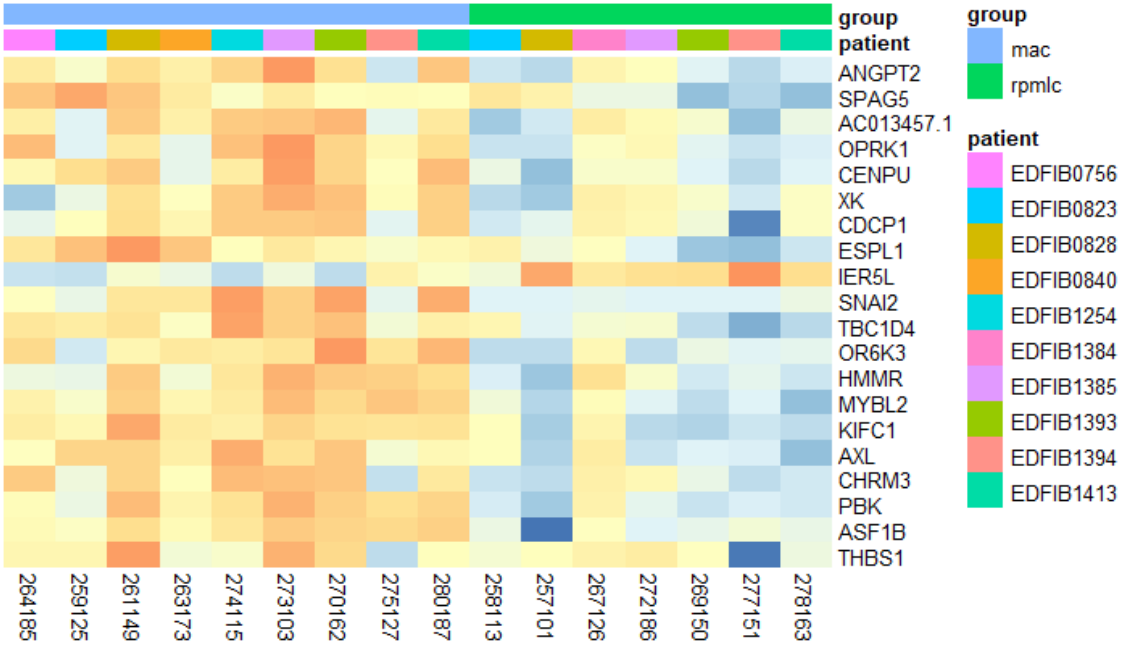

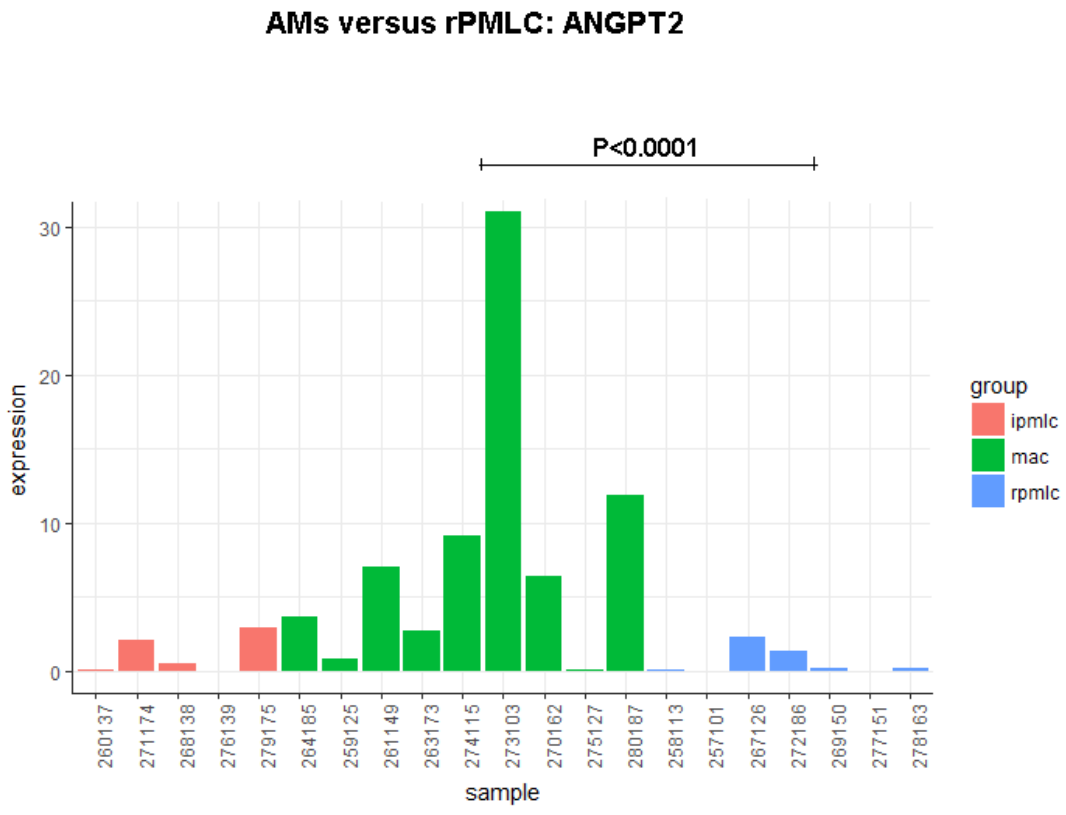

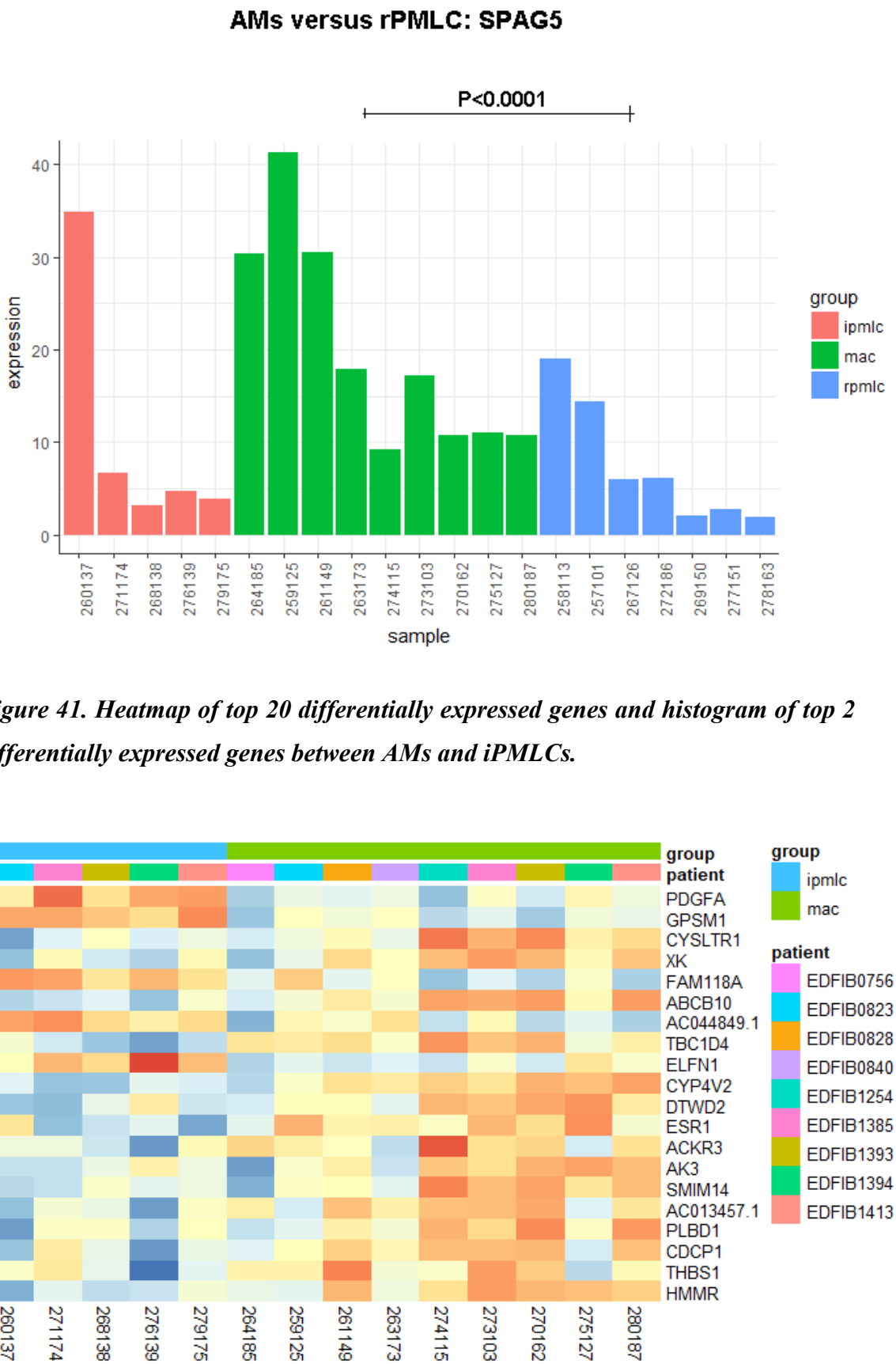

Figure 41. Heatmap of top 20 differentially expressed genes and histogram of top 2 differentially expressed genes between AMs and iPMLCs.

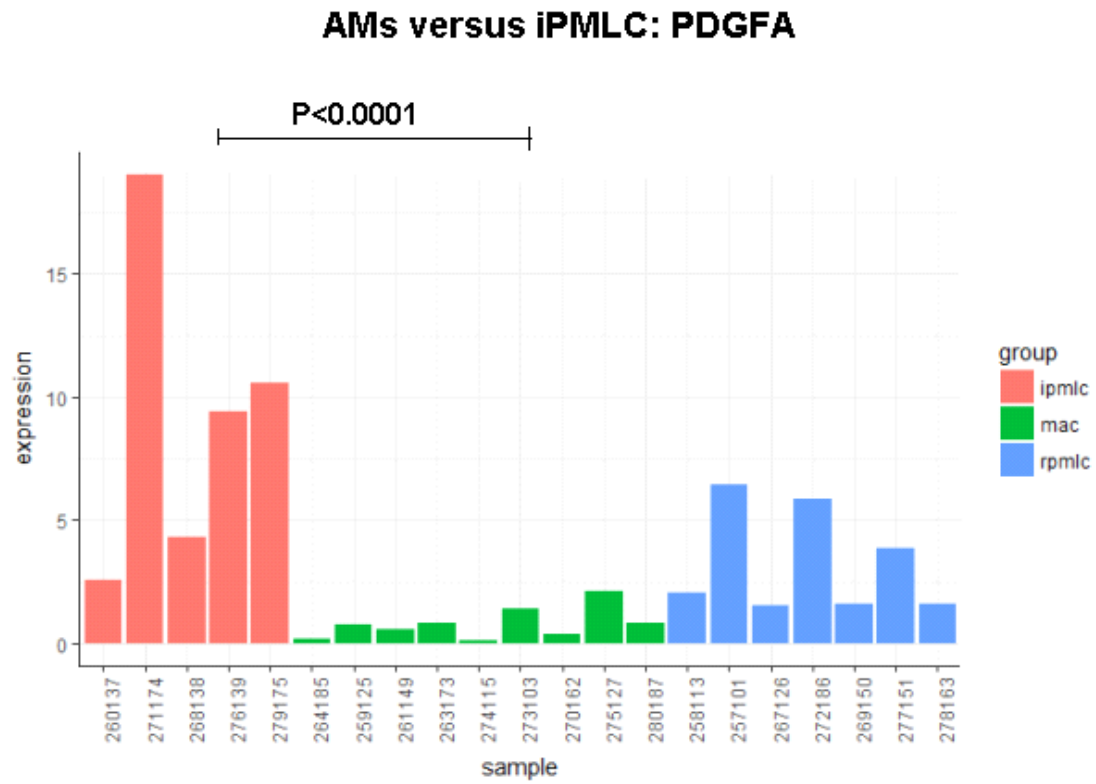
AMs versus iPMLC: PDGFA
P<0.0001
expression
15
10
5
0
260137
271174
268138
276139
279175
264185
259125
261149
263173
274115
273103
270162
275127
280187
258113
257101
267126
272186
269150
277151
278163
sample
group
ipmlc
mac
rpmlc

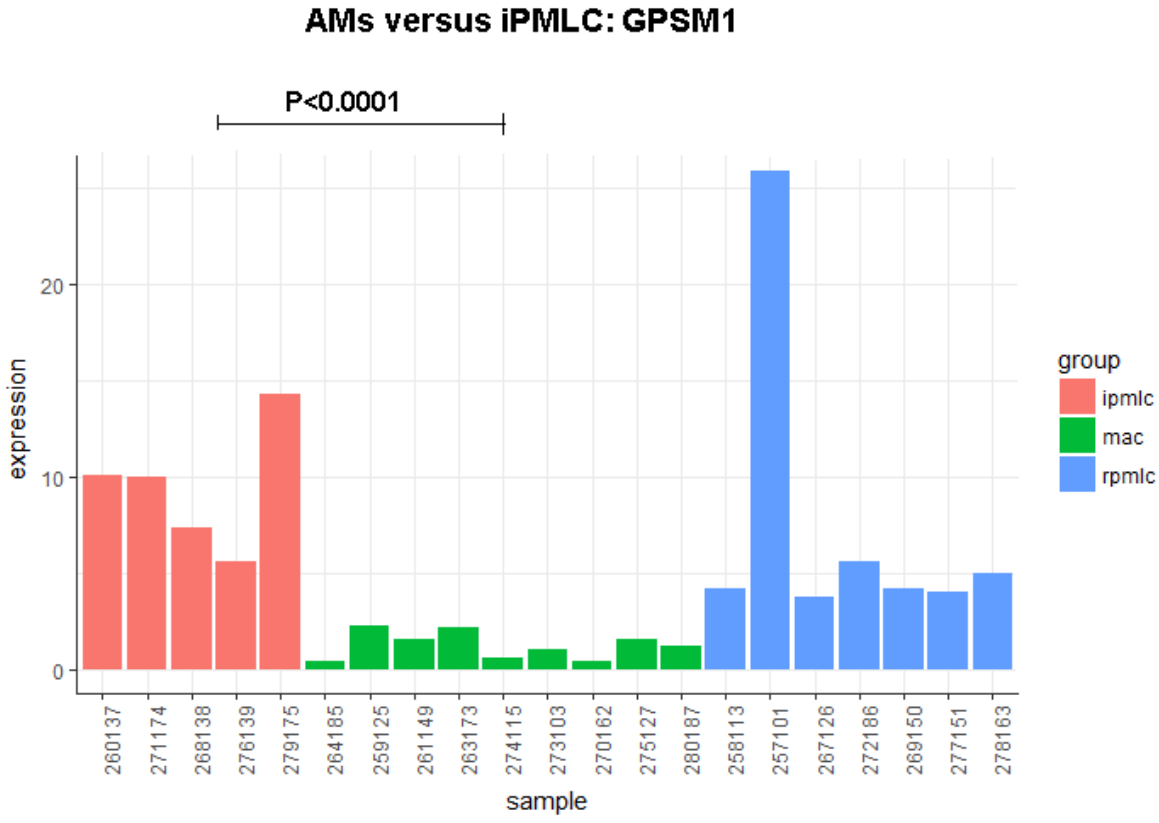
AMs versus iPMLC: GPSM1
P<0.0001
expression
20
10
0
260137
271174
268138
276139
279175
264185
259125
261149
263173
274115
273103
270162
275127
280187
258113
257101
267126
272186
269150
277151
278163
sample
group
ipmlc
mac
rpmlc

Figure 42. Heatmap of top 20 differentially expressed genes and histogram of top 2 differentially expressed genes between iPMLCs and rPMLCs.

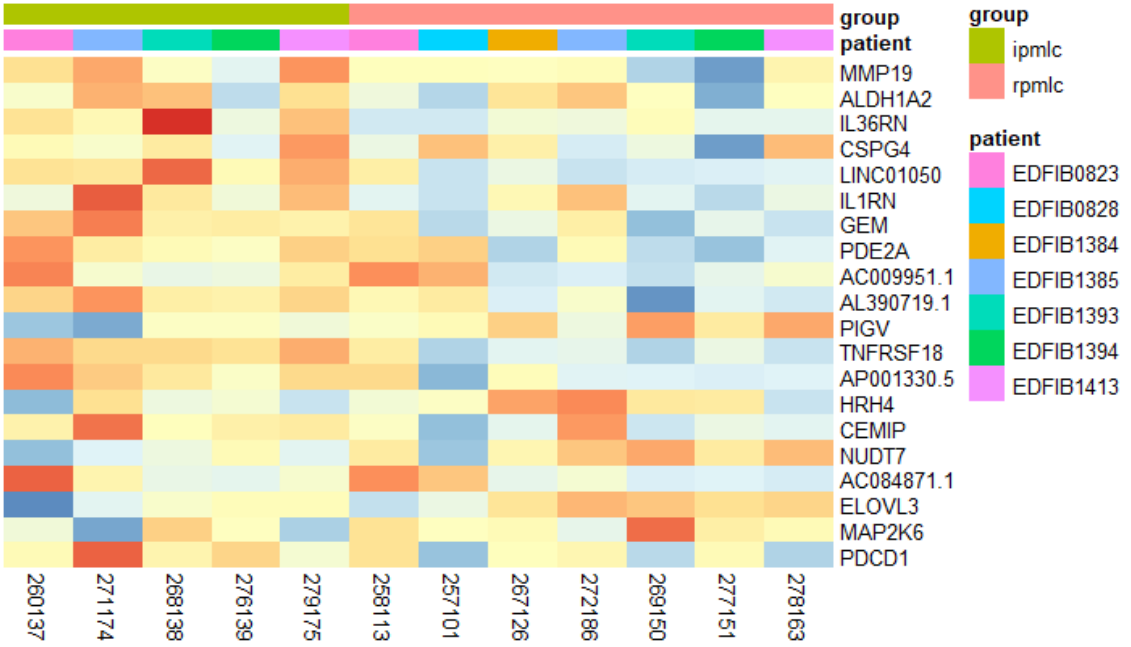

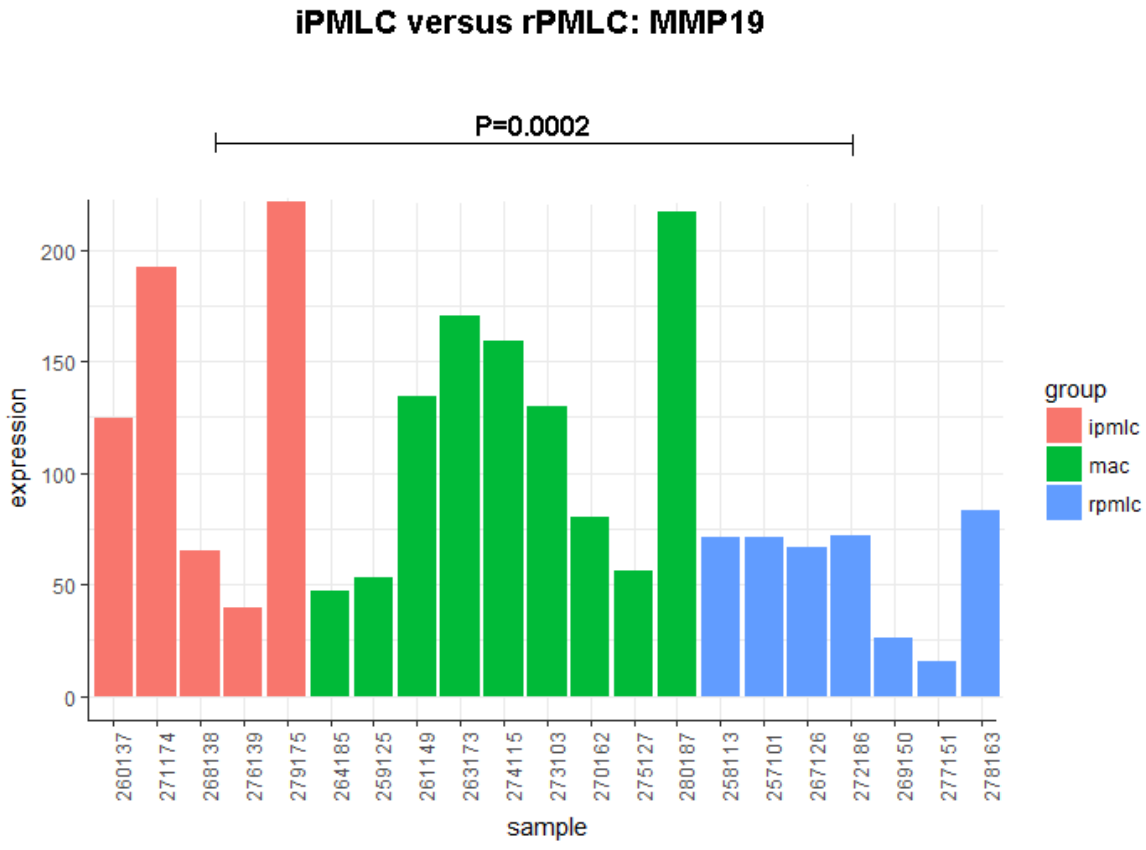

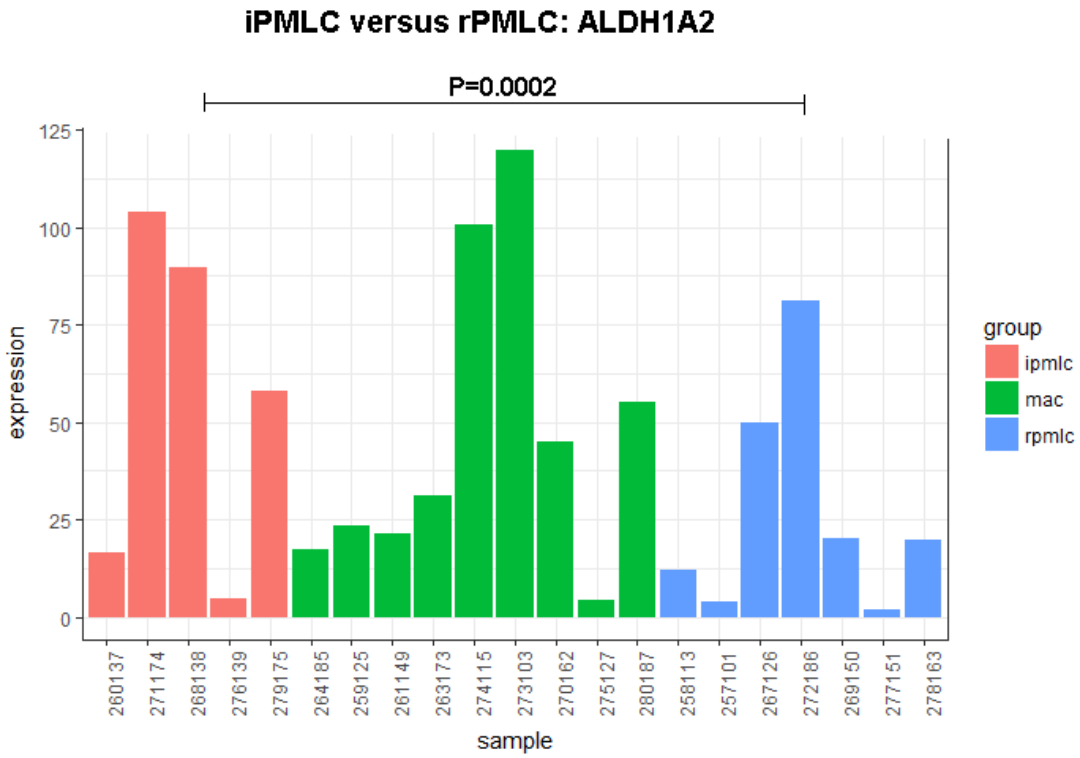

RNA gene sequencing revealed a number of significantly differentially expressed genes between AM vs rPMLC, AM vs iPMLC and iPMLC vs rPMLC groups. In the AM versus rPMLC group, ANGPT2, SPAG5, AC013457.1, OPRK1, CENPU, XK, CDCP1, ESPL1, IER5L, SNAI2, TBC1D4, OR6K3, HMMR, MYBL2, KIFC1, AXL, CHRM3, PBK, ASF1B and THBS1 were all significantly differentially expressed (all P<0.0001). In the AM versus iPMLC group, PDGFA, GPSM1, CYSLTR1, XK, FAM118A, ABCB10, AC044849.1, TBC1D4, ELFN1, CYP4V2, DTWD2, ESR1, ACKR3, AK3, SMIM14, AC013457.1, PLBD1, CDCP1, THBS1 and HMMR were all significantly differentially expressed (all P<0.0001). In the iPMLC versus rPMLC group, MMP19, ALDH1A2, IL36RN, CSPG4, LINC01050, IL1RN, GEM, PDE2A, AC009951.1, AL390719.1, PIGV, TNFRSF18, AP001330.5, HRH4, CEMIP, NUDT7, AC084871.1, ELOVL3, MAP2K6 and PDCD1 were all significantly differentially expressed (all P<0.002). A literature search on each of the genes revealed that most of the top sixty differentially expressed genes could be clustered together by their involvement in one of three main pathways; apoptosis, G-protein coupled receptor signalling pathways and angiogenesis. All three of these pathways play a role in the pathogenesis of IPF and may represent future targets for further research to develop targeted therapy.

4.3 Discussion

Idiopathic pulmonary fibrosis is a lethal, chronic, progressive interstitial lung disease of unknown aetiology. Because of it's poor prognosis, and no curative therapy, reliable methods of both differentiating IPF from the other ILDs and also predicting disease progression are of great benefit. Several studies have reported considerable interobserver variation[96,97] and interlobar variability[96,98] in the histological interpretation of the ILDs, and so it has been suggested that histopathologic examination alone from SLB sampling is less reliable as a pivotal investigation in diagnosing ILD. Numerous studies have also demonstrated interobserver variation in the interpretation of HRCT findings alone[96,99,100] and also when HRCT appearances and histopathology are examined in combination[32,96]. The sensitivity and specificity of HRCT for the diagnosis of IPF have been reported as approximately 43 to 78% and 90 to 97% respectively[96]. Furthermore Flaherty et al demonstrated that an HRCT pattern consistent with IPF is only present in around half of patients with histologically confirmed UIP and is associated with mid to late-stage disease and a particularly poor prognosis[32,96]. Both UIP HRCT and histopathologic appearances can also be seen in association with drug exposure, environmental factors and connective tissue disease[96,101].

Prior to the 2011 ATS/ERS/JRS/ALAT guideline, differential cell count in BAL was considered a key step in the IPF diagnostic pathway. However in 2011, BAL was completely removed from the diagnostic algorithm. Bronchoalveolar lavage has been pivotal in elucidating the key immune effector cells driving the inflammatory process in IPF[102,103]. A number of BAL cellular components are reported as being elevated in patients with IPF, including polymorphonuclear leukocytes, neutrophil products, eosinophils, eosinophil products, activated alveolar macrophages, alveolar macrophage products, cytokines, chemokines, immune complexes and fibroblastic growth factors[102,103]. BAL fluid analysis in IPF typically shows an increase in total cell count, polymorphonucleated neutrophils (>5%) and eosinophils (>2%)[16,102,104–107]. It has been shown however that there is no correlation between the percentages of BAL cell types and various clinical parameters, serum tests or lung function studies[102]. It has been reported that 70-90% of patients with IIP have a BAL neutrophilia (>5%). The presence of a BAL neutrophilia increases the likelihood of an underlying fibrotic process such as IPF, RA-ILD, asbestosis or fibrotic sarcoidosis, and is directly linked to the extent of

reticular change on HRCT[102]. Whilst raised BAL neutrophils (>5%) may be characteristic of IPF, it is not diagnostic. In IPF, 40-60% of patients will also have an associated increase in BAL eosinophils (>2%)[102]. Numerous studies have reported that BAL is a safe, well-tolerated diagnostic procedure in ILD, and carries far fewer risks than SLB.

Our study demonstrates a composite assessment of the roles of BAL in the clinical pathway of patients presenting with suspected IPF from diagnosis to prognostic stratification and additionally explores the safety and tolerability of the procedure. In our study of 325 suspected IIP patients, 128 underwent BAL at presentation. Based on ATS/ERS HRCT criteria, 22 were categorised as 'definite UIP', 62 as 'probable UIP' and 44 as 'inconsistent with UIP'. BAL granulocytes ≥3% and lymphocytes <20% were considered consistent with IPF, as suggested by consensus guidelines. Our data suggests that BAL differential cell count is consistent with IPF in the majority of patients with IPF (86.9%, n=73/84) in which HRCT appearances are considered either 'definite' (90.0%, n=20/22) or 'probable' (85.5%, n=53/62) UIP pattern. In our cohort, BAL DCC in patients with HRCT defined 'definite' and 'probable' UIP were similar, however differed significantly from other types of ILD with patterns 'inconsistent with' and IPF diagnosis. Both at baseline and at 12 month BAL, there were no significant differences in BAL DCC percentages or absolute cell count in any cell type between progressor and non-progressor groups.

Numerous study groups report that BAL is a useful technique for the differential diagnosis of various ILDs and with well documented typical BAL features of sarcoidosis, hypersensitivity pneumonitis, occupational lung disease and RB-ILD, it should be considered an important adjuvant in the diagnostic work-up. A study by Domagala-Kulawik and colleagues revealed a significant relation between the total cell count and ILD diagnosis[108]. They also found significant differences between ILD groups in total AM, lymphocyte, neutrophil and eosinophil counts. The additional value of BAL in the diagnostic pathway in IPF specifically has also been explored in several studies. Oshimo et al evaluated the clinical utility of BAL for the diagnosis of IPF and found that 8% (n=6/74) of their cohort were diagnosed with IPF based on consistent HRCT, pulmonary function and clinical findings, but demonstrated a lymphocytosis of >30% in BAL cell differentials. Further examinations by means of surgical lung biopsy

in 2 patients and subsequent outcomes in 4 patients clarified the final diagnosis of idiopathic NSIP in 3 patients and of EAA in 3 patients, therefore BAL lymphocytosis changed the diagnostic perception in all 6 patients. They concluded that BAL differential cell count continues to have a role in the diagnostic evaluation of IPF since 1 in 12 of their patients with 'definite UIP' HRCT appearances had cell counts inconsistent with the diagnosis[96]. In our cohort, 9.1% (n=2/22) of patients with 'definite UIP' HRCT appearances had a BAL DCC that was inconsistent with IPF (granulocytes <3% or lymphocytes >20%). Neither of these patients were fit enough to undergo repeat BAL at 12 months. In the 'probable UIP' HRCT group, 14.5% (n=9/62) had inconsistent with IPF BAL DCCs. Two patients went on to have SLB and UIP was confirmed histologically in both. Five patients had a repeat BAL 12 months later, and of the 5, 4 patients had DCCs that were consistent with IPF on repeat. Our data shows that mortality in patients with suspected IPF and a BAL differential cell count consistent with IPF was no different to those with a BAL DCC inconsistent with IPF (P=0.425, HR 1.590 (95% CI 0.502 – 4.967)). Furthermore, there was also no significant difference in disease progression in either group (P=0.885, HR 1.08 (95% CI 0.367 – 3.106)).

The value of BAL differential cell count in predicting survival in IPF has been a topic of rich debate. A large scale multivariate analysis by Kinder et al demonstrated that BAL neutrophilia >3% significantly predicted mortality independently of confounding variables including age, sex, smoking status and lung function. Their study however is not without its limitations, including an extended follow up period of over 14 years, during which time there may have been several changes in the diagnosis and management of IPF, and also most importantly, a lack of HRCT diagnosis in their patients[104]. In contrast, Veeraghavan et al reported no significant predictive effect of BAL neutrophilia on survival when its value was studied retrospectively in a cohort of histologically proven IPF patients. These patients were diagnosed by the 'gold standard' by means of surgical lung biopsy, however the study was limited by a small cohort of only 35 patients[105]. Whilst previous studies have demonstrated that BAL granulocystosis or neutrophilia may be an important diagnostic and prognostic indicator in IPF[96,104,106], our data does not suggest any significant predictive effects. Kaplan Meier curves showing 2 and 5 year mortality in patients with BAL neutrophils of >3% vs <3% showed no significant difference in either 2 or 5 year survival between groups.

Previous studies have also reported that the absence of a lymphocytosis in BAL is important for the diagnosis of IPF[96,101], however no exact cut-off level has been evaluated. The 2002 ATS/ERS Consensus Classification suggested that lymphocyte counts greater than 15%, which is the upper limit of normal, might be suggestive of an alternative diagnosis such as NSIP, COP, EAA or sarcoidosis[68,96]. Our study demonstrated that a cut-off level of 20% for lymphocytes in BAL could discriminate between IPF and non-IPF favourably, however the value of a lymphocytosis as a predictor of survival was much less convincing with Kaplan Meier curves showing no significant difference in either 2 or 5 year survival between patients with BAL lymphocytes of <20% and those with BAL lymphocytes >20%.

It is widely accepted that alveolar macrophages are an integral part of the lung's reparative mechanism following injury, and in IPF they contribute to the pathogenesis by releasing pro-fibrotic mediators promoting fibroblast proliferation and collagen deposition. It is well documented that macrophage polarisation phenotype is broadly heterogeneic depending on their microenvironment. However little exists in the literature regarding the alveolar macrophage polarisation phenotype in IPF specifically. The M1 macrophage phenotype is characterised by the production of high levels of pro-inflammatory cytokines, and strong microbicidal properties with an ability to facilitate resistance to pathogens. Polarisation into M1 (pro-inflammatory or classically activated) macrophages occurs in response to bacterial LPS and products secreted by activated T helper 1 lymphocytes and natural killer (NK) cells, including IFN-γ, TNF-α and granulocyte-macrophage colony stimulating factor. M1 macrophages release pro-inflammatory cytokines such as TNF-α, IL-12, IL-6, IL-18, IL-23 and NO, which help drive antigen specific Th1 and Th17 cell inflammatory responses[109]. Phenotypically M1 macrophages express high levels of major histocompatibility complex class II, CD68 marker and co-stimulatory molecules CD80 and CD86.

M2 (anti-inflammatory or alternatively activated) macrophages are induced by fungal cells, immune complexes, helminth infections, glucocorticosteroids, complement components, apoptotic cells, and a number of T helper 2 lymphocyte-related cytokines including IL-4, IL-13, IL-10, macrophage colony stimulating factor and TGF-β. They

release inflammatory mediators. M2 macrophages have immunomodulatory functions and are involved in phagocytosis, parasite control, angiogenesis, wound healing and tumour promotion[109]. M2 macrophage activation has been reported in a number of disease pathologies including asthma, host response to parasitic infections, wound repair, fibrosis, granulomatous disease, atheromatous plaque deposition and in response to tumour-associated macrophages[62]. Phenotypically M2 macrophages can be further divided into subsets (M2a, M2b and M2c) depending on their gene expression profiles[110,111]. The M2a subtype is elicited in response to IL-4, IL-13 and fungal or helminth infections, M2b by IL-1 receptor ligands, immune complexes and LPS, and M2c by IL-10, TGF-β and glucocorticosteroids.

The two populations can be differentiated from each other with specific antibodies against their surface markers. CD163 is a transmembrane protein expressed on monocyte/ macrophage cell lines. It is been reported that increased CD163 expression occurs during resolution of inflammation and the wound healing process[109,112]. CD206 (mannose receptor) is a C-type lectin expressed predominantly by most tissue macrophages, dendritic cells and specific lymphatic or endothelial cells. Both molecules are reported as markers of M2 macrophages. M1 detection is more contentious as no single, widely accepted marker has ever been described. It is well recognised that the idea of AMs being polarised into two distinct populations, M1 and M2, is an oversimplification. Macrophage differentiation is highly dynamic. Unlike the irreversible changes in the phenotype of lymphocytes following exposure to polarising cytokines, macrophages can rapidly switch from one phenotype to another, in a transient and plastic process. There is a growing body of evidence to suggest that spatiotemporal activation of nuclear factor kappa-light-chain-enhancer of activated B cells (NF-B) is one of the most prominent regulators of the plasticity of macrophages seen in many disease courses. It has been shown that in the early phase of tumorigenesis, NF-B activation in M1 macrophages causes cancer-related inflammation, however during the late stages of tumorigenesis, macrophages are re-programmed to M2-like tumour-associated macrophages, with low NF-B activation and high immunosuppressive capacity[57]. A similar switch has been reported in the course of sepsis in which NF-B activation drives the initial inflammatory response, whilst during the later stages macrophages are polarised to an anti-inflammatory, tumour-growth promoting M2 phenotype, with reduced NF-B activation[57]. These findings are

supported by a study by Pawel Wojtan et al describing macrophage polarisation in ILD. Their group used CD40 as a marker of M1 macrophages and CD163 as a marker of M2 macrophages, but found the summation of the percentages of cells stained with anti-CD40 and anti-CD163 was greater than 100%, suggesting the presence of both markers of M1 and M2 on the cells. There was also a very low proportion of unstained cells, indicating a number of cells did not express M1 or M2 markers, and may have been in an intermediate stage of polarisation between pro- and anti-inflammatory states[109]. This finding was supported by a study by SJ Allden et al, who noted AMs from ILD lacked a distinct pattern of polarisation with cells widely expressing both M1 and M2 markers[113]. It has also been demonstrated by MJ Davis et al that macrophages are capable of complete repolarisation from M2 to M1 in vitro, and can reverse their polarisation depending on the chemokine environment[57,114].

CD71 (transferrin receptor 1) is a membrane glycoprotein that plays an important role in cellular uptake of iron. All proliferating cells in the hematopoietic system express CD71 and whilst CD71 is a well known marker for cell proliferation and activation[115], it's role in IPF is uncertain. A small number of studies have reported that CD71 expression may distinguish subsets of human alveolar macrophages, with SJ Allden and colleagues reporting CD71 expression highlighted distinct populations of cells in human BAL. CD71 expression was high on AMs, and CD11c+CD71+ cells expressed significantly more HLA-DR, CD86, CD206 and CD163 compared to CD11c+CD71- cells. Furthermore, the two populations were functionally distinct with a significantly higher population of CD11c+CD71+ AMs having phagocytosed bacteria and increased proportion of CD11c+CD71- cells producing NO[113].

My study demonstrated the presence of a distinct AM polarisation phenotype in the IPF patient population with a significantly increased M2 (specifically M2a) subset. In addition, I was able to demonstrate that AM phenotypes can be predictive of disease progression in IPF with characteristic predictors of stable disease at presentation including low CD71, low CD206 and high CD163 expression on AMs. A higher M2 (specifically M2a) population relative to M1 macrophages at presentation was also suggestive of a more indolent course. In my study, IPF patients with rapid disease progression had significantly increased AM expression of CD71 and CD206, and significantly reduced expression of CD163. The finding that survival was significantly

worse in patients with high CD71 expression, led to the description of an AM phenotype that was predictive of disease progression in IPF, and a finding that survival was significantly different between $CD71^{high}CD206^{high}CD163^{low}$, $CD71^{high/low}CD206^{high/low}CD163^{high/low}$ and $CD71^{low}CD206^{low}CD163^{high}$ groups.

It has been reported previously that expansion of novel subpopulations of pulmonary monocyte-like cells, rPMLC (HLA-DR+CD14++CD16+ cells) and iPMLC (HLA-DR+CD14++CD16- cells) occurs in inflammatory lung disease, however their presence and significance in fibrotic lung disease is unknown. It is widely accepted that monocytes and macrophages contribute significantly to the disease process in IPF, and this is supported by a number of studies investigating the molecular events leading to pulmonary fibrosis[116]. AMs are the predominant cell type in the healthy lung, and under normal conditions, are maintained by both local proliferation of resident pulmonary macrophages and extravasation of circulating monocytes, which are derived from bone marrow[116]. It has been suggested that in inflammatory lung disease, increased numbers of monocytes are recruited to the bronchoalveolar space from the pulmonary circulation[116]. It has also been reported that in smokers, and patients with sarcoidosis, IPF, extrinsic allergic alveolitis (EAA), bronchogenic cancer, asthma and HIV, AMs exhibit increased expression of monocyte-lineage surface antigens[116].

CD14 is a receptor for LPS that has high level expression in normal blood monocytes, and low level expression in the CD14+/CD16+ monocyte subset, and in mature AMs[116]. CD16 is a low-affinity receptor for IgG. It has low level expression on blood monocytes, but is highly expressed on end-stage differentiated macrophages[116]. HLA-DR is a major histocompatibility complex class II molecule and is expressed on both blood monocytes and AMs, with considerably higher staining intensity in AMs[116]. CD11b is an integrin expressed on the surface of many leukocytes including monocytes, neutrophils, natural killer cells, granulocytes and macrophages. It is involved in the regulation of leukocyte adhesion and migration to mediate the inflammatory response, and also functions in phagocytosis and extravasation. Krombach et al demonstrated an increased monocyte population in the lungs of patients with chronic inflammatory lung disease. They found a predominance of cells with a monocyte-like phenotype of the total AM population with cells displaying increased expression of CD14 and CD11b, and reduced expression of CD16. They found that in BAL fluid of patients with chronic inflammatory lung

disease, increased numbers of monocyte-like cells were present, exhibiting optical properties of blood monocytes and an immunophenotype in between that of blood monocytes and AMs[116].

A small number of studies have investigated monocyte phenotype, function and their lineage in the human lung. Brittan et al characterised human monocyte subsets, neutrophils and T-regs in both peripheral blood and BAL fluid cells in healthy volunteers exposed to either inhaled bacterial LPS or normal saline. They reported the presence of a human PMLC population with distinct resident and inducible PMLC subsets post LPS-inhalation. The iPMLC subpopulation were HLA-DR+CD14++CD16- cells, and increased significantly following LPS compared with saline, significant increases in pulmonary neutrophils and significant decreases in pulmonary T-regs were also noted[49]. A previous study had reported a population of monocytes with reduced phagocytic capacity and increased expression of HLA-DR, CD80 and CD86, markers of dendritic cell maturation, in sputum from healthy volunteers following LPS inhalation[49,117]. A second study had reported the presence of a 'small sputum macrophage' in patients with COPD. Frankenberger et al found that a large proportion of CD14+ macrophages in COPD patients had lower forward scatter on flow cytometry, and termed them 'small macrophages'. These cells were found to have high CD14 and HLA-DR expression, and higher levels of TNF compared to large macrophages. TNF was also inducible by LPS preferentially in the small macrophages, suggesting the cells were highly active inflammatory cells. The group concluded these cells were of the monocyte/macrophage lineage[49,118].

Brittan and colleagues proposed that during self-limiting lung inflammation, inducible CD14++CD16- monocytes rapidly infiltrate the lung alongside neutrophils, from blood. PMLCs were not believed to be dendritic cells as they expressed CD11b and high levels of CD14[49,50]. In their study, the numbers of resident PMLCs in the lung remained unchanged following LPS inhalation, suggesting there was no phenotypic switch from rPMLC to iPMLCs. They proposed that rPMLCs were endogenous to the lung and were involved in the maintenance of macrophage homeostasis by undergoing local proliferation and macrophage differentiation. Phenotypically, rPMLCs had significantly higher expression of the proliferation marker Ki67, the transferring receptor CD71, and the macrophage mannose receptor CD206. The scavenger receptor

CD163 and the mature macrophage marker 25 F9 were also expressed by a higher proportion of rPMLCs compared to iPMLCs, however this did not reach significance. Functional differences were also reported in that AMs had a significantly increased ability to undergo phagocytosis when compared to PMLCs in BAL fluid and dexamethasone was found to significantly suppress IL-8 and IL-6 secretion by AMs, but not by iPMLCs after 24 hours of treatment. No significant differences in IL-6, IL-8 or TNFα production by iPMLCs compared to AMs were noted[50].

My study aimed to quantify and characterise the PMLC population in the lungs of IPF patients. I found that the percentage of BAL rPMLCs was significantly higher in patients with IPF versus both non-fibrotic ILD and controls. Furthermore, the BAL rPMLC percentage was significantly increased in IPF progressor versus non-progressor groups. Disease progression in IPF was associated with an increased percentage of BAL rPMLCs and a reduced percentage of iPMLCs, and a significantly reduced iPMLC:rPMLC ratio at presentation. My study also identified a number of key differentially expressed genes by RNA gene sequencing between AM vs rPMLC, AM vs iPMLC and iPMLC vs rPMLC groups, suggesting that these cell types are different functionally as well as phenotypically.

IPF is thought to occur following injury to type I alveolar cells, which leads to AEC apoptosis and disruption of the AEC cell layer. Remaining AECs are aberrantly activated and secrete profibrotic cytokines (for example TGF) that promote recruitment and activation of inflammatory cells and fibroblasts. Chemokines and growth factors present in the provisional matrix result in an influx of fibroblasts and epithelial to mesenchymal transition (EMT) of local AECs. These fibroblasts are then activated by TGF into highly contractile myofibroblasts , which are the primary cell for collagen deposition, matrix production and tissue remodelling. Apoptosis is a highly organised physiological event that is fundamental in a variety of normal developmental and homeostatic processes[119]. Epithelial cell apoptosis is a persistent finding in lung tissue from patients with IPF and in the murine bleomycin-induced fibrosis models[119]. There is evidence to suggest lung myofibroblasts have a resistance to apoptosis in IPF[119]. These mechanisms may be pivotal to the underlying pathogenesis in IPF. A number of genes involved in apoptosis were differentially expressed between AMs and rPMLCs, AMs and iPMLCs and iPMLCs and rPMLCs in our RNA gene sequencing study. In the

AM versus rPMLC group, SPAG5, CENPU, ESPL1, SNAI2, MYBL2 and AXL were all significantly differentially expressed. In the AM versus iPMLC group, ACKR3 was significantly differentially expressed, and in the iPMLC versus rPMLC group, MMP19, PDE2A, TNFRSF18, CEMIP, MAP2K6 and PDCD1 were all significantly differentially expressed. This may be a significant finding as it suggests that these cells are different both phenotypically and functionally, and in view of the fact that a number of genes are differentially expressed in a small number of pathways already documented as relevant in IPF pathogenesis (namely apoptosis, G-protein coupled receptor signalling and angiogenesis), may be important clinically, as they may represent future targets for further biochemical and molecular research to understand the pathogenesis in IPF, but also for future therapeutic strategies.

Nintedanib, one of the two licensed drug treatments for IPF inhibits multiple receptor tyrosine kinases, and has been shown to slow progression of lung function decline in IPF[120]. As receptor tyrosine kinases predominantly signal through the Ras/mitogen-activated protein kinase signalling cascade, this pathway may be responsible for many of the pro-fibrotic responses observed in IPF[120]. Recent evidence suggests that the cyclic adenosine monophosphate (cAMP) pathway can inhibit mitogen-activated protein kinase signalling and also reduce fibroblast function via the binding of agonist to G protein-coupled receptors, which leads to adenylyl cyclase activation and increased levels of cAMP, which then leads to inhibition of lung fibroblast migration, proliferation and differentiation. It has been demonstrated that PGE2 acting at PGE2 receptors 2 and 4, and iloprost acting at the prostacyclin receptor reduced proliferation and differentiation of lung fibroblasts via cAMP accumulation and protein kinase A (PKA) activation[120]. In addition, it has been shown that inhibition of phosphodiesterases which catalyse cAMP degradation lead to reduced pulmonary fibrosis in the bleomycin mouse model[120]. A number of genes involved in G protein-coupled receptor signalling pathways were differentially expressed in our study. The majority of diffentially expressed genes were between the AM vs iPMLC group (GPSM1, CYSLTR1, ELFN1 and ACKR3) and the AM vs rPMLC group (OPRK1, OR6K3 and CHRM3). However HRH4 was also differentially expressed between iPMLC and rPMLC groups, suggesting PMLCs may play an important role in these pathways.

IPF not only destroys the lung parenchyma, but also the pulmonary vasculature with aberrant microvascular and macrovascular remodelling[121]. Aberrant vascular remodelling in IPF was reported in a study by Turner-Warwick demonstrating anastomoses between the systemic and pulmonary microvasculature and extensive neovascularisation within areas of fibrosis[121,122]. Further studies have demonstrated that vascular heterogeneity exists in the IPF lung, with areas of increased vascularisation often at the interface with normal parenchyma, and areas of reduced vascularity often in the most severely affected fibrotic areas[121,123]. A number of genes involved in angiogenesis were differentially expressed in our study (PDGF-A, THBS1, ANGPT2 and MMP19). Homeostatic control of angiogenesis depends on a careful balance between stimulatory and inhibitory factors. Keane et al reported that an imbalance in the expression of angiogenic chemokines (CXCL5, CXCL8) versus angiostatic factors (CXCL10) was present in IPF, resulting in angiogenesis[121,124]. Other reported factor include VEGF, PEDF, ang-1, ang-2 and nuclear factor B[121]. A better understanding of vascular remodelling in the IPF lung is required before targeted therapies can be considered.

Limitations of the study

Our study has a number of limitations. It is a single centre study of a small number of IPF patients which was not repeated in a validation cohort. Our control patients were often not healthy volunteers, but rather patients undergoing bronchoscopy for another indication, for example a single episode of haemoptysis. Many of the control patients were also smokers. The data has not been adjusted for confounding factors such as smoking status, age, sex and baseline lung function and so there will undoubtedly be an element of bias. Another important caveat of our study is that almost a quarter (22%) of lavaged patients died or were deemed too frail to undergo a repeat procedure at 12 months, and so the truly progressive subpopulation may have been missed. Due to time limitations on the day of the BAL procedure, a number of samples were frozen after cell sorting, with cDNA and RNA extractions performed at a later date. Whilst attempts were made to limit the number of freeze-thaw cycles to one or two, some samples may have been frozen/thawed more than this, which would undoubtedly lead to cell damage and loss of material. Another limitation is that I did not use a live/dead cell marker when staining my samples. Dead cells have greater autofluorescence and increased non-

specific antibody binding, which can lead to false positives. Identification of weakly positive samples and rare populations is also more difficult. I used forward and side scatter gating strategies to remove dead cells and debris at the beginning of my analysis, however this will not have excluded all of them.

BAL itself may cause a degree of pulmonary inflammation. Our BAL always sampled only one segment of the right middle lobe, and so we did not sample the area most severely affected by disease on HRCT. BAL only retrieves cells freely mobilised from the alveolar space, and so we may have have retrieved reduced numbers of the cells of interest in doing this. However total cell counts in our study were consistently between 10 and 20 million cells per patient, and percentages of AMs, neutrophils, eosinophils and lymphocytes were consistent with other studies. Our classification of resident and inducible PMLC subpopulations mirrored the terms described previously by Brittan and colleagues and were based on the variable expression of the monocyte markers CD14 and CD16, and the shift in the ratio of these cells in LPS-mediated acute lung inflammation. Their study had its own limitations, and whilst their data was broadly supportive that rPMLCs are endogenous to the lung and iPMLCs are sequestered from circulation, this has not yet been proven. There also remains very little information regarding the function of these cells. Due to time constraints on the day of the BAL procedure, these cells were only obtained from 5 patients, and flow sorting of these cells in my study yielded a small and finite number of cells. The samples from the 5 patients were pooled together to provide enough cells for RNA sequencing. Although pooling leads to a decrease in biological variation, it also leads to the loss of individual-specific information which is essential in biomarker studies. Both small sample size and pooling of samples can lead to an increase in false positive and false negative results.

4.4 Conclusions

Prior to the 2011 ATS/ERS/JRS/ALAT guideline, BAL DCC was considered a key step in the IPF diagnostic algorithm, however in the current guideline it is no longer advocated. BAL and repeat BAL in IPF is feasible and safe (<1.5%) mortality. Our study suggests BAL has only limited clinical value in the diagnosis of patients with suspected IPF and HRCT scans consistent with definite or possible UIP. Baseline BAL

DCC could not predict disease progression as there were no significant differences in BAL DCC between definite and possible IPF, or progressor and non-progressor groups. Of those that underwent repeat BAL, disease progression was not associated with a change in DCC. It is also worth noting that in our population, BAL DCC was inconsistent with IPF in 1 in 10 patients with 'definite UIP' and 1 in 6 patients with 'possible UIP' HRCT patterns. Whilst the implications of this are uncertain, it may highlight a need to question a diagnosis of IPF in selected patients, and perhaps consider alternative management plans, for example a trial of steroids in patients with a BAL lymphocytosis and disease progression.

Our data emphasise the presence of a novel human alveolar macrophage polarisation phenotype in IPF. Our study is clinically relevant as it suggests there is a distinct relationship between AM subtypes, cell-surface expression markers and disease progression in IPF. This may be utilised to investigate new targets for future therapeutic strategies. Our data mirrors previous work by Brittan et al, suggesting that pulmonary monocyte-like cells may play an important role in the pathogenesis of IPF. We found that disease progression is associated with significantly increased numbers of rPMLC in BAL and that the ratio of iPMLC:rPMLC at baseline BAL may predict disease progression. Furthermore RNA gene sequencing revealed that these cells differed functionally as well as phenotypically, therefore strengthening our hypothesis that they may be important in disease pathogenesis. This study emphasises the importance of this distinct subpopulation of PMLCs in predicting disease progression in IPF, and may also represent a novel target for future therapeutic strategies as modulation of these myeloid phenotypes may be of therapeutic value.

Chapter 5

Disease progression in IPF can be predicted by a combination of physiological parameters, HRCT scoring and biomarker profiling

5.1 Introduction

5.1.1 General introduction

The natural history of IPF is very variable and the course of disease in individual patients can be difficult to predict. Some patients progress slowly over a period of many years, others show periods of relative stability interspersed with acute deteriorations in respiratory function, whilst around one fifth of patients with IPF experience rapid decline leading to death within 12 months of presentation.

The pathogenesis of IPF is complex and poorly understood, but it is thought to be due to aberrant wound healing in response to repetitive alveolar injury. This leads to abnormal fibroblast proliferation, differentiation and activation, which then drives expansion of the extracellular matrix with extensive remodelling and loss of normal lung architecture[2]. Although the initial trigger for the development of IPF remains unknown, it is generally accepted that the disease occurs following repeated injury by environmental exposures in genetically susceptible individuals[5].

It is estimated that around 20% of IIPs have a genetic component, and familial cases with the most commonly affected genes reported being those involved in surfactant processing and telomere biology, were first described in the 1950s[2]. Genetics also play a role in sporadic IPF with polymorphisms in the promoter for the gene encoding the salivary mucin 5b (MUC5B) and for the Toll-interacting protein (TOLLIP) reported as being associated with an increased risk of developing IPF, although both ensue a relatively mild disease phenotype[2].

Challenges posed by the management of the ILDs include the difficulty of early diagnosis of IPF, difficulties differentiating IPF from the other IIPs and the impossibility of predicting patient outcome. Even with the benefit of a surgical lung biopsy and an MDT experienced in ILD, around 10% of patients are still deemed to have unclassifiable disease, with overlap features between entities[46]. Futhermore, as discussed previously, a lung biopsy is not always feasible in an elderly population with frequent comorbidities. Small uncertainties with regards to diagnosis can lead to major uncertainties in management. With the recent discovery and approval of two new antifibrotic drugs (pirfenidone and nintedanib) for the treatment of IPF, accurate phenotyping of ILD patients is paramount.

The demand to distinguish IPF from the other IIPs and the need to predict individual patient outcome has prompted a wealth of research into novel diagnostic and prognostic biomarkers over the last 5 years. Useful biomarkers must be readily detectable in biological fluid obtained by non-invasive and reproducible methods, and must demonstrate sufficient sensitivity and specificity by appropriate statistical analysis[56]. The development of new technologies such as genomics and proteomics which can reveal genetic mutations, polymorphisms, proteins, peptides and other molecules with potential roles as biological indicators in the diagnosis and prognosis of IPF has driven a growing field of research[56]. It is envisaged that biomarkers will assist in clinical decision making and will aid clinicians in stratifying patients into different endotypes, however they also have the potential to aid cohort enrichment in clinical trials[2]. Whilst several studies have identified circulating mediators that may predict disease progression in IPF, they have not been validated in 'real-life' patient cohorts, outside of clinical trials. To date there are no proven biomarkers that predict disease progression or response to treatment and no single biomarker has yet provided sufficient evidence to be implemented in routine clinical practice.

5.1.2 Hypothesis and aims

Idiopathic pulmonary fibrosis (IPF) is a devastating form of chronic lung injury of unknown aetiology characterized by progressive lung scarring. It is a very heterogeneous disease and around 10-15% of patients die or lose ≥10% FVC within 12 months ('progressors'). Patients are typically risk stratified using a combination of clinical variables including history and examination findings, pulmonary function testing, exercise capacity, radiological appearances and histological features, however these variables are poorly reflective of disease pathogenesis and cannot accurately predict clinical outcome. More recently, several prognostic scoring systems and biomarkers have been described to predict disease progression but most were derived from clinical trial patients or tertiary referral centres and none have been validated in separate cohorts. We hypothesised that disease progression in IPF can be confidently predicted by a combination of HRCT scoring and serum biomarker profiling. We aimed to identify a unique protein signature of IPF progressor versus non-progressor patients, and develop a regression model incorporating physiological, HRCT and biomarker data to predict disease progression in a unique population of incident treatment naïve IPF patients.

5.1.3 Experimental methodology

Patient selection and the Edinburgh Lung Fibrosis Biobank

The Edinburgh Lung Fibrosis research database was established in 2002, and was designed to capture the nature the natural history of ILD in patient's referred to the specialist adult ILD clinic. The dataset from 01/01/02-31/12/14 is summarised in Table 7. All subjects were fully consented and ethical approval was obtained for all protocols and procedures (LREC 06/S0703/53). Study cohorts consisted of locally referred, consecutively presenting patients with ILD presenting since 01/01/02. For all patients, diagnosis, investigation, management and follow-up was as per the Edinburgh local policy. This included a detailed clinical history, examination, autoantibody screen,

HRCT and pulmonary function testing. Follow-up included 6 monthly PFTs and clinic review, with less than 1% of the study population being lost to follow-up**.** Disease progression was defined as death or ≥10% decline in FVC within 12 months of baseline BAL or serum. All HRCT scans were reviewed by an expert thoracic radiologist and discussed in a multidisciplinary meeting with at least two respiratory physicians with ILD subspecialty expertise. Patient HRCT scans were categorised into 'definite', 'probable' or 'inconsistent with' UIP patterns based on 2011 ATS/ERS criteria, and were then scored on percentage of total lung fibrosis, percentage of periphery involved and degree of bronchiolar dilatation (0,1,2,3).

In addition to this dataset, since 2007 a unique biobank has been collected comprising of baseline and serial samples from 575 patients. Baseline BAL samples were obtained from 94 IPF patients (32 progressors, 62 non-progressors) and repeat BAL was performed at 12 months in 60 patients (16 progressors, 44 non-progressors). Baseline serum samples were obtained in 216 IPF patients (102 progressors, 114 non-progressors) and 118 patients went on to have successive serum samples 12 months later (38 progressors, 80 non-progressors). Most of the patients had matched BAL and serum samples, and less than 2% had received IPF-directed therapy. The Edinburgh Lung Fibrosis study biobank is summarised in Table 32.

Table 32. Summary of the available samples in the Edinburgh IPF biobank according to patient phenotype.

	Progressors		**Non-Progressors**		**Controls (aged matched healthy volunteers)**
	Definite IPF Age (SD)	Probable IPF Age (SD)	Definite IPF Age (SD)	Probable IPF Age (SD)	Controls Age (SD)
Baseline serum samples	N=38 73.9 years (9.5)	N=64 74.0 years (7.8)	N=46 71.2 years (8.7)	N=68 73.6 years (8.1)	N=64 67.1 years (9.3)

0 and 12 month serum samples	N=25 73.8 years (9.1)	N=13 75.3 years (5.3)	N=33 71.0 years (8.1)	N=47 73.5 years (7.1)	0
Baseline BAL samples	N=15 66.9 years (9.0)	N=17 76.1 years (5.8)	N=27 71.3 years (6.8)	N=35 72.1 years (5.9)	N=9 62.6 years (7.8)
0 and 12 month BAL samples	N=8 69.6 years (10.3)	N=8 74.8 years (4.2)	N=20 71.3 years (7.5)	N=24 70.8 years (6.4)	0

Processing of BALF and serum

BALF was filtered through a 40µm cell strainer and total cell count obtained using an automated NucleoCounter. BALF was then centrifuged at 1200rpm for 10 mins at 4°C and the supernatant was removed and stored at -80°C. Cells were resuspended in IMDM at a concentration of 1 million cells per ml for flow cytometry. One million cells were removed for cytospin processing, briefly 10x100µl aliquots were cytocentrifued onto superfrost glass slides at 300g for 3 mins. Slides were then placed in methanol for 2 minutes and allowed to dry. One slide was then placed in DiffQuick Red for 2 minutes, then DiffQuick Blue for 90 seconds for staining.

Serum samples were centrifuged at 2500rpm for 10 minutes at 4°C and then serum was collected and stored at -80°C.

ELISAs

Analysis of cytokines and mediators in BALF and serum were performed using DuoSet ELISA kits from R&D Systems, according to the manufacturer's instructions. ELISA plates were analysed using a Synergy-HT microplate reader using Gen5 data analysis software.

Proteomic Arrays

Initially, unbiased semi-quantitative commercially bought proteomic array kits were used to detect proteins of interest in BALF of IPF progressors and non-progressors (R&D, Human Angiogenesis Array cat# ARY007, Human Chemokine Array cat# ARY017, Human Protease/Protease Inhibitor Array cat# ARY025 and Human Soluble Receptor, Non-haematopoietic Panel Array cat# ARY012). Protocols were followed as per manufacturer's instruction, however briefly capture antibodies were spotted in duplicate on nitrocellulose membranes, BAL samples were pooled, diluted and mixed with a cocktail of biotinylated detection antibodies and sample/antibody mixtures were then incubated with the array. Any analyte/detection antibody complexes present were bound by their cognate immobilised capture antibody on the membrane, Streptavidin-Horseradish Peroxidase and chemiluminescent detection reagents were then added, and a signal was produced in proportion to the amount of analyte bound. IPF Progressor and Non-Progressor groups were compared by pooling fluid containing 50µg of protein (protein determined via Pierce BCA assay, ThermoFisher cat# 23225) each from four IPF patients from each group. Image J was used to measure pixel density between proteins and controls, giving a semi-quantitative numerical value for comparison between groups. These values were plotted on a graph and a linear regression line was fitted with 90% confidence bands added, proteins of interest were identified as outliers. These initial experiments were performed in collaboration with Ross Mills, PhD student, Centre For Inflammation, Queens Medical Research Institute Edinburgh. Examples of the film, dot-blot analysis technique and numerical values obtained are shown in Figure 43.

Figure 43. Example of semi-quantitative dot-blot proteomic array.

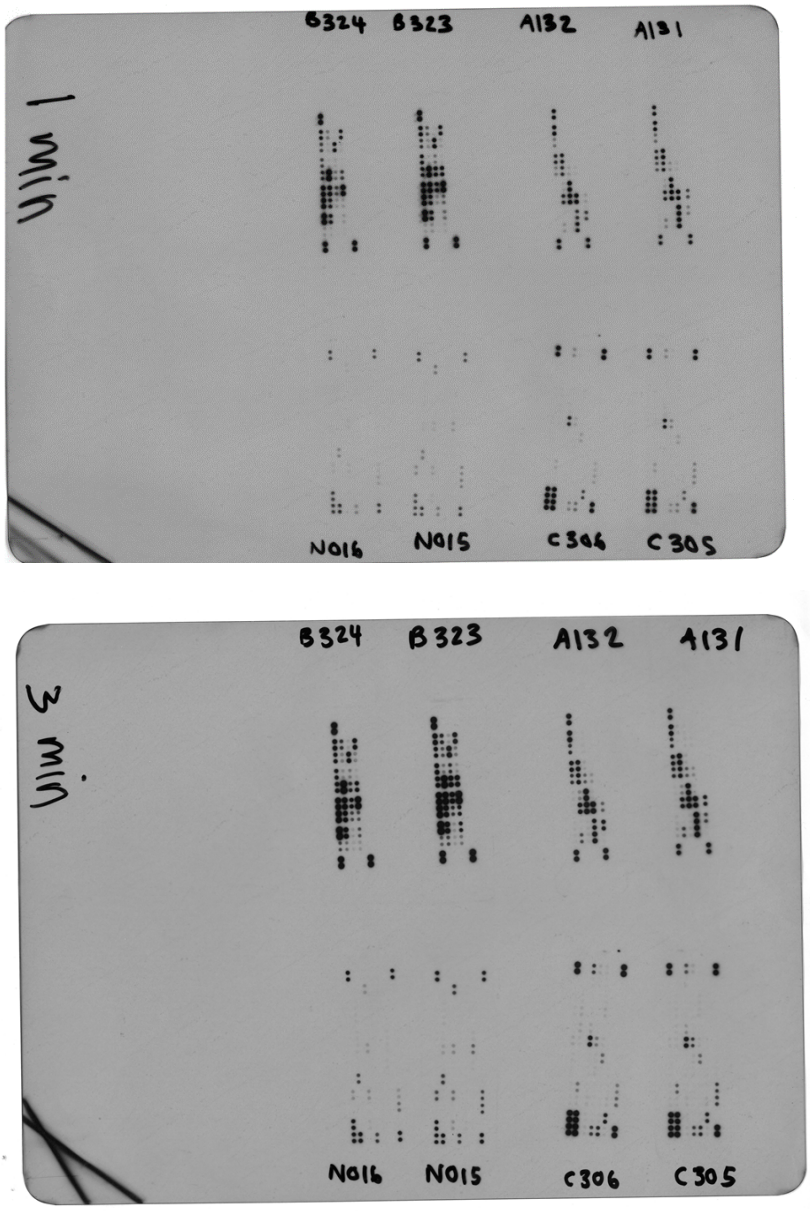

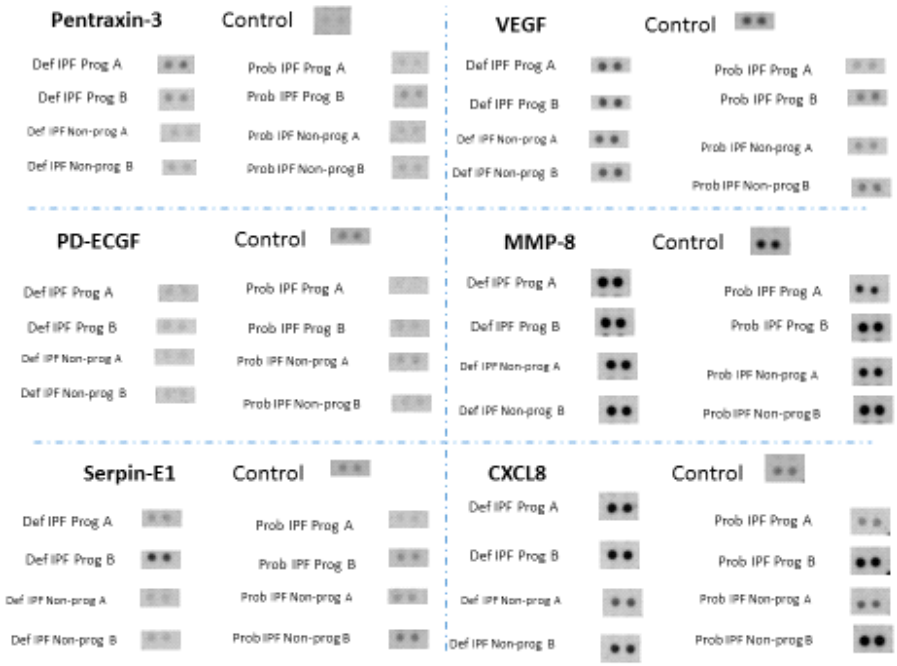

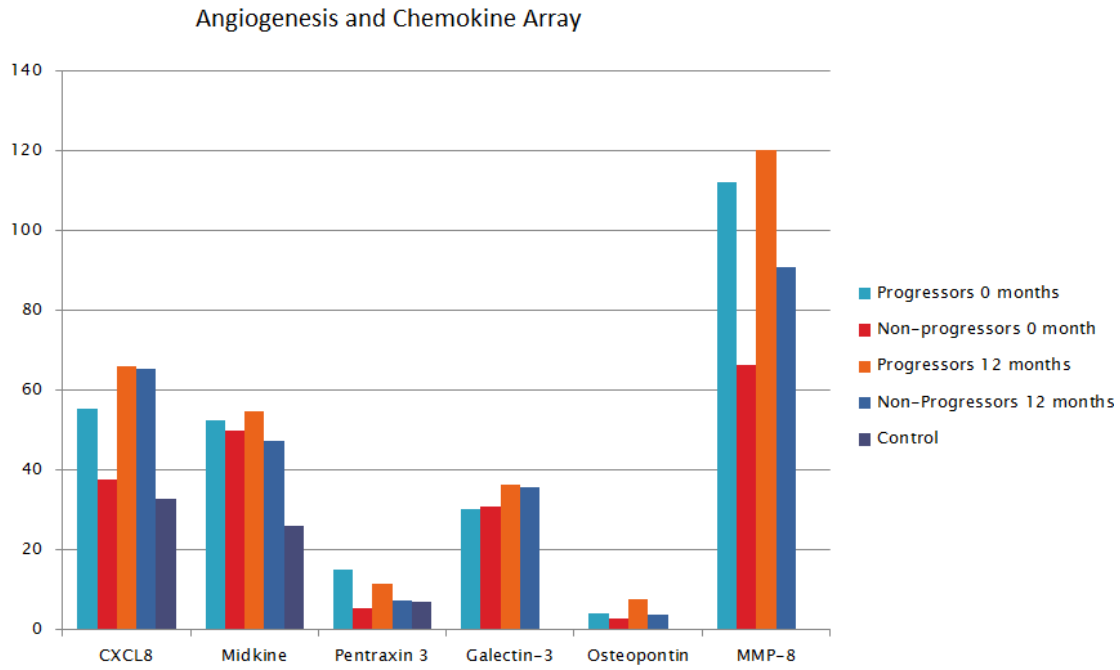

For the angiogenesis kit, baseline BAL proteins of interest included EGF, IGFBP-1, IGFBP- 2, IL-8/CXCL8, MMP8, MMP9, Pentraxin 3, Platelet Factor 4, CXCL16, Serpin F1 and uPA. Outliers in the chemokine kit were IL-16, CXCL4, CXCL7,

CXCL8, CXCL17, Chemerin, CCL17 and CCL18. Outliers in the Protease kit were MMP1, MMP7, MMP8, MMP10, Cathespin E, Cathespin S, Kallikrein 6, Kallikrein 7, Kallikrein 13 and Proteinase 3, and in the Protease Inhibitor kit; Trappin-2, Serpin A5, Serpin A8, Serpin B5, Serpin B6, Serpin B8, Fetuin B and TFPI-2. Outliers in the soluble receptor and non-haematopoietic kits were CXCL8, Galectin-3BP, Galectin-3, ACE, BCAM, CD58, CD99, Integrin B2, Lipocalin-2, Osteopontin and Thrombospondin, and ESAM, bIG-H3, CRELD2, ECM-1, EpCAM, MUCHDL, Nectin-2, SREC-II and VCAM-1 respectively. Proteins of interest, as represented as outliers, are shown in Figure 44.

Figure 44. Proteins of interest identified as outliers on semi-quantitative proteomic kit screening.

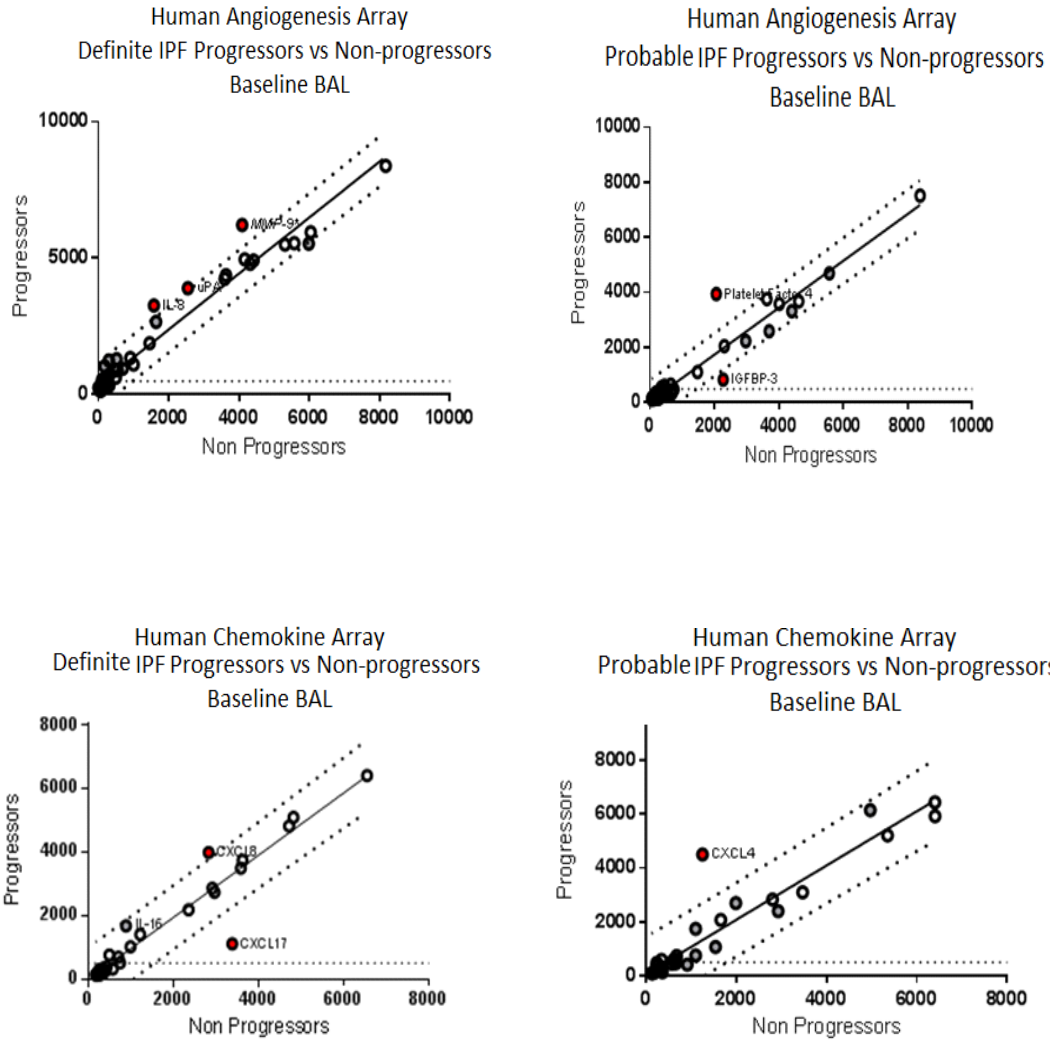

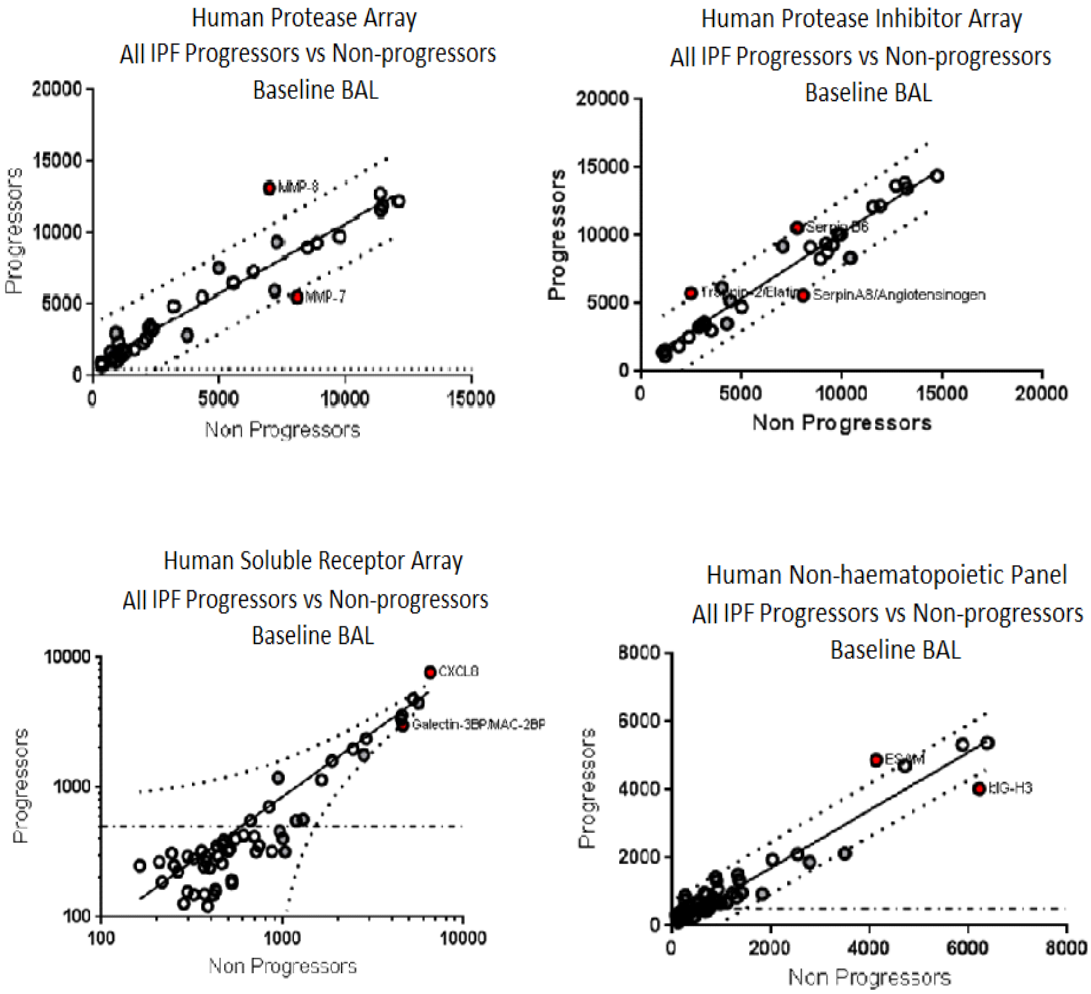

Based on the results of dot-blot proteomic screening arrays and a literature review of current biomarkers undergoing investigation, a new panel of potential biomarkers (n=22 analytes) were identified for analysis with semi-biased Luminex Magnetic Screening Assay kits (R&D), in the hope of identifying additional key protein candidates. The proteins selected for the assay are reported in Table 33.

Table 33. Analytes included in Luminex Magnetic Screening Assay.

Analyte	Analyte	Analyte	Analyte
Amphiregulin	IL-10	CXCL1/GRO alpha	Pentraxin 3
CCL2/MCP-1	MMP-7	CXCL8/IL-8	Periostin/OSF-2
CCL5/RANTES	MMP-8	CXCL10/IP-10	SP-D
CCL18/PARC	IL-33	EGF	VEGF
CCL26/Eotaxin-3	MMP-1	Galectin-3	
Chi3-L1	MIF	Osteopontin	

Protocols were followed as per manufacturer's instructions, however briefly analyte-specific antibodies were pre-coated onto magnetic microparticles, microparticles, standards and samples were pipetted into wells and immobilised antibodies were bound to the analyte of interest, plates were washed, then a biotinylated antibody cocktail specific to analytes of interest were added, plates were again washed, then Steptavidin-PE was added to bind to the biotinylated antibody. Plated were again washed, then read using the Bio-Plex 200 HTF analyser (one LED identifies analyte and one determines magnitude of PE-derived signal, which is directly proportional to amount of analyte bound).

Patients were categorised into definite IPF progressor, probable IPF progressor, definite IPF non-progressor, probable IPF non-progressor and healthy control groups. Luminex Magnetic Screening Assay was performed on BALF and serum samples, first in a Test Cohort of 4 patients per group, then in a Validation Cohort of 8 patients per IPF group and 5 controls. As no significant differences were found in the protein signature between definite and probable IPF groups (data not shown), definite and probable IPF groups were combined allowing a test cohort of 8 progressors and 8 non-progressors and a validation cohort of 16 progressors and 16 non-progressors for statistical analysis. BALF was normalised to 10µg of protein per sample (protein determined via Pierce BCA assay, ThermoFisher cat# 23225). Serum was utilised at either 1:2 or 1:50 dilution depending on manufacturer's instruction.

Statistical analysis

GraphPad prism (version 6, GraphPad Software Inc., CA, USA) was used for data analysis. Normally distributed data were analysed by unpaired or paired t-test and expressed as mean (SD). Data that were not normally distributed were reported as median (interquartile range) and analysed by Mann Whitney U test or Wilcoxon signed rank test. Kruskal-Wallis test with Dunn's Multiple Comparison Test was used to calculate differences between multiple groups. Linear logistic regression was used on each predictor separately to assess its importance in terms of p-value of the associated weight. The top two variables were then used to learn a decision tree. *P* values of <0.05 were considered significant.

5.2 Results

5.2.1 Clinical parameters predictive of disease Progression

A number of studies have reported the merits of utilising different combinations of clinical, physiological, radiological and serological parameters in devising prognostic scoring systems to predict survival in IPF. However there remains no single risk model that has been validated and accepted in routine clinical practice. The Composite Physiologic Index (CPI) was described by Wells et al[37]. They reported that a combination of FVC, FEV_1 and DLCO values correlated with the extent of fibrosis on HRCT. The CPI was thought not only to closely reflect the morphologic extent of pulmonary fibrosis but also to provide a more accurate prognostic determinant in IPF than an individual PFT value alone. The formula used to calculate the CPI is as follows

- extent of disease on CT = 91.0 − (0.65 × percent predicted diffusing capacity for carbon monoxide [DL_{CO}]) − (0.53 × percent predicted FVC) + (0.34 × percent predicted FEV_1).

When the CPI formula was applied to the Edinburgh IPF patient cohort, significant differences in survival were demonstrated between the four quartiles (P<0.0001). This is demonstrated in Figure 45 below.

Figure 45. Kaplan Meier survival curves grouped by quartiles of Composite Physiological Index .

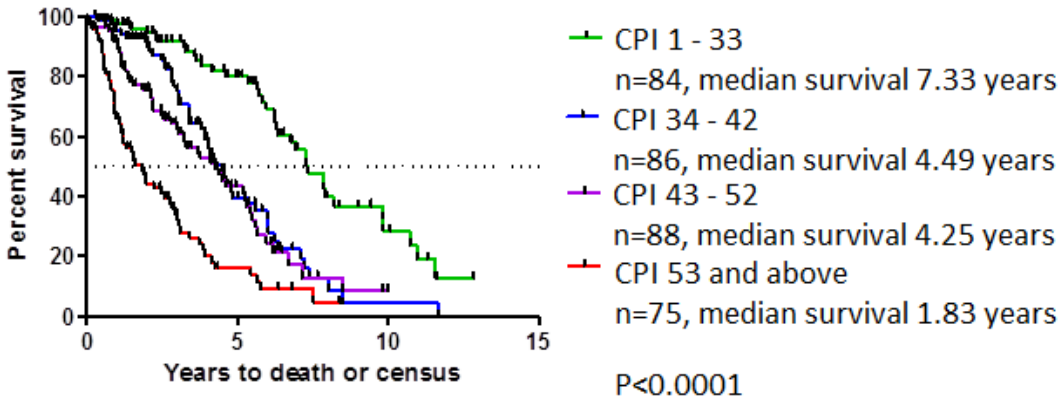

The GAP Index was developed using data from three large distinct patient cohorts (N=558) and was proposed as a prognostic staging system in IPF by Ley and colleagues[38]. The model included four baseline clinical variables (gender, age, FVC and DLCO) and categorised patients into three severity groups with 1-year mortality risks of 6%, 16% and 39% respectively. A description of the GAP Index scoring system and predicted 1-, 2- and 3-year mortality for scores of 0-3, 4-5 and 6-8 are shown in Figure 46 below.

Figure 46. GAP Index scoring system and predicted 1-, 2- and 3-year mortality for scores of 0-3, 4-5 and 6-8.

Risk factor	Score
Gender	
Female	0
Male	+1
Age	
≤60 years	0
61-65 years	+1
>65 years	+2
Predicted FVC	
>75%	0
50-75%	+1
<50%	+2
Predicted DLCO	
>55%	0
36-55%	+1
≤35%	+2
Unable to perform	+3

GAP Index	1 year mortality	2 year mortality	3 year mortality
0-3	5.6%	10.9%	16.3%
4-5	16.2%	29.9%	42.1%
6-8	39.2%	62.1%	76.8%

A GAP index was also calculated for each patient in the Edinburgh IPF cohort. Among our patients with definite IPF (n=164), scores of 0-3 (n=77), 4-5 (n=69) and 6-8 (n=18) predicted one year mortality of 5.6%, 16.2% and 39.2% respectively. Actual one year mortality in each of these groups was 2.7%, 6.7% and 18.7% respectively. Two and three year mortality was also calculated as shown in Figure 47 below. Median survival was calculated in each group and was 5.7 years for the GAP index 0-3 group, 2.8 years

in the GAP index 4-5 group and 2.6 years in the GAP index 6-8 group (p <0.0001). The percentage of patients deceased at census date in each group was 69.6%, 87.9% and 100.0% respectively (p <0.0001). Although the GAP index is not validated in patients with 'probable IPF', we report similar results in this population as demonstrated in Figure 48 below. When definite and probable IPF patient groups were combined into an 'all IPF' cohort, survival remained significantly different between the 3 groups, and the predicted 1-, 2- and 3-year mortality was found to be very similar to the observed mortality. This data is shown in Figure 49 below.

Figure 47. Kaplan-Meier survival curves and observed and predicted 1-, 2- and 3-year mortality based on GAP Index applied to the Edinburgh 'Definite IPF' cohort.

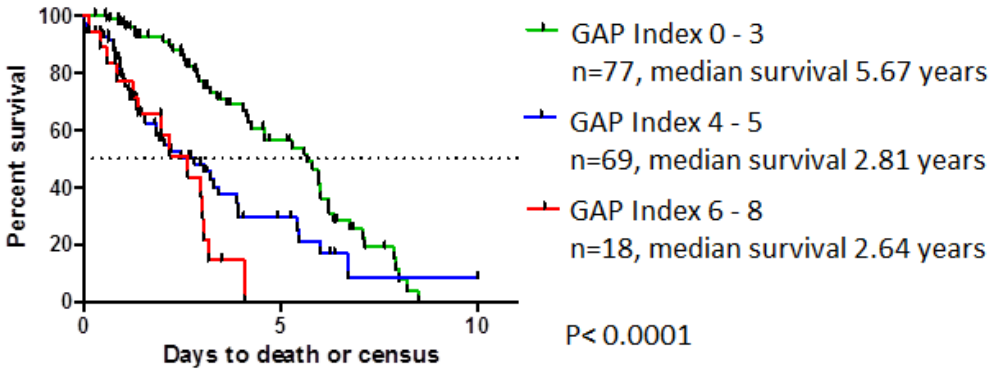

GAP Index	Observed 1 year mortality	Predicted 1 year mortality	Observed 2 year mortality	Predicted 2 year mortality	Observed 3 year mortality	Predicted 3 year mortality
0 – 3	2.7%	5.6%	21.7%	10.9%	22.2%	16.3%
4 – 5	6.7%	16.2%	39.1%	29.9%	38.9%	42.1%
6 – 8	18.7%	39.2%	44.9%	62.1%	55.6%	76.8%

Figure 48. Kaplan-Meier survival curves and observed and predicted 1-, 2- and 3-year mortality based on GAP Index applied to the Edinburgh 'Probable IPF' cohort.

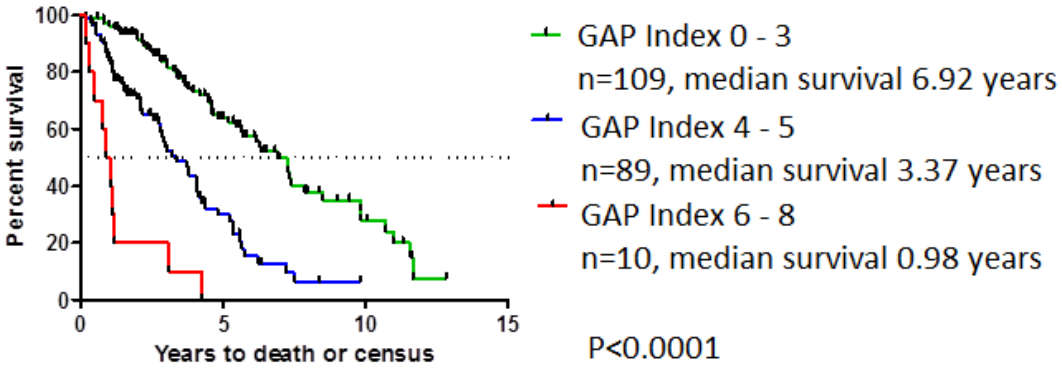

GAP Index	Observed 1 year mortality	Predicted 1 year mortality	Observed 2 year mortality	Predicted 2 year mortality	Observed 3 year mortality	Predicted 3 year mortality
0 – 3	2.8%	5.6%	14.6%	10.9%	50.0%	16.3%
4 – 5	7.3%	16.2%	28.1%	29.9%	80.0%	42.1%
6 – 8	14.7%	39.2%	40.4%	62.1%	80.0%	76.8%

Figure 49. Kaplan-Meier survival curves and observed and predicted 1-, 2- and 3-year mortality based on GAP Index applied to the Edinburgh 'All IPF' cohort.

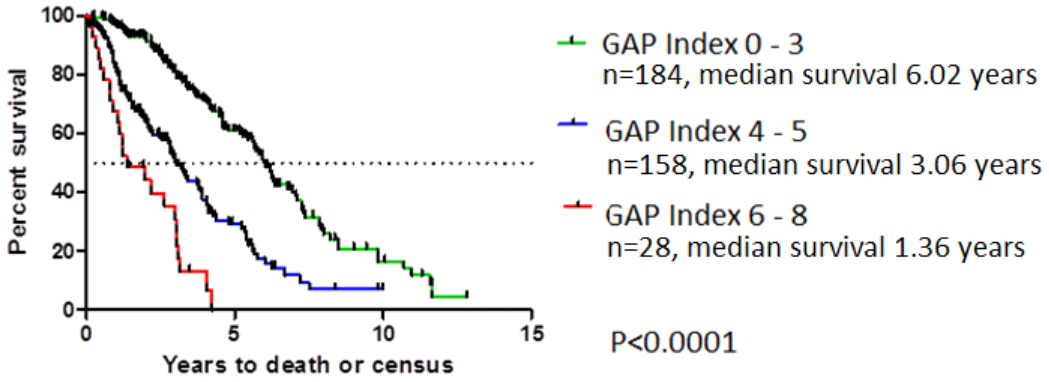

GAP Index	Observed 1 year mortality	Predicted 1 year mortality	Observed 2 year mortality	Predicted 2 year mortality	Observed 3 year mortality	Predicted 3 year mortality
0 – 3	2.7%	5.6%	4.3%	10.9%	16.3%	16.3%
4 – 5	17.7%	16.2%	32.9%	29.9%	42.4%	42.1%
6 – 8	32.1%	39.2%	53.6%	62.1%	64.3%	76.8%

Du Bois et al devised a scoring system capable of independently predicting mortality using data from two clinical trials (N=1099)[41]. The IPF score determined 1-year mortality in IPF patients using a number of PFT and clinical indicators. Parameters included in the model were age, respiratory hospitalisations, %predicted FVC and change in %predicted FVC over a 24 week period. In order to improve the ability of the model to predict 1-year survival, 6MWD and 24 week change in 6MWD were later added. The scoring system and predicted 1-year mortality data is shown in Table 34 below.

Table 34. Du Bois IPF score.

Risk Factor	Score	Total Risk Score	Expected 1-Year Risk of Death
Age			
<60 years	0	0–4	<2%
60-69 years	+4	8–14	2–5%
≥70 years	+8	16–21	5–10%
Respiratory hospitalization in past 6 months		22–29	10–20%
No	0	30–33	20–30%
Yes	+14	34–37	30–40%
Predicted Baseline FVC		38–40	40–50%
≥80%	0	41–43	50–60%
66-79%	+8	44–45	60–70%
51-65%	+13	47–49	70–80%
≤50%	+18	>50	>80%
24-Week Change in Predicted FVC			
≥ -4.9%	0		
-5% to -9.9%	+10		
≤ -10%	+21		

Among our patients with IPF, scores of 0-21 (n=236), 22-40 (n=85) and 41-61 (n=11) predicted median survival of 5.8 years, 3.6 years (HR 2.02; 95%CI 1.26 to 3.23) and 0.6 years (HR 14.2; 95%CI 7.47 to 26.8) respectively (P< 0.001). Mortality was similar for patients with probable UIP who did and did not have a surgical lung biopsy after adjusting for the IPF Score (HR 1.06; 95%CI 0.56 to 1.99, likelihood ratio statistic 0.03, P = 0.86). In our 'definite IPF' patient cohort, IPF scores of 0-21, 22-40 and 41-61 predicted 1 year mortality as 0-10%, 10-50% and 50->80% respectively. Observed 1 year mortality in each of the 3 groups was 5.8%, 18.8% and 66.7% (P<0.0001). Similar data was demonstrated in the 'probable IPF' group. When both groups were combined into an 'all IPF' cohort, the model was still accurate in predicting 1 year survival,

however the variation for expected mortality in each of the 3 groups is large. This data is shown in Figures 50 – 52 below.

Figure 50. Kaplan-Meier survival curves and observed and expected 1-year mortality based on du Bois IPF score applied to the Edinburgh 'Definite IPF' cohort.

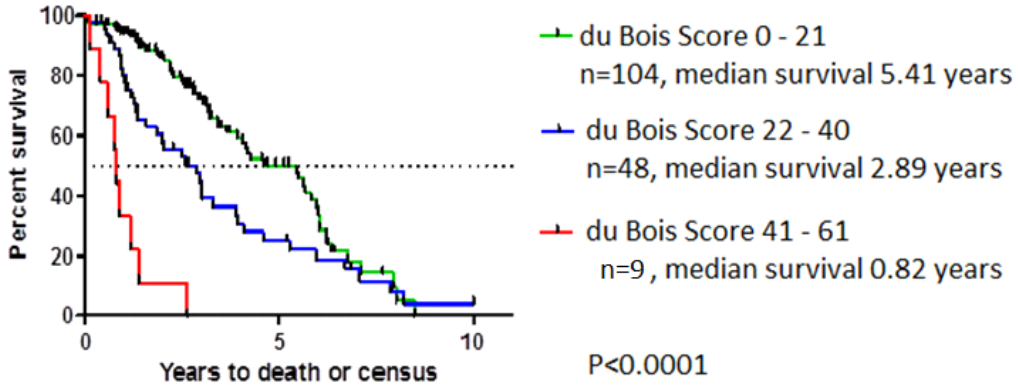

du Bois Score	Observed 1 year mortality	Expected 1 year mortality
0 - 21	5.8%	0 - 10%
22 - 40	18.8%	10 - 50%
41 - 61	66.7%	50 - >80%

Figure 51. Kaplan-Meier survival curves and observed and expected 1-year mortality based on du Bois IPF score applied to the Edinburgh 'Probable IPF' cohort.

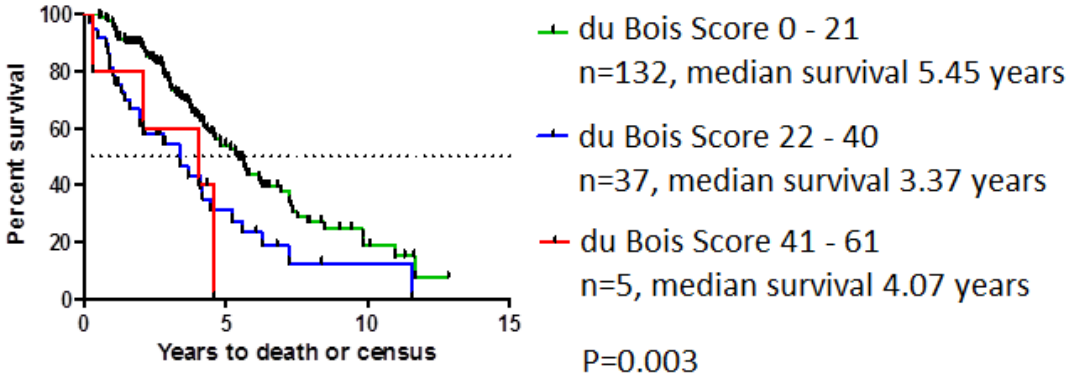

du Bois Score	Observed 1 year mortality	Expected 1 year mortality
0 - 21	1.5%	0 - 10%
22 - 40	18.9%	10 - 50%
41 - 61	20.0%	50 - >80%

Figure 52. Kaplan-Meier survival curves and observed and expected 1-year mortality based on du Bois IPF score applied to the Edinburgh 'All IPF' cohort.

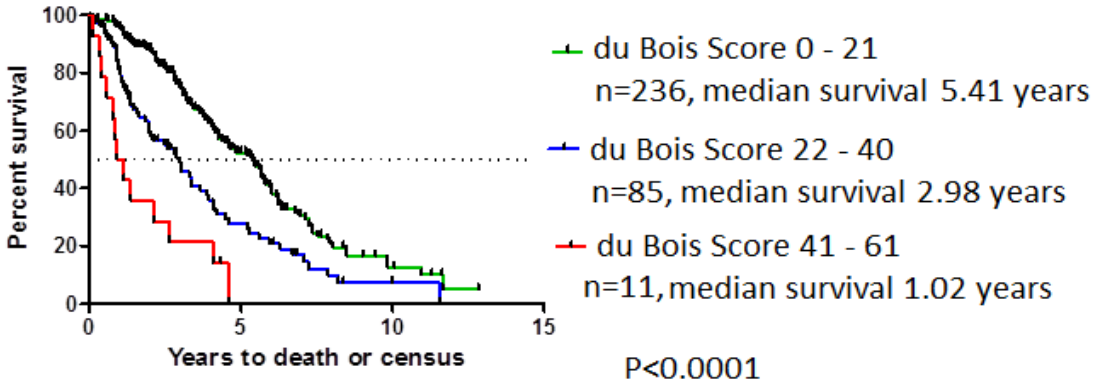

du Bois Score	Observed 1 year mortality	Expected 1 year mortality
0 - 21	3.4%	0 - 10%
22 - 40	18.8%	10 - 50%
41 - 61	63.6%	50 - >80%

5.2.2 BAL biomarker profiling

Luminex Magnetic Screening Assay identified a number of protein candidates that warranted further investigation into their utility as a potential biomarker for disease progression in IPF. In BALF, CHI3-L1 and MCP-1 levels were significantly elevated in patients with IPF vs controls, there was also a trend for increased PARC (CCL18) levels in IPF vs controls, and in IPF progressors vs non-progressors, however this did not reach significance. VEGF levels were significantly decreased in IPF vs controls, and reduced in IPF progressors vs on-progressors, although this did not reach significance. Galectin-3 levels were significantly increased in IPF progressors vs non-progressors. These data are shown in Figure 53 below. There were no differences between IPF and control patients, or IPF progressors vs non-progressor groups in MMP1, MIF, SP-D, IP10, Gro-alpha, IL8 or RANTES BAL fluid levels. Amphiregulin, periostin, EGF, pentraxin-3, osteopontin, IL33, Eotaxin-3, IL10, IL17e and IL-12 p70 levels were all below the level of detection of BALF (data not shown).

Figure 53. BAL fluid protein levels in training and validation cohorts.

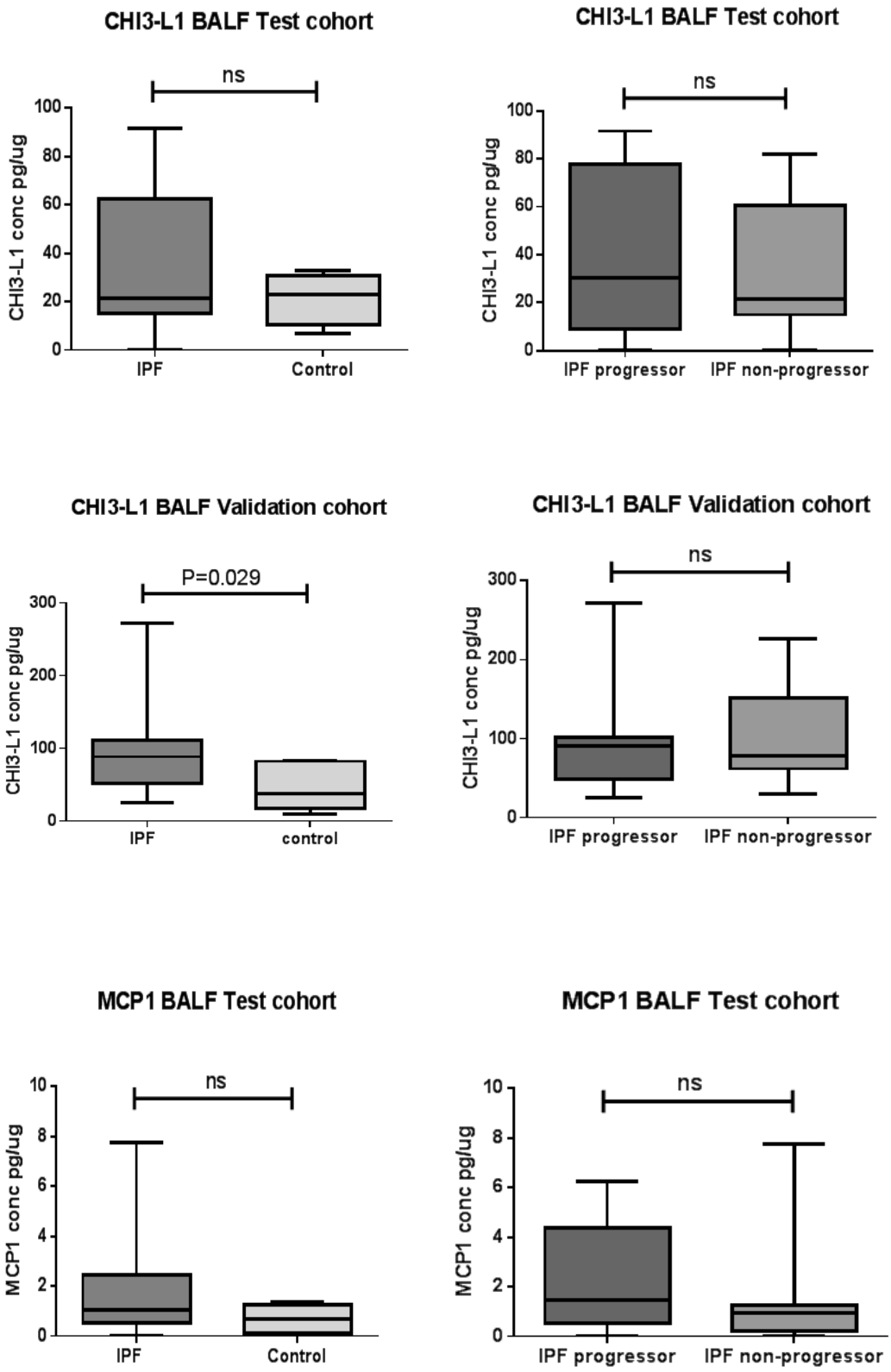

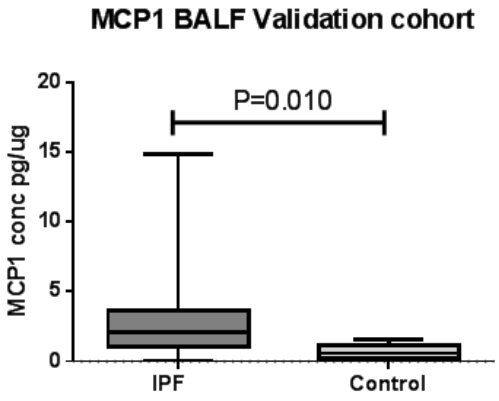
MCP1 BALF Validation cohort
P=0.010
MCP1 conc pg/ug
20
15
10
5
0
IPF
Control

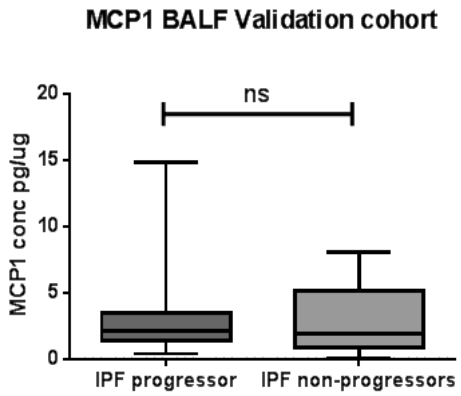
MCP1 BALF Validation cohort
ns
MCP1 conc pg/ug
20
15
10
5
0
IPF progressor
IPF non-progressors

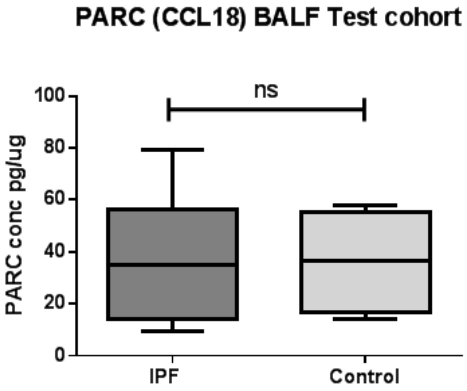
PARC (CCL18) BALF Test cohort
ns
PARC conc pg/ug
100
80
60
40
20
0
IPF
Control

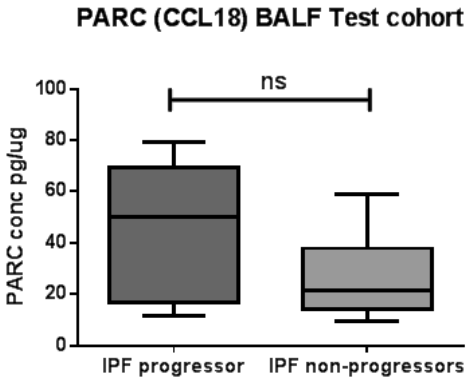
PARC (CCL18) BALF Test cohort
ns
PARC conc pg/ug
100
80
60
40
20
0
IPF progressor
IPF non-progressors

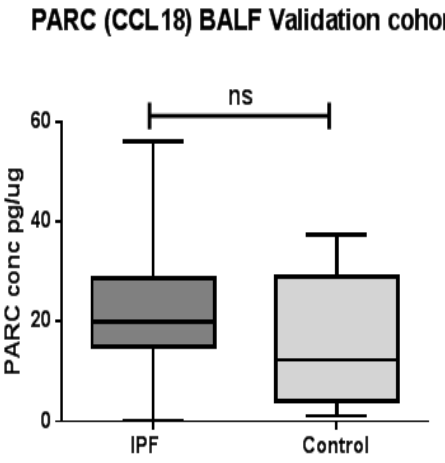
PARC (CCL18) BALF Validation cohort
ns
PARC conc pg/ug
60
40
20
0
IPF
Control

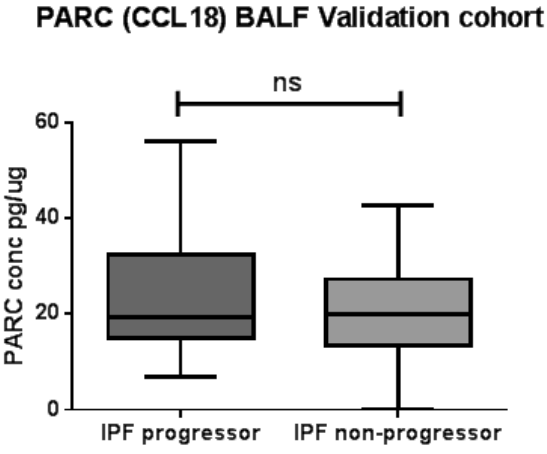
PARC (CCL18) BALF Validation cohort
ns
PARC conc pg/ug
60
40
20
0
IPF progressor
IPF non-progressor

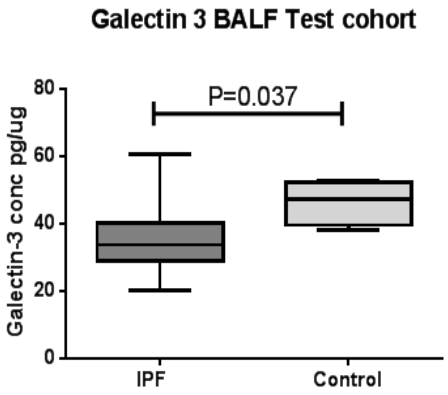
Galectin 3 BALF Test cohort
P=0.037
Galectin-3 conc pg/ug
80
60
40
20
0
IPF
Control

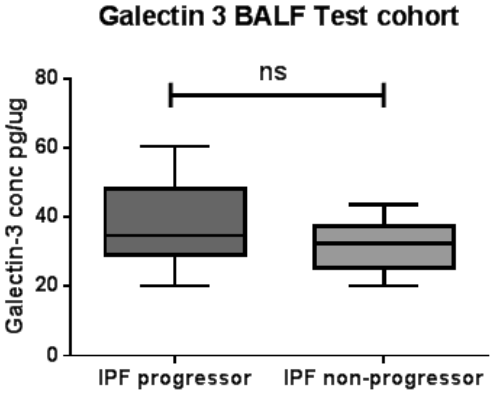
Galectin 3 BALF Test cohort
ns
Galectin-3 conc pg/ug
80
60
40
20
0
IPF progressor
IPF non-progressor

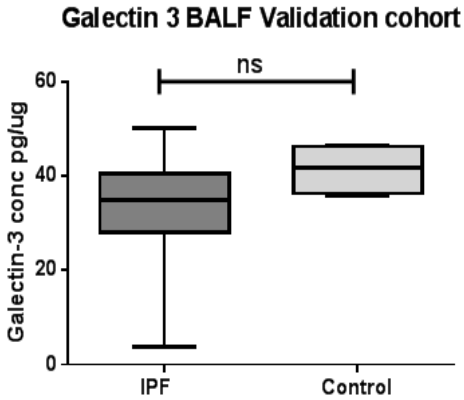
Galectin 3 BALF Validation cohort
ns
Galectin-3 conc pg/ug
60
40
20
0
IPF
Control

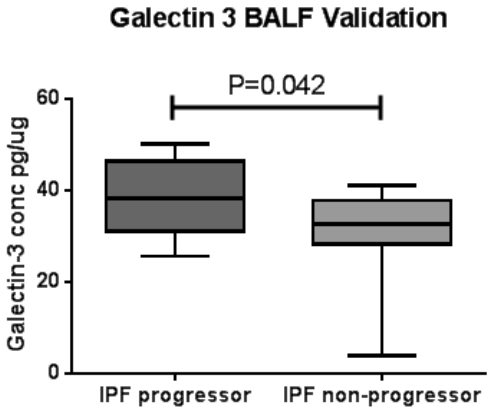
Galectin 3 BALF Validation
P=0.042
Galectin-3 conc pg/ug
60
40
20
0
IPF progressor
IPF non-progressor

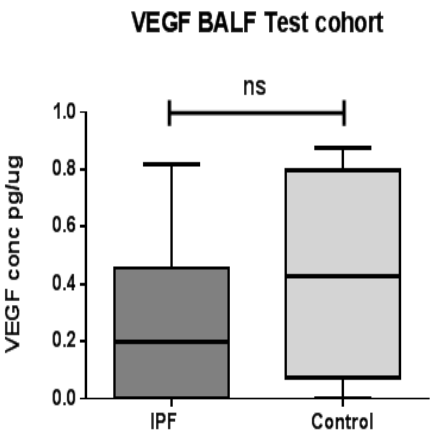
VEGF BALF Test cohort
ns
VEGF conc pg/ug
1.0
0.8
0.6
0.4
0.2
0.0
IPF
Control

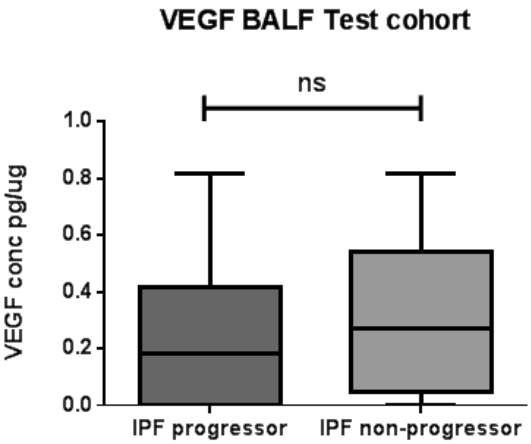
VEGF BALF Test cohort
ns
VEGF conc pg/ug
1.0
0.8
0.6
0.4
0.2
0.0
IPF progressor
IPF non-progressor

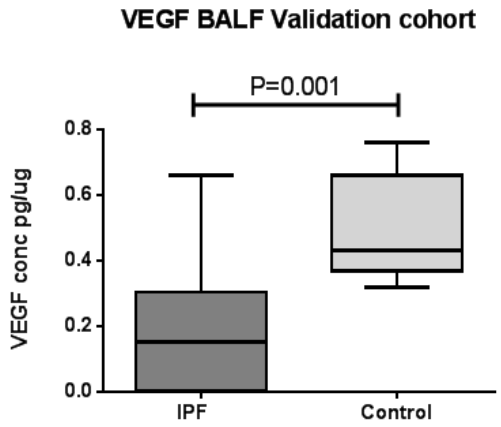

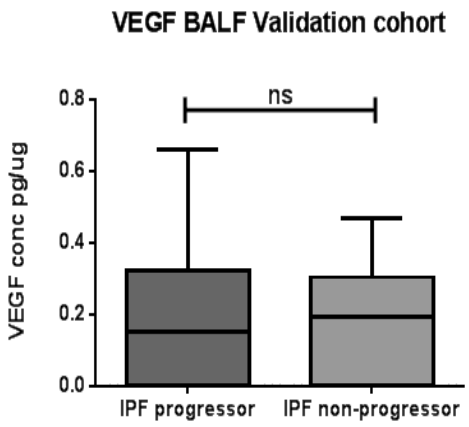

5.2.3 Serum biomarker profiling

In serum, MMP1, periostin, osteopontin, SP-D, IP10, MCP-1, IL8 and PARC (CCL18) levels were all significantly increased in IPF patients vs controls. Periostin, SP-D and gro-alpha levels were also significantly increased in IPF progressors vs non-progressors. CHI3-L1 levels were increased in IPF vs controls and in IPF progressors vs non-progressors, MCP1 levels were increased in IPF vs controls, and osteopontin and IL8 levels were increased in IPF progressors vs non-progressors, however none of these differences reached significance. These data are shown in Figure 54 below. There were no differences in IPF and control patients, or IPF progressors vs non-progressors in serum MIF, VEGF, EGF, pentraxin-3, RANTES or galectin-3 levels. Amphiregulin, IL33, eotaxin-3, IL10, IL17e and IL-12 p70 levels were all below the level of detection in serum (data not shown).

Figure 54. Serum protein levels in training and validation cohorts.

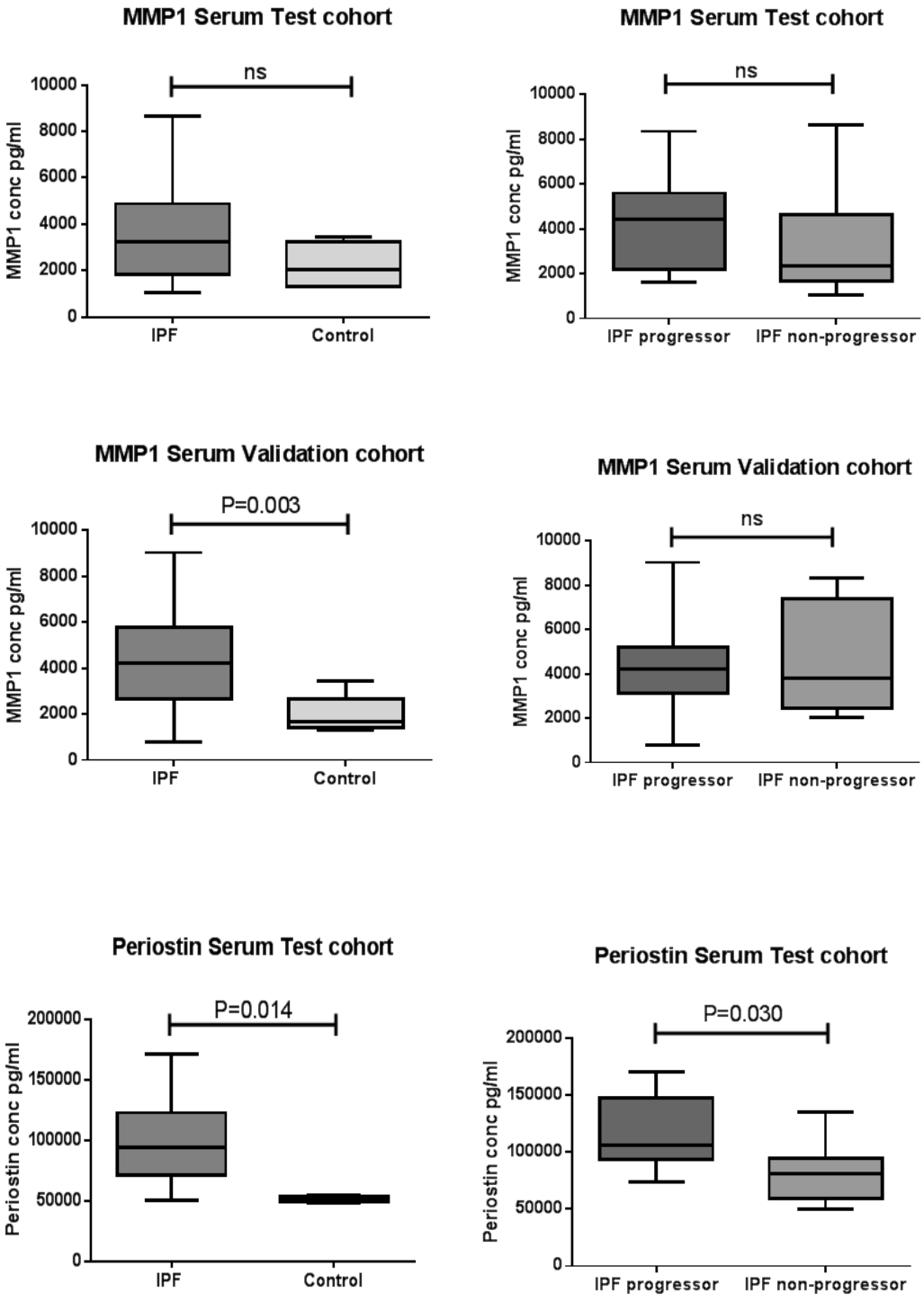

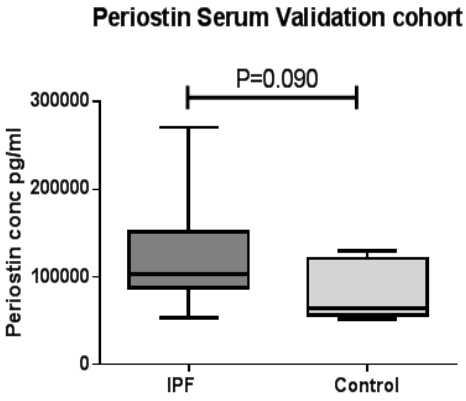
Periostin Serum Validation cohort
P=0.090
Periostin conc pg/ml
300000
200000
100000
0
IPF
Control

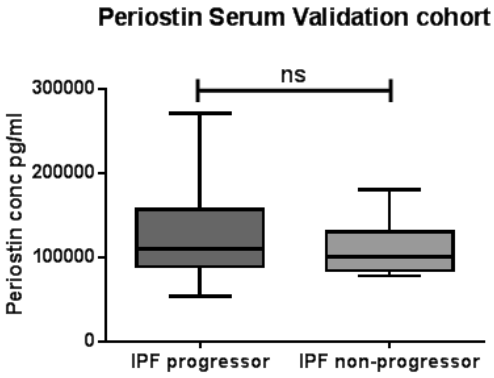
Periostin Serum Validation cohort
ns
Periostin conc pg/ml
300000
200000
100000
0
IPF progressor
IPF non-progressor

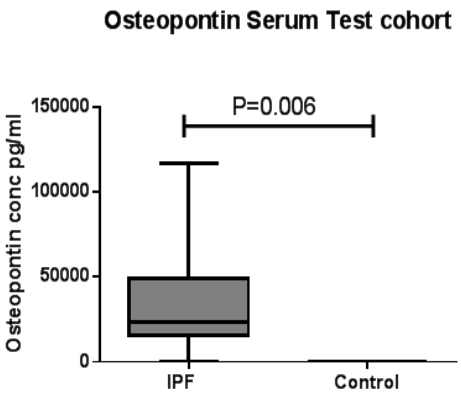
Osteopontin Serum Test cohort
P=0.006
Osteopontin conc pg/ml
150000
100000
50000
0
IPF
Control

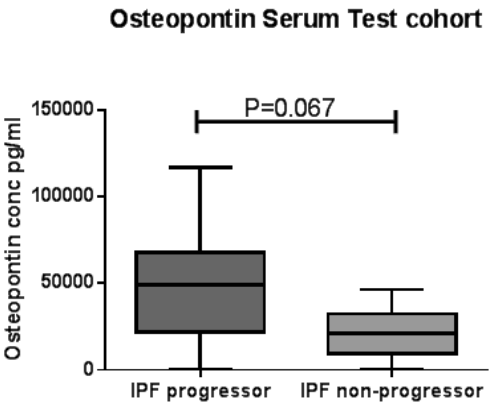
Osteopontin Serum Test cohort
P=0.067
Osteopontin conc pg/ml
150000
100000
50000
0
IPF progressor
IPF non-progressor

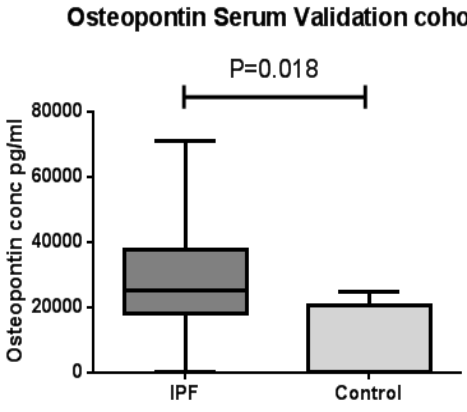
Osteopontin Serum Validation cohort
P=0.018
Osteopontin conc pg/ml
80000
60000
40000
20000
0
IPF
Control

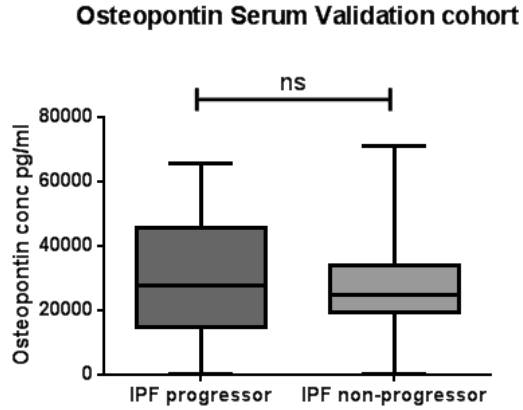
Osteopontin Serum Validation cohort
ns
Osteopontin conc pg/ml
80000
60000
40000
20000
0
IPF progressor
IPF non-progressor

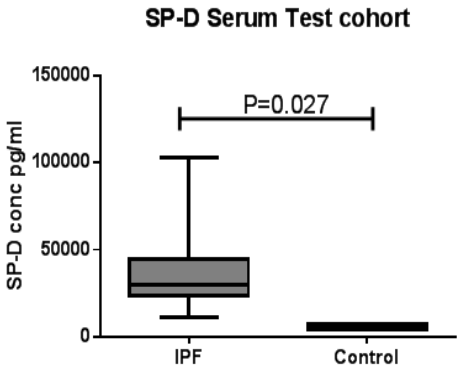
SP-D Serum Test cohort
SP-D conc pg/ml
150000
100000
50000
0
P=0.027
IPF
Control

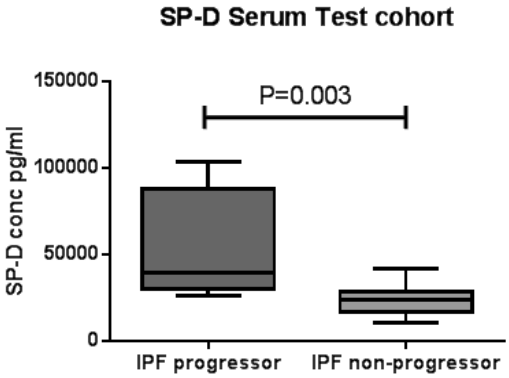
SP-D Serum Test cohort
SP-D conc pg/ml
150000
100000
50000
0
P=0.003
IPF progressor
IPF non-progressor

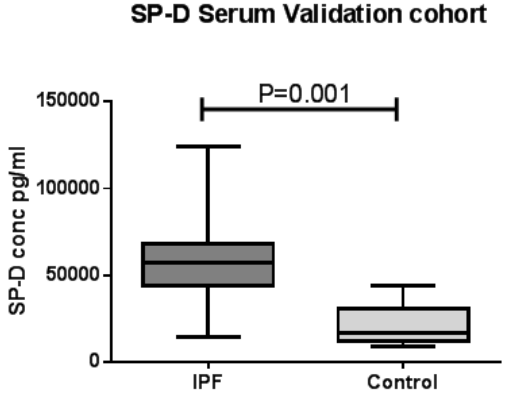
SP-D Serum Validation cohort
SP-D conc pg/ml
150000
100000
50000
0
P=0.001
IPF
Control

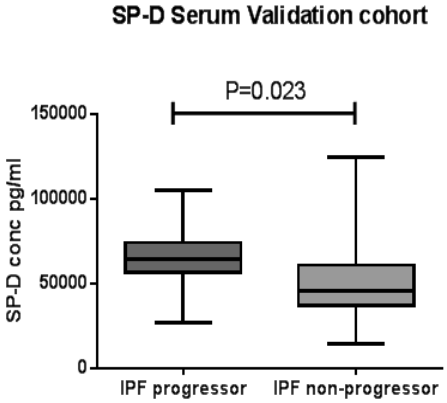
SP-D Serum Validation cohort
SP-D conc pg/ml
150000
100000
50000
0
P=0.023
IPF progressor
IPF non-progressor

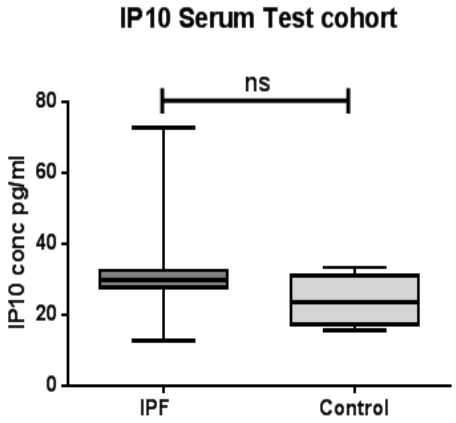
IP10 Serum Test cohort
IP10 conc pg/ml
80
60
40
20
0
ns
IPF
Control

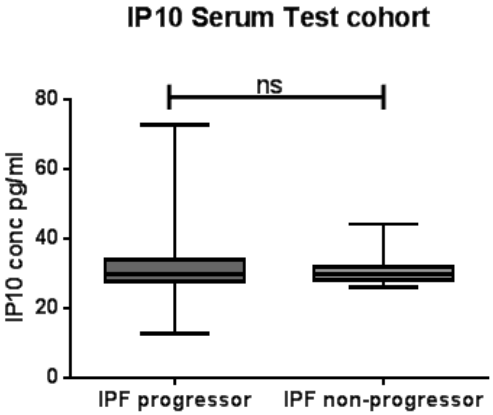
IP10 Serum Test cohort
IP10 conc pg/ml
80
60
40
20
0
ns
IPF progressor
IPF non-progressor

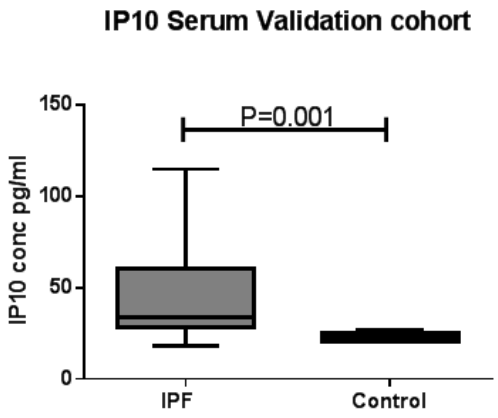
IP10 Serum Validation cohort
P=0.001
IP10 conc pg/ml
150
100
50
0
IPF
Control

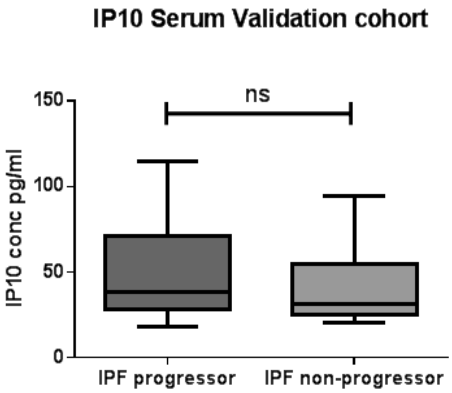
IP10 Serum Validation cohort
ns
IP10 conc pg/ml
150
100
50
0
IPF progressor
IPF non-progressor

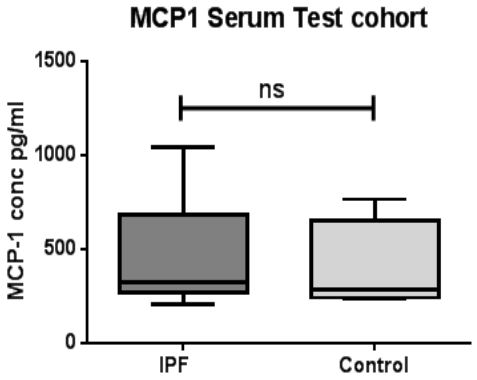
MCP1 Serum Test cohort
ns
MCP-1 conc pg/ml
1500
1000
500
0
IPF
Control

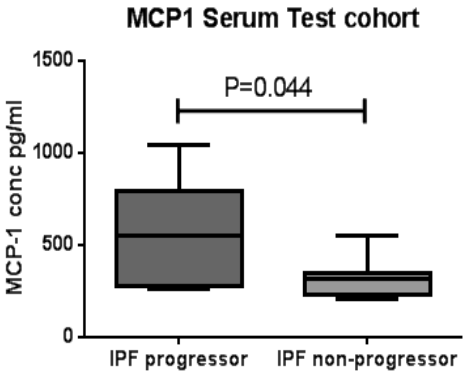
MCP1 Serum Test cohort
P=0.044
MCP-1 conc pg/ml
1500
1000
500
0
IPF progressor
IPF non-progressor

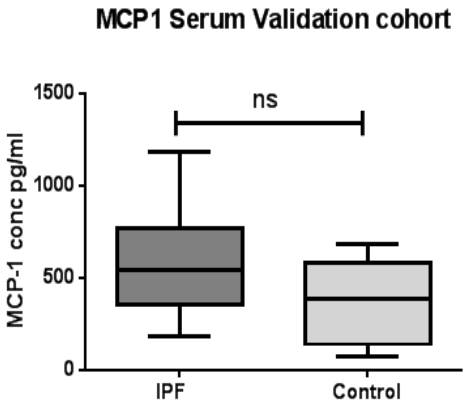
MCP1 Serum Validation cohort
ns
MCP-1 conc pg/ml
1500
1000
500
0
IPF
Control

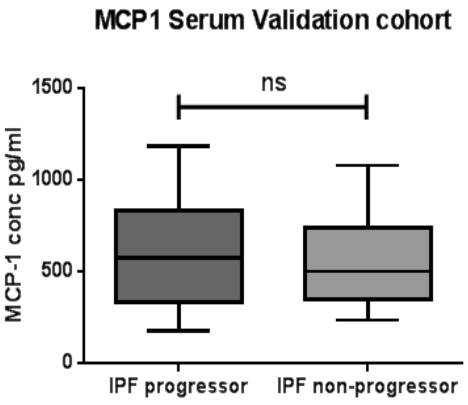
MCP1 Serum Validation cohort
ns
MCP-1 conc pg/ml
1500
1000
500
0
IPF progressor
IPF non-progressor

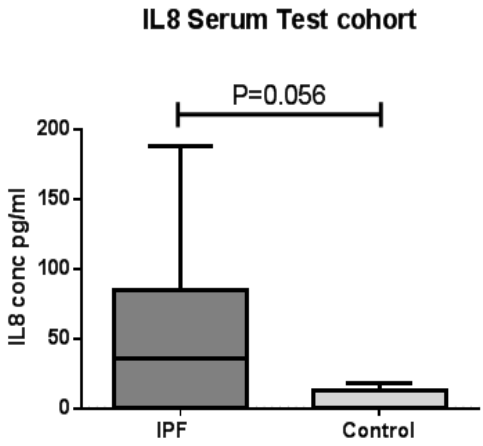
IL8 Serum Test cohort
P=0.056
IL8 conc pg/ml
200
150
100
50
0
IPF
Control

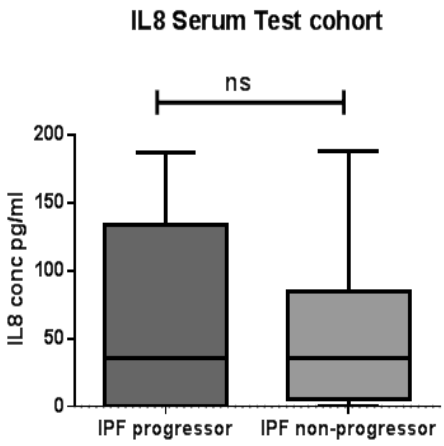
IL8 Serum Test cohort
ns
IL8 conc pg/ml
200
150
100
50
0
IPF progressor
IPF non-progressor

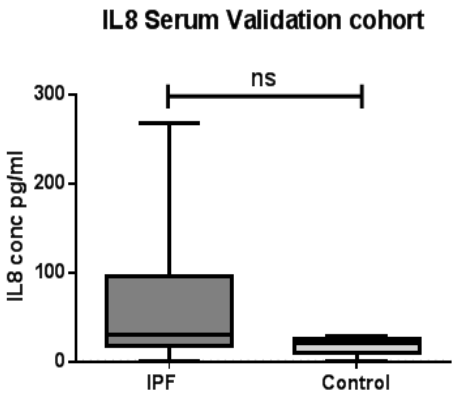
IL8 Serum Validation cohort
ns
IL8 conc pg/ml
300
200
100
0
IPF
Control

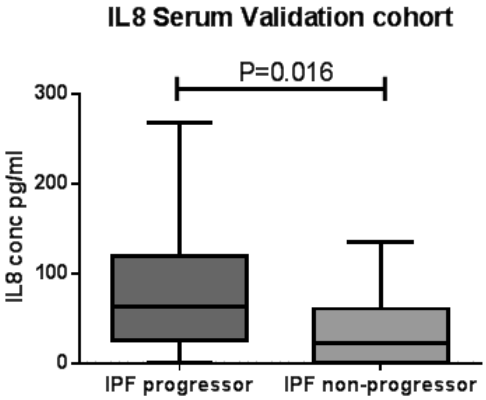
IL8 Serum Validation cohort
P=0.016
IL8 conc pg/ml
300
200
100
0
IPF progressor
IPF non-progressor

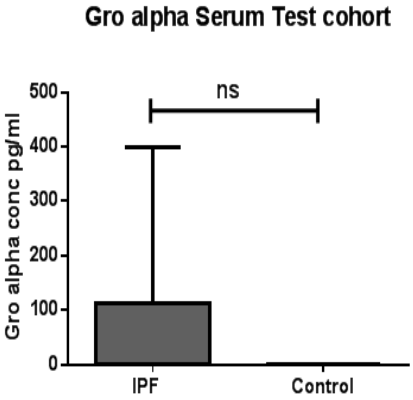
Gro alpha Serum Test cohort
ns
Gro alpha conc pg/ml
500
400
300
200
100
0
IPF
Control

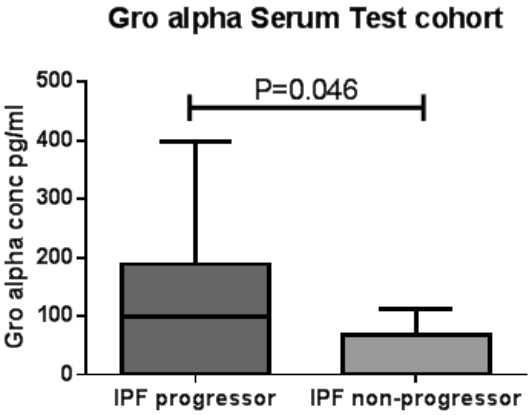
Gro alpha Serum Test cohort
P=0.046
Gro alpha conc pg/ml
500
400
300
200
100
0
IPF progressor
IPF non-progressor

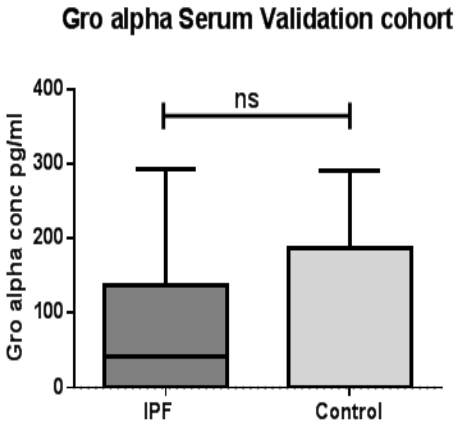
Gro alpha Serum Validation cohort
Gro alpha conc pg/ml
400
300
200
100
0
ns
IPF
Control

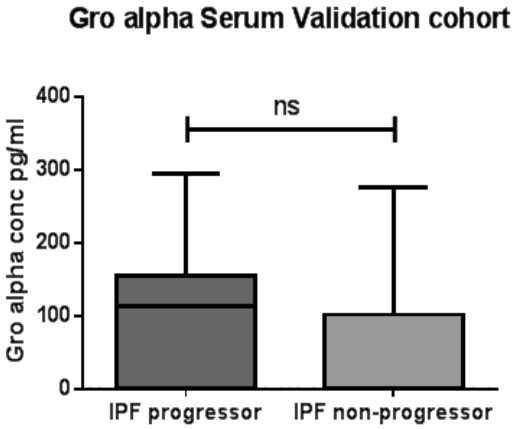
Gro alpha Serum Validation cohort
Gro alpha conc pg/ml
400
300
200
100
0
ns
IPF progressor
IPF non-progressor

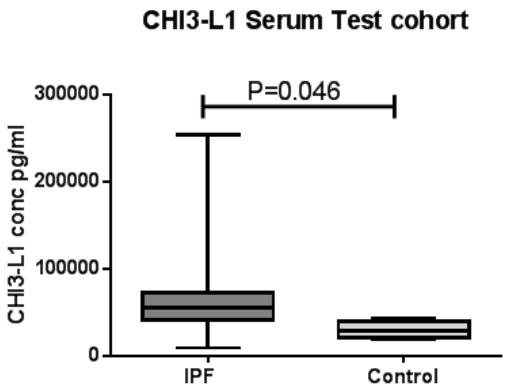
CHI3-L1 Serum Test cohort
CHI3-L1 conc pg/ml
300000
200000
100000
0
P=0.046
IPF
Control

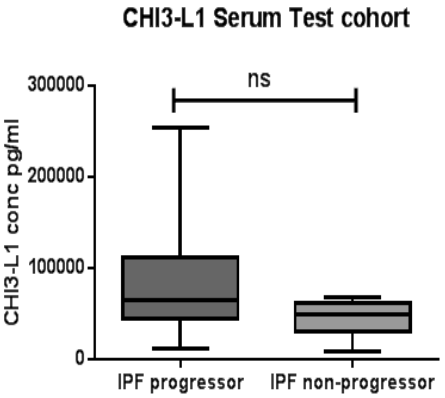
CHI3-L1 Serum Test cohort
CHI3-L1 conc pg/ml
300000
200000
100000
0
ns
IPF progressor
IPF non-progressor

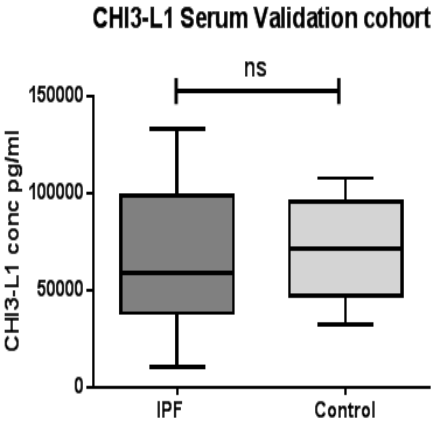
CHI3-L1 Serum Validation cohort
CHI3-L1 conc pg/ml
150000
100000
50000
0
ns
IPF
Control

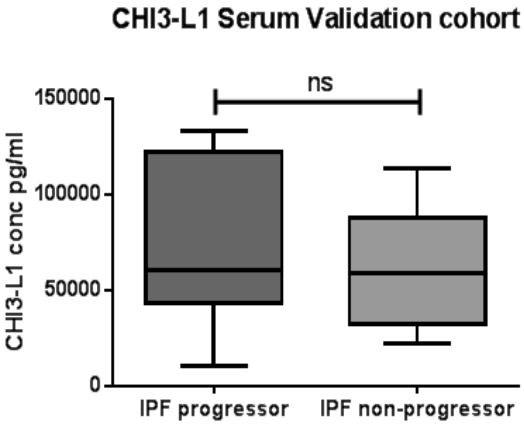
CHI3-L1 Serum Validation cohort
CHI3-L1 conc pg/ml
150000
100000
50000
0
ns
IPF progressor
IPF non-progressor

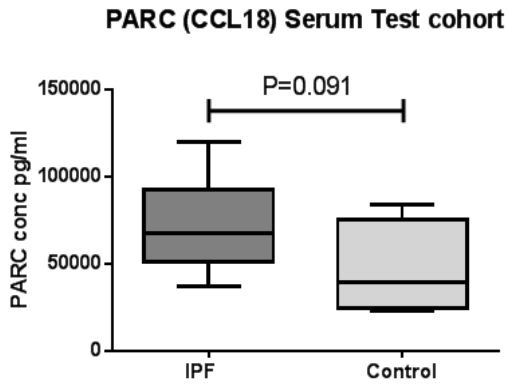

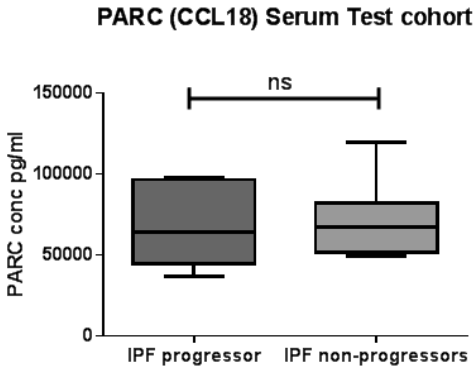

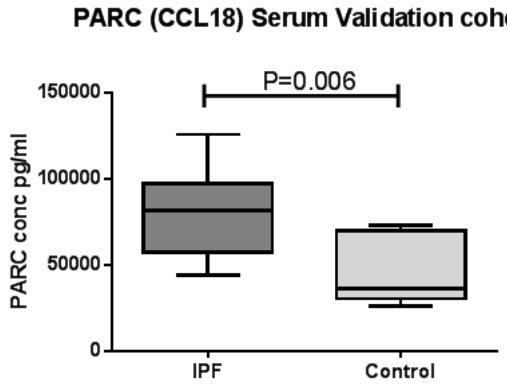

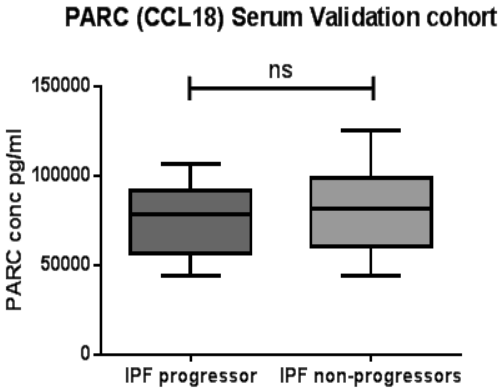

In order to investigate whether any of the analytes tested may have potential for use as a predictive biomarker for disease progression in IPF, ROC curve analysis was performed to assess the sensitivity and specificity above or below a cut off threshold for each protein. The results of this are demonstrated in Table 35.

Table 35. ROC curve analysis for Luminex serum proteins of interest.

Protein	Cut-off value 1 (pg/ml)	Sensitivity 1 (%)	Specificity 1 (%)	Cut-off value 2 (pg/ml)	Sensitivity 2 (%)	Specificity 2 (%)
MMP1	>3738	61%	58%	>7686	9%	83%
MIF	>13975	63%	50%	>54363	33%	83%
VEGF	>102.7	67%	54%	>186.6	25%	83%
Periostin	>97532	67%	54%	>133365	33%	83%
CHI3-L1	>48689	61%	38%	>88259	41%	82%
EGF	>306.2	63%	60%	>506.5	33%	83%
Pentraxin3	>535.2	63%	30%	>3518	25%	83%
Osteopontin	>24370	63%	58%	>47311	33%	83%
SP-D	>51530	71%	88%	>51016	75%	83%
IP10	>31.49	63%	58%	>45.49	33%	83%
MCP1	>480.8	63%	55%	>669.7	42%	83%
Gro-alpha	>120.2	73%	67%	>140.3	53%	84%
IL8	>29.46	63%	63%	>83.66	42%	83%
PARC	<82822	63%	38%	<50352	17%	83%
RANTES	>36570	61%	63%	>43844	44%	83%
Galectin3	<17837	63%	29%	<10855	33%	83%

Following on from this analysis, a number of proteins were identified for investigation into their use in combination in an attempt to improve sensitivity and specificity. Contingency tables (Vassarstats.net) were used to identify the sensitivity, specificity and positive and negative predictive values when different combinations of proteins at different cut-off thresholds were used. For example, if we look at a combination of SP-D, gro-alpha and RANTES for predicting disease progression in IPF, a serum SP-D level of >51016pg/ml and a gro-alpha level of >140.3pg/ml and a RANTES level of >52418pg/ml yields a sensitivity of 96% and a specificity of 80%. The positive predictive value of this combination was 81% and the negative predictive value was 95%. If we use another combination of SP-D >51016pg/ml, gro-alpha >129.1pg/ml and IL8 >201.3pg/ml, sensitivity was 91%, specificity was 80%, and the positive and negative predictive values were 81% and 91% respectively. An example of how these values were calculated is demonstrated in Figure 55 below.

Figure 55. Example of different combinations of biomarkers to yield sensitivity, specificity, positive and negative predictive values for disease progression in IPF.

IPF Progressors	IPF Progressors	IPF Non-Progressors	IPF Non-Progressors	IPF Non-Progressors	IPF Non-Progressors
SP-D	Gro-alpha	RANTES	SP-D	Gro-alpha	RANTES
26615.3	130.84	116365	10751.74	113.08	41100
30187.74	83.84	53291	14078.21	0	44574.19
30737.36	208.26	48141	15686.32	0	122940
30960.8	92.81	31658.48	20765.88	0	46773
45729.78	398.28	24860.5	23184.58	0	36795.5
46630.7	0	56786.85	24872.22	0	25817.5
51706.32	0	23304.5	26447.66	92.02	33118.5
55223.99	141.71		26573.37	0	33768.31
57896.23	127.32	79912.83	29406.66	0	36428
58370	293.58	125416.5	33792.43	0	31525.16
62973.38	242.23	27677	33883.46	113.08	35437
63079.95	0	72862	35816.95	0	51545.14
65957.9	159.89	72415.5	39301.08	104.25	33403.24
66073.07	0	34066.45	41392.61	0	23202.63
66903.97	0	15896.55	42008.06	0	42693.5
68746.8	0	37609.03	43425.04	84.42	42868.2
75801.24	0	86496.5	43743.83	0	14385.27
81965.02	100.57	33888.5	47116.77	0	20097.88
86755.69	133.24	39398.35	48673.47	0	18979.15
94606.71	138.94	36722.29	50678.96	0	31872.07
99958.12	0	39291.5	51353.77	275.89	43112.85
103429.9	0	37547	56211.25	243.93	36711
104773.3	138.94	29707	63862.12	92.81	37928.99
			83649.43	133.24	29829.72
			124247.9	0	46710.45

	Disease Absent	**Disease Present**
Test positive	5	22
Test negative	20	1

Above data were entered into Calculator 1 on Vassarstats for analysis

Proteomic analysis highlighted several proteins that differed between IPF and controls, and progressor and non-progressor groups. The most notable were EGF, IL-8, Pentraxin-3, CXCL17, CHI3-L1, MCP1, CCl18, VEGF and Galectin-3 in BALf, and MMP1, Periostin, Osteopontin, SP-D, IP10, MCP1, IL8, CCL18 and Gro-alpha in serum. Many of these biomarkers have been described previously, however they have not been validated in a 'real-life' patient cohort, such as those in our study. Based on this preliminary data, further work to devise a prediction model including clinical and serological data was undertaken.

5.2.4 Paired biomarker profiling

BAL

BAL was performed at presentation (baseline) and at 12 months. Luminex Magnetic Screening Assay kits (R&D) were used to detect proteins of interest in BAL fluid in paired samples from 61 patients (21 IPF progressors, 40 IPF non-progressors). BALF was normalised to 10μg of protein per sample (protein determined via Pierce BCA assay, ThermoFisher cat# 23225). A similar panel of potential biomarkers (n=32) were used as described in previous work with the addition of ten analytes following recently reported proteins of interest in the literature, these included amphiregulin, MCP-1 (CCL2), RANTES (CCL5), PARC (CCL18), eotaxin-3 (CCL26), Chi3-L1, GRO alpha (CXCL1), IL-8 (CXCL8), IP-10 (CXCL10), EGF, IL-10, MMP7, MMP8, IL-33, MMP1, MIF, osteopontin, pentraxin 3, periostin, SP-D, TNFα , TIMP-1, IL1-ra, IL-13, PDGF-AA, PDGF-BB, HGF, VEGF, galectin 3, galectin 1, serpin e1 and IFNγ. Significant characteristics of disease progression at 12 month BAL were increased BAL amphiregulin and PDGF-AA levels, a significant increase in MMP8 between 0 and 12 month BALs in IPF progressors, and a significant decrease in amphiregulin levels between 0 and 12 month BALs in IPF non-progressors. This data is shown in Figure 56 below. Other important findings were a reduction in EGF, SP-D, IL-13 and TIMP1 levels between 0 and 12 month BALs in IPF non-progressors, at baseline 0 month BAL Galectin-1 levels were increased and IL-13 levels were decreased in the IPF progressor group, and at 12 month BAL IFNγ levels were increased in IPF progressors, however

none of these findings reached significance. These data are shown in Figure 57. There were no significant differences in MMP1, MIF, periostin, CHI3-L1, osteopontin, TNFα, IL1-ra or HGF levels between progressor and non-progressor groups at 0 and 12 months, or between 0 and 12 month BALs within groups (data not shown).

Figure 56**. **Significant findings in BAL biomarker profiling at 0 and 12 month BALs.

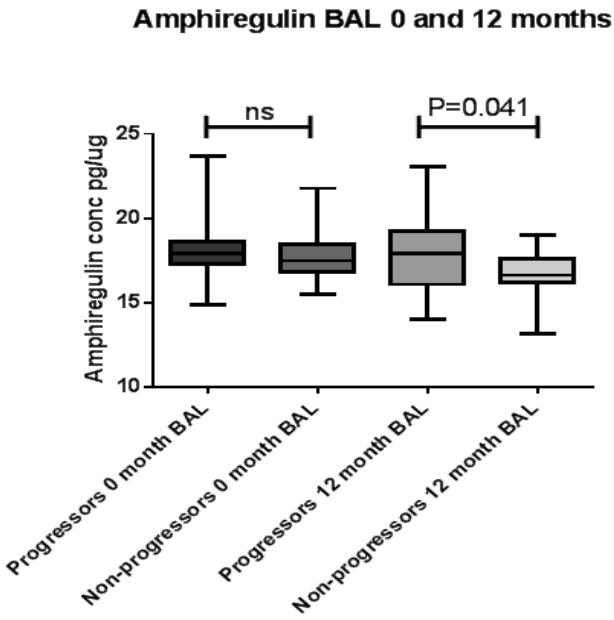

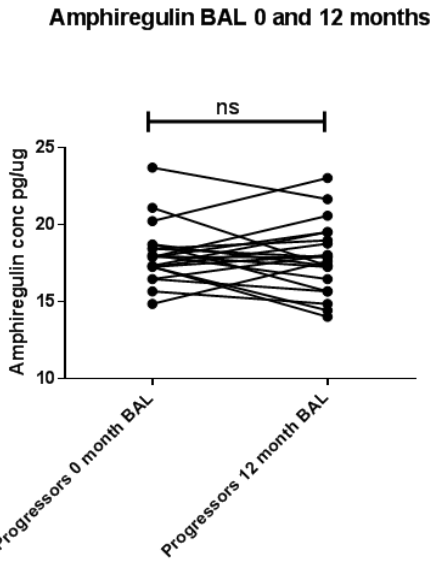

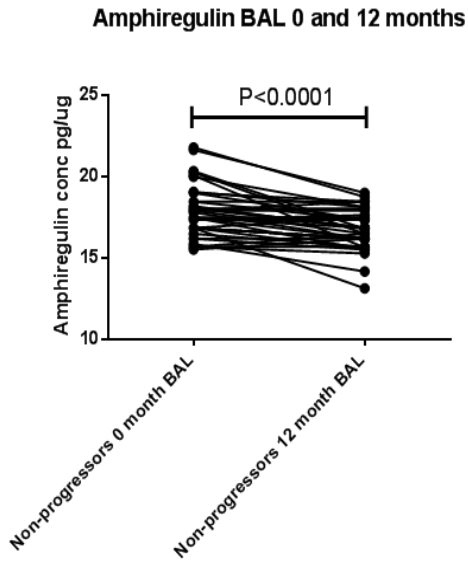

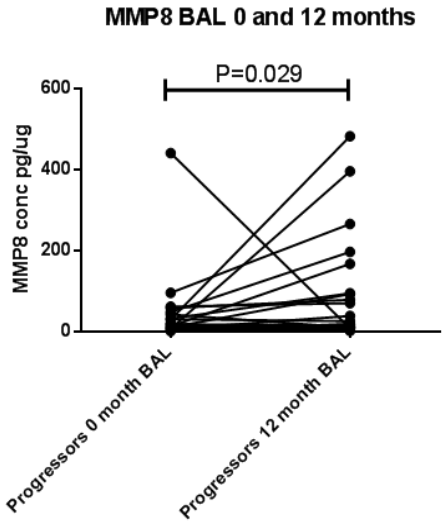
MMP8 BAL 0 and 12 months
P=0.029
MMP8 conc pg/ug
600
400
200
0
Progressors 0 month BAL
Progressors 12 month BAL

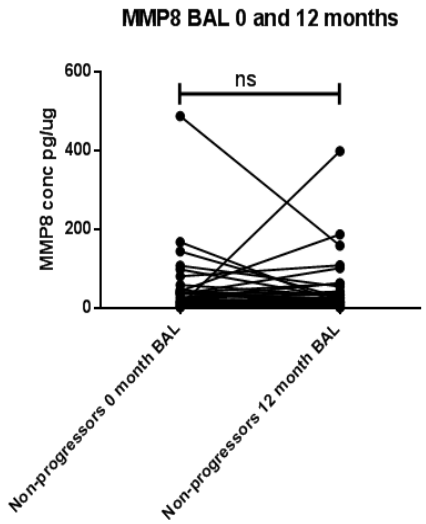
MMP8 BAL 0 and 12 months
ns
MMP8 conc pg/ug
600
400
200
0
Non-progressors 0 month BAL
Non-progressors 12 month BAL

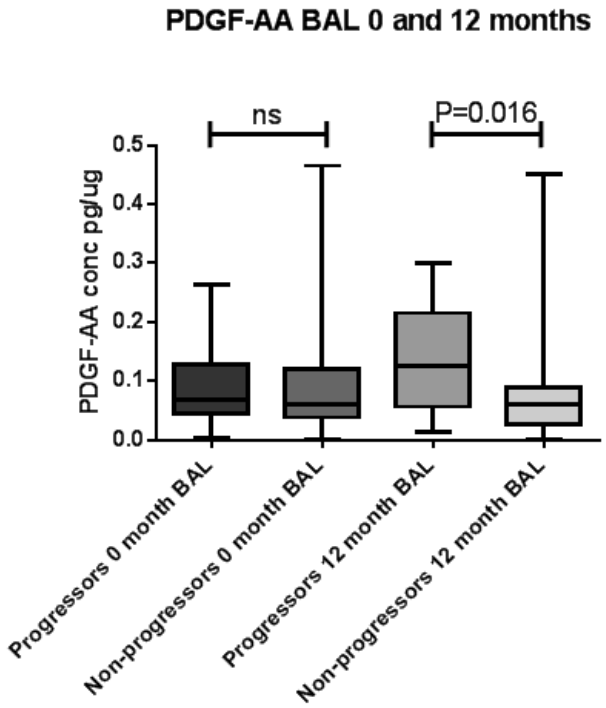
PDGF-AA BAL 0 and 12 months
ns
P=0.016
PDGF-AA conc pg/ug
0.5
0.4
0.3
0.2
0.1
0.0
Progressors 0 month BAL
Non-progressors 0 month BAL
Progressors 12 month BAL
Non-progressors 12 month BAL

Figure 57. Additional findings in BAL biomarker profiling at 0 and 12 month BALs.

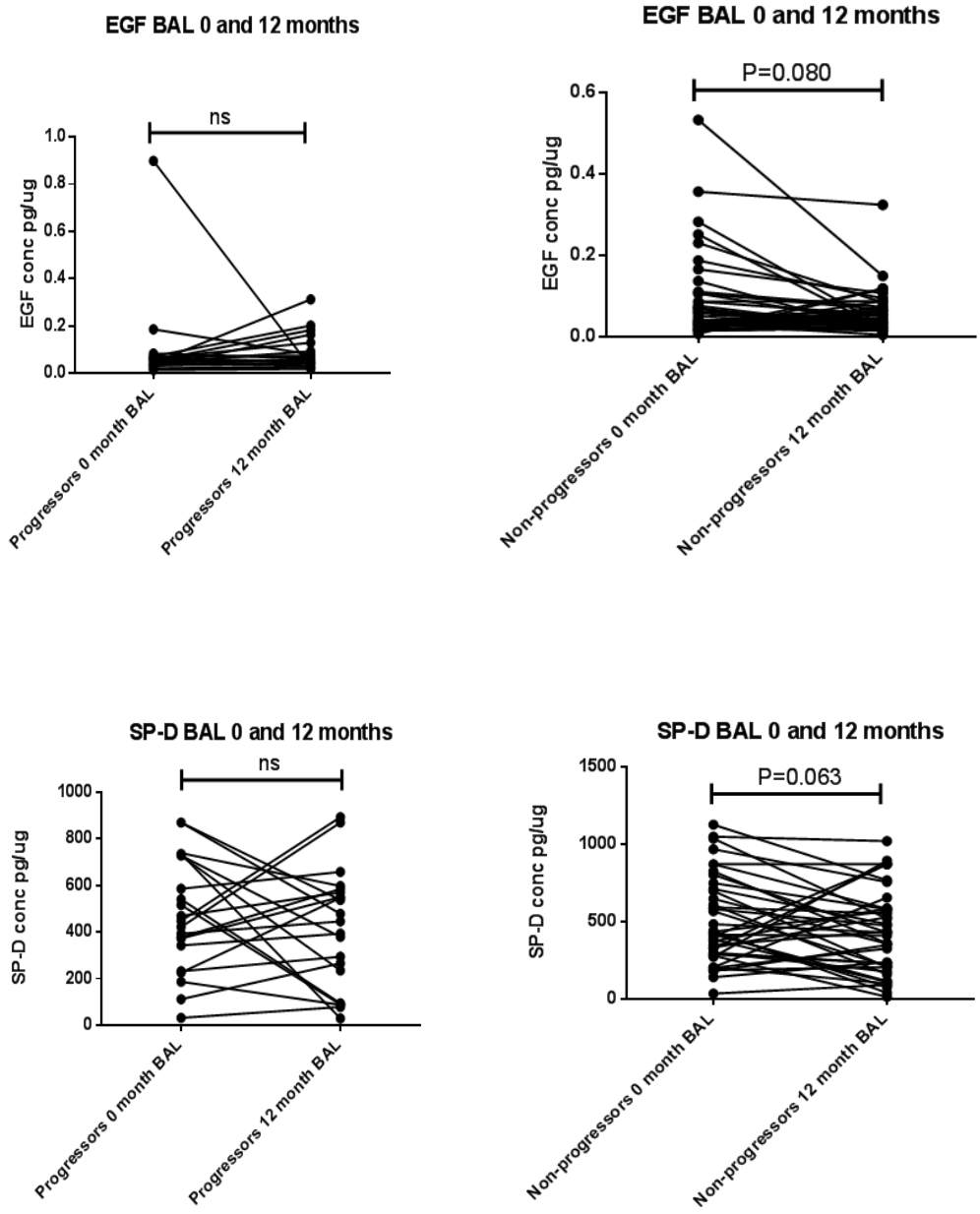

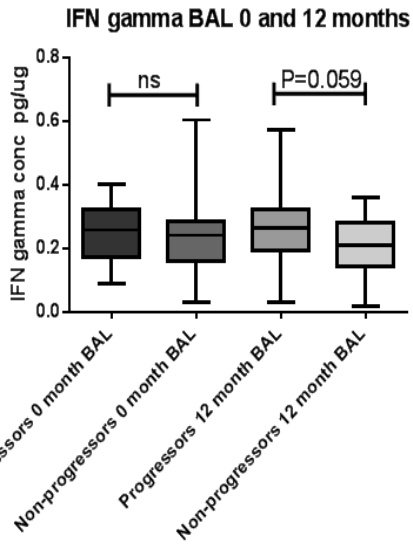
IFN gamma BAL 0 and 12 months
IFN gamma conc pg/ug
0.8
0.6
0.4
0.2
0.0
ns
P=0.059
Progressors 0 month BAL
Non-progressors 0 month BAL
Progressors 12 month BAL
Non-progressors 12 month BAL

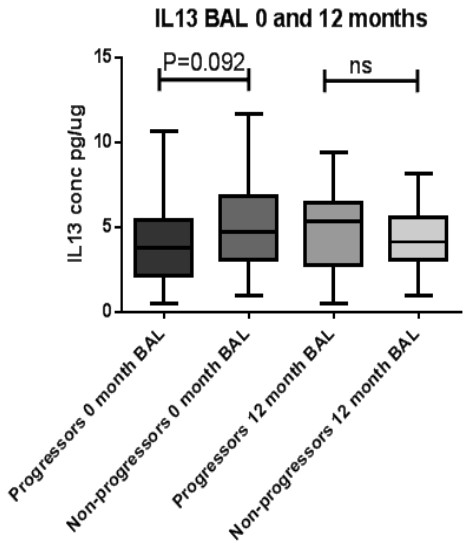
IL13 BAL 0 and 12 months
IL13 conc pg/ug
15
10
5
0
P=0.092
ns
Progressors 0 month BAL
Non-progressors 0 month BAL
Progressors 12 month BAL
Non-progressors 12 month BAL

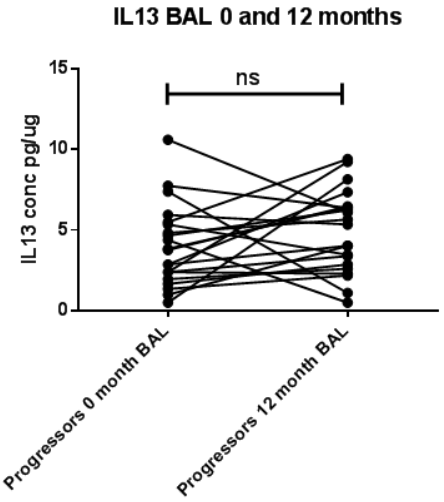
IL13 BAL 0 and 12 months
IL13 conc pg/ug
15
10
5
0
ns
Progressors 0 month BAL
Progressors 12 month BAL

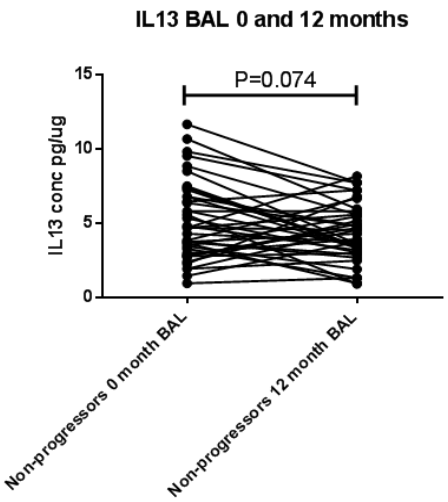
IL13 BAL 0 and 12 months
IL13 conc pg/ug
15
10
5
0
P=0.074
Non-progressors 0 month BAL
Non-progressors 12 month BAL

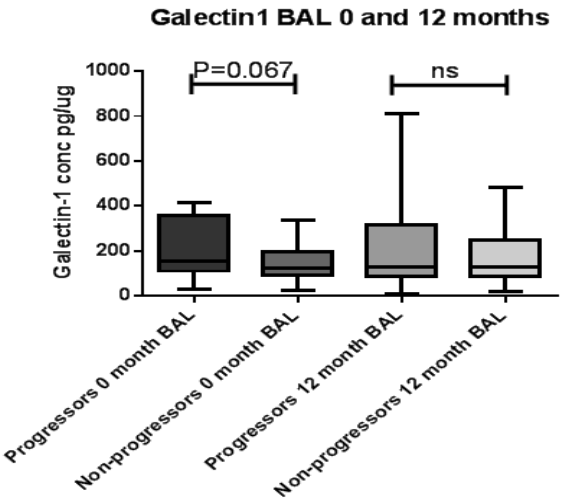
Galectin1 BAL 0 and 12 months
Galectin-1 conc pg/ug
1000
800
600
400
200
0
P=0.067
ns
Progressors 0 month BAL
Non-progressors 0 month BAL
Progressors 12 month BAL
Non-progressors 12 month BAL

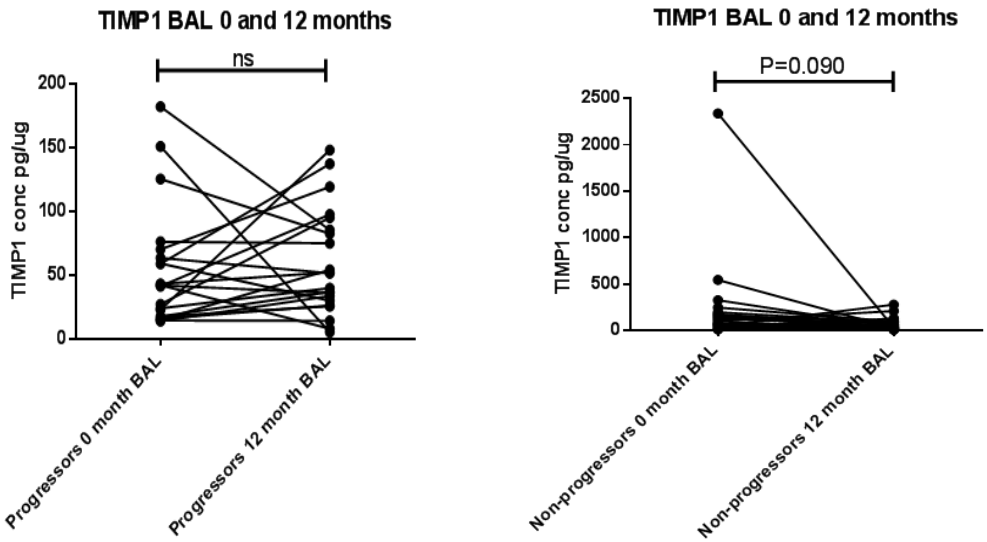

Serum

Serum samples were obtained from patients at presentation (baseline) and at 12 months. Luminex Magnetic Screening Assay kits (R&D) were used to detect proteins of interest in serum in paired samples from 59 patients (21 IPF progressors, 38 IPF non-progressors). Serum was prepared at either a 1:2 or 1:50 dilution as per manufacturer instructions. A similar panel of potential biomarkers (n=26) were used as described in previous work, these included MCP-1 (CCL2), RANTES (CCL5), PARC (CCL18), Chi3-L1, IL-8 (CXCL8), IP-10 (CXCL10), EGF, MMP8, MMP1, MIF, osteopontin, pentraxin 3, periostin, SP-D, TNF , TIMP-1, IL-1 ra, IL-13, PDGF-AA, PDGF-BB, HGF, VEGF, galectin 3, galectin 1, serpin e1 and IFN . Six analytes were dropped from the panel (amphiregulin, eotaxin3, gro alpha, IL-10, MMP7 and IL33), as previous work had shown these analytes were rarely detected in serum using Luminex Magnestic Screening Assays. Significant characteristics of disease progression on serum obtained at 12 months were increased serum SP-D and galectin-1 levels in progressors versus non-progressors, a significant increase in periostin, CHI3-L1, SP-D, TNF, galectin-1, MMP8 and IL-8 levels between serum obtained at 0 and 12 month in IPF progressors, and a significant decrease in EGF, TNF, pentraxin-3, IFN and CCL18 levels between 0 and 12 month sera in IPF non-progressors. This data is shown in Figure 58 below. There were no significant differences in MMP1, MIF, osteopontin, IL-1 ra, TIMP1, IL-13, PDGF-AA, VEGF, IP-10, MCP1, RANTES, galectin-3, PDGF-BB, serpin e1 or HGF

levels between progressor and non-progressor groups at 0 and 12 months, or between 0 and 12 month sera within groups (data not shown).

Figure 58. Significant findings in serum biomarker profiling at 0 and 12 months.

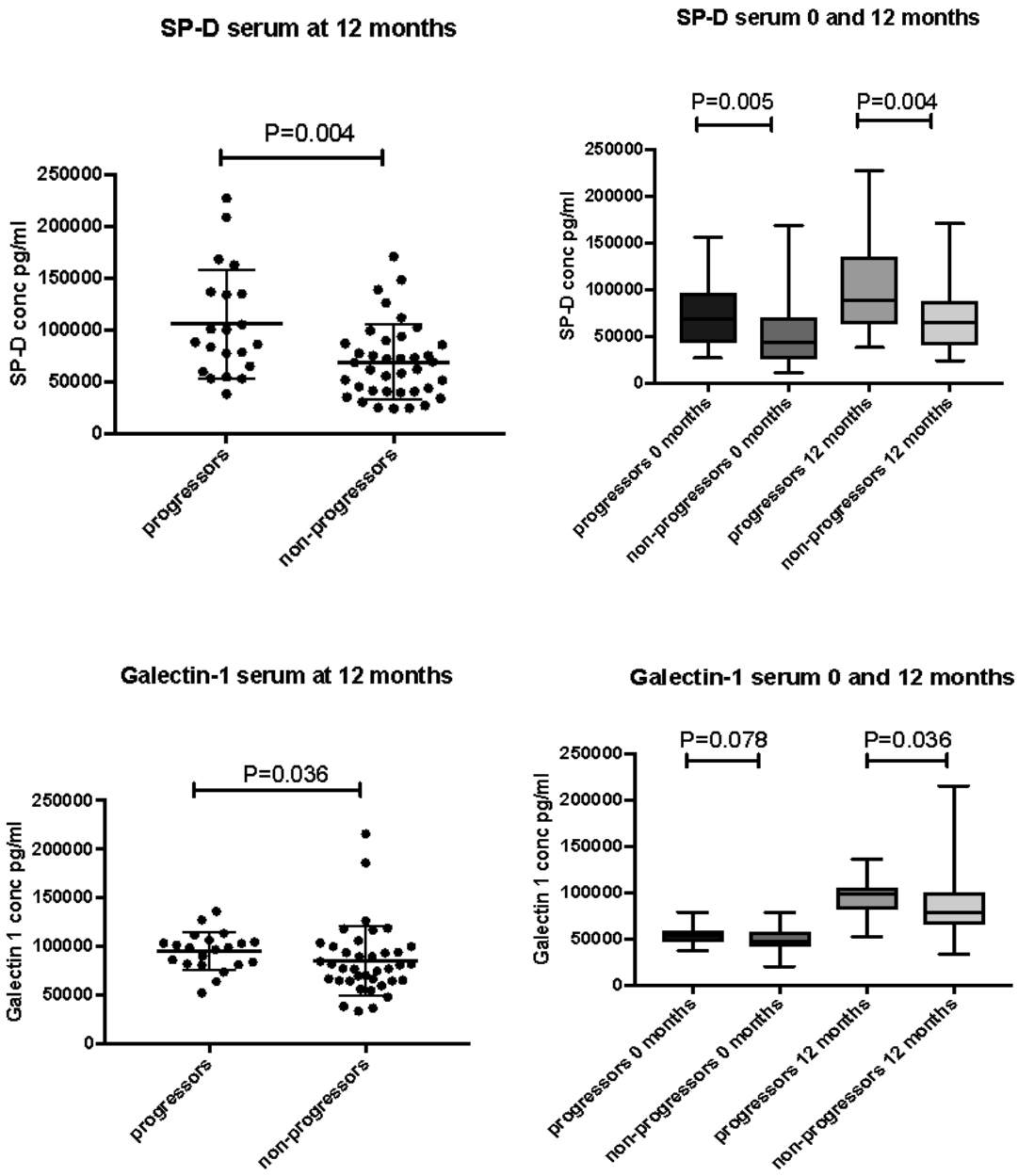

Periostin serum 0 and 12 months progressors

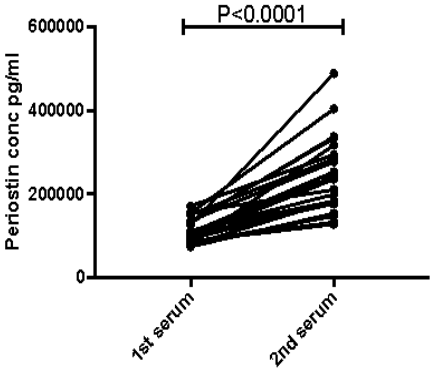

Periostin serum 0 and 12 months non-progressors

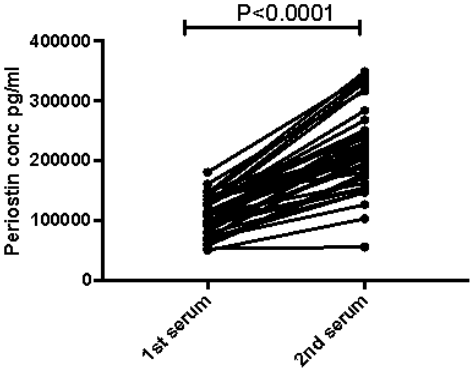

Chi3-L1 serum 0 and 12 months progressors

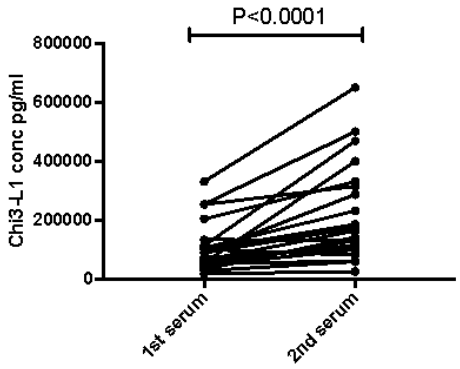

Chi3-L1 serum 0 and 12 months non-progressors

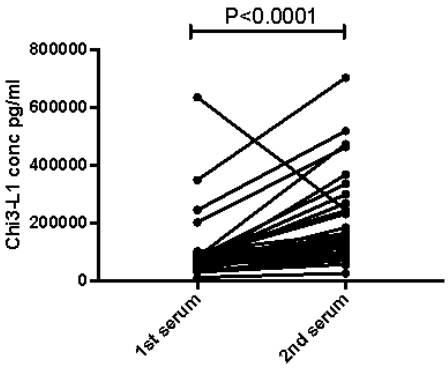

SP-D serum 0 and 12 months progressors

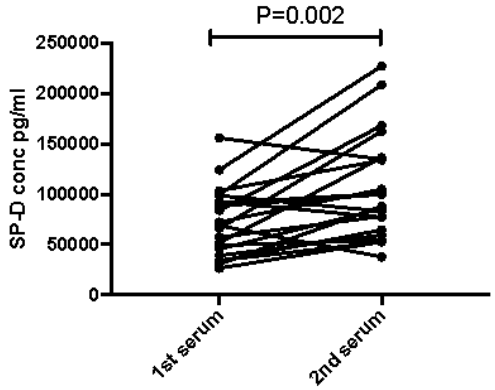

SP-D serum 0 and 12 months non-progressors

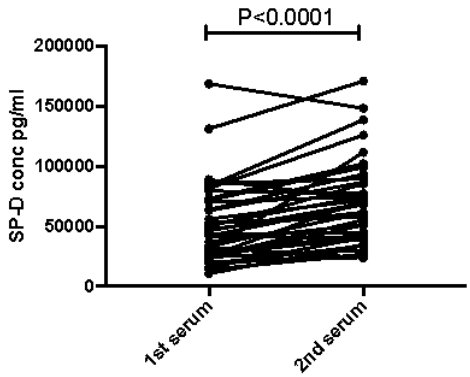

EGF serum 0 and 12 months progressors

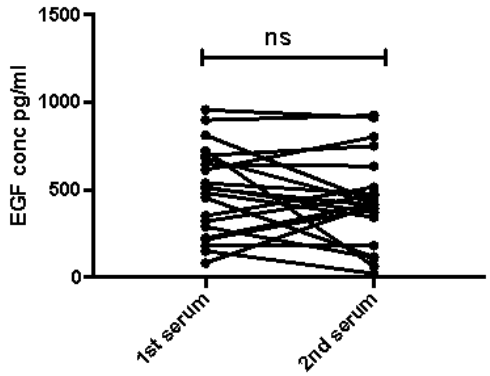

EGF serum 0 and 12 months non-progressors

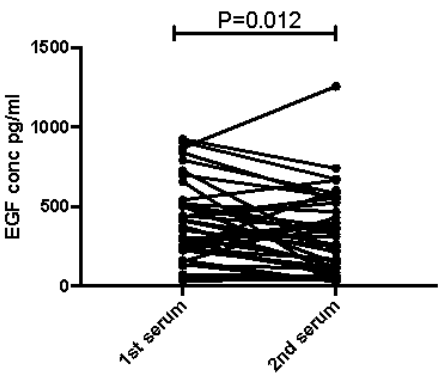

TNF alpha serum 0 and 12 months progressors

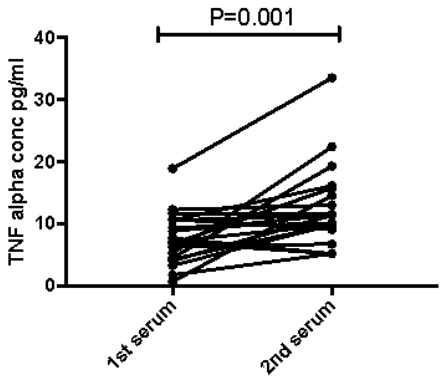

TNF alpha serum 0 and 12 months non-progressors

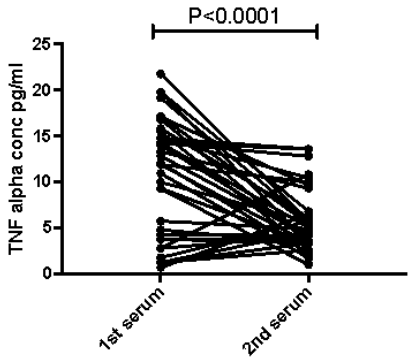

IFN gamma serum 0 and 12 months progressors

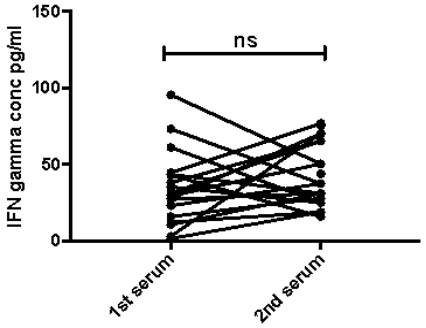

IFN gamma serum 0 and 12 months non-progressors

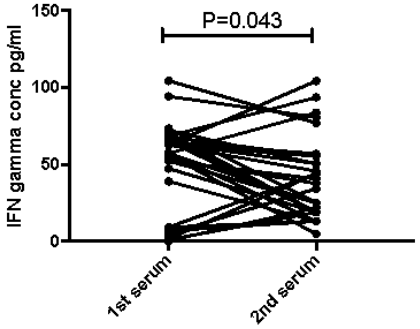

Galectin 1 serum 0 and 12 months progressors

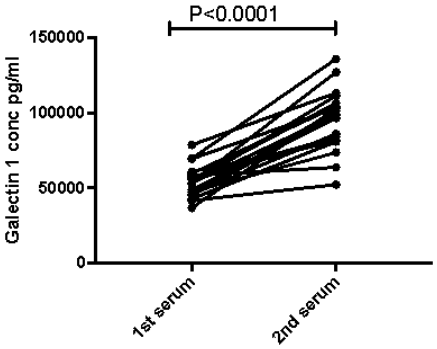

Galectin 1 serum 0 and 12 months non-progressors

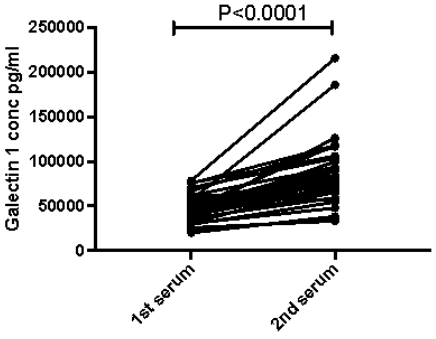

MMP8 serum 0 and 12 months progressors

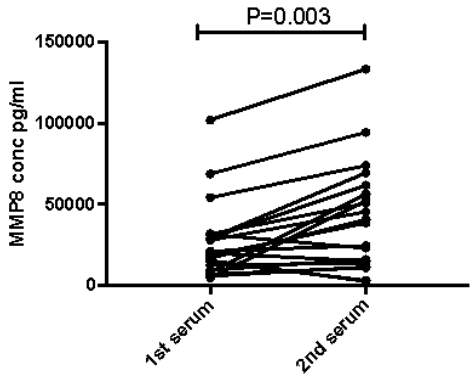

MMP8 serum 0 and 12 months non-progressors

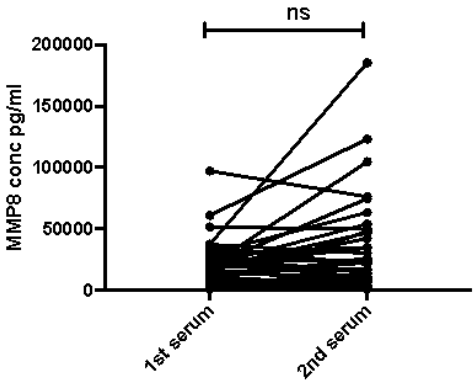

Pentraxin 3 serum 0 and 12 months progressors

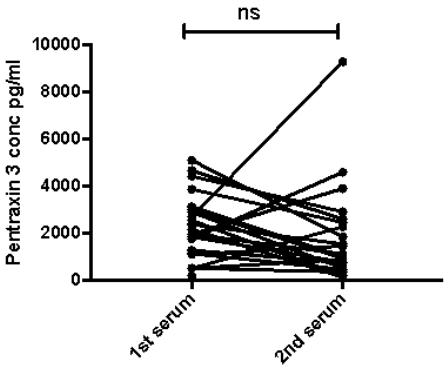

Pentraxin 3 serum 0 and 12 months non-progressors

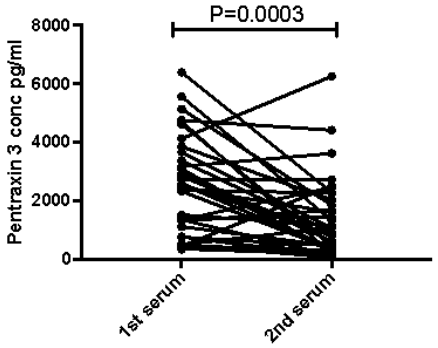

IL8 serum 0 and 12 months progressors

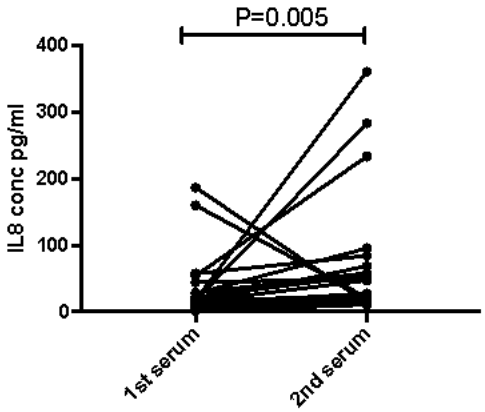

IL8 serum 0 and 12 months non-progressors

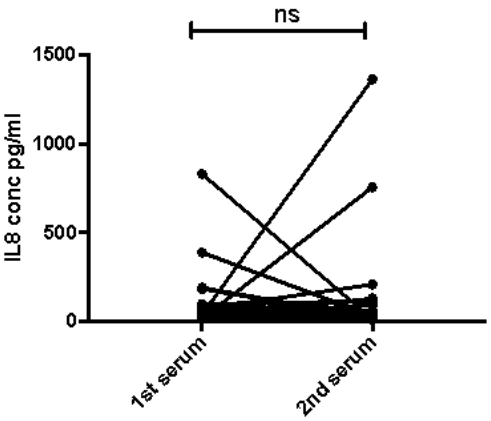

CCL18 serum 0 and 12 months progressors

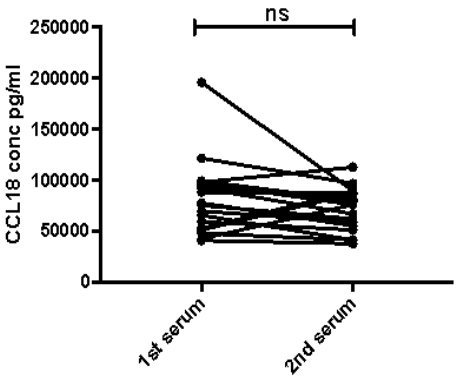

CCL18 serum 0 and 12 months non-progressors

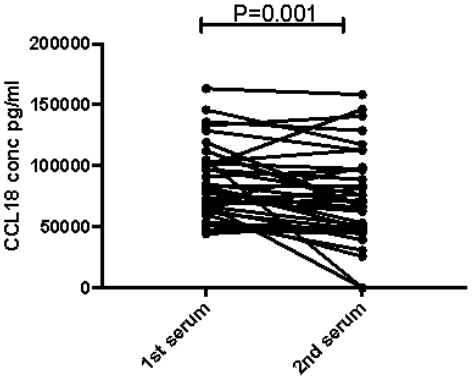

5.2.5 Linear regression modelling and decision tree learning

Serum was obtained at presentation (baseline) and at 12 months. Luminex Magnetic Screening Assay kits (R&D) were used to detect serum biomarkers in a training cohort (n=48; progessors n=22, non-progressors n=26) and then a validation cohort (n=160; progressors n=77, non-progressors n=83) of IPF patients. Serum was utilised at either 1:2 or 1:50 dilution depending on manufacturer's instruction. Potential biomarkers (n=32) were pre-selected from either previously published studies of IPF biomarkers or our hypothesis-driven profiling from previous work. Biomarkers included in the model were amphiregulin, MCP-1 (CCL2), RANTES (CCL5), PARC (CCL18), eotaxin-3 (CCL26), Chi3-L1, GRO alpha (CXCL1), IL-8 (CXCL8), IP-10 (CXCL10), EGF, IL-10, MMP7, MMP8, IL-33, MMP1, MIF, osteopontin, pentraxin 3, periostin, SP-D, TNF , TIMP-1, IL1-ra, IL-13, PDGF-AA, PDGF-BB, HGF, VEGF, galectin 3, galectin 1, serpin e1 and IFN . Serological data was combined with clinical parameters including patient age, sex, smoking status, lung function data including baseline percentage predicted FEV_1, FVC and TCO, and HRCT data including CT category, % fibrosis on HRCT, % periphery involved and degree of bronchiolar dilatation. We also applied previously reported predictive tools such as the GAP Index, du Bois score and CPI Index to the Edinburgh IPF cohort to include in the model. Patient demographic data, HRCT scoring, clinical scoring models and serum biomarker data for serum training and validation cohorts are demonstrated in Table 36 below.

Table 36. Patient demographic data, HRCT scoring, clinical scoring models and serum biomarker data.

	Test cohort			Validation cohort		
	IPF Progressor N=22	**IPF Non-Progressor N=26**	**P-value**	**IPF Progressor N=77**	**IPF Non-Progressor N=83**	**P-value**
Age in years (SD)	70.0 (9.2)	71.1 (7.7)	0.634	74.3 (7.7)	73.9 (9.3)	0.762
Male (%)	19 (86.4)	16 (61.5)	0.056	58 (75.3)	51 (61.4)	0.060
Never smoked (%)	5 (22.7)	7 (26.9)	0.740	19 (24.7)	18 (21.7)	0.654
Ex-smoker (%)	14 (63.6)	16 (61.5)	0.882	54 (70.1)	56 (67.5)	0.724
Current smoker (%)	3 (13.6)	3 (11.5)	0.828	4 (5.2)	9 (10.8)	0.196
VC in Litres (IQR)	2.99 (2.31, 3.29)	3.01 (2.20, 3.20)	0.706	2.62 (2.04, 3.28)	2.73 (2.02, 3.19)	0.813
VC %predicted in Litres (IQR)	73.0 (67.0, 92.6)	95.0 (81.5, 103.3)	0.022	89.0 (71.6, 103.2)	90.6 (78.3, 103.4)	0.163
TLCO (mm/min/ mmHg) (IQR)	4.30 (3.33, 5.10)	3.69 (3.18, 4.60)	0.478	3.28 (2.38, 4.15)	3.69 (2.74, 4.56)	0.033
TLCO %predicted (IQR)	49.4 (42.0, 56.1)	52.1 (52.6, 59.1)	0.339	41.6 (35.0, 51.9)	51.4 (39.3, 59.7)	0.017
Definite UIP HRCT (%)	7 (31.8)	6 (23.1)	0.504	21 (27.3)	21 (25.3)	0.775
Probable UIP HRCT (%)	15 (68.2)	20 (76.9)	0.503	56 (72.7)	62 (74.7)	0.774
% total fibrosis HRCT (IQR)	40.0 (35.0, 60.0)	30.0 (25.0, 40.0)	0.001	35.0 (25.0, 55.0)	25.0 (20.0, 40.0)	0.008
% periphery involved (IQR)	90.0 (90.0, 95.0)	80.0 (32.5, 90.0)	0.049	75.0 (40.0, 90.0)	70.0 (36.3, 85.0)	0.187
Bronchiolar dilatation [0-3] (SD)	1.36 (1.05)	0.62 (0.70)	0.013	0.90 (0.75)	0.74 (0.58)	0.155
GAP Score (SD)	4.05 (1.33)	2.85 (0.97)	0.002	4.10 (1.43)	3.36 (1.25)	0.002

Du Bois Score	30.14 (13.50)	10.57 (9.03)	<0.0001	28.74 (14.54)	13.57 (9.02)	<0.0001
CPI Index	49.55 (15.05)	41.26 (7.95)	0.032	48.54 (15.97)	42.40 (14.81)	0.013
Serum SP-D pg/ml (SD)	65652.09 (23489.68)	40833.12 (23557.32)	0.004	105752.99 (74678.11)	56183.18 (33571.91)	0.0008
Serum Periostin pg/ml (SD)	127017.14 (48885.01)	98870.48 (30468.10)	0.019	115376.66 (32705.52)	111265.36 (34397.71)	0.440
Serum MMP7 pg/ml (SD)	1637.85 (796.38)	1303.76 (1077.63)	0.048	4708.41 (3886.95)	2672.48 (1759.96)	0.024

Vital capacity and TLCO were significantly reduced in the progressors versus the non-progressor group. Patients in the progressor group had significantly increased total fibrosis percentage, peripheral involvement percentage and degree of bronchiolar dilatation on HRCT than the non-progressors. GAP score, du Bois score and CPI index scores were also significantly higher in the progressor group versus the non-progressors. In the serum test cohort (n=48), six proteins were noted to be significantly increased in the IPF progressor group compared to the IPF non-progressor group; periostin, EGF, SP-D, MMP7, IFNγ and galectin1. This data is shown in Figure 59. There were no significant differences between progressor and non-progressor groups in MMP1, MIF, CHI3-L1, osteopontin, TNFα, TIMP1, MMP8, IL1-ra, IL-13, PDGF-AA, HGF, pentraxin 3, VEGF, IP10, MCP1, gro-alpha, IL8, PARC, RANTES, galectin 3, PDGF-BB or serpin e1 levels (data not shown). In the serum validation cohort (n=160), amphiregulin, osteopontin, SP-D, galectin 1, MMP7, HGF and CHI3-L1 were all significantly elevated in the IPF progressors vs non-progressors. TNFα, IFNγ, IL-13 and PDGF-AA were all significantly increased in the IPF non-progressor group. These data are shown in Figure 60. There were no significant differences between IPF progressor and non-progressor groups in MMP1, MIF, periostin, EGF, TIMP1, MMP8, IL1-ra, PDGF-BB or serpin e1 levels (data not shown).

Figure 59. Serum protein levels in test cohort (n=48).

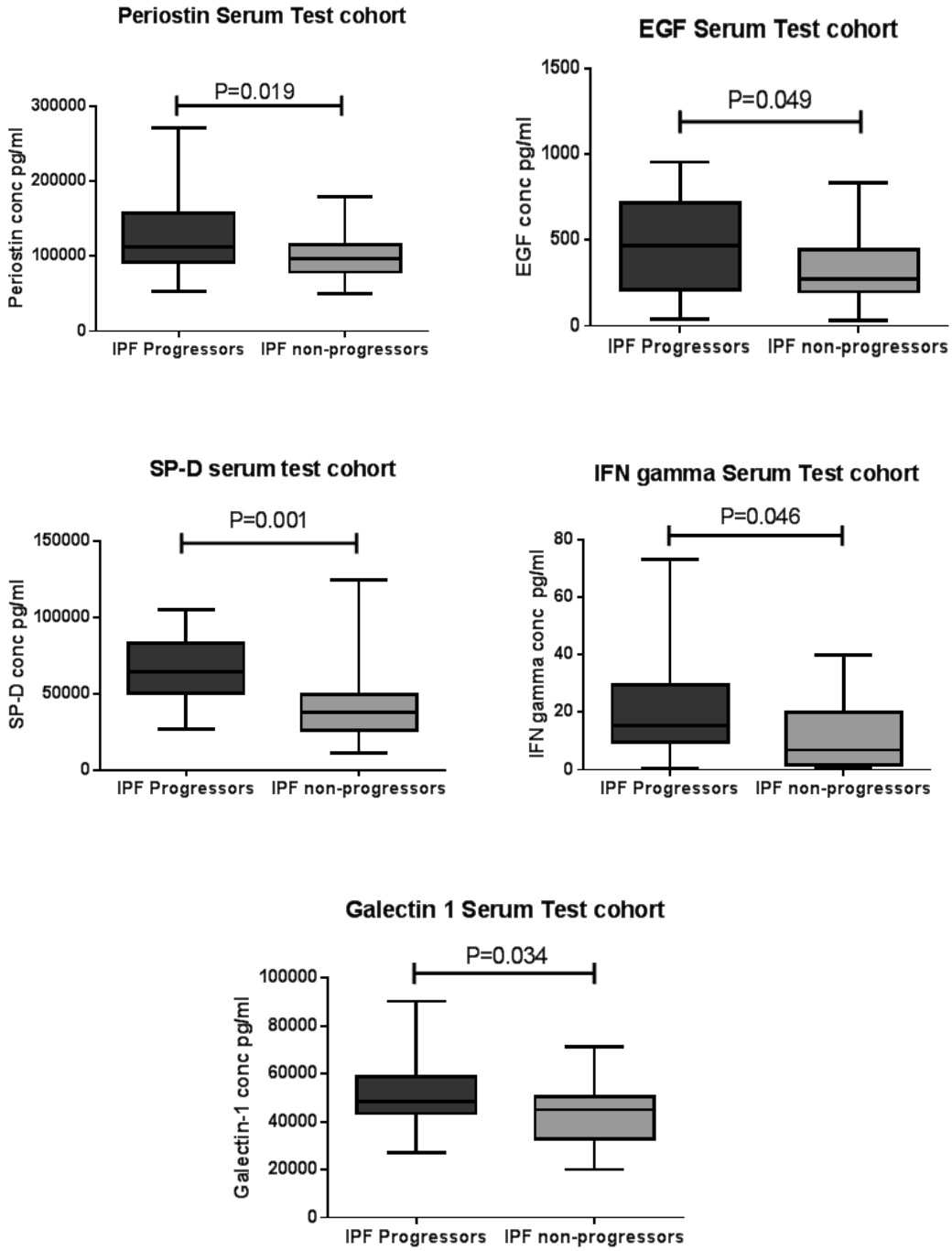

Figure 60. Serum protein levels in validation cohort (n=160).

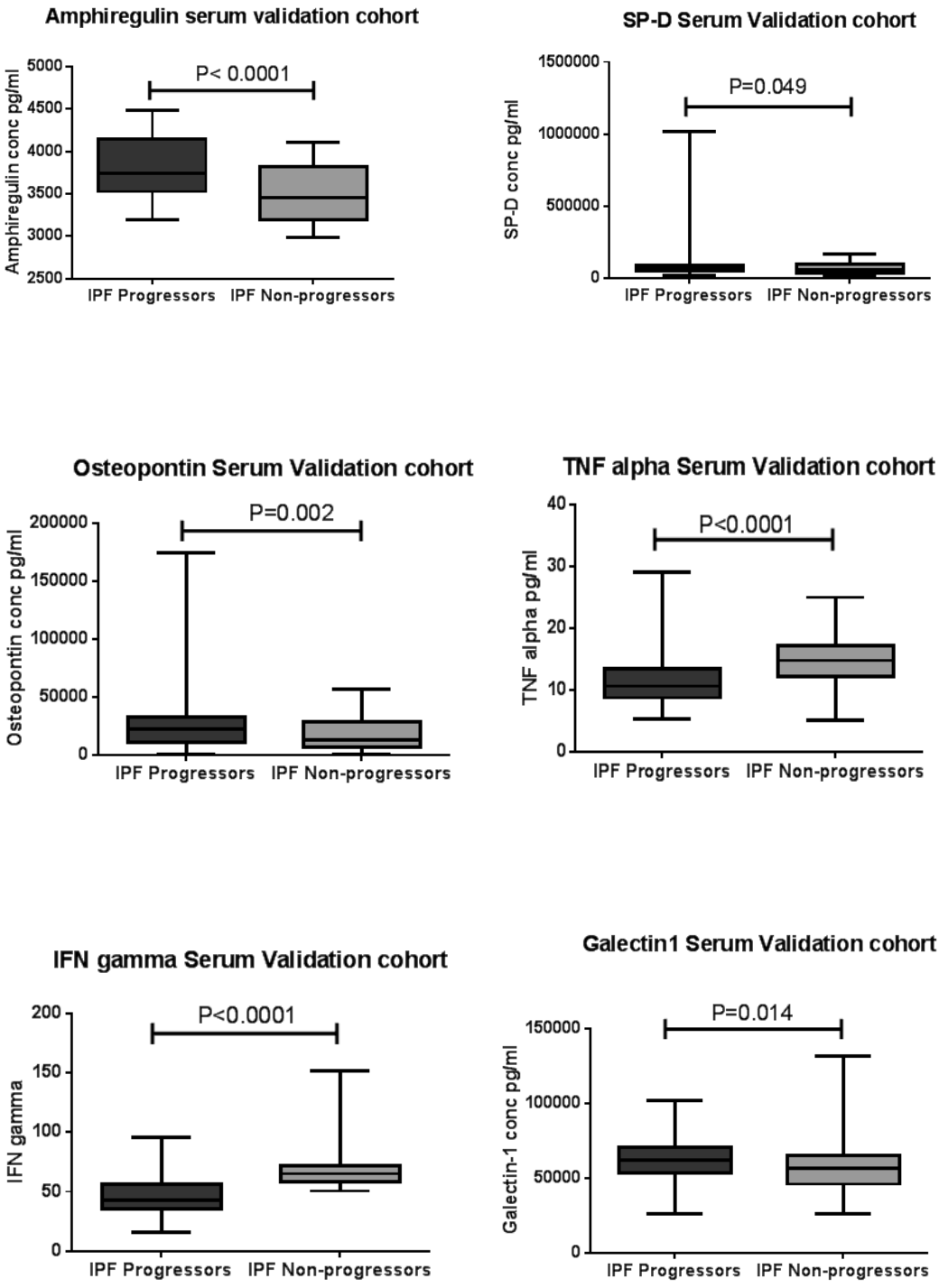

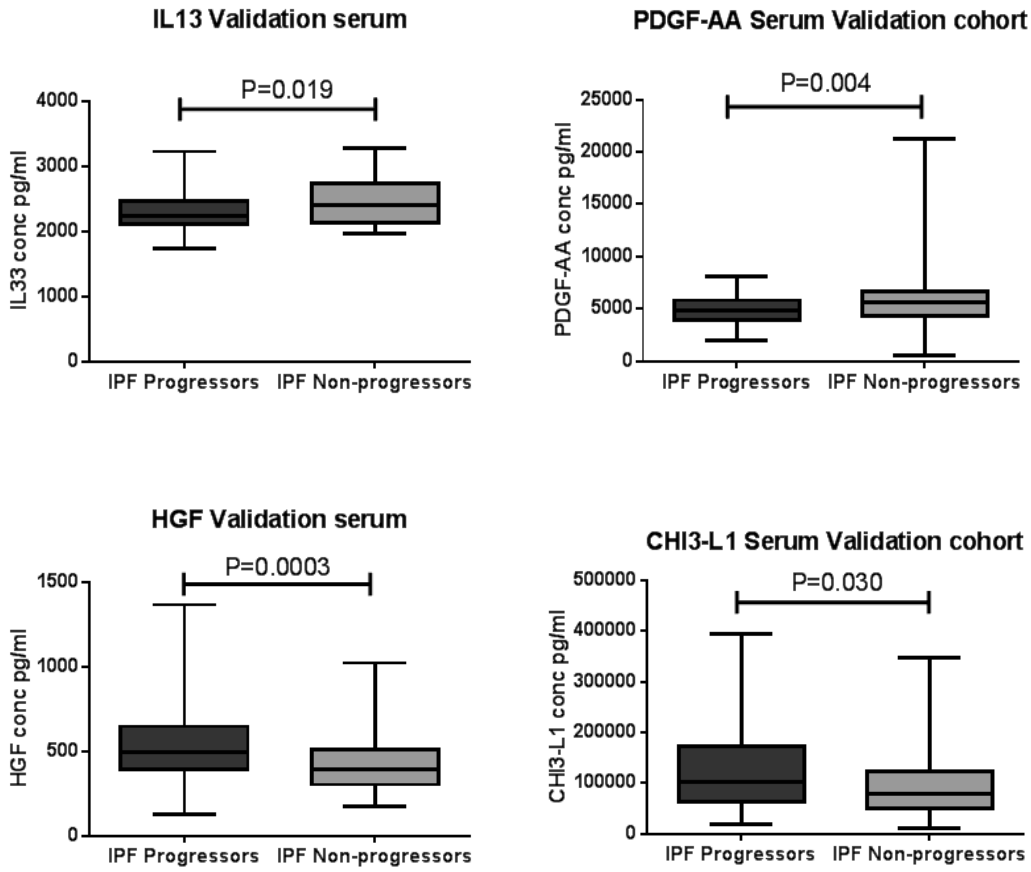

Linear logistic regression was performed in collaboration with Dr Sohan Seth, PhD (Institute for Adaptive and Neural Computation, School of Informatics, University of Edinburgh) and was used on each predictor separately to assess its importance in terms of P-value of the associated weight, the top two variables were then used to learn a decision tree. Disease progression was confidently predicted by a combination of clinical and serological variables. The current data showed that the most informative variables in predicting disease progression in IPF were % fibrosis (coefficient 0.88, P-value 0.01), % periphery involved (coefficient 0.82, P-value 0.03), % predicted FVC (coefficient 1.02, P-value 0.01), periostin pg/ml (coefficient 0.82, P-value 0.03) and SP-D pg/ml (coefficient 1.24, P-value 0.00). A linear regression model using the best two variables, % predicted FVC and serum SP-D, yielded a sensitivity of 86.4%, specificity of 92.3%, positive predictive value of 90.5% and negative predictive value of 88.9% for disease progression in IPF. Analysis of the two parameters relative to disease and the subsequent decision tree are demonstrated in Figures 61 and 62 below. Linear logistic regression modelling work to apply the predictive model to the validation

cohort is currently ongoing. Unfortunately due to time limitations, I was unable to include the results of this in this thesis.

Figure 61. Analysis of the two parameters relative to disease.

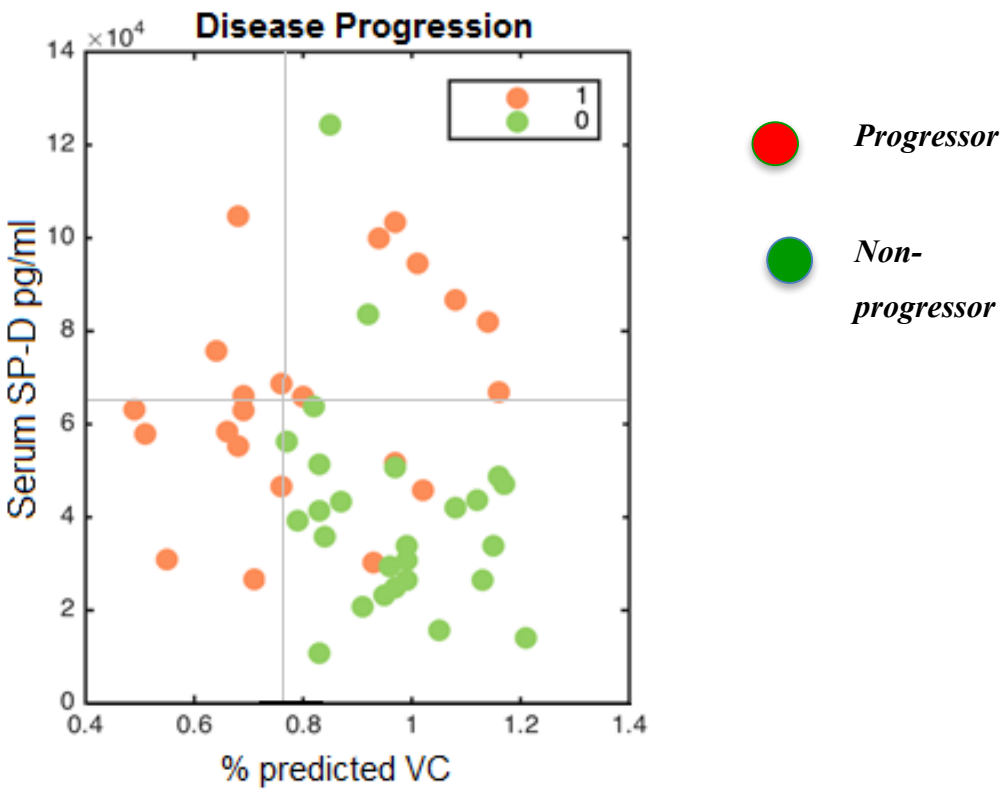

Figure 62. Decision tree predictive of disease progression in IPF.

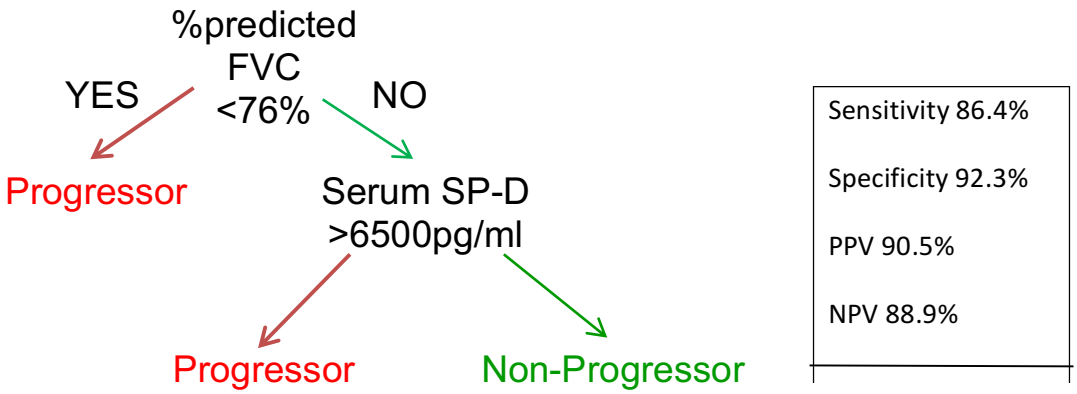

5.2.6 A phase IIa clinical trial of TD139, a Galectin-3 inhibitor

Patients from cohorts 1, 2 and 3 of the trial that had received TD139 at a dose of 0.3mg, 3mg or 10mg were pooled together to form a 'TD139 group', and were compared with patients who had received placebo in cohorts 1, 2 and 3, termed the 'control group'. Flow cytometry of BAL samples from the pooled TD139 group revealed there was a significant decrease in the galectin 3 geometric mean of alveolar macrophages between day 1 and day 14 BALs after two weeks of treatment with TD139 (P=0.0001). There was no significant change in the galectin 3 geometric mean of alveolar macrophages between day 1 and day 14 BALs in the control group. This data is shown in Figure 63 below. There were no significant changes between day 1 and day 14 BALs in the pooled TD139 group in % of B-cells, % of PMLCs, % of iPMLCs, % of rPMLCs, % of neutrophils, % of CD3+ cells, % of CD4+ cells, % of CD8+ cells, % of HLA-DR+ cells, % of M1 AM phenotype cells, % of M2a AM phenotype cells, % of M2c AM phenotype cells, % of CD71+ cells, % of CCL18+ cells or % of fibrocytes when measured by flow cytometry.

Figure 63. Galectin 3 geometric mean of alveolar macrophages between day 1 and day 14 BALs in pooled TD139 and control groups.

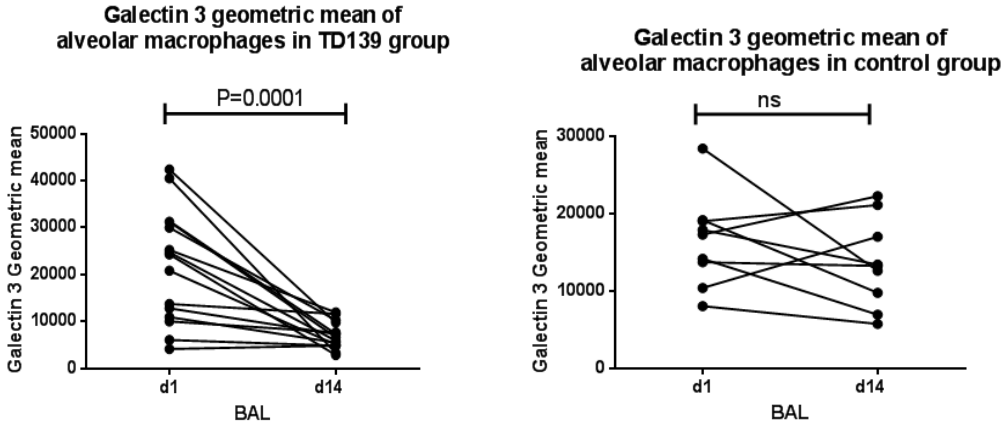

Luminex Magnetic Screening Assays (described previously) were used to assess whether there were any significant changes in a number of proteins expressed in BAL

fluid and in plasma of patients in control and TD139 groups between day 1 and day 14 BALs. The proteins of interest were selected based on previously reported studies of IPF biomarkers or hypothesis-driven profiling from my previous work, also described in this thesis.

In BALF there was a significant difference in the percentage change of galectin 3 levels between control and 10mg TD139 dose groups (P=0.007). ANOVA statistics revealed there was a significant difference in percentage change of galectin 3 levels in BALF between control, 0.3mg, 3mg and 10mg TD139 dose groups (P=0.001). There was also a significant difference in percentage change in MMP1 levels between control and the 10mg TD139 dose groups (P=0.029). ANOVA also revealed significant differences between control, 0.3mg, 3mg and 10mg TD139 dose groups in the percentage change of galectin 1, gro-alpha and IL-8 levels in BALF (P=0.017, P=0.020 and P=0.034 respectively). There were no differences in perentage change of MMP7, IP10, MCP1, MIF, CHI3-L1, SP-D, PAI, CCL18, TNFα, MMP8 or IL-1 ra levels in BALF between the groups. This data is shown in Figure 64 below.

Figure 64. Percentage change in BAL fluid proteins of interest between day 1 and day 14 BALs in TD139 and control groups, measured by Luminex Magnestic Screening Assay.

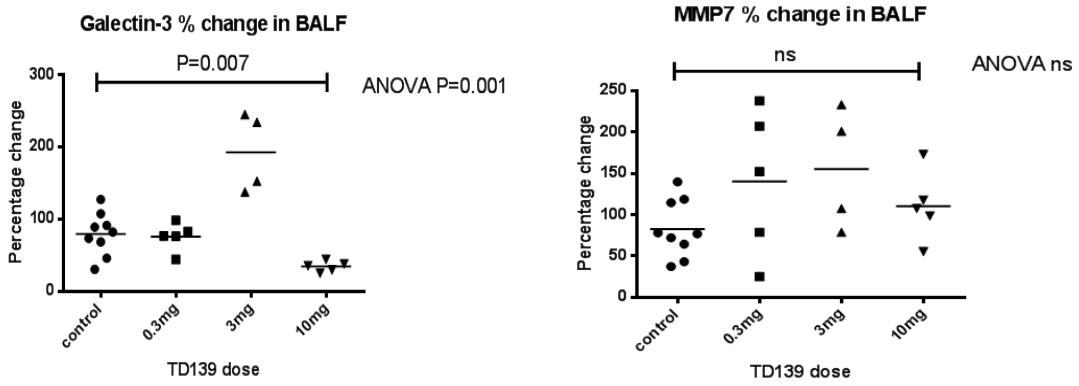

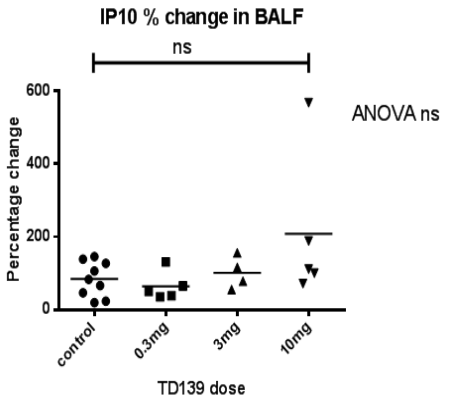
IP10 % change in BALF
ns
ANOVA ns
Percentage change
600
400
200
0
control
0.3mg
3mg
10mg
TD139 dose

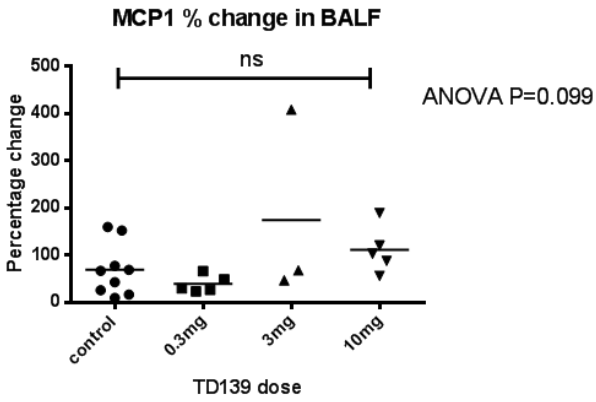
MCP1 % change in BALF
ns
ANOVA P=0.099
Percentage change
500
400
300
200
100
0
control
0.3mg
3mg
10mg
TD139 dose

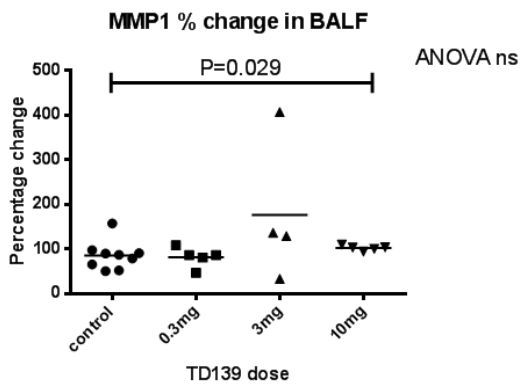
MMP1 % change in BALF
P=0.029
ANOVA ns
Percentage change
500
400
300
200
100
0
control
0.3mg
3mg
10mg
TD139 dose

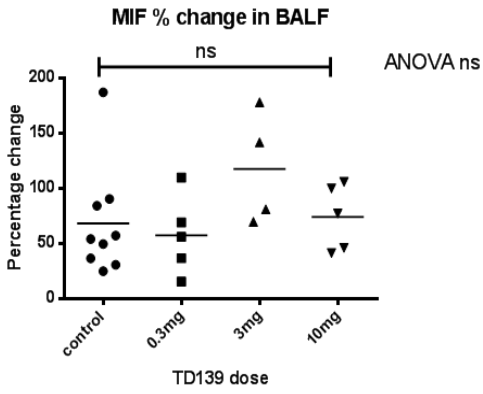
MIF % change in BALF
ns
ANOVA ns
Percentage change
200
150
100
50
0
control
0.3mg
3mg
10mg
TD139 dose

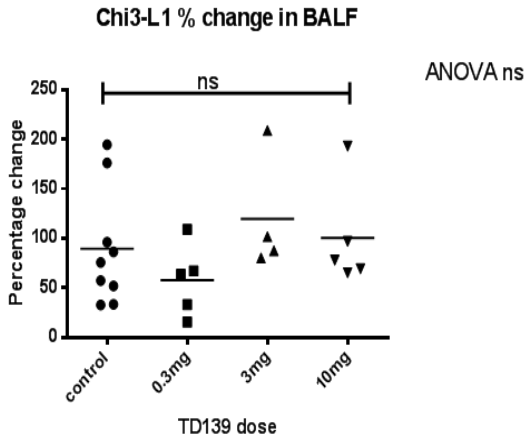
Chi3-L1 % change in BALF
ns
ANOVA ns
Percentage change
250
200
150
100
50
0
control
0.3mg
3mg
10mg
TD139 dose

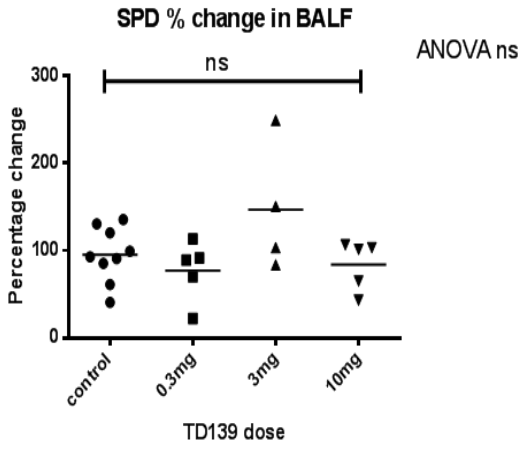
SPD % change in BALF
ns
ANOVA ns
Percentage change
300
200
100
0
control
0.3mg
3mg
10mg
TD139 dose

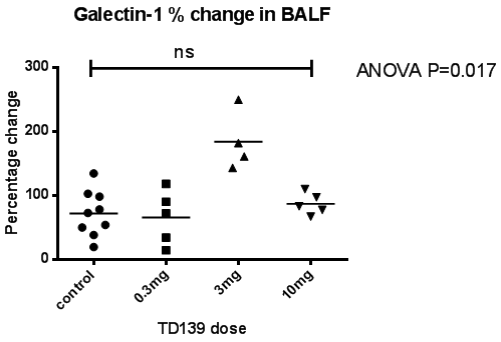
Galectin-1 % change in BALF
ns
ANOVA P=0.017
Percentage change
300
200
100
0
control
0.3mg
3mg
10mg
TD139 dose

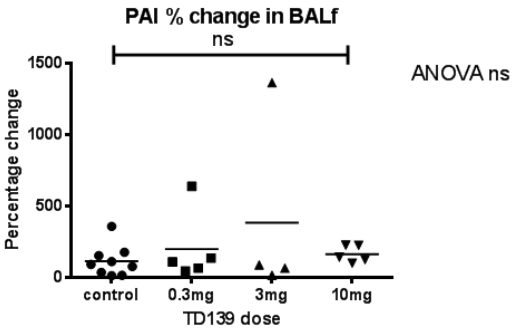
PAI % change in BALf
ns
ANOVA ns
Percentage change
1500
1000
500
0
control
0.3mg
3mg
10mg
TD139 dose

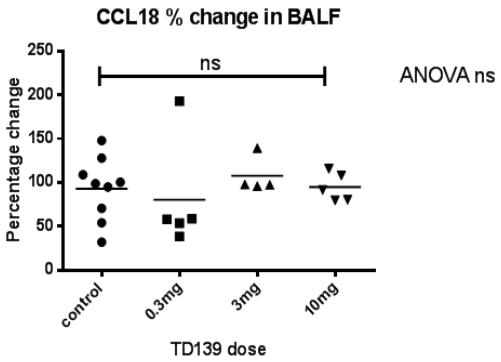
CCL18 % change in BALF
ns
ANOVA ns
Percentage change
250
200
150
100
50
0
control
0.3mg
3mg
10mg
TD139 dose

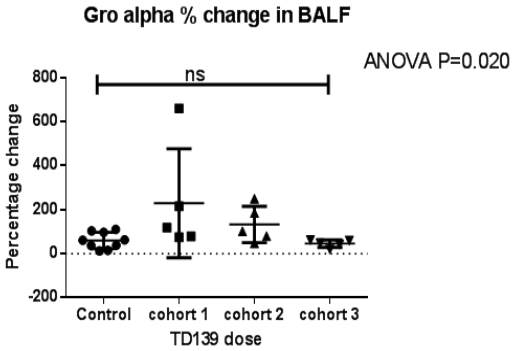
Gro alpha % change in BALF
ns
ANOVA P=0.020
Percentage change
800
600
400
200
0
-200
Control
cohort 1
cohort 2
cohort 3
TD139 dose

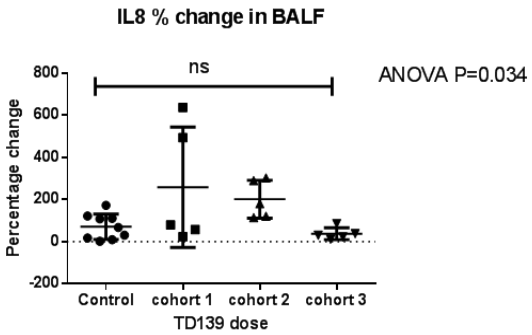
IL8 % change in BALF
ns
ANOVA P=0.034
Percentage change
800
600
400
200
0
-200
Control
cohort 1
cohort 2
cohort 3
TD139 dose

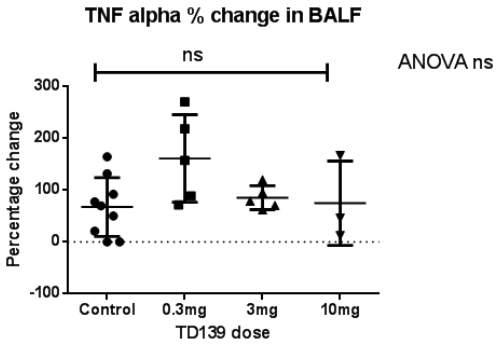
TNF alpha % change in BALF
ns
ANOVA ns
Percentage change
300
200
100
0
-100
Control
0.3mg
3mg
10mg
TD139 dose

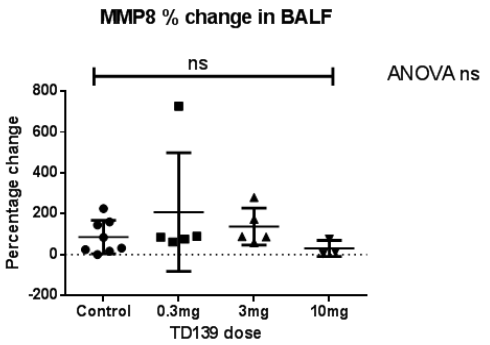
MMP8 % change in BALF
ns
ANOVA ns
Percentage change
800
600
400
200
0
-200
Control
0.3mg
3mg
10mg
TD139 dose

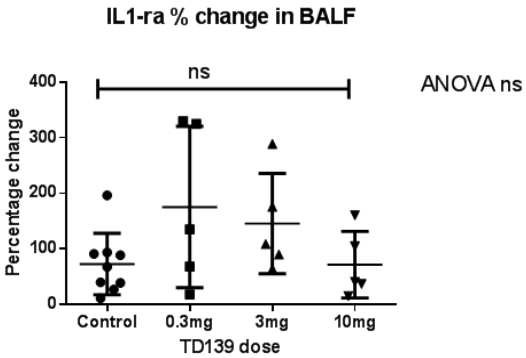
IL1-ra % change in BALF
ns
ANOVA ns
Percentage change
400
300
200
100
0
Control
0.3mg
3mg
10mg
TD139 dose

In plasma, ANOVA statistics demonstrated a significant difference in percentage change of PDGF-BB and PAI levels between control and TD139 groups, between day 1 and day 14 BALs (P=0.034 and P=0.028 respectively). Significant difference in percentage change of eotaxin (P=0.046), CHI3-L1 (P=0.012), MMP8 (P=0.029), HGF (P=0.019), galectin 3 (P=0.049), PDGF-BB (P=0.019) and PAI (P=0.029) plasma levels were noted between control and Td139 dose groups. There were no significant differences in percentage change of pentraxin 3, MCP1, IP10, IL8, TNFα, galectin 1, periostin, SP-D, TIMP1, MMP1, MIF, IL-1 ra, osteopontin, PDGF-AA, CCL18, rantes or MMP7 plasma levels between the groups, as determined by ANOVA. This data is demonstrated in Figure 65 below.

Figure 65. Percentage change in plasma proteins of interest between day 1 and day 14 BALs in TD139 and control groups, measured by Luminex Magnestic Screening Assay.

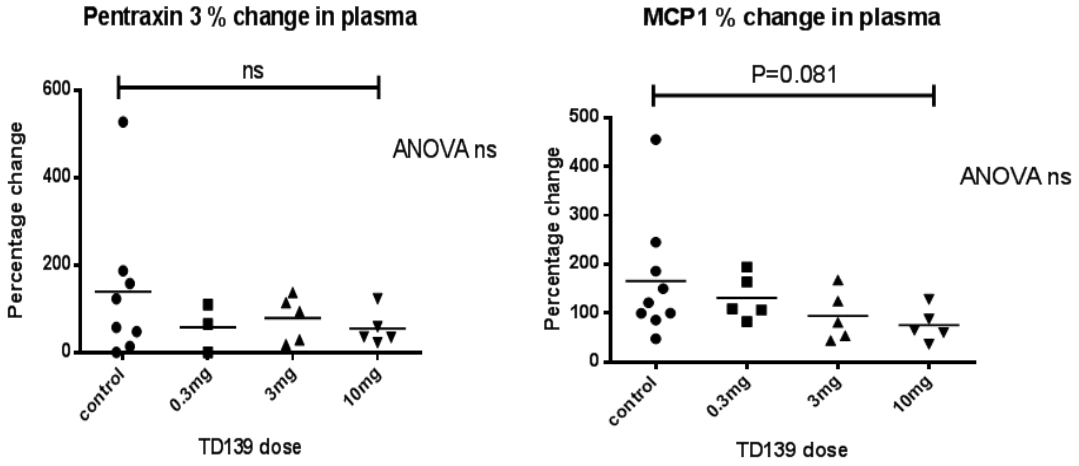

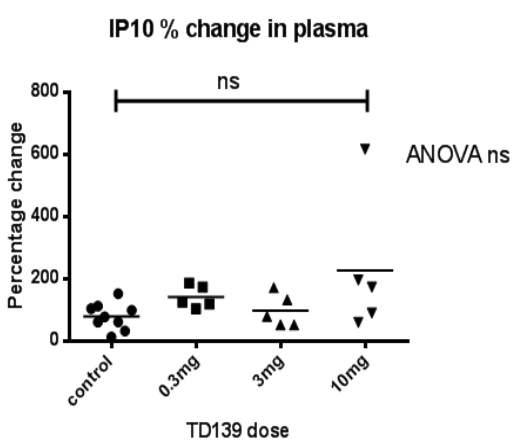
IP10 % change in plasma
ns
ANOVA ns
Percentage change
800
600
400
200
0
control
0.3mg
3mg
10mg
TD139 dose

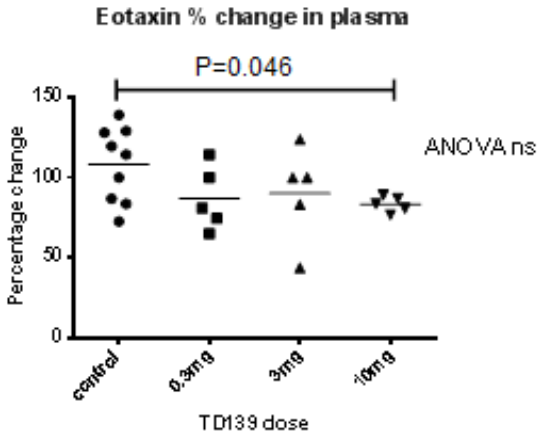
Eotaxin % change in plasma
P=0.046
ANOVA ns
Percentage change
150
100
50
0
control
0.3mg
3mg
10mg
TD139 dose

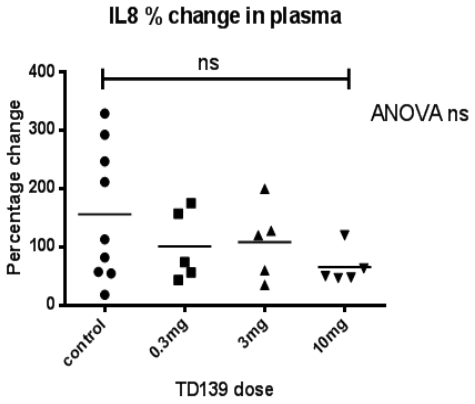
IL8 % change in plasma
ns
ANOVA ns
Percentage change
400
300
200
100
0
control
0.3mg
3mg
10mg
TD139 dose

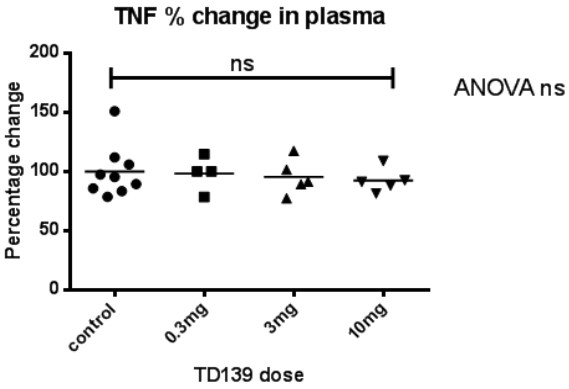
TNF % change in plasma
ns
ANOVA ns
Percentage change
200
150
100
50
0
control
0.3mg
3mg
10mg
TD139 dose

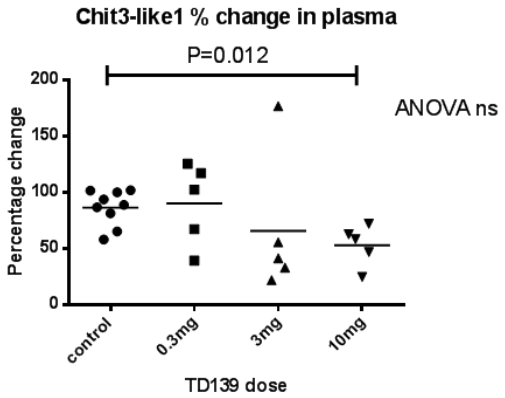
Chit3-like1 % change in plasma
P=0.012
ANOVA ns
Percentage change
200
150
100
50
0
control
0.3mg
3mg
10mg
TD139 dose

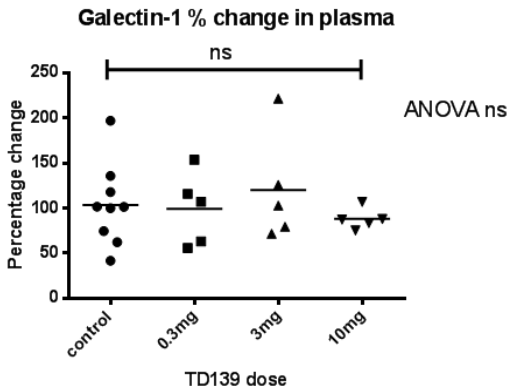
Galectin-1 % change in plasma
ns
ANOVA ns
Percentage change
250
200
150
100
50
0
control
0.3mg
3mg
10mg
TD139 dose

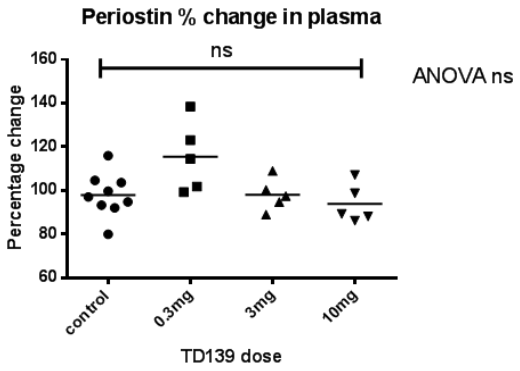
Periostin % change in plasma
ns
ANOVA ns
Percentage change
160
140
120
100
80
60
control
0.3mg
3mg
10mg
TD139 dose

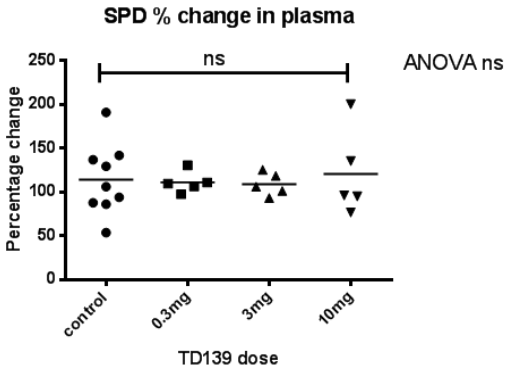
SPD % change in plasma
ns
ANOVA ns
Percentage change
250
200
150
100
50
0
control
0.3mg
3mg
10mg
TD139 dose

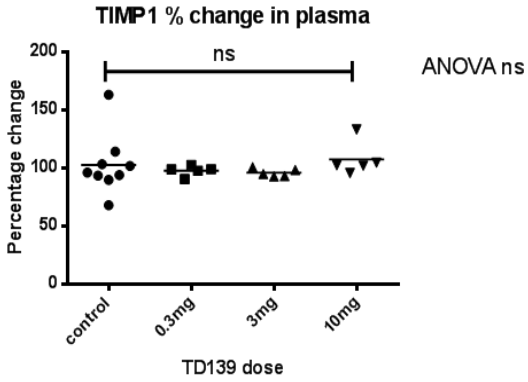
TIMP1 % change in plasma
ns
ANOVA ns
Percentage change
200
150
100
50
0
control
0.3mg
3mg
10mg
TD139 dose

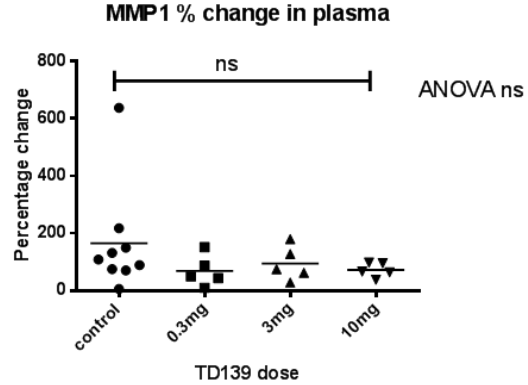
MMP1 % change in plasma
ns
ANOVA ns
Percentage change
800
600
400
200
0
control
0.3mg
3mg
10mg
TD139 dose

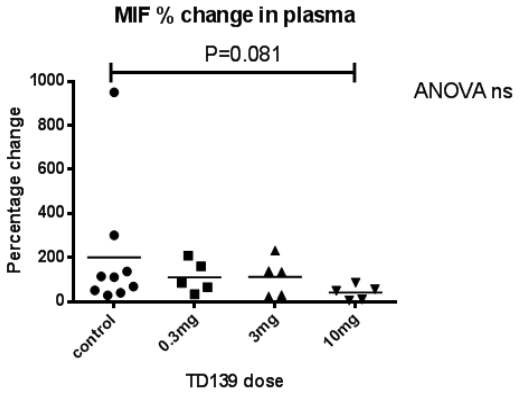
MIF % change in plasma
P=0.081
ANOVA ns
Percentage change
1000
800
600
400
200
0
control
0.3mg
3mg
10mg
TD139 dose

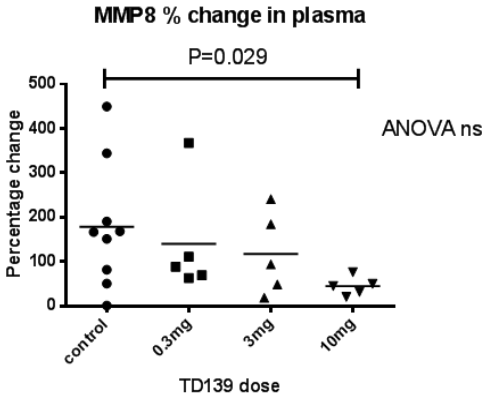
MMP8 % change in plasma
P=0.029
ANOVA ns
Percentage change
500
400
300
200
100
0
control
0.3mg
3mg
10mg
TD139 dose

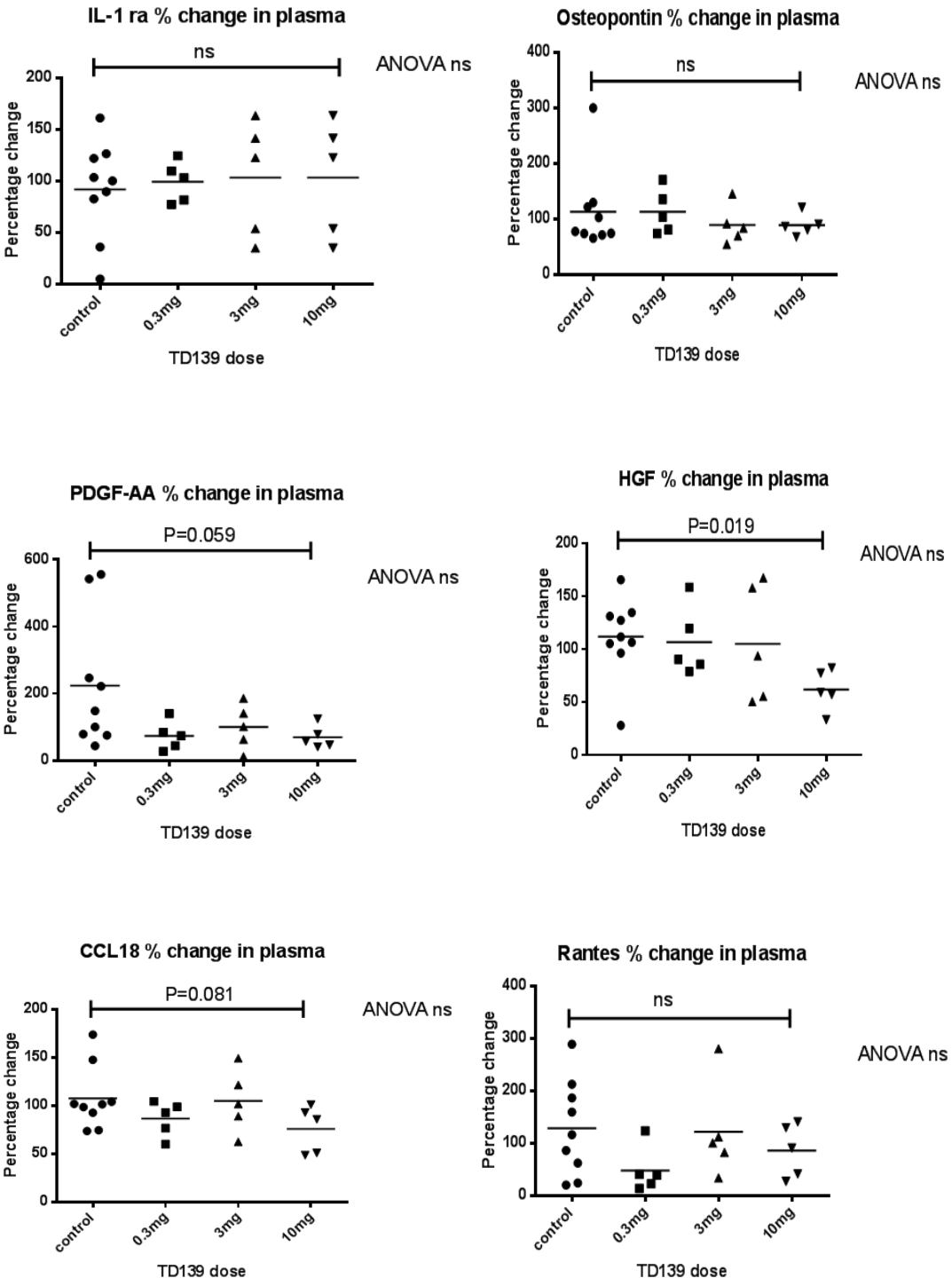
IL-1 ra % change in plasma
ns
ANOVA ns
Percentage change
200
150
100
50
0
control
0.3mg
3mg
10mg
TD139 dose
Osteopontin % change in plasma
ns
ANOVA ns
Percentage change
400
300
200
100
0
control
0.3mg
3mg
10mg
TD139 dose
PDGF-AA % change in plasma
P=0.059
ANOVA ns
Percentage change
600
400
200
0
control
0.3mg
3mg
10mg
TD139 dose
HGF % change in plasma
P=0.019
ANOVA ns
Percentage change
200
150
100
50
0
control
0.3mg
3mg
10mg
TD139 dose
CCL18 % change in plasma
P=0.081
ANOVA ns
Percentage change
200
150
100
50
0
control
0.3mg
3mg
10mg
TD139 dose
Rantes % change in plasma
ns
ANOVA ns
Percentage change
400
300
200
100
0
control
0.3mg
3mg
10mg
TD139 dose

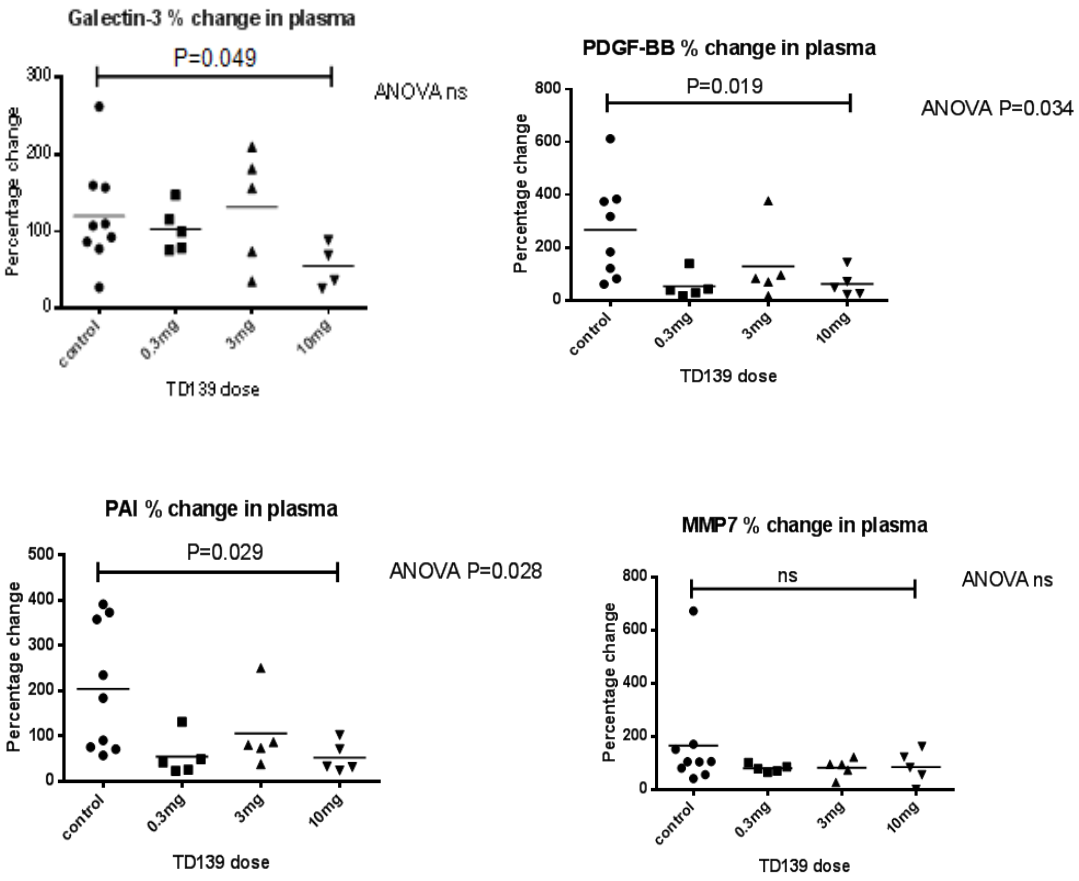

When qPCR was used to quantify gene expression of galectin 3, CCL18, CD163, CD206, IL10, CD80 and TGFβ, the percentage change of galectin 3 expression was significantly different between the control and 10mg TD139 dose group (P=0.0001). ANOVA statistics showed significant differences between control, 0.3mg, 3mg and 10mg TD139 dose groups (P=0.004). There was also a significant increase in percentage change of CD163 expression between the control and 0.3mg TD139 dose group (P=0.019), however ANOVA did not reveal and significant change between the groups as a whole (P=0.098). There were no significant differences in percentage change of expression of CCL18, CD206, IL10, CD80 or TGFβ between groups. When the 0.3mg, 3mg and 10mg TD139 dose groups were pooled into a 'TD139 group' versus 'controls', there were no significant percentage changes in expression of galectin 3, CCL18, CD163, CD206, IL10, CD80 or TGFβ when measured by qPCR. These data are shown in Figure 66 below.

Figure 66. Percentage change in galectin 3, CCL18, CD163, CD206, IL10, CD80 and TGF- expression between day 1 and day 14 BALs in TD139 and control groups, measured by qPCR.

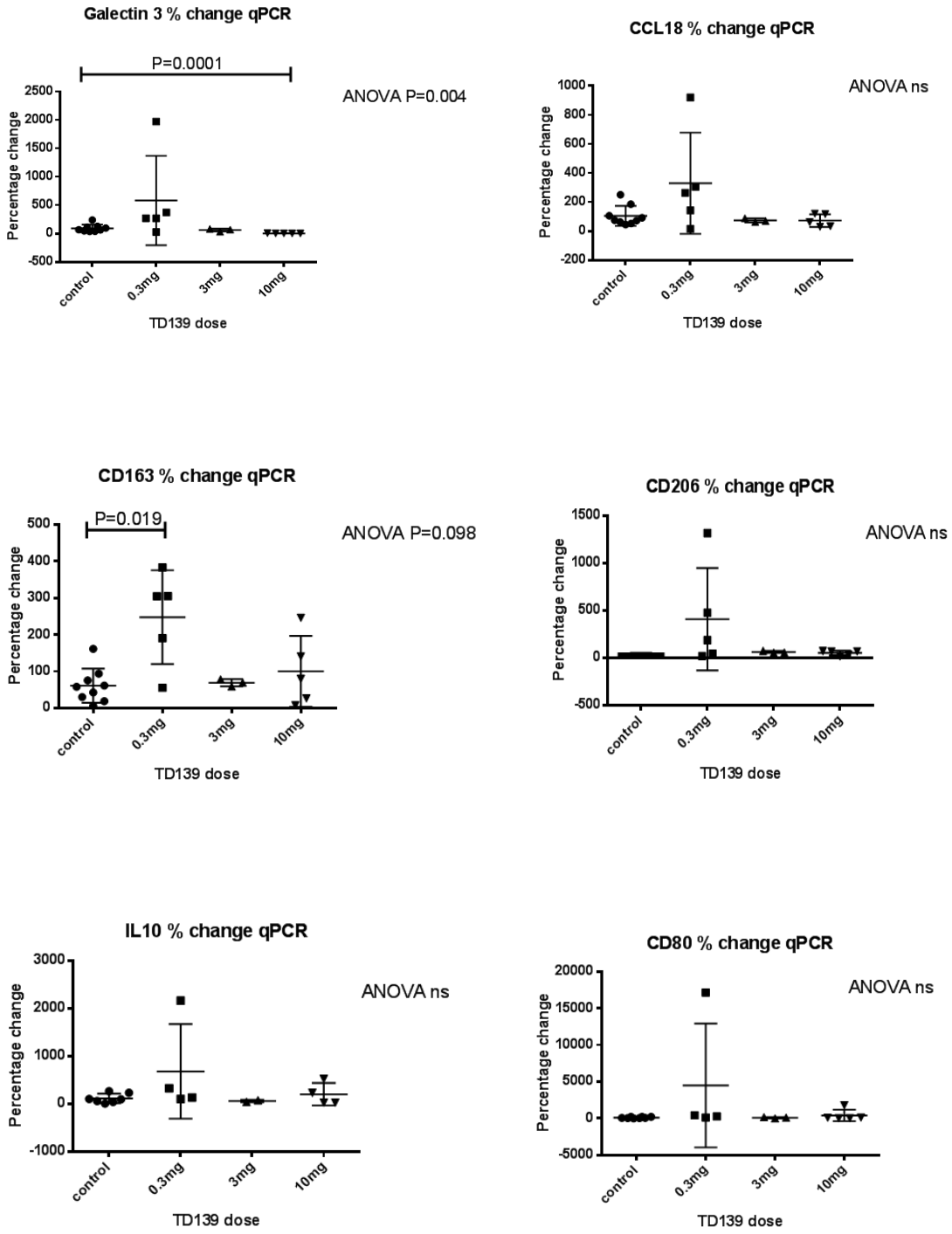

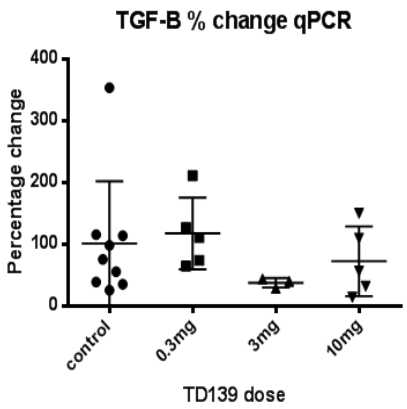
TGF-B % change qPCR
Percentage change
400
300
200
100
0
control
0.3mg
3mg
10mg
TD139 dose

ANOVA ns

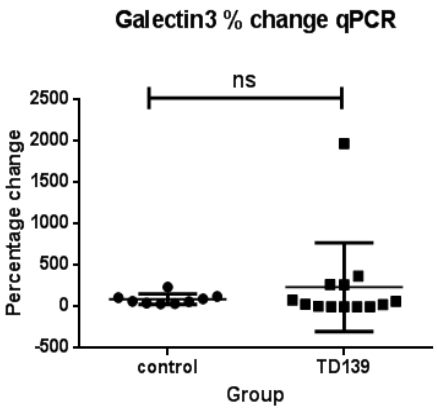
Galectin3 % change qPCR
ns
Percentage change
2500
2000
1500
1000
500
0
-500
control
TD139
Group

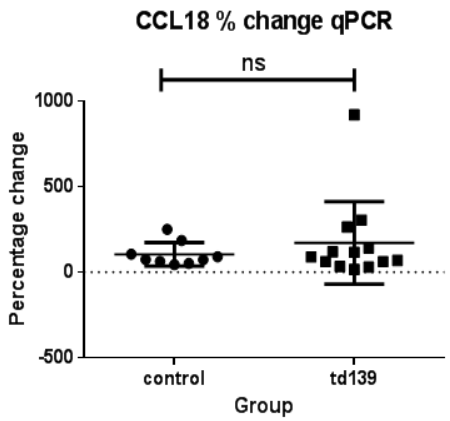
CCL18 % change qPCR
ns
Percentage change
1000
500
0
-500
control
td139
Group

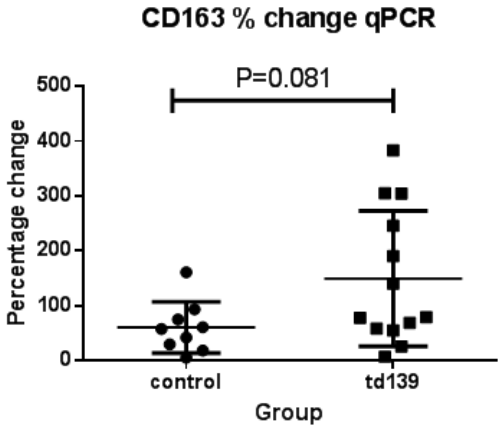
CD163 % change qPCR
P=0.081
Percentage change
500
400
300
200
100
0
control
td139
Group

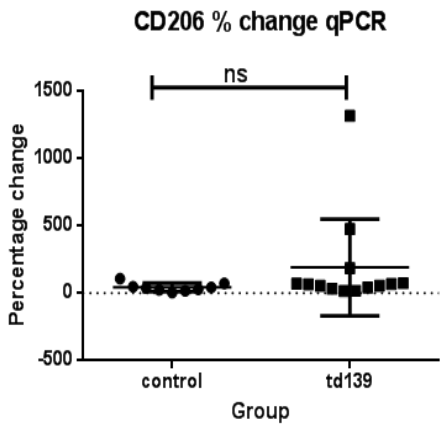
CD206 % change qPCR
ns
Percentage change
1500
1000
500
0
-500
control
td139
Group

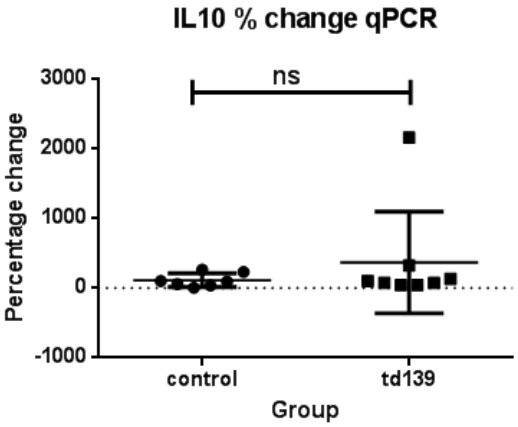
IL10 % change qPCR
ns
Percentage change
3000
2000
1000
0
-1000
control
td139
Group

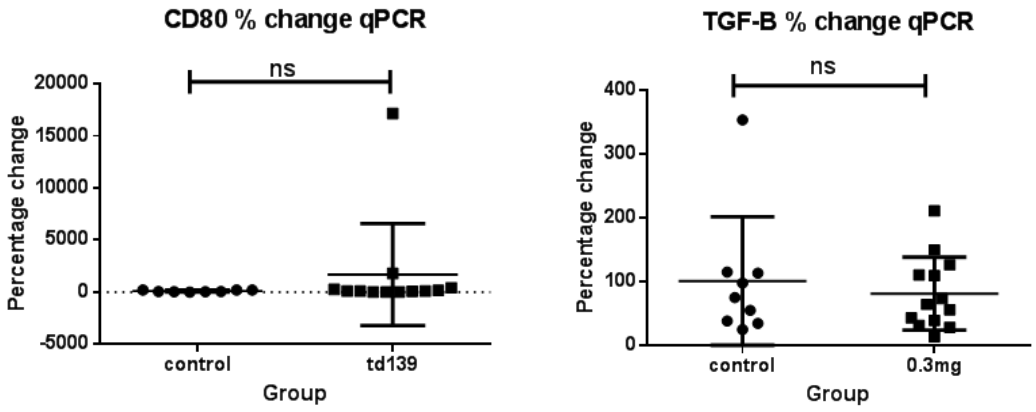

5.3 Discussion

Whilst obtaining a timely and confident diagnosis of IPF remains paramount in managing patients with suspected ILD, there remains a large unmet clinical need for accurate and validated prediction models to identify the subset of patients (around 15%) that will progress rapidly with worsening respiratory function and death within a year of presentation. The pathogenesis of IPF is a complex and multi-faceted process, and it remains poorly understood. It is clear that no single protein biomarker will have the ability to confidently predict disease progression with high sensitivity, specificity, PPV and NPV values in IPF, however perhaps in combination with clinical, physiological and radiological parameters, risk stratification for progression could be improved.

It was previously thought that IPF was a result of generalised inflammation followed by widespread parenchymal fibrosis, however this theory came into question after a number of clinical trials investigating the effect of anti-inflammatory drugs and immune modulators on the natural course of the disease revealed a minimal effect only. The current theory is that IPF results after an unknown endogenous or environmental stimulus (for example smoke, environmental pollutants, dust, viral infections, gastro-oesophageal reflux disease, chronic aspiration) disrupts the homeostasis of alveolar epithelial cells, which leads to diffuse epithelial cell activation and aberrant epithelial cell repair[125]. Following injury, aberrant activation of alveolar epithelial cells drives the migration, proliferation and activation of mesenchymal cells, which leads to the formation of fibroblastic/ myofibroblastic foci and exaggerated accumulation of

extracellular matrix[126]. It has been reported that activated alveolar epithelial cells secrete a number of potent fibrogenic cytokines and growth factors including TNF-α, TGF-β, PDGF, IGF-1 and ET-1[126–128]. These cytokines and growth factors are involved in the migration and proliferation of two of the key effector cells in fibrogenesis; fibroblasts, which transform into myofibroblasts, and myofibroblasts, which release a number of extracellular matrix proteins[126,129]. This in turn leads to tissue remodelling and irreversible destruction of the normal architecture of the lung parenchyma.

It has been well documented that myofibroblasts must undergo apoptosis for normal wound healing to occur. Harari et al reported that production of TGF-β promotes an anti-apoptotic phenotype in fibroblasts contributing to the pathogenesis of IPF[126]. Failure of apoptosis results in the accumulation of myofibroblasts, which then leads to increased extracellular matrix production, persistent tissue contraction and formation of scar tissue[126]. It has been shown that myofibroblasts in areas of fibroblastic foci in IPF undergo less apoptotic activity than the myofibroblasts in fibromyxoid lesions of bronchiolitis obliterans, therefore supporting this theory[130].

There have been a number of attempts to risk stratify patients with IPF using a combination of clinical variables including history and examination findings, pulmonary function testing, exercise capacity, radiological appearances and histological features, however these variables are poorly reflective of disease pathogenesis and can only be of use when patients are grouped into large cohorts and put into scoring systems, not for estimating individual patient risk in a clinical setting. It is well documented that IPF is a heterogeneous disease, and there is a definite need to identify 'personalised' prognostic biomarkers which may in turn lead to novel targets and the advent of personalised medicines. I applied a number of prognostic scoring systems to the Edinburgh IPF cohort with variable results. I have already shown that phenotypically, there was no apparent difference between patients with 'definite' and 'possible' UIP and so both cohorts were grouped together for the application of risk stratification scoring models. The du Bois score was found to be accurate in predicting 1 year mortality in both 'definite', 'possible' and 'all' IPF groups, however the margins for predicted mortality were very broad. The score has also never been formally validated.

Ley et al developed the GAP model in 2012. It's simple nature has allowed the GAP index to be widely studied and it is the only scoring system of it's kind to have been validated around the world from centres in USA, Italy and South Korea[38,131,132]. The GAP score is perhaps the most well known scoring system in IPF and is the simplest to calculate. The four variables included in the model (gender, age, percentage predicted FVC, percentage predicted DLCO) are commonly measured at the initial visit and are easily followed up. In a study of 268 South Korean patients with IPF, Kim at al showed the GAP model predicted 1-year mortality well and that the differences between the predicted and observed mortality were not significant. However they found that 2- and 3-year mortality were not predicted accurately, and there were significant differences between the predicted and observed risk. They also found that by multivariate analysis, mortality correlated independently with sex, age, lower FVC and lower DLCO, the same variables included in the GAP model[132]. Lee and colleagues reported the relation between the GAP score (0-7) and the GAP stage (I-III) in 1228 IPF patients. They found that all GAP variables showed significant association with prognosis except gender. They found that advanced GAP stage was associated with poor prognosis, and that higher GAP scores were significantly associated with male gender, aging and poor lung function, in parallel with the original GAP model definition[131]. The GAP score is not validated in 'possible UIP', however when the GAP score was applied to the Edinburgh 'definite' and 'possible' UIP cohorts separately, predictions for 1-, 2- and 3- year mortality were only moderately accurate. When the cohorts were combined as an 'all IPF' cohort, the accuracy of the predicted mortality to the observed mortality was much improved. The differences in survival between patients with a low, medium and high GAP score were significantly different in all 3 cohorts.

Numerous studies have attempted to identify diagnostic and predictive biomarkers in IPF, however because of it's variable and unpredictable course, and the lack of easily reproducible relevant patient outcomes, clinical research in IPF remains challenging. Multiple single centre studies report upregulation of various proteins in IPF, however until recently, these studies were limited in size and lacked validation. There has been increasing evidence of late, that when taken together changes in blood proteins (for example KL-6, SP-A, MMP-7, CCL-18) or cells (fibrocytes and T-cell subpopulations) can be of value in diagnosis and prognostication.

Biomarkers can be divided into diagnostic, prognostic, disease activity and treatment efficacy biomarkers, depending on the information that they provide. There have been multiple reports in recent years of peripheral blood molecular biomarkers able to differentiate patients with IPF from controls. These included KL-6, surfactant proteins SP-A and SP-D, matrix metalloproteases MMP-1 and MMP-7, YKL-40 (CHI3-L1)[61]. Unfortunately many of these studies did not include smoking controls, or other ILDs, and when replication cohorts were performed, these patients also had increased levels of the marker[61]. A study by Rosas and colleagues used targeted proteomics to develop a protein signature that included MMP-1, MMP-7, MMP-8, IGFBP-1 and TNFRSA1F and distinguished patients with IPF from controls with a sensitivity of 98.6% and a specificity of 98.1%[60]. They compared MMP-1 and MMP-7 protein levels in plasma of both IPF vs controls and in IPF vs COPD, sarcoidosis and hypersensitivity pneumonitis. They found that MMP-1 and MMP-7 levels were significantly higher in IPF patients and could detect IPF from HP with a sensitivity of 96.3% and a specificity of 87.2%[60]. They went on to perform a validation cohort which confirmed MMP-7 levels were significantly increased in patients with IPF vs controls, but were also significantly increased in patients with subclinical ILD vs controls, therefore suggesting it could be used as a potential biomarker for early detection. MMP-1 and MMP-7 levels were significantly elevated in both plasma and BAL fluid of patients with IPF versus control individuals[60,61].

Recent trials have supported peripheral blood biomarkers as important adjuvants in predicting disease progression in IPF at presentation. Multiple study groups have reported a number of different protein biomarkers with variable results. KL-6 (also known as MUC-1) is a mucinous high-molecular weight glycoprotein, expressed on type 2 pneumonocytes. It has been reported to be elevated in both serum and bronchoalveolar lavage fluid of patients with interstitial pneumonia, and high blood concentrations of KL-6 have repeatedly been shown to be predictive of decreased survival in IPF. The majority of these studies were of small cohort size, and were not replicated in validation cohorts, however the studies were undoubtedly consistent and therefore KL-6 is considered a potential marker in disease stratification[61]. Additional studies of note include the work by Prasse et al, who showed that serum CCL18 levels were able to predict lung function and survival outcomes in a prospectively collected

cohort of 72 patients with IPF[58,61]. Kinder et al reported serum SP-A was a predictor of early mortality in a study of 81 IPF patients[43,61] and Korthagen and colleagues showed that high serum levels of YKL-40 (an inflammatory glycoprotein otherwise known as CHI3-L1) could differentiate between two distinct groups with significantly different survival (HR for serum YKL-40 (cut-off 79ng/ml) as 10.9 (95% CI 1.9–63.8, $P < 0.01$) in a cohort of 79 IPF patients[61,65].

In my study, BAL fluid levels of CHI3-L1, CCL-18 and MCP were significantly higher in IPF patients versus controls, which is consistent with current literature. Galectin-3 levels were significantly increased in IPF progressors versus non-progressors, and CCL-18 levels were higher in progressors, however this did not reach significance. VEGF is a signal protein involved in angiogenesis, I found levels were significantly reduced in patients with IPF versus controls, and were lower in IPF progressor versus non-progressor patients, however this did not reach significance. This result is consistent with a study by Murray et al examining the association of VEGF with the IPF disease state and preclinical pathogenesis. They reported that tissue and circulating levels of VEGF were significantly reduced in IPF patients, particularly in those with a rapidly progressive phenotype, when compared with healthy controls. In addition, they showed that lung-specific overexpression of VEGF significantly protected mice following intratracheal bleomycin, with a decrease in fibrosis and bleomycin-induced cell death in VEGF transgenic mice, suggesting beneficial roles for VEGF during lung fibrosis by modulation of epithelial homeostasis via the endothelium[133].

My study was also consistent with a number of studies describing serum proteins of interest in IPF in the current literature. In my study, serum concentrations of MMP-1, periostin, osteopontin, SP-D, IP-10, MCP-1, IL-8 and CCL-18 were all significantly increased in patients with IPF versus controls. This is in keeping with current literature[46]. Periostin, SP-D, GRO-alpha (otherwise known as CXCL-1), EGF, IFNγ, galectin-1, amphiregulin, osteopontin and HGF levels were all significantly higher in IPF progressors versus non-progressors. CHI3-L1 levels were higher in both IPF patients vs controls and in IPF progressors vs non-progressors. IL-8 levels were also increased in IPF progressors vs non-progressors, however this did not reach significance. This data is in keeping with recent studies reporting GRO-alpha, periostin and SP-D expression in IPF. Antoniou et al showed both serum and BAL levels of

GRO-alpha were significantly increased in patients with IPF versus healthy subjects[134]. Okamoto et al identified periostin in the lungs of Japanese patients with IPF and showed that serum periostin levels were higher in IPF patients than in controls[135,136]. It was then reported by Uchida et al that bleomycin injury caused increased periostin expression, and that periostin-deficient mice were protected from bleomycin-induced lung fibrosis[135,137]. More recently Naik and colleagues confirmed an excess of periostin in the lungs of IPF patients, and showed that periostin was produced by IPF fibroblasts. They also found that blood periostin levels were predictive of clinical progression at 48 weeks (HR 1.47, 95% CI 1.03-2.10, $P<0.05$)[135]. A systematic review and meta-analysis by Wang et al investigating the impact of SP-D levels on prognosis in IPF found that serum SP-D levels were significantly increased in patients with IPF compared to both patients with pulmonary infections and healthy controls. Furthermore there was a significant association between higher SP-D levels and increased risk of death, without heterogeneity (HR: 2.11, 95% CI 1.60 - 2.78, $P<0.001$)[138].

In my prediction model for disease progression in IPF, I aimed to identify a unique protein signature that could be used in combination with clinical parameters to predict patients likely to progress rapidly. In light of the vast heterogeneity in IPF, it is clear that no single biomarker would be adequately sensitive and specific for this when used alone. I set targets of sensitivity greater than 60% and specificity greater than 80% for my model as these values would be deemed sufficient for use in clinical practice. In my study I described a prediction model combining clinical, physiological and biological variables, and found that accuracy in predicting disease progression was highest when these parameters were used in combination. Initially I combined a number of serum protein biomarkers and found that by selecting out the top three proteins that were predictive of disease progression in the model, and by setting cut off values for each, combining serum SP-D, GRO-alpha and RANTES (CCL-5) concentrations could predict rapid progression at a sensitivity of 96%, specificity of 80%, PPV 81% and NPV 95%. Another combination of SP-D, GRO-alpha and IL-8 levels predicted disease progression at a sensitivity of 91%, specificity 80%, PPV 81% and NPV 91%. Additional clinical and radiological variables identified by the model as being significantly associated with disease progression were the volume of fibrosis on HRCT (%), percentage of lung periphery involved on HRCT and percentage of predicted FVC at baseline. The model identified the best two variables as percentage of predicted FVC

and serum SP-D level, and when these two variables alone were entered into the model, disease progression in IPF could be predicted at a sensitivity of 86.4%, specificity of 92.3%, PPV 90.5% and NPV 88.9%. Richards et al applied targeted proteomics to screen plasma for 95 different proteins of interest in a derivation cohort of 140 IPF patients, and then a validation cohort of 101 IPF patients with replicable results. They found that high plasma concentrations of MMP-7, ICAM-1 and IL-8 were predictive of poor overall survival in both cohorts[45,61]. This group then went on to describe a personal clinical and molecular mortality prediction index (PCMI) model incorporating sex, percent predicted FVC, percent predicted DLCO and plasma MMP-7 level that was highly predictive of early mortality with a C-index of 84[61]. This data is supportive of my own findings that the use of molecular markers can improve upon clinical prediction models in IPF.

In order for a molecular biomarker to seem plausible, it would ideally reflect the pathobiological mechanism driving disease progression in IPF, and have been studied first in animal models. Studies would ideally show a significantly different protein signature in IPF patients versus healthy controls and in IPF progressor patients versus non-progressor patients. This would ideally be followed by significant increases or decreases in the concentrations of proteins of interest in patients over a 12 month period. In my study, BAL fluid obtained at presentation (0 months) and then at 12 months revealed significantly increased amphiregulin and PDGF-AA concentrations at 12 months in the IPF progressor group. Between 0 and 12 month BALs there was a significant increase in MMP-8 in the progressor group and a significant decrease in amphiregulin in the non-progressor group. To my knowledge, there are no other studies that have investigated changes in the IPF proteome in BAL fluid with BAL at presentation (0 months) and then a repeat BAL at 12 months. In addition, in serum profiling, SP-D and galectin-1 were significantly higher at baseline in progressor versus non-progressor patients, and there was a significant increase in serum SP-D and galectin-1 levels between serum samples obtained at 0 (presentation) and at 12 months.

Little is known about the exact role of amphiregulin in the pathogenesis of pulmonary fibrosis however dysregulated amphiregulin expression and EGFR activation have been described in animal models of pulmonary fibrosis. Zhou et al showed that TGF-β1 significantly induced the expression of amphiregulin in lung fibroblasts in vitro and in

murine lungs in vivo[139]. Amphiregulin has been shown before in mouse models that it is an essential factor for the development of inflammation-induced fibrotic diseases. It has also been shown that amphiregulin is strongly elevated specifically in IPF patients, but not in patients of other lung diseases. A number of studies have reported the association between PDGF and TGF-β in the development of organ fibrosis[140]. Myofibroblasts (or activated mesenchymal cells) cause excessive deposition of extracellular matrix which in turn leads to fibrosis. PDGF is involved in the expansion of myofibroblasts by driving their proliferation, migration and survival. Trojanowska reported PDGF levels are elevated in the fibrotic lesions of various organs. PDGF-A is produced by myofibroblasts and PDGF-B by alveolar macrophages in pulmonary fibrosis[140]. MMP-8 is expressed by polymorphonuclear cells, activated monocytes, macrophages, lymphocytes, lung epithelial cells, fibroblasts, fibrocytes, dendritic cells and NK cells[141]. MMP-8 is regulated by TGFβ and TNFα in fibroblasts and IL-1 and CD40 ligand in mononuclear phagocytes[141]. Plasma MMP-8 levels have been reported as being increased in patients with IPF, however plasma and BALF levels do not appear to correlate with decline in lung function or mortality[141]. García-Prieto et al showed that MMP-8 knock out mice were protected from bleomycin-mediated pulmonary fibrosis[141,142], but had increased accumulation of macrophages in the lung during the acute inflammatory phase. MMP-8 may be involved in the pathogenesis of pulmonary fibrosis by upregulating fibrocyte migration into the lung, leading to increased fibroproliferative response to injury[141].

Galectin-3 is a member of the galectin family of galactoside binding lectins. It exists both intra- and extracellularly and binds to glycosylated proteins. Previous studies have demonstrated that galectin-3 plays a central role in the development and progression of liver, kidney and lung fibrosis[143]. Organ fibrosis occurs due to the activation of macrophages and the recruitment and activation of myofibroblasts, galectin-3 drives both of these pathways. TGFβ has been shown to play a key role in pulmonary fibrosis by inducing EMT, ECM production and apoptosis of AECs. It has also been shown that pulmonary fibrosis can be reduced by inhibiting TGFβ activity[143]. TD139 is a specific inhibitor of the galactoside binding pocket of galectin-3. It was developed by a team of scientists from Lund University, Sweden, and Edinburgh University, UK, and is formulated for inhalation, which enables direct targeting the fibrotic tissue in the lungs,

while minimizing systemic exposure. MacKinnon and colleagues previously showed that TD139 blocked TGF-β-induced β-catenin activation in vitro and in vivo and attenuated the late-stage progression of lung fibrosis after bleomycin. In addition, they found that patients with stable IPF had elevated levels of galectin-3 in BAL fluid and in serum when compared with patients with NSIP and controls. They also found that galectin-3 levels rose sharply during an acute exacerbation of IPF, and therefore suggested that galectin-3 may be a marker of active fibrosis in IPF[62,143]. The Galecto trial was a randomised, double-blind, multicenter, placebo-controlled, phase IIa study, designed to assess the safety, tolerability, PK and PD characteristics of TD139 in 24 IPF patients. I was able to perform flow cytometry and Luminex Magnestic Screening Assays on BAL and plasma samples to assess whether there were any notable differences in a number of proteins of interest linked to IPF-pathogenesis, after patients were treated with an inhaled galectin-3 inhibitor for a two week period. The results of the PK/PD studies are outwith the remit of this thesis and have been presented previously. In my study, I found TD139 was both safe and well tolerated in IPF patients. In addition, suppression of galectin-3 was replicated by FACS analysis in AMs, and by measuring galectin-3 levels in BAL fluid by Luminex Magnetic Screening Assay. A number of proteins of interest were significantly different between control and 0.3mg, 3mg and 10mg TD139 dose groups in both BAL fluid (galectin-3, MMP1, galectin-1, gro-alpha) and in plasma (eotaxin, CHI3-L1, MMP8, HGF, galectin-3, PDGF-BB, PAI). There were also significant differences in markers of macrophage activation (CD163) between the groups. This is supportive of previous studies demonstrating galectin-3 plays an important role in IPF pathogenesis and has downstream actions on a number of mediators and cytokines involved in the development of IPF. Inhibition of galectin-3 may have the potential to reduce pulmonary fibrosis in man and following the results of this trial, a phase IIb trial is currently in development.

Limitations of the study

Our study has a number of limitations. Whilst our cohort of IPF patients was prospectively recruited as consecutive incident cases, the analyses were performed retrospectively. Many of the BAL and serum samples used for biomarker profiling were over 5 years old, and had been frozen at 80C in storage since sample processing. It is

uncertain how much degradation of protein and material occurs over time when samples are stored for such prolonged periods. Again a number of these samples will also have undergone a number of freeze/thaw cycles, which will also undoubtedly lead to loss of material and degradation of the sample. I attempted to limit the number of freeze/thaw cycles of samples to once or twice, but the samples were shared with a number of other PhD students in the laboratory, and so a few of the samples may have been frozen/thawed more than this. Another limitation was the Luminex Magnetic Screening Assays themselves. In serum, the manufacturer (R&D) recommended diluting serum samples to a 1:2 or 1:50 dilution. The majority of the analytes fell between the top and bottom values of the standard curve when utilised at the correct dilution. Samples outwith 10% of either the top or bottom reading were deemed outliers and were excluded from analysis. In BAL, it was more difficult to adjust for the total protein in each BAL sample. Test plates were performed with the BAL fluid volume containing 5 and 10g of protein per well, and most analytes fell between the top and bottom values of the standard curve using 10g of protein, and so this was chosen going forward, however a number of samples and anaytes fell off the standard curve and so had to be excluded from analysis. If I had not been limited by time, I would have gone on to perform ELISAs on each of the low or high level expression analytes to obtain more individualised and accurate results. Another important limitation of the study is that almost a quarter (22%) of lavaged patients died or were deemed to frail to undergo a repeat procedure at 12 months, and so the truly progressive subpopulation may have been missed. This was slightly less of a problem in serum sampling as most patients managed to attend to have serum samples taken, despite clear evidence of progression with a >10% decline in VC on lung function testing. Our laboratory routinely records VC rather than FVC. In patients with restrictive lung disease, it is reasonable to assume that these two measures will be similar. Lastly, the prediction model for IPF progression has not yet been tested in a validation cohort of patient. Work to undertake this is currently ongoing, but unfortunately due to time limitations, the results could not be included in this thesis.

5.4 Conclusions

Although the aetiology of IPF remains unknown and the pathogenesis poorly understood, recent advances defining clinical and pathological features of IPF have led to a better understanding of the molecular pathways that are abnormally activated in the disease. There is no animal model that reliably replicates the pathobiological changes seen in IPF. The most commonly used model in the study of the molecular pathways of pulmonary fibrosis is the bleomycin model of lung injury, however pathological changes seen in this model do not mirror those seen in IPF. In the bleomycin model, the fibrosis develops over a number of months, and is patchy and usually bronchocentric, whereas in IPF fibrosis occurs over a number of years, and has subpleual dominance and areas of fibroblastic foci[144]. The bleomycin lung fibrosis model has been used to identify mediators that have potential to cause lung fibrosis and to describe specific molecular mechanisms in the pathogenesis of fibrosis. However any findings in mice must be confirmed in translational studies in humans with fibrotic lung disease prior to any consideration in clinical practice[144].

Clinicians face multiple challenges in the management of IPF. Obtaining an accurate and timely diagnosis remains fundamental, however there are a distinct lack of clinical and molecular indicators of disease progression that can be readily measured in clinical practice. With the recent approval of two new drug treatments for IPF, there is also an absence of simple short-term measures of therapeutic response, both in terms of response to these new drugs, and in the context of clinical trials. The median survival remains very poor at 3-5 years, however the disease is hugely heterogeneic with disease courses ranging from slowly evolving disease over a decade, to rapid deterioration and death within 12 months[145].

The clinical variables available to predict the risk of mortality and disease progression in IPF are currently inadequate. Additional non-invasive and reproducible markers are required to improve existing risk model templates. In recent years large numbers of BAL and peripheral blood proteins and cytokines have been studied as potential biomarkers of disease progression in IPF. Biomarkers may have many different applications including predisposition to disease, diagnostic, prognostic, prediction of

response to treatment and acting as a surrogate endpoint in clinical trials, however their main function is to meet an unmet clinical need. Good biomarkers should have high sensitivity/specificity, be cost effective, non-invasive, easily reproducible and widely available[20]. There has been a wealth of evidence from centres around the world detailing numerous potential biomarkers and proteins of interest predictive of disease progression in IPF in recent years, however many of these studies reported small sample size, lacked the appropriate adjustments for confounding factors such as age, smoking status, sex and significant co-morbidity, and lacked the appropriate replication and validation required for consideration in clinical practice.

Meta-analysis of the most commonly described potential biomarkers has shown that there is a clear distinction between the peripheral blood protein signature in patients with IPF compared to healthy control individuals. The distinction however is less clear cut when patients with IPF are compared to patients with other chronic lung diseases such as COPD, sarcoidosis and the other IIPs. A possible strategy for overcoming this disparity could be to utilise datasets such as the Lung Genomics Resource Consortium (LGRC), which contains patient demographic data and analysis of multiple chronic lung diseases and well as smoking and non-smoking controls, which could allow investigators to detect potential novel biomarkers that are disease specific[20,144].

In summary, the recently described outcome prediction models based on peripheral blood appear to hold significant promise in risk stratification in IPF. It has been demonstrated by multiple studies that the most accurate of models incorporate a combination of clinical, physiological and biological parameters, rather that utilising one single biomarker alone. A small number or recent studies, including my own, report prediction models and unique protein signatures in well- phenotyped cohorts of IPF patients, and show replicable results in both test and validation cohorts. This shows that integration of both clinical and molecular variables in predicting risk of progression in IPF is feasible, and could be performed in routine clinical practice. These findings may provide a basis for future investigation on predicting outcomes and personalised treatment in this heterogeneous disease.

Chapter 6

General Discussion and Conclusions

The term interstitial lung disease is used to describe a group of over 200 different diseases affecting the lung, all of which display marked variability in clinical course, treatment and prognosis. Clinicians strive to differentiate patients with an identifiable cause such as connective tissue disease, environmental triggers, drugs, allergens and occupational exposures, from those without, termed the idiopathic interstitial pneumonias. A limited number of disease patterns occur in the lung in response to injury, and so the ILDs are largely characterised by varying degrees of parenchymal inflammation and fibrosis, not only between the different disease groups, but also among patients with the same disease. The last decade has witnessed significant changes in the field of ILD with an increasing incidence and a more complex disease classification. Despite significant advances, progress has been limited by a poor understanding of the pathological mechanisms of disease. It is largely accepted that aberrant wound healing occurs in response to repetitive alveolar injury, which results in abnormal fibroblast proliferation, differentiation and activation, leading to expansion of extracellular matrix with excess collagen deposition and loss of normal lung architecture. In their most severe forms these diseases lead to progressive loss of lung function, respiratory failure and death, however there is significant patient heterogeneity and great variability in disease progression rates. Distinguishing the various forms of pulmonary fibrosis is fundamental in determining correct management and in predicting prognosis.

IPF is the commonest IIP with an incidence of approximately 5000 cases per year in the UK, and affecting mainly older male smokers. It is a chronic and progressive form of lung scarring with a median survival time worse than many cancers at 3-5 years, and no curative therapy. The current international consensus guideline recommends that around two thirds of IPF patients can be diagnosed on the basis of clinical and radiological (HRCT) appearances that are typical for UIP, however the remainder should undergo SLB to obtain a confident diagnosis. The gold standard is that all

patients must undergo MDT discussion and a diagnosis can only be reached after consideration of all clinical, radiological and histological parameters.

Obtaining a confident and timely diagnosis of IPF is important for many reasons. Unlike the CTD-ILDs, for example systemic sclerosis, IPF does not respond to immunosuppressive therapies such as cyclophosphamide and rituximab, in contrast there is evidence that immunomodulation may worsen outcomes[2,21]. There is also evidence that steroids, a treatment used for many of the mimics of IPF, is harmful when used in IPF patients. With the recent NICE approval of two drugs, pirfenidone and nintedanib, for IPF, diagnostic accuracy and phenotyping are important components both for facilitating early treatment in clinical practice, and in epidemiological study of the natural history of the disease. We found that change in VC from presentation to 6 months was predictive of mortality in both 'definite' and 'possible' IPF cohorts alike, and suggest clinicians may use clinical measures alongside a related prognostic IPF index (for example GAP Index) to make prognostic statements in both groups. Furthermore, among patients in whom SLB would be advised according to international guidelines, after adjusting for these IPF scores there was no difference in mortality among patients who did and did not have a biopsy, therefore potentially negating the need for an invasive procedure in this elderly population.

Despite international guidelines that patients have histological confirmation of a diagnosis of IPF, mortality between patients diagnosed by HRCT or by biopsy was similar, but 30-day mortality for the SLB group was 7.5%. Advanced age is a strong predictor of IPF and the majority of patients in our cohort aged over 65 years with 'possible UIP' HRCT appearances had UIP on biopsy. Notably there was no difference in mortality between patients diagnosed on HRCT or by SLB. The observation that around 20% of patients were deceased at 1 year, regardless of how the diagnosis was made is important. These patients are 'rapid progressors' and cannot be identified by HRCT or biopsy characteristics. Several prognostic scoring systems based on clinical, physiological, radiological and serological parameters have been reported in the literature to predict survival in IPF, however there is no single risk model that has been validated, accepted and adopted in clinical practice.

There is a limited number of observational studies describing the natural history and characteristics of patients with IPF outside of clinical trials. Most IPF studies have recruited younger patients with more preserved lung function than real world patients. Our data show the PANTHER and CAPACITY eligibility criteria promote this younger/milder phenotype. When ASCEND eligibility criteria were applied to our real world cohort, eligible patients were much younger, but with a much lower VC than non-eligible patients. Only INPULSIS criteria generated eligible patients that were of a similar age and lung function as non-eligible patients. The generalisabilty of IPF clinical trial data to real world patients is important to clinicians and patients. It has been well documented that mortality in IPF is high (around 20% per year), however this has not been reflected in placebo arms or past clinical trials with mortality ranging from 2.3% to 7.8%. This may be explained by our observation that patients recruited to clinical trials in IPF tend to be younger, present fewer comorbidities, have better lung function and well characterised disease severity, when compared to real world IPF patients. The majority of our Edinburgh IPF cohort would have been excluded from recent clinical trials and we have shown that the outcome of non-eligible patients was different to eligible patients, therefore limiting the generalisability of clinical trials to our everyday clinical practice. By comparing the baseline characteristics and natural history of IPF patients deemed eligible or not eligible for recent trials, we found that the INPULSIS trial is more generalisable to real world IPF patients than PANTHER, CAPACITY and ASCEND.

Reliable methods of predicting disease progression and survival are of great clinical value in IPF. Prior to the 2011 guideline, differential cell count in BAL was an important part of the diagnostic algorithm, however was removed from the guideline in 2011. BAL has been crucial in identifying the key immune effector cells driving the inflammatory process in IPF, and BAL DCCs may be of additional diagnostic benefit, even in patients with ‘definite UIP’ HRCT appearances. It is thought that low-grade inflammation, oxidative cell injury and an abnormal healing process drive the development of UIP, and since macrophages are integral to lung tissue repair and homeostasis, play a central role in IPF. Previous studies have demonstrated BAL neutrophilia may be an important diagnostic and prognostic indicator in IPF, however our data does not suggest any significant predictive effects.

It is now accepted that macrophage polarisation phenotype is dynamic and broadly heterogenic depending on the local microenvironment. However there are few reports in the literature detailing the alveolar macrophage polarisation phenotype in IPF specifically. My study demonstrated a distinct AM polarisation phenotype in the IPF patient population with a significantly increased M2 (specifically M2a) subset. Furthermore, I showed that AM phenotypes can be predictive of disease progression in IPF with characteristic predictors of stable disease at presentation including low CD71, low CD206 and high CD163 AM expression. IPF patients with rapid disease progression had significantly increased AM expression of CD71 and CD206, and significantly decreased CD163 expression, survival was also significantly worse in patients with high AM CD71 expression. The AM phenotype predictive of disease progression in IPF was $CD71^{high}CD206^{high}CD163^{low}$, mortality was significantly higher in this group when compared to those with a $CD71^{low}CD206^{low}CD163^{high}$ phenotype.

It is well documented that monocytes and macrophages contribute significantly to the disease process in IPF. It has also been reported that expansion of novel subpopulations of pulmonary monocyte-like cells occurs in inflammatory lung disease, however their role in fibrotic lung disease is largely unknown. My study aimed to quantify and characterise the PMLC population in BALF cells from IPF patients. I found the percentage of BAL resident PMLCs was significantly higher in patients with IPF versus both non-fibrotic ILD and controls. In addition, the percentage of BAL resident PMLCs was significantly increased in IPF progressor versus non-progressor groups. Disease progression in IPF was associated with an increased percentage of BAL resident PMLCs and a decreased percentage of BAL inducible PMLCs, and a significantly reduced iPMLC:rPMLC ratio at presentation. Our study is clinically relevant as it suggests there is a distinct relationship between AM subtypes, cell-surface expression markers and disease progression in IPF. Future research may build upon this to investigate new targets for further therapeutic strategies. PMLCs may also represent a novel target for future approaches as modulation of these myeloid phenotypes may be of therapeutic value.

The drive to distinguish IPF from the other IIPs and the need to predict individual patient outcome has prompted a wealth of research into novel diagnostic and prognostic biomarkers over the last 5 years. The clinical variables available to predict the risk of

mortality and disease progression in IPF are currently inadequate. Additional non-invasive and reproducible markers are required to improve existing risk model templates. In recent years large numbers of BAL and peripheral blood proteins have been studied as potential biomarkers of disease progression in IPF. It is clear that no single protein biomarker will have the ability to confidently predict disease progression with high sensitivity, specificity, PPV and NPV values in IPF, however in combination with clinical, physiological and radiological parameters, risk stratification can be improved.

My study was consistent with the current literature describing serum proteins of interest as potential biomarkers in IPF. I found serum concentrations of MMP-1, periostin, osteopontin, SP-D, IP-10, MCP-1, CHI3-L1, IL-8 and CCL-18 were all significantly increased in patients with IPF versus controls. Furthermore, periostin, SP-D, GRO-alpha, EGF, IFNγ, galectin-1, CHI3-L1, amphiregulin, osteopontin and HGF levels were all significantly higher in IPF progressors versus non-progressors. This data is all in keeping with recent reports in the literature. I then developed a prediction model combining clinical, physiological and biological variables, and found accuracy in predicting disease progression was highest when these parameters were used in combination. The top four proteins that were predictive of disease progression in the model were serum SP-D, GRO-alpha, RANTES and IL-8. Additional clinical and radiological variables identified by the model as being significantly associated with disease progression were volume of fibrosis on HRCT (%), percentage of lung periphery involved on HRCT and percentage of predicted FVC at baseline. The best two variables were serum SP-D level and percentage of predicted FVC, and when applied in combination in the model, predicted disease progression at a sensitivity of 86.4%, specificity of 92.3%, PPV 90.5% and NPV 88.9%. My study complements a small number of recent studies that report prediction models and unique protein signatures in well-phenotyped cohorts of IPF patients, and show replicable results in both test and validation cohorts. This shows that integration of both clinical and molecular variables in predicting risk of progression in IPF is feasible, and could be performed in routine clinical practice. These findings may provide a basis for future investigation on predicting outcomes and personalised treatment in this heterogeneous disease.

Chapter 7

Abstracts Presented and Publications

Publications (Abstracts)

- Nicol LM, Muralidharan V, Mills R, Brittan M, Marwick JA, MacKinnon AC, Graham C, McAllister DA, McFarlane PA, Wallace WA, Stewart G, Simpson J, Howie SE, Murchison JT, Hirani N. *The Clinical Value And Feasibility Of Repeat Bronchoalveolar Lavage In Idiopathic Pulmonary Fibrosis.* Am J Respir Crit Care Med (Abstract). 191;2015:A2526.

- Nicol LM, Muralidharan V, Mills R, Brittan M, Marwick JA, MacKinnon AC, Graham C, McAllister DA, McFarlane PA, Wallace WA, Stewart G, Simpson J, Howie SE, Murchison JT, Hirani N. *The Diagnostic And Prognostic Value Of Bronchoalveolar Lavage Differential Cell Count In Definite And Possible Idiopathic Pulmonary Fibrosis.* Am J Respir Crit Care Med (Abstract). 191;2015:A1560.

- Nicol LM, McFarlane PA, AC, Graham C, McAllister DA, Wallace WA, Stewart G, Howie SE, Murchison JT, Hirani N. *Generalisability of recent clinical trials in idiopathic pulmonary fibrosis to everyday clinical practice.* European Respiratory Journal Sep 2015, 46 (suppl 59) OA4501 (Absract).

- Nicol LM, McFarlane PA, AC, Graham C, McAllister DA, Wallace WA, Stewart G, Howie SE, Murchison JT, Hirani N. *The clinical value of surgical lung biopsy in 225 patients with suspected interstitial lung disease.* European Respiratory Journal Sep 2015, 46 (suppl 59) PA4856 (Abstract).

- Nicol LM, Brittan M, Marwick JA, MacKinnon AC, Mills R, McFarlane PA, Wallace WA, Stewart S, Simpson J, Rossi A, Howie SE, Murchison JT, Hirani N. *Disease progression in idiopathic pulmonary fibrosis is associated with an increased subpopulation of resident pulmonary monocyte like cells in bronchoalveolar lavage.* Am J Respir Crit Care Med (Abstract). 193;2016:A4538

- Nicol LM, Brittan M, Marwick JA, MacKinnon AC, Mills R, McFarlane PA, Wallace WA, Stewart S, Simpson J, Rossi A, Howie SE, Murchison JT, Hirani N. *A unique human alveolar macrophage polarization phenotype is associated with disease progression in idiopathic pulmonary fibrosis.* Am J Respir Crit Care Med (Abstract). 193;2016:A6603.

- Nicol LM, Brittan M, Marwick JA, MacKinnon AC, Mills R, McFarlane PA, Wallace WA, Stewart S, Simpson J, Rossi A, Howie SE, Murchison JT, Hirani N. *Identification of alveolar macrophage phenotypes predictive of disease progression in idiopathic pulmonary fibrosis.* QJM: monthly journal of the Association of Physicians Sept 2016;109(suppl_1):S2-S2 .

- Nicol LM, Mills R, Seth S, Brittan M, Marwick JA, MacKinnon AC, McFarlane PA, Wallace WA, Stewart S, Simpson J, Rossi A, Howie SE, Murchison JT, Hirani N. *Prognostically predictive biomarkers for IPF; a longitudinal cohort study of treatment naive patients*. QJM: monthly journal of the Association of Physicians Sept 2016;109(suppl_1):S38-S38.

Spoken Presentations

- 'Identification of alveolar macrophage phenotypes predictive of disease progression in idiopathic pulmonary fibrosis.' Nicol LM, Brittan M, Marwick J et al.
    - International Colloquium on Lung and Airway Fibrosis (ICLAF) 24th – 28th September 2016, Dublin

- 'Generalisability of recent clinical trials in idiopathic pulmonary fibrosis to everyday clinical practice.' Nicol LM, McFarlane PA, AC, Graham C, McAllister DA, Wallace WA, Stewart G, Howie SE, Murchison JT, Hirani N.

    - European Respiratory Society International Congress 29th September 2015, Amsterdam

Poster Presentations

- ‘Prognostically predictive biomarkers for IPF; a longitudinal cohort study of treatment naive patients.’ Nicol LM, Mills R, Seth S et al.
    - Poster presentation and discussion session, International Colloquium on Lung and Airway Fibrosis (ICLAF), 24th – 28th September 2016, Dublin

- ‘Disease progression in idiopathic pulmonary fibrosis is associated with an increased subpopulation of resident pulmonary monocyte like cells in bronchoalveolar lavage.’ Nicol LM, Brittan M, Marwick J et al.
    - Poster presentation and discussion session at American Thoracic Society meeting, San Francisco, May 2016.

- ‘A unique human alveolar macrophage polarization phenotype is associated with disease progression in idiopathic pulmonary fibrosis.’ Nicol LM, Brittan M, Marwick J et al.
    - Poster presentation and discussion session at American Thoracic Society meeting, San Francisco, May 2016.

- The clinical value of surgical lung biopsy in 225 patients with suspected interstitial lung disease. Nicol LM, Graham C, McAllister DA et al.
    - Poster presentation and discussion session, European Respiratory Society 2015 International Congress, September 2015, Amsterdam

- The Clinical Value And Feasibility Of Repeat Bronchoalveolar Lavage In Idiopathic Pulmonary Fibrosis. Nicol LM, Muralidharan V, Mills R et al.
    - Poster presentation and discussion session, American Thoracic Society 2015 International Conference, May 2015, Denver

- The Diagnostic And Prognostic Value Of Bronchoalveolar Lavage Differential Cell Count In Definite And Possible Idiopathic Pulmonary Fibrosis. Nicol LM, Muralidharan V, Mills R et al.

    - Poster presentation, American Thoracic Society 2015 International Conference, May 2015, Denver

Reference List

1. Raghu, G. *et al.* An Official ATS/ERS/JRS/ALAT Statement: Idiopathic pulmonary fibrosis: Evidence-based guidelines for diagnosis and management. *Am. J. Respir. Crit. Care Med.* **183,** 788–824 (2011).
2. Mikolasch, T. A., Garthwaite, H. S. & Porter, J. C. Update in diagnosis and management of interstitial lung disease. *Clinical medicine (London, England)* 16(6):s71-s78 (2016). doi:10.7861/clinmedicine.16-6-s71
3. Gribbin, J. *et al.* Incidence and mortality of idiopathic pulmonary fibrosis and sarcoidosis in the UK. *Thorax* **61,** 980–985 (2006).
4. Sgalla, G., Biffi, A. & Richeldi, L. Idiopathic pulmonary fibrosis: Diagnosis, epidemiology and natural history. *Respirology* (2016). doi:10.1111/resp.12683
5. Wuyts, W. A. *et al.* The pathogenesis of pulmonary fibrosis: A moving target. *European Respiratory Journal* 41(5): 1207-1218 (2013). doi:10.1183/09031936.00073012
6. Kim, H. J., Perlman, D. & Tomic, R. Natural history of idiopathic pulmonary fibrosis. *Respiratory Medicine* 109(6):661-70 (2015). doi:10.1016/j.rmed.2015.02.002
7. Ley, B., Collard, H. R. & King Jr, T. E. Clinical course and prediction of survival in idiopathic pulmonary fibrosis. *Am. J. Respir. Crit. Care Med.* **183,** 431–40 (2011).
8. Hlastala M, B. A. *Physiology of Respiration*. (Oxford University Press, 2001).
9. Abbas A, Lichtman A, P. S. *Basic Immunology*. (Elsevier, 2015).
10. Wynn, T. A. & Vannella, K. M. Macrophages in Tissue Repair, Regeneration, and Fibrosis. *Immunity* 44:450-462 (2016). doi:10.1016/j.immuni.2016.02.015
11. Strieter, R. M. What Differentiates Normal Lung Repair and Fibrosis?: Inflammation, Resolution of Repair, and Fibrosis. *Proc. Am. Thorac. Soc.* **5,** 305–310 (2008).
12. Kolahian, S., Fernandez, I. E., Eickelberg, O. & Hartl, D. Immune mechanisms in pulmonary fibrosis. *American Journal of Respiratory Cell and Molecular Biology* 55(3): 309-22 (2016). doi:10.1165/rcmb.2016-0121TR
13. O'Dwyer, D. N., Ashley, S. L. & Moore, B. B. Influences of innate immunity, autophagy, and fibroblast activation in the pathogenesis of lung fibrosis. *Am. J. Physiol. - Lung Cell. Mol. Physiol.* **311,** L590-601 (2016).
14. Byrne, A. J., Maher, T. M. & Lloyd, C. M. Pulmonary Macrophages: A New Therapeutic Pathway in Fibrosing Lung Disease? *Trends in Molecular Medicine* 22(4): 303-316 (2016). doi:10.1016/j.molmed.2016.02.004
15. Renzoni, E., Srihari, V. & Sestini, P. Pathogenesis of idiopathic pulmonary fibrosis: review of recent findings. *F1000Prime Rep.* **6,** 69 (2014).
16. Travis, W. D. *et al.* An official American Thoracic Society/European Respiratory Society statement: Update of the international multidisciplinary classification of the idiopathic interstitial pneumonias. *Am. J. Respir. Crit. Care Med.* **188,** 733–748 (2013).
17. Fell, C. D. *et al.* Clinical predictors of a diagnosis of idiopathic pulmonary fibrosis. *Am. J. Respir. Crit. Care Med.* **181,** 832–7 (2010).
18. Spagnolo, P., Maher, T. M. & Richeldi, L. Idiopathic pulmonary fibrosis: Recent advances on pharmacological therapy. *Pharmacol. Ther.* **152,** 18–27 (2015).
19. Kreuter, M., Bonella, F., Wijsenbeek, M., Maher, T. M. & Spagnolo, P. Pharmacological Treatment of Idiopathic Pulmonary Fibrosis: Current

Approaches, Unsolved Issues, and Future Perspectives. *BioMed Research International* 2015:329481 (2015). doi:10.1155/2015/329481
20. Tzouvelekis, A., Bonella, F. & Spagnolo, P. Update on therapeutic management of idiopathic pulmonary fibrosis. *Ther. Clin. Risk Manag.* **11,** 359–370 (2015).
21. Idiopathic, T. & Fibrosis, P. Prednisone, Azathioprine, and N -Acetylcysteine for Pulmonary Fibrosis. *N. Engl. J. Med.* **366,** 1968–1977 (2012).
22. Noble, P. W. *et al.* Pirfenidone in patients with idiopathic pulmonary fibrosis (CAPACITY): Two randomised trials. *Lancet* **377,** 1760–9 (2011).
23. Covvey, J. R. & Mancl, E. E. Recent Evidence for Pharmacological Treatment of Idiopathic Pulmonary Fibrosis. *Ann. Pharmacother.* **48,** 1611–1619 (2014).
24. King, T. E. *et al.* A phase 3 trial of pirfenidone in patients with idiopathic pulmonary fibrosis. *N. Engl. J. Med.* **370,** 2083–2092 (2014).
25. Richeldi, L. *et al.* Efficacy and safety of nintedanib in idiopathic pulmonary fibrosis. *N. Engl. J. Med.* **370,** 2071–2082 (2014).
26. Nathan, S. D. *et al.* Long-term course and prognosis of idiopathic pulmonary fibrosis in the new millennium. in *Chest* 140(1): 221-9 (2011). doi:10.1378/chest.10-2572
27. Nadrous, H. F., Myers, J. L., Decker, P. A. & Ryu, J. H. Idiopathic Pulmonary Fibrosis in Patients Younger Than 50 Years. *Mayo Clin. Proc.* **80,** 37–40 (2005).
28. Han, M. K. *et al.* Sex differences in physiological progression of idiopathic pulmonary fibrosis. *Eur. Respir. J.* **31,** 1183–8 (2008).
29. Alakhras, M., Decker, P. A., Nadrous, H. F., Collazo-Clavell, M. & Ryu, J. H. Body mass index and mortality in patients with idiopathic pulmonary fibrosis. *Chest* **131,** 1448–1453 (2007).
30. Jegal, Y. *et al.* Physiology is a stronger predictor of survival than pathology in fibrotic interstitial pneumonia. *Am. J. Respir. Crit. Care Med.* **171,** 639–644 (2005).
31. Latsi, P. I. *et al.* Fibrotic idiopathic interstitial pneumonia: The prognostic value of longitudinal functional trends. *Am. J. Respir. Crit. Care Med.* **168,** 531–537 (2003).
32. Flaherty, K. R. *et al.* Radiological versus histological diagnosis in UIP and NSIP: Survival implications. *Thorax* **58,** 143–148 (2003).
33. Sumikawa, H. *et al.* Computed tomography findings in pathological usual interstitial pneumonia: Relationship to survival. *Am. J. Respir. Crit. Care Med.* **177,** 433–9 (2008).
34. Lynch, D. A. *et al.* High-resolution computed tomography in idiopathic pulmonary fibrosis: Diagnosis and prognosis. *Am. J. Respir. Crit. Care Med.* **172,** 488–93 (2005).
35. Lee, H. Y. *et al.* High-resolution CT findings in fibrotic idiopathic interstitial pneumonias with little honeycombing: Serial changes and prognostic implications. *Am. J. Roentgenol.* **199,** 982–9 (2012).
36. King, T. E., Tooze, J. a, Schwarz, M. I., Brown, K. R. & Cherniack, R. M. Predicting survival in idiopathic pulmonary fibrosis: scoring system and survival model. *Am. J. Respir. Crit. Care Med.* **164,** 1171–81 (2001).
37. Wells, A. U. *et al.* Idiopathic pulmonary fibrosis: A composite physiologic index derived from disease extent observed by computed tomography. *Am. J. Respir. Crit. Care Med.* **167,** 962–9 (2003).
38. Ley, B. *et al.* A multidimensional index and staging system for idiopathic pulmonary fibrosis. *Ann. Intern. Med.* **156,** 684–91 (2012).
39. Ley, B. *et al.* Unified baseline and longitudinal mortality prediction in idiopathic

pulmonary fibrosis. *Eur. Respir. J.* **45,** 1374–81 (2015).
40. Du Bois, R. M. *et al.* Ascertainment of individual risk of mortality for patients with idiopathic pulmonary fibrosis. *Am. J. Respir. Crit. Care Med.* **184,** 459–66 (2011).
41. Du Bois, Roland M, Alberta C, B. W. et al. A novel clinical prediction model for near-term mortality in patients with idiopathic pulmonary fibrosis (IPF). *Am. J. Respir. Crit. Care Med.* **187,** A2357 (2013).
42. Mura, M. *et al.* Predicting survival in newly diagnosed idiopathic pulmonary fibrosis: a 3-year prospective study. *Eur. Respir. J.* **40,** 101–9 (2012).
43. Kinder, B. W. *et al.* Serum surfactant protein-A is a strong predictor of early mortality in idiopathic pulmonary fibrosis. *Chest* **135,** 1557–63 (2009).
44. Song, J. W. *et al.* Blood biomarkers MMP-7 and SP-A: Predictors of outcome in idiopathic pulmonary fibrosis. *Chest* **143,** 1422–9 (2013).
45. Richards, T. J. *et al.* Peripheral blood proteins predict mortality in idiopathic pulmonary fibrosis. *Am. J. Respir. Crit. Care Med.* **185,** 67–76 (2012).
46. De Lauretis, A. & Renzoni, E. A. Molecular Biomarkers in Interstitial Lung Diseases. *Mol. Diagn. Ther.* **18,** 505–522 (2014).
47. Willems, S. *et al.* Multiplex protein profiling of bronchoalveolar lavage in idiopathic pulmonary fibrosis and hypersensitivity pneumonitis. *Ann. Thorac. Med.* **8,** 38–45 (2013).
48. Hambly, N., Shimbori, C. & Kolb, M. Molecular classification of idiopathic pulmonary fibrosis: Personalized medicine, genetics and biomarkers. *Respirology* 20(7):1010-22 (2015). doi:10.1111/resp.12569
49. Brittan, M. *et al.* A novel subpopulation of monocyte-like cells in the human lung after lipopolysaccharide inhalation. *Eur. Respir. J.* **40,** 206–214 (2012).
50. Brittan, M. *et al.* Functional characterisation of human pulmonary monocyte-like cells in lipopolysaccharide-mediated acute lung inflammation. *J. Inflamm. (Lond).* **31,** 11–9 (2014).
51. Vuga, L. J. *et al.* C-X-C motif chemokine 13 (CXCL13) is a prognostic biomarker of idiopathic pulmonary fibrosis. *Am. J. Respir. Crit. Care Med.* **189,** 966–74 (2014).
52. Gilani, S. R. *et al.* CD28 down-regulation on circulating CD4 T-cells is associated with poor prognoses of patients with idiopathic pulmonary fibrosis. *PLoS One* **5,** e8959 (2010).
53. Ley, B., Brown, K. K. & Collard, H. R. Molecular biomarkers in idiopathic pulmonary fibrosis. *Am. J. Physiol. Lung Cell. Mol. Physiol.* **307,** L681–L691 (2014).
54. Kahloon, R. A. *et al.* Patients with idiopathic pulmonary fibrosis with antibodies to heat shock protein 70 have poor prognoses. *Am. J. Respir. Crit. Care Med.* **187,** 768–775 (2013).
55. Belghith, M. *et al.* TGF-β-dependent mechanisms mediate restoration of self-tolerance induced by antibodies to CD3 in overt autoimmune diabetes. *Nat. Med.* **9,** 1202–1208 (2003).
56. Bargagli, E., Prasse, A., Olivieri, C., Muller-Quernheim, J. & Rottoli, P. Macrophage-derived biomarkers of idiopathic pulmonary fibrosis. *Pulmonary Medicine* (2011). doi:10.1155/2011/717130
57. Wang, N., Liang, H. & Zen, K. Molecular mechanisms that influence the macrophage M1-M2 polarization balance. *Frontiers in Immunology* 5:614 (2014). doi:10.3389/fimmu.2014.00614
58. Prasse, A. *et al.* Serum CC-chemokine ligand 18 concentration predicts outcome

in idiopathic pulmonary fibrosis. *Am. J. Respir. Crit. Care Med.* **179,** 717–723 (2009).
59. Takahashi, H. *et al.* Serum surfactant proteins A and D as prognostic factors in idiopathic pulmonary fibrosis and their relationship to disease extent. *Am. J. Respir. Crit. Care Med.* **162,** 1109–1114 (2000).
60. Rosas, I. O. *et al.* MMP1 and MMP7 as potential peripheral blood biomarkers in idiopathic pulmonary fibrosis. *PLoS Med.* **5,** e93 (2008).
61. Zhang, Y. & Kaminski, N. Biomarkers in idiopathic pulmonary fibrosis. *Current Opinion in Pulmonary Medicine* 18(5): 441-446 (2012). doi:10.1097/MCP.0b013e328356d03c
62. MacKinnon, A. C. *et al.* Regulation of Alternative Macrophage Activation by Galectin-3. *J. Immunol.* **180,** 2650–8 (2008).
63. Henderson, N. C. *et al.* Galectin-3 expression and secretion links macrophages to the promotion of renal fibrosis. *Am. J. Pathol.* **172,** 288–98 (2008).
64. Henderson, N. C. *et al.* Galectin-3 regulates myofibroblast activation and hepatic fibrosis. *Proc. Natl. Acad. Sci.* **103,** 5060–5 (2006).
65. Korthagen, N. M. *et al.* Serum and BALF YKL-40 levels are predictors of survival in idiopathic pulmonary fibrosis. *Respir. Med.* **105,** 106–113 (2011).
66. Moeller, A. *et al.* Circulating fibrocytes are an indicator of poor prognosis in idiopathic pulmonary fibrosis. *Am. J. Respir. Crit. Care Med.* **179,** 588–594 (2009).
67. Walsh, S. L. F. Multidisciplinary evaluation of interstitial lung diseases: Current insights. *Eur. Respir. Rev.* **26,** 170002 (2017).
68. Travis, W. D. *et al.* American thoracic society/European respiratory society international multidisciplinary consensus classification of the idiopathic interstitial pneumonias. in *American Journal of Respiratory and Critical Care Medicine* 165(2):277-304 (2002). doi:10.1164/ajrccm.165.2.ats01
69. Jo, H. E., Randhawa, S., Corte, T. J. & Moodley, Y. Idiopathic Pulmonary Fibrosis and the Elderly: Diagnosis and Management Considerations. *Drugs Aging* **33,** 321–34 (2016).
70. Kim, R. & Meyer, K. C. Therapies for interstitial lung disease: past, present and future. *Ther. Adv. Respir. Dis.* **2,** 319–38 (2008).
71. Meyer, K. C. Diagnosis and management of interstitial lung disease. *Transl. Respir. Med.* **2,** 4 (2014).
72. Hutchinson, J. P., McKeever, T. M., Fogarty, A. W., Navaratnam, V. & Hubbard, R. B. Surgical lung biopsy for the diagnosis of interstitial lung disease in England: 1997-2008. *Eur. Respir. J.* **48,** 1453–1461 (2016).
73. Hutchinson, J. P., Fogarty, A. W., McKeever, T. M. & Hubbard, R. B. In-hospital Mortality Following Surgical Lung Biopsy for Interstitial Lung Disease in the USA: 2000-2011. *Am. J. Respir. Crit. Care Med.* (2015). doi:10.1164/rccm.201508-1632OC
74. Nguyen, W. & Meyer, K. C. Surgical lung biopsy for the diagnosis of interstitial lung disease: a review of the literature and recommendations for optimizing safety and efficacy. *Sarcoidosis, Vasc. Diffus. Lung Dis.* **30,** 3–16 (2013).
75. Dindo, D., Demartines, N. & Clavien, P. A. Classification of surgical complications: A new proposal with evaluation in a cohort of 6336 patients and results of a survey. *Annals of Surgery* 240(2): 205-213 (2004). doi:10.1097/01.sla.0000133083.54934.ae
76. Quan, H. *et al.* Updating and validating the charlson comorbidity index and score for risk adjustment in hospital discharge abstracts using data from 6 countries.

Am. J. Epidemiol. **173,** 676–682 (2011).
77. Du Bois, R. M. *et al.* Forced vital capacity in patients with idiopathic pulmonary fibrosis: Test properties and minimal clinically important difference. *Am. J. Respir. Crit. Care Med.* **184,** 1382–1389 (2011).
78. Bjoraker, J. A. *et al.* Prognostic significance of histopathologic subsets in idiopathic pulmonary fibrosis. *Am. J. Respir. Crit. Care Med.* **157,** 199–203 (1998).
79. Nicholson, A. G., Colby, T. V., Dubois, R. M., Hansell, D. M. & Wells, A. U. The prognostic significance of the histologic pattern of interstitial pneumonia in patients presenting with the clinical entity of cryptogenic fibrosing alveolitis. *Am. J. Respir. Crit. Care Med.* **162,** 2213–2217 (2000).
80. Demedts, M. *et al.* High-Dose Acetylcysteine in Idiopathic Pulmonary Fibrosis. *N. Engl. J. Med.* **353,** 2229–2242 (2005).
81. King, T. E. *et al.* BUILD-3: A randomized, controlled trial of bosentan in idiopathic pulmonary fibrosis. *Am. J. Respir. Crit. Care Med.* **184,** 92–99 (2011).
82. Richeldi, L. *et al.* Efficacy of a tyrosine kinase inhibitor in idiopathic pulmonary fibrosis. *N. Engl. J. Med.* **365,** 1079–1087 (2011).
83. Martinez, F. J. *et al.* The clinical course of patients with idiopathic pulmonary fibrosis. *Ann. Intern. Med.* **142,** 963–967 (2005).
84. Nicholson, A. G. *et al.* The relationship between individual histologic features and disease progression in idiopathic pulmonary fibrosis. *Am. J. Respir. Crit. Care Med.* **166,** 173–177 (2002).
85. King, T. E. *et al.* Effect of interferon gamma-1b on survival in patients with idiopathic pulmonary fibrosis (INSPIRE): a multicentre, randomised, placebo-controlled trial. *Lancet* **374,** 222–8 (2009).
86. Raghu, G. *et al.* Treatment of idiopathic pulmonary fibrosis with Ambrisentan: A parallel, randomized trial. *Ann. Intern. Med.* **158,** 641–9 (2013).
87. King, T. E. *et al.* BUILD-1: A randomized placebo-controlled trial of bosentan in idiopathic pulmonary fibrosis. *Am. J. Respir. Crit. Care Med.* **177,** 75–81 (2008).
88. Raghu, G. *et al.* Efficacy of simtuzumab versus placebo in patients with idiopathic pulmonary fibrosis: a randomised, double-blind, controlled, phase 2 trial. *Lancet Respir. Med.* **5,** 22–32 (2017).
89. Atkins, C. P., Loke, Y. K. & Wilson, A. M. Outcomes in idiopathic pulmonary fibrosis: A meta-analysis from placebo controlled trials. *Respir. Med.* **108,** 376–387 (2014).
90. Wells, A. U. *et al.* Hot off the breath: Mortality as a primary end-point in IPF treatment trials: The best is the enemy of the good. *Thorax* 67: 938-940 (2012). doi:10.1136/thoraxjnl-2012-202580
91. Raghu, G. *et al.* Idiopathic pulmonary fibrosis: Clinically meaningful primary endpoints in phase 3 clinical trials. *American Journal of Respiratory and Critical Care Medicine* 185: 1044-1048 (2012). doi:10.1164/rccm.201201-0006PP
92. Karimi-Shah, B. A. & Chowdhury, B. A. Forced Vital Capacity in Idiopathic Pulmonary Fibrosis — FDA Review of Pirfenidone and Nintedanib. *N. Engl. J. Med.* **372,** 1189–1191 (2015).
93. Corte, T. J. *et al.* Use of intravenous cyclophosphamide in known or suspected, advanced non-specific interstitial pneumonia. *Sarcoidosis Vasc. Diffus. Lung Dis.* **26,** 132–138 (2009).
94. Park, I. N. *et al.* Clinical course and lung function change of idiopathic nonspecific interstitial pneumonia. *Eur. Respir. J.* **33,** 68–76 (2009).

95. Pellegrino, R. *et al.* Interpretative strategies for lung function tests. *Eur. Respir. J.* **26,** 948–968 (2005).
96. Ohshimo, S. *et al.* Significance of bronchoalveolar lavage for the diagnosis of idiopathic pulmonary fibrosis. *Am. J. Respir. Crit. Care Med.* (2009). doi:10.1164/rccm.200808-1313OC
97. Nicholson, A. G. *et al.* Inter-observer variation between pathologists in diffuse parenchymal lung disease. *Thorax* **59,** 500–505 (2004).
98. Flaherty, K. R. *et al.* Histopathologic variability in usual and nonspecific interstitial pneumonias. *Am. J. Respir. Crit. Care Med.* **164,** 1722–1727 (2001).
99. Hunninghake, G. W. *et al.* Utility of a lung biopsy for the diagnosis of idiopathic pulmonary fibrosis. *Am. J. Respir. Crit. Care Med.* **164,** 193–196 (2001).
100. Collins, C. D. *et al.* Observer variation in pattern type and extent of disease in fibrosing alveolitis on thin section computed tomography and chest radiography. *Clin. Radiol.* **49,** 236–240 (1994).
101. Nagai, S., Handa, T., Ito, Y., Takeuchi, M. & Izumi, T. Bronchoalveolar lavage in idiopathic interstitial lung diseases. *Semin. Respir. Crit. Care Med.* **28,** 496–503 (2007).
102. Pesci, A., Ricchiuti, E., Ruggiero, R. & De Micheli, A. Bronchoalveolar lavage in idiopathic pulmonary fibrosis: What does it tell us? *Respir. Med.* **104,** 570–573 (2010).
103. Costabel, U. & Guzman, J. Bronchoalveolar lavage in interstitial lung disease. *Curr. Opin. Pulm. Med.* **7,** 255–61 (2001).
104. Kinder, B. W. *et al.* Baseline BAL neutrophilia predicts early mortality in idiopathic pulmonary fibrosis. *Chest* **133,** 226 (2008).
105. Veeraraghavan, S. *et al.* BAL findings in idiopathic nonspecific interstitial pneumonia and usual interstitial pneumonia. *Eur. Respir. J.* **22,** 239 (2003).
106. Tabuena, R. P. *et al.* Cell profiles of bronchoalveolar lavage fluid as prognosticators of idiopathic pulmonary fibrosis/usual interstitial pneumonia among Japanese patients. *Respiration* **72,** 490–8 (2005).
107. Ju Ryu, Y. *et al.* Bronchoalveolar lavage in fibrotic idiopathic interstitial pneumonias. *Respir. Med.* **101,** 655–60 (2007).
108. Domagała-Kulawik, J., Skirecki, T., Maskey-Warzechowska, M., Grubek-Jaworska, H. & Chazan, R. Bronchoalveolar Lavage Total Cell Count in Interstitial Lung Diseases—Does It Matter? *Inflammation* **35,** 803–809 (2012).
109. Wojtan, P., Mierzejewski, M., Osińska, I. & Domagała-Kulawik, J. Macrophage polarization in interstitial lung diseases. *Cent. Eur. J. Immunol.* **41,** 159–164 (2016).
110. Mantovani, A. *et al.* The chemokine system in diverse forms of macrophage activation and polarization. *Trends in Immunology* 25(12): 677-86 (2004). doi:10.1016/j.it.2004.09.015
111. Roszer, T. Understanding the mysterious M2 macrophage through activation markers and effector mechanisms. *Mediators of Inflammation* 1–16 (2015). doi:10.1155/2015/816460
112. Kowal, K. *et al.* CD163 and its role in inflammation. *Folia Histochemica et Cytobiologica* 49: 365-374 (2011). doi:10.5603/FHC.2011.0052
113. Allden S, Toshner R, Byrne A, Lloyd C, M. T. Expression of CD71 on alveolar macrophages reveals distinct cell populations in human bronchoalveolar lavage from patients with interstitial lung disease. *Am J Respir Crit Care Med* **193,** A6605 (2016).
114. Davis, M. J. *et al.* Macrophage M1 / M2 Polarization Dynamically Adapts to

Changes in. *MBio* **4,** e00264-13 (2013).
115. Liu, Q. *et al.* Significance of CD71 expression by flow cytometry in diagnosis of acute leukemia. *Leuk. Lymphoma* **55,** 892–898 (2014).
116. Krombach, F. *et al.* Characterization and quantification of alveolar monocyte-like cells in human chronic inflammatory lung disease. *Eur. Respir. J.* **9,** 984–991 (1996).
117. Alexis, N. E. *et al.* Acute LPS inhalation in healthy volunteers induces dendritic cell maturation in vivo. *J. Allergy Clin. Immunol.* **115,** 345–350 (2005).
118. FRANKENBERGER, M. *et al.* Characterization of a population of small macrophages in induced sputum of patients with chronic obstructive pulmonary disease and healthy volunteers. *Clin. Exp. Immunol.* **138,** 507–516 (2004).
119. Uhal, B. D. The role of apoptosis in pulmonary fibrosis. *European Respiratory Review* 17: 138-144 (2008). doi:10.1183/09059180.00010906
120. Roberts M, Broome R, Kent T, Charlton S, R. E. The inhibition of human lung fibroblast proliferation and differentiation by Gs-coupled receptors is not predicted by the magnitude of cAMP response. *Respir. Res.* **19,** (2018).
121. Barratt, S. & Millar, A. Vascular remodelling in the pathogenesis of idiopathic pulmonary fibrosis. *QJM* **107,** 515–519 (2014).
122. TURNER-WARWICK, M. PRECAPILLARY SYSTEMIC-PULMONARY ANASTOMOSES. *Thorax* **167,** 438–43 (1963).
123. Ebina, M. *et al.* Heterogeneous Increase in CD34-positive Alveolar Capillaries in Idiopathic Pulmonary Fibrosis. *Am. J. Respir. Crit. Care Med.* **169,** 1203–8 (2004).
124. Keane, M. P. *et al.* The CXC chemokines, IL-8 and IP-10, regulate angiogenic activity in idiopathic pulmonary fibrosis. *J. Immunol.* **159,** 1437–43 (1997).
125. Verma, S. & Slutsky, A. S. Idiopathic Pulmonary Fibrosis — New Insights. *N. Engl. J. Med.* **356,** 1370–2 (2007).
126. Harari, S. & Caminati, A. IPF: New insight on pathogenesis and treatment. *Allergy: European Journal of Allergy and Clinical Immunology* 65(6):537-53 (2010). doi:10.1111/j.1398-9995.2009.02305.x
127. Visscher, D. W. Histologic Spectrum of Idiopathic Interstitial Pneumonias. *Proc. Am. Thorac. Soc.* **3,** 322–9 (2006).
128. Chen, H. *et al.* Triptolide suppresses paraquat induced idiopathic pulmonary fibrosis by inhibiting TGFB1-dependent epithelial mesenchymal transition. *Toxicol. Lett.* **284,** 1–9 (2018).
129. Giménez, A. *et al.* Dysregulated collagen homeostasis by matrix stiffening and TGF-β1 in fibroblasts from idiopathic pulmonary fibrosis patients: Role of FAK/Akt. *Int. J. Mol. Sci.* **18,** 16–23 (2017).
130. Thannickal, V. J. & Horowitz, J. C. Evolving concepts of apoptosis in idiopathic pulmonary fibrosis. *Proc. Am. Thorac. Soc.* **3,** 350–6 (2006).
131. Lee, S. H. *et al.* Predicting survival of patients with idiopathic pulmonary fibrosis using GAP score: A nationwide cohort study. *Respir. Res.* **17,** 131 (2016).
132. Kim, E. S. *et al.* Validation of the GAP score in Korean patients with idiopathic pulmonary fibrosis. *Chest* **147,** 430–437 (2015).
133. Murray, L. A. *et al.* Antifibrotic role of vascular endothelial growth factor in pulmonary fibrosis. *JCI insight* **2,** (2017).
134. Antoniou, K. M. *et al.* Different angiogenic activity in pulmonary sarcoidosis and idiopathic pulmonary fibrosis. *Chest* **130,** 928–8 (2006).
135. Naik, P. K. *et al.* Periostin promotes fibrosis and predicts progression in patients with idiopathic pulmonary fibrosis. *Am. J. Physiol. Lung Cell. Mol. Physiol.* **303,**

L1046–L1056 (2012).
136. Okamoto, M. *et al.* Periostin, a matrix protein, is a novel biomarker for idiopathic interstitial pneumonias. *Eur. Respir. J.* **37,** 1119–1127 (2011).
137. Uchida, M. *et al.* Periostin, a matricellular protein, plays a role in the induction of chemokines in pulmonary fibrosis. *Am. J. Respir. Cell Mol. Biol.* **46,** 677–686 (2012).
138. Wang, K., Ju, Q., Cao, J., Tang, W. & Zhang, J. Impact of serum SP-A and SP-D levels on comparison and prognosis of idiopathic pulmonary fibrosis. *Med. (United States)* **96,** e7083 (2017).
139. Zhou, Y. *et al.* Amphiregulin, an epidermal growth factor receptor ligand, plays an essential role in the pathogenesis of transforming growth factor-β-induced pulmonary fibrosis. *J. Biol. Chem.* **287,** 41991–2000 (2012).
140. Trojanowska, M. Role of PDGF in fibrotic diseases and systemic sclerosis. in *Rheumatology* 47 Suppl 5: v2-4 (2009). doi:10.1093/rheumatology/ken265
141. Craig, V. J., Zhang, L., Hagood, J. S. & Owen, C. A. Matrix metalloproteinases as therapeutic targets for idiopathic pulmonary fibrosis. *American Journal of Respiratory Cell and Molecular Biology* 53(5):585-600 (2015). doi:10.1165/rcmb.2015-0020TR
142. García-Prieto, E. *et al.* Resistance to bleomycin-induced lung fibrosis in MMP-8 deficient mice is mediated by interleukin-10. *PLoS One* **5,** e13242 (2010).
143. Li, L. -c., Li, J. & Gao, J. Functions of Galectin-3 and Its Role in Fibrotic Diseases. *J. Pharmacol. Exp. Ther.* **351,** 336–343 (2014).
144. Wolters, P. J., Collard, H. R. & Jones, K. D. Pathogenesis of idiopathic pulmonary fibrosis. *Annu. Rev. Pathol.* **9,** 157–179 (2014).
145. Guiot, J., Moermans, C., Henket, M., Corhay, J.-L. & Louis, R. Blood Biomarkers in Idiopathic Pulmonary Fibrosis. *Lung* **195,** 273–280 (2017).